Drought in southern Africa:
structure, characteristics and impacts

Hector Chikoore

Thesis

To fulfill requirements for the degree

DOCTOR OF PHILOSOPHY

Department of Geography and Environmental Studies

Faculty of Science and Agriculture

UNIVERSITY OF ZULULAND

South Africa

December 2016

To my mother - Lyness Chikoore

“But blessed is the one who trusts in the LORD,
whose confidence is in him.
They will be like a tree planted by the water
that sends out its roots by the stream.
It does not fear when heat comes;
its leaves are always green.
It has no worries in a year of drought
and never fails to bear fruit.”

Jeremiah 17:7-8 (Holy Bible, New International Version)

ACKNOWLEDGEMENTS

This PhD thesis was supervised by Professor Mark R. Jury of the University of Puerto Rico, Mayaguez and supported by a bursary from South Africa's Department of Science and Technology/National Research Foundation - Alliance for Collaboration on Climate and Earth Systems Science (ACCESS). The administrative and moral support of colleagues in the Department of Geography and Environmental Studies (University of Zululand) is greatly appreciated.

The datasets employed in this thesis were obtained from several global and national climate, hydrology and agriculture centers. The following are acknowledged for data used in this study:- National Oceanic and Atmospheric Administration (NOAA) Physical Services Division (PSD), National Centers for Environmental Prediction - National Center for Atmospheric Research (NCEP-NCAR), European Center for Medium-Range Weather Forecasting (ECMWF), University of East Anglia's Climatic Research Unit (CRU), National Aeronautics and Space Administration (NASA), United States Geological Survey (USGS), United States Department of Agriculture (USDA), the Statistics Division of the Food and Agriculture Organization (FAOSTAT) and Zambezi River Authority (ZRA). The Moderate Resolution Imaging Spectroradiometer (MODIS) mission scientists and related NASA personnel are acknowledged for providing some data employed in this study. Data portals from International Research Institute for Climate and Society (IRI), Royal Netherlands Meteorological Institute (KNMI) and NCEP were used to access and analyze some of the data. The Center for Ocean-Land-Atmosphere Studies Grid Analysis and Display System and RStudio were used to manipulate and visualize some of the climate reanalyses.

Some of the analyses and write-up were done at the Abdus Salam International Center for Theoretical Physics, Trieste; the University of Puerto Rico, Mayaguez and the Japan Agency for Marine-Earth Science and Technology, Yokohama. Dr. Mary-Jane Bopape read a draft of this thesis and gave useful insights. Dr. J.V. Ratnam, Dr. Tak Ikeda, Thabo Mpanza, Innocent Mbokodo and Farai Dondofema were helpful with accessing and visualizing datasets in various platforms.

ABSTRACT

Drought is a complex, slow onset phenomenon which is a recurring and inevitable feature of the regional climate of southern Africa. This thesis focuses on the structure and characteristics of meteorological droughts in southern Africa and their impacts on surface soil moisture, agricultural yields and surface hydrology. In exploring drought characteristics in southern Africa (15-28°S, 22-32°E) monthly satellite datasets and reanalysis models are employed for the period from the austral summer of 1979-80 to that of 2011-12. Drought frequency and severity are determined using a Precipitation minus Evapotranspiration anomaly index which is related to the self-calibrating Palmer Drought Severity Index. It is found that sensible heat flux is strongly correlated with potential evapotranspiration and may be a useful drought indicator. Seven droughts are identified using the drought index with most occurring in the early part of the study period (1979-1995), whilst the 1992 drought was the most severe.

It is shown that rain trends in the study region are neutral but sensible heat flux exhibits an upward trend suggesting reduced available water for evaporation from the land surface. Changes in evaporation due to warmer temperatures may become more important than changes in precipitation in the surface water balance over southern Africa. While rainfall, outgoing longwave radiation and soil moisture composite anomalies are greatest over Zimbabwe, potential evapotranspiration, air temperature and vegetation anomalies maximize over the western Limpopo valley. The droughts identified in this study are among the 10 hottest seasons during the study period and area associated with increased probability of heat waves.

The immediate cause of meteorological drought over southern Africa is the establishment and persistence of the mid-tropospheric Botswana High which intensifies displacing the tropical rain belts equatorward whilst cloud bands shift to the warm ocean east of Madagascar. The jet stream is strengthened and displaced equatorward as the Angola Low weakens at the surface. The low-level moisture flux from the Indian Ocean is reduced and westerly wind anomalies become dominant. The vertical structure of zonal and meridional winds and vertical motion from the surface to 100 hPa exhibits enhanced subsidence in the area bounded by 18-38°E and between 10-30°S during drought seasons. This is a key finding as it shows that

drought tends to be widespread over southern Africa covering an area extending from South Africa's KwaZulu-Natal to northern Malawi.

The El Niño Southern Oscillation signal is the dominant mode of variability particularly over the eastern sector of southern Africa. Five of seven droughts identified occurred during an El Niño event while some were enhanced by a positive phase of the Indian Ocean Dipole. There is a strong link between upper divergence and the Indian Ocean Dipole, where upper convergence over central South Africa and Botswana results in sinking motion. Fluctuations in sea-level pressure over the adjacent tropical Atlantic Ocean due to Benguela Niños act to modulate the Angola Low and moisture convergence over southern Africa such that sometimes the west coastal margins experience a wet anomaly as the rest of the region endures drought.

This thesis also investigates relationships between drought and environmental and socio-economic indicators such as soil moisture, streamflow, lake levels, vegetation indices, maize yields and agricultural productivity. Strong negative soil moisture anomalies occur over the region during drought with a maximum over Zimbabwe affecting maize yields there. The El Niño impact on maize, Lake Kariba reservoir levels and vegetation is comparable to the impact on rainfall. Successive drought periods have had greater impact on livelihoods and economies of southern Africa which are heavily dependent on rain-fed agriculture.

CONTENTS

Acknowledgements ..... *iii*
Abstract ..... *iv*
List of Figures ..... *x*
List of Tables ..... *xiii*
List of Acronyms ..... *xiv*

CHAPTER 1 ..... **1**

1.1 HYDROLOGY 1
1.2 VEGETATION 2
1.3 AGRICULTURAL SYSTEMS 2
1.4 MEAN CLIMATE 3
1.5 BACKGROUND AND MOTIVATION 8
1.6 THESIS AIM, OBJECTIVES AND RESEARCH QUESTIONS 10
1.6.1 Aim *10*
1.6.2 Objectives *10*
1.6.3 Research questions *10*
1.8 SELECTION OF STUDY AREA 11
1.9 THESIS STRUCTURE 11

CHAPTER 2 ..... **16**

2.1 INTRODUCTION 16
2.2 DROUGHT CLASSIFICATION 17
2.3 DROUGHT MONITORING USING DROUGHT INDICES 19
2.3.1 Palmer Drought Severity Index *20*
2.3.2 Standardized Precipitation Index *21*
2.3.3 Vegetation indices *21*
2.3.4 Percent of normal rainfall index *22*
2.3.5 Other drought indices *23*
2.4 CAUSES AND PREDICTION OF DROUGHT 23
2.4.1 Atmospheric circulation *24*
2.4.2 Land-surface temperatures *25*
2.4.3 Sea surface temperatures *26*
2.4.4 Soil moisture content *30*
2.4.5 Other causes of drought *31*
2.5 CHARACTERISTICS OF DROUGHT 32
2.5.1 Drought severity or intensity *32*
2.5.2 Drought duration *32*
2.5.3 Aerial extent of drought *33*
2.6 DROUGHT IMPACTS 34
2.6.1 Environmental impacts *35*
2.6.2 Economic impacts *36*
2.6.3 Social impacts *37*
2.7 DROUGHT PREPAREDNESS, MITIGATION AND RESPONSE 37
2.8 DROUGHT IN SOUTHERN AFRICA 39
2.9 TEMPORAL TRENDS OF DROUGHT 43
2.10 SUMMARY 44

CHAPTER 3 ..... **47**

3.1 INTRODUCTION 47
3.2 DESCRIPTION AND SOURCES OF DATA 49
3.2.1 Rainfall *49*
3.2.2 Relative humidity *50*
3.2.3 Outgoing longwave radiation *51*
3.2.4 Circulation parameters *51*

3.2.5 Surface heat fluxes *54*
3.2.6 Evapotranspiration and potential evapotranspiration *55*
3.2.7 Land-surface and maximum air temperature *56*
3.2.8 Sea-surface temperatures *57*
3.2.9 ENSO indices *57*
3.2.10 Indian Ocean indices *58*
3.2.11 Surface soil moisture *58*
3.2.12 Normalized Difference Vegetation Index *59*
3.2.13 Crop yield and value of agricultural production *60*
3.2.14 Hydrological data *60*
3.3 Research Methods 61
3.3.1 Drought index *62*
3.3.2 Climatologies and anomalies *63*
3.3.3 Correlation and trend analysis *64*
3.3.4 Wavelet analysis *64*
3.3.5 EOF analysis *65*
3.3.6 Composite analysis *66*
3.3.7 Event scale analysis *67*
3.4 NOAA Earth System Research Laboratory 67
3.5 KNMI Climate Explorer 68
3.6 IRI Climate Data Library 68
3.7 Grid Analysis and Display System (GrADS) 68
3.8 Summary 69

CHAPTER 4 76

4.1 Introduction 76
4.2 Rainfall 76
4.2.1 Spatial patterns *76*
4.2.2 Annual cycle and intraseasonal variability *79*
4.2.3 Inter-annual variability *80*
4.3 Outgoing longwave radiation 81
4.4 Land surface temperature 82
4.5 Maximum temperature 82
4.6 Potential evapotranspiration, sensible heat flux and net radiation 83
4.7 Summary and discussion 84

CHAPTER 5 99

5.1 Introduction 99
5.2 Mean circulation 99
5.3 Large scale circulation anomalies inducing drought 102
5.3.1 Low level circulation *103*
5.3.2 Vorticity and divergence *103*
5.3.3 Middle level circulation *104*
5.3.4 Upper level winds *105*
5.3.5 Vertical structure *105*
5.4 Atmospheric moisture 106
5.5 Global remote mechanisms of drought 107
5.5.1 Sea-surface temperature anomalies *107*
5.5.2 El Niño Southern Oscillation *108*
5.5.3 El Niño and non-El Niño droughts: 1984 and 1992 events *109*
5.5.4 Indian Ocean influences *110*
5.5.5 Atlantic Ocean influences *111*
5.6 Tropical cyclones and drought 112
5.7 Summary and discussion 113

CHAPTER 6 137

6.1 Introduction 137

6.2 Soil moisture 138
6.3 Maize 139
6.3.1 Climate requirements 139
6.3.2 Maize yields 140
6.3.3 Value of agricultural production 141
6.4 Normalized Difference Vegetation Index (NDVI) 142
6.5 Surface hydrology 144
6.5.1 Annual cycles and interannual variability 144
6.5.2 Low flow and deficit characteristics 145
6.5.3 Lake Kariba 146
6.6 Summary and discussion 147

CHAPTER 7 164

7.1 Introduction 164
7.2 Thesis findings and conclusions 165
7.2.1 Recent drought events: 1979-2012 165
7.2.2 Rainfall and evapotranspiration 166
7.2.3 Radiation and temperature 167
7.2.4 Meteorological propagation and diagnostics 167
7.2.5 Remote influences 169
7.2.6 Space-time variability 171
7.2.7 Drought impact 172
7.3 Implications: Drought in a wider context 174
7.4 Future work 176
7.5 Solutions in drought management 178

REFERENCES 181

LIST OF FIGURES

Figure 1:1 The southern African study area and the countries involved, with the elevation (meters Above Mean Sea Level (AMSL) indicated in shading colours..... 14
Figure 1:2 The vegetation biomes of southern Africa (adapted from http://exploringafrica.matrix.msu.edu/map-three/) 15
Figure 1:3 Corn/maize production (ton/province) in southern Africa shown in shading. The inset shows the main focus of this study which is an important region for agriculture (adapted from http://fas.usda.gov/pecad/pecad.html)..... 15
Figure 2:1 Propagation of drought in the climate system (after Wilhite 2000a) 46
Figure 2:2 Positive and negative modes of the Indian Ocean Dipole (source: JAMSTEC 2015). The red color represents warmer SSTs whilst blue indicates colder. 46
Figure 3:1 Distribution of GPCC rain gauges over the study area indicated by shading. The white spaces indicate no rain gauges in those gridboxes. 71
Figure 3:2 Mean annual cycles of GPCC, GPCP, ERA-Int and CFS-R rainfall datasets over the southern Africa region..... 72
Figure 3:3 Mean annual cycles of LHF from MERRA, ERAInt and CFS-R reanalyses for the southern Africa region 72
Figure 3:4 Annual cycle of SHF from MERRA, ERAInt and CFS-R reanalyses. 73
Figure 3:5 El Niño regions used to measure the strength of El Niño over the equatorial Pacific Ocean (source: Climate Prediction Center www.cpc.noaa.gov).. 73
Figure 3:6 Mean annual cycles of LHF, SHF and PET over the southern Africa region 74
Figure 3:7 Mean annual cycle of P-E over southern Africa 74
Figure 3:8 Interannual variability of PDSI and P-E anomaly over southern Africa. The P-E index exhibits a weak upward trend (R^2=0.2192) whilst the PDSI is neutral (R^2=0.02)..... 75
Figure 4:1 Long term (1980-2012) mean summer (DJF) GPCP precipitation (shaded in mm/day) over southern Africa and the adjacent oceans..... 87
Figure 4:2 Mean GPCP Precipitation (mm/day) for wet years minus dry years over southern Africa and the adjacent oceans 88
Figure 4:3 Composite mean GPCP precipitation anomaly (shaded in mm/day) for droughts over southern Africa and the adjacent oceans 89
Figure 4:4 Summer (DJF) GPCP precipitation anomalies (shaded in mm/day) over southern Africa and the adjacent oceans during the seven drought seasons identified in this study. The same scale is used for comparisons. 90
Figure 4:5 (a) EOF1 (24% variance) (b) EOF2 (16% variance) and (c) EOF3 (9% variance) of summer (DJF) rainfall over southern Africa 91
Figure 4:6 Interannual variability of GPCP precipitation (mm/day) over southern Africa (averaged over 22-32E; 15-28°S): 1979-2012 92
Figure 4:7 Morlet wavelet analysis of GPCP precipitation for the southern Africa region (averaged over 22-32E; 15-28°S)..... 92
Figure 4:8 Mean annual cycle of NCEP OLR (Wm^{-2}) over southern Africa (averaged over 22-32E; 15-28°S): 1979-2012 93
Figure 4:9 Composite mean NCEP OLR anomalies (shaded in Wm^{-2}) for the seven drought seasons over southern Africa and the adjacent oceans..... 93
Figure 4:10 Interannual variability of NCEP OLR anomalies (Wm^{-2}) over southern Africa (averaged over 22-32E; 15-28°S): 1979-2012 94

Figure 4:11 Spatial patterns of long-term mean daily MODIS land surface temperature (shaded in °C) over southern Africa during summer (DJF) 95
Figure 4:12 Mean annual cycle of MODIS land surface temperature (°C) over southern Africa (averaged over 22-32E; 15-28°S) 95
Figure 4:13 Mean annual cycle of NCEP maximum air temperature (°C) over southern Africa (averaged over 22-32E; 15-28°S) 96
Figure 4:14 Composite mean NCEP maximum air temperature (shaded in °C) anomaly for drought over southern Africa 96
Figure 4:15 Long-term (1960-2012) NCEP maximum air temperature (°C) anomalies over southern Africa (averaged over 22-32E; 15-28°S) 97
Figure 4:16 Interannual variability of surface evaporation (mm/day) over southern Africa (averaged over 22-32E; 15-28°S) 97
Figure 4:17 Mean annual cycles of PET (mm/day) and MERRA SHF (Wm^{-2}) over southern Africa (averaged over 22-32E; 15-28°S) 98
Figure 4:18 Composite mean anomalies of NCEP PET (shaded in Wm^{-2}) over southern Africa during drought periods 98
Figure 5:1 Composite mean summer (DJF) NCEP sea level pressure (shaded in hPa) over southern Africa and the adjacent oceans: 1979-2012..... 116
Figure 5:2 Mean summer (DJF) NCEP surface winds (vector) and wind speed (shaded in m/s) over southern Africa and the adjacent oceans..... 116
Figure 5:3 Mean summer sea surface temperature (shaded in °C) over the southeast Atlantic Ocean and the southwest Indian Ocean showing ocean currents adjacent to southern Africa (Adapted from http://oceancurrents.rsmas.miami.edu)..... 117
Figure 5:4 Mean summer (DJF) NCEP geopotential height (shaded in m) at 500 hPa over southern Africa and the adjacent oceans 118
Figure 5:5 Mean summer (DJF) upper level (200 hPa) NCEP vector winds over and wind speed (shaded in ms^{-1}) southern Africa and the adjacent oceans. The jet stream is in shades of red 118
Figure 5:6 Composite mean (a) NCEP geopotential height (shaded in m) anomalies at 850 hPa and (b) associated low level (850-700 hPa) NCEP wind (vector) anomalies for drought periods over southern Africa and the adjacent oceans. A wind scale vector is shown. 119
Figure 5:7 Composite mean NCEP surface wind (vector) and GPCP precipitation (shaded in mm/day) anomalies over southern Africa and the adjacent oceans for drought seasons. A wind scale vector is shown. 120
Figure 5:8 Composite mean NCEP relative vorticity (shaded in s^{-1}) for 250-200 hPa (above) and for 850–700 hPa (below) over southern Africa and adjacent oceans for drought seasons (each with its own scale x 10^{-5}). 121
Figure 5:9 Composite mean NCEP divergence for 250-200hPa (above) and for 850-700 hPa (below) during drought seasons over southern Africa and adjacent oceans (each with its own scale x 10^{-5}). 121
Figure 5:10 Composite mean summer (DJF) NCEP (a) geopotential height (shaded in m) and (b) associated wind vector anomalies at 500 hPa over southern Africa and the adjacent oceans during drought seasons. A wind scale vector is shown in (b). 122
Figure 5:11 Composite summer (DJF) mean NCEP geopotential height (shaded in m) and wind vector anomalies at 500 hPa over southern Africa for each of the seven drought seasons. A wind scale vector is shown. 123
Figure 5:12 Composite mean upper level (250-200 hPa) NCEP wind (vector) anomalies over southern Africa and adjacent oceans for drought seasons. A wind scale vector is shown. 124

Figure 5:13 Composite mean vertical NCEP geopotential height (shaded in m) anomalies over southern Africa (averaged for 22-32°E; 15-28°S) during drought seasons from (a) west-east and from (b) north-south..... 125
Figure 5:14 Composite mean vertical structure of NCEP circulation over southern Africa showing meridional, zonal and vertical wind (vector) anomalies from 1000-100 hPa during drought seasons from (a) west-east and from (b) south-north. A wind scale vector is shown. 126
Figure 5:15 Composite mean NCEP relative humidity (shaded in %) anomalies over southern Africa (averaged over 22-32°E; 15-28°S,) vertically from 1000-300 hPa during drought periods from (a) west-east and from (b) south-north 127
Figure 5:16 Correlation of PC1 of GPCP precipitation anomalies with HadISST1 anomalies (1960-2008). A southern Africa rain index is used. The shaded areas are significant at 90% or more. 128
Figure 5:17 NOAA OISST sea-surface temperature (shaded in °C) anomalies over the tropical oceans during NDJ for the seven drought seasons analyzed in this study 129
Figure 5:18 Variability of SOI and P-E anomalies over southern Africa (averaged over 22-32E; 15-28S): 1979-2012 130
Figure 5:19 Correlation between NOAA CPC Southern Oscillation Index and GPCP precipitation during the austral summer over southern Africa and the adjacent oceans. The shaded areas are significant at 90% or more. 131
Figure 5:20 Correlation of summer DJF Niño3.4 index with GPCP precipitation over southern Africa and the adjacent oceans. The shaded areas are significant at 90% or more. 131
Figure 5:21 1997/98 summer (DJF) GPCP precipitation (mm/day) anomalies over southern Africa and the adjacent oceans 132
Figure 5:22 Correlation of summer (DJF) Niño 3.4 and NCEP geopotential height at 500 hPa over southern Africa and the adjacent oceans. The shaded areas are significant at 90% or more. 132
Figure 5:23 Correlation of summer (DJF) Niño 3.4 with NCEP omega at 500 hPa over southern Africa and the adjacent oceans. The shaded areas are significant at 90% or more..... 133
Figure 5:24 Correlation of summer (DJF) Niño 3.4 with 850 hPa geopotential height over southern Africa and the adjacent oceans. The shaded areas are significant at 90% or more..... 133
Figure 5:25 Variability of DMI and P-E index over southern Africa (averaged over 22-32E, 15-28S): 1979-2012 134
Figure 5:26 Variability of IOSD and P-E index over southern Africa (averaged over 22-32E, 15-28S): 1979-2012 134
Figure 5:27 (a) Composite mean NOAA OISST sea-surface temperature (°C) anomalies for all drought seasons over the southeast Atlantic Ocean and the Southwest Indian Ocean near Africa and (b) associated NCEP SLP (shaded in hPa) anomalies 135
Figure 5:28 (a) Vertical structure of NCEP circulation (wind vector) and (b) composite mean GPCP precipitation (shaded in mm/day) anomalies during the Jan-Mar 1984 drought season over southern Africa and the adjacent oceans 136
Figure 6:1 Mean annual cycles of GRACE soil moisture and the P-E index over southern Africa 149
Figure 6:2 Interannual variability of surface GRACE soil moisture (kgm^{-2}) over southern Africa (2001-12) 149

Figure 6:3 Composite mean CPC surface soil moisture (v2) anomalies during late summer to early autumn (February-April) over southern Africa for drought periods. Values are given in mm. 150
Figure 6:4 Correlation between CPC surface soil moisture (v2) and GPCP precipitation in southern Africa. The shaded grid boxes are significant at 90% or more. 151
Figure 6:5 Interannual variability of combined FAOSTAT maize yields (ton/ha) for southern Africa (1961-2012). Trend is slightly upward despite the low yields of 1983-84, 1991/92 and 151
Figure 6:6 Variability of FAOSTAT maize yields (ton/ha) for Botswana and Zimbabwe: 1960-2012 152
Figure 6:7 Detrended FAOSTAT maize yields (ton/ha) and seasonal rainfall (sigma) anomalies over southern Africa: 1980-2012 152
Figure 6:8 Combined FAOSTAT maize yields (ton/ha) anomaly for the southern Africa region 153
Figure 6:9 FAOSTAT value of agricultural productivity (for maize in US$) in southern Africa 153
Figure 6:10 Mean annual cycles of NDVI and surface soil moisture (kg of water/m^3 of soil) 154
Figure 6:11 Anomalies of late summer mean NOAA NESDIS NDVI over southern Africa: 1982-2006 154
Figure 6:12 USGS NDVI anomalies over southern Africa for the seven drought seasons analyzed in this study 155
Figure 6:13 Variability of NDVI and MODIS LST (°C) anomalies over southern Africa (averaged over 22-32E; 15-28S): 1982-2012 156
Figure 6:14 NASA Giovanni mean surface runoff over southern Africa ($10^{-6}kgm^{-2}s^{-1}$) 157
Figure 6:15 Interannual variability of NASA Giovanni surface runoff ($kgm^{-2}s^{-1}$) over southern Africa (averaged over 22-32E; 15-28S) 157
Figure 6:16 Drainage basins of the Zambezi and Limpopo Rivers with weirs shown upstream. Lake Kariba is also shown along the Zambezi between Zambia and Zimbabwe. 158
Figure 6:17 Mean annual cycle of Zambezi River flows (m^3s^{-1}) at Victoria Falls 159
Figure 6:18 Mean annual cycle of flow volumes (mill cub met) of the upper Limpopo River at Botswana (A5H006) 159
Figure 6:19 Interannual variability of ZRA Zambezi River peak flow (m^3s^{-1}) at Victoria Falls 160
Figure 6:20 Interannual variability of late summer flows (mill cub met) of the upper Limpopo River at Botswana 160
Figure 6:21 Annual minimum flows (m^3s^{-1}) of the Zambezi River at Victoria Falls (1948-2010) 161
Figure 6:22 Mean annual cycle of reservoir levels (m) at Lake Kariba along the Zambezi River 161
Figure 6:23 Variability of Lake levels (m) at Kariba: 1960-2012 (source: Zambezi River Authority) 162
Figure 6:24 Anomalies of reservoir levels (m) for Lake Kariba: 1963-2012 (data source: Zambezi River Authority) 162
Figure 6:25 May-July averaged Kariba Reservoir Index correlated with DJF precipitation. The shaded grids are at 90% significance or more. 163

Figure 6:26 Nov-Jan averaged Nino 3.4 correlated with Kariba Reservoir Index lagged (90% significance) 163

LIST OF TABLES

Table 3-1 Summary of the variables, parameters and fields obtained and analyzed in this thesis 70
Table 3-2 Ranked drought events identified by a P-E anomaly index over southern Africa 70
Table 4-1 Ranked Tmax (°C) for February from 1979-2012. The definitive selection of drought seasons identified in Table 3.2 with the most negative P-E anomalies are shown with an asterisk. 86
Table 4-2 Eigenvalues, percentages of variance explained (%) by EOF1 to EOF4, and accumulated variance (%) 86
Table 5-1 ENSO events during 1979-2012 based on the SOI 115
Table 6-1 Ranked NDVI anomalies over southern Africa (averaged over 22-32E; 15-28S). The definitive selection of drought seasons identified in Table 3.2 with the most negative P-E anomalies shown with an asterisk. 148

LIST OF ACRONYMS

AAO	Antarctic Oscillation
ARC	Agriculture Research Council (South Africa)
CAPE	Convective Available Potential Energy
CMAP	Climate Prediction Center Merged Analysis of Precipitation
CMIP	Coupled Model Intercomparison Project
CPC	Climate Prediction Center
CRU	Climate Research Unit
CSIRO	Commonwealth Scientific and Industrial Research Organization
DJF	December January February
ECMWF	European Center for Medium-Range Weather Forecasts
ENSO	El Niño Southern Oscillation
EOF	Empirical Orthogonal Function
ET	Evapotranspiration
FAOSTAT	Food and Agriculture Organization (United Nations): Statistics Division
FEWS NET	Famine Early Warning Systems Network
GCM	General Circulation Model
GPCC	Global Precipitation Climatology Center
GPCP	Global Precipitation Climatology Project
GRACE	Gravity Recovery And Climate Experiment
IOD	Indian Ocean Dipole
IOSD	Indian Ocean Subtropical Dipole
IPCC	Intergovernmental Panel on Climate Change
IRI	International Research Institute for Climate and Society
ITCZ	Inter-Tropical Convergence Zone
JFM	January February March
JJA	June July August
KNMI	Royal Netherlands Meteorological Institute
LHF	Latent Heat Flux
LST	Land Surface Temperature
MCC	Mesoscale Convective Complex
MERRA	Modern Era Retrospective-Analysis for Research and

	Applications
MODIS	Moderate Resolution Imaging Spectroradiometer
MSL	Mean Sea Level
MSLP	Mean Sea Level Pressure
NASA	National Aeronautics and Space Administration
NCAR	National Center for Atmospheric Research
NCEP	National Centers for Environmental Prediction
NDJ	November December January
NDVI	Normalized Difference Vegetation Index
NOAA	National Oceanic and Atmospheric Administration
NWP	Numerical Weather Prediction
OND	October November December
OLR	Outgoing Longwave Radiation
PC	Principal Component
PCA	Principal Components Analysis
PDSI	Palmer Drought Severity Index
PET	Potential Evapotranspiration
QBO	Quasi Biennial Oscillation
RH	Relative Humidity
scPDSI	self-calibrating Palmer Drought Severity Index
SHF	Sensible Heat Flux
SLP	Sea Level Pressure
SOI	Southern Oscillation Index
SST	Sea Surface Temperature
SPEI	Standardized Precipitation - Evapotranspiration Index
SPI	Standardized Precipitation Index
Tmax	Maximum Temperature
USGS	United States Geological Survey
VIs	Vegetation Indices
WASP	Weighted Anomaly Standardized Precipitation
WMO	World Meteorological Organization
ZRA	Zambezi River Authority

Chapter 1

INTRODUCTION

Subtropical southern Africa has a warm dry climate influenced by complex regional topography, disparate ocean currents (Lindesay 1998) and its position between a tropical monsoon and mid-latitude frontal weather. The region lies atop the African plateau above 1000 m in altitude (Mugara 1997; Lindesay 1998) only falling below 600 m in a few river valleys (Figure 1.1). The high topography falls steeply through a sharp escarpment to the narrow coasts particularly in the south and southeast. This complex topography regulates the flow of river basins, and creates meso-climate regimes within a large seasonal cycle (Hart *et al.* 2012).

1.1 Hydrology

The Zambezi River basin has the largest catchment area in southern Africa and is the fourth largest river system in Africa after the Nile, Congo and Niger. The river rises in highland Zambia in the northwest and flows through Angola, Namibia, Botswana, Zimbabwe and northern Mozambique before emptying into the Indian Ocean. The Zambezi drainage basin covers eight countries including Malawi and Tanzania. The Okavango, Limpopo and Vaal-Orange River systems are dominant south of the Zambezi catchment. Apart from the Vaal-Orange system, most of the river systems of southern Africa flow eastwards into the Indian Ocean. A number of dams are impounded on major river systems to supply water for domestic and industrial use and for irrigated agriculture.

Southern Africa experiences water deficits due to seasonal rainfall and constantly high evaporation. Greater demand for surface and underground water resources is expected with about 2% population growth by 2030 (African Development Bank 2012). Whilst most of southern Africa (south of the Zambezi valley) is already water stressed, it is expected that by 2025 South Africa might be experiencing absolute water scarcity (United Nations Economic Commission for Africa 1999). An increase in the occurrence of meteorological

droughts would aggravate the situation and possibly result in severe socio-economic consequences on countries and communities of southern Africa.

1.2 Vegetation

The natural vegetation of southern Africa is characterized by grasslands, savannas, fynbos, Karoo and desert biomes. In the west are the Nama-Karoo and desert biomes where the soil is nearly bare and characterized by scattered vegetation cover. Woodlands and forests occur in the east, and contain great diversity as documented by Rutherford and Westfall (1986). A large area of southern Africa is covered by grassland savannas and deciduous forests (Jury *et al.* 1997a; Rutherford 2004; Figure 1.2)

It is long established in plant ecology that the distribution of vegetation cover is strongly related to the mean climate (Rutherford 2004). Vegetation growth and senescence have been linked to soil moisture availability (Chikoore 2005) which is a function of the rainfall regime. The east of southern Africa may be defined as sub-humid supporting forests and woodlands.

The health of vegetation, particularly grasslands, also affects livestock production and wildlife survival. During severe droughts such as 1992, the livestock population was decimated as the grasslands and drinking holes had dried up (Vogel 1994).

1.3 Agricultural systems

The regional agriculture is dominated by maize production, mixed pastoral systems with small grains (sorghum/millet) and pastoralism for the semi-arid areas where rainfall is unreliable. The maize crop is most important as it forms the staple food for most of the population (Moeletsi 2010; Moeletsi *et al.* 2011). Significantly, the majority of rural populations of southern Africa are communal or smallholder farmers and their livelihoods depend mostly on rain-fed agriculture or livestock production.

The agricultural systems of southern Africa are predominantly rain-fed (Mason and Jury 1997) especially in the semi-arid regions of Africa where irrigation systems are not well

developed (Camberlin *et al.* 2009). Rain-fed crop production is particularly sensitive to prolonged mid-season dry spells, especially in the marginally watered central Kalahari zone (on 20°E).

Except for industrialized and diversified South Africa, most economies of southern Africa and rural livelihoods rely heavily on rain-fed agriculture and are affected by large shifts in rainfall. Severe crop damage, decreased livestock, widespread food and water shortages, and sometimes loss of lives have resulted from recurrent droughts over the region. Hence drought events over southern Africa often turn from natural hazards into natural disasters (Manatsa *et al.* 2007).

1.4 Mean climate

The climate of southern Africa is largely semi-arid and highly variable from intraseasonal to inter-annual and longer time scales (Walker 1990; Levey and Jury 1996; Mason and Jury 1997; Lindesay 1998: Landman and Mason 1999; Reason and Mulenga 1999; Tennant and Hewitson 2002; Cook *et al.* 2004). Spatial gradients of climate parameters, land surface characteristics (including vegetation and soil moisture) and ocean temperatures regulate the regional climate. The west of the subcontinent is arid, dominated by the Namib Desert which is one of the driest regions on earth. The aridity of the west is largely due to a combination of the influence of the cold eastern boundary Benguela Ocean Current and subtropical subsidence restricting convection and cloud development (Muller *et al.* 2008).

An important oceanographic feature of the west coastline of southern Africa is the Benguela upwelling system (Andrews and Hutchings 1980) which extends from the Cape Point to the border between Namibia and Angola (Fennel 1999; Nelson and Hutchings 1983). Upwelling is at a maximum around 25°S decreasing to the north and south (Fennel 1999). From time to time, warm anomalies in the Benguela upwelling system have been observed and termed Benguela Niños which result in higher than normal rainfall along the Namibia/Angola coastal areas (Hansingo and Reason 2009).

The presence of the warm western boundary Agulhas Current flowing polewards in the southwest Indian Ocean results in enhanced convection, frequent cloudiness and high rainfall over the eastern seaboard. A strong correlation (R=+0.88, 99% confidence) has been found between local SSTs and coastal rainfall (Jury *et al* 1993a). The influence of the Agulhas Current on rainfall may be a result of increased surface latent heat flux and enhanced cyclonic activity in the greater Agulhas region (Reason 2001b).

Gradients of rainfall over the subcontinent are discernible in the mean pattern from annual rainfall less than 20 mm over the Namib Desert to more than 1000 mm over the east coast (Richard and Poccard 1998). Rainfall generally increases equatorward maximizing in the deep tropics with annual rainfalls exceeding 2000 mm in some highland areas of Malawi (Malawi Meteorological Services 2011).

Temporally, the rainfall over much of southern Africa is strongly seasonal (Torrance 1972; Hsu and Wallace 1976; Vigaud *et al.* 2009), dominated by the north-south seasonal migration of the tropical rain belts (Christensen *et al.* 2007), primarily the Inter-Tropical Convergence Zone (ITCZ). Wet summers characterize much of the regional climate with more than 80% of annual rainfall received from October to March (Lindesay 1998, Richard *et al.* 2000). The rest of the year is predominantly dry with little or no rainfall. April-May and September-October may be considered as transition periods (Mugara 1997). Hence the meteorological year over the subcontinent commences in July of one year ending in June of the following year.

Sometimes early rains fall during October and on occasion the season may extend well into April. Typically, the rainfall season is composed of an alternating sequence of wet and dry spells (Makarau 1995). The onset, duration and cessation of the rainy season can vary significantly from year to year.

A region on the southwest margins of the subcontinent including the Western and Northern Cape Provinces (South Africa) and parts of southern Namibia is characterized by a Mediterranean type distribution of rainfall, peaking in winter. Winter rainfall in this

region is largely produced by cold fronts (which migrate equatorward during the austral winter) and mid-tropospheric cut-off lows. Sometimes ridging Atlantic Ocean anticyclones bring cold and moist air resulting in coastal rain. Rainfall occurs nearly all year round along the Cape south coast of South Africa with nearly half (~46%) of the rainfall produced by ridging highs (Engelbrecht *et al.* 2015).

Peak summer rainfall occurs during December-February (DJF) and is associated with deep convection in the ITCZ (Jury and Mwafulirwa 2002; Todd *et al.* 2004; Jury 2012). The ITCZ is a zone of convergence of trade winds in the equatorial trough associated with deep cumulonimbus convection, thunderstorms and high rainfall. It is the dominant rainfall producing system over the subcontinent. Rainfall over southern Africa maximizes zonally along about 15°S extending from Angola, through Zambia to northern Mozambique and across the Mozambique Channel to northern Madagascar, coinciding with the mean position of the ITCZ (Trzaska 2010). Over the mainland, this area of maximum rainfall corresponds to the drainage basin of the Zambezi River.

Despite a unimodal distribution of rainfall, it is often considered that the summer rainfall season over southern Africa has two distinct periods: the early summer from October to December (OND) and the late summer from January to March (JFM). The early summer is dominated by extra-tropical influences whilst the tropical circulation is the main feature of the late summer (D'Abreton and Lindesay 1993). During some seasons, an intervening dry period occurs from early to mid-January separating the early summer influenced by baroclinic westerly wave disturbances from the barotropic easterly wave perturbations of the late summer (Makarau and Jury 1997).

South of the Zambezi valley, Tropical-Temperate Troughs (TTTs) and associated cloud bands are major rainfall producing systems (Harrison 1984; Todd and Washington 1999; Usman and Reason 2004; Fauchereau *et al.* 2009). TTTs link meso-scale convection in the deep tropics to synoptic scale mid-latitude westerly waves (Hart *et* al 2013) and therefore act to transfer tropical moisture and energy to the mid-latitudes. Planetary scale Rossby waves, convection from the land surface (Hart *et al.* 2010) and enhanced low-

level humidity and latent heat (Macron *et al.* 2014) are important for the development of TTTs. They contribute 30-50% of annual rainfall over South Africa (Hart *et al.* 2013). During seasons of average or above average rainfall, these bands of cloud and rainfall extend from a tropical heat low over southeast Angola (Angola Low) to a westerly wave southeast of South Africa (Muller *et al.* 2008; Mulenga 1998). More TTT events develop during La Niña seasons than during El Niño (Ratna *et al.* 2013). Being an important source of rainfall in the subtropics, the establishment and frequency of cloud bands determine the quality of a given season.

During drier or drought seasons, cloud bands shift eastwards and rainfall is thus displaced to the warm ocean east of Madagascar (Jury 1992; Lindesay 1998; Cook 2000; Reason *et al.* 2000; Chikoore and Jury 2010). The Angola Low plays a critical role in drawing moisture from the tropical Atlantic Ocean (Macron *et al.* 2014) but it tends to weaken during dry (or drought) years and El Niño years. However, during the strong 1997/98 El Niño, the Angola Low and cloud bands were strengthened resulting in a wetter than expected rainy season (Reason and Jagadheesha 2005). Mechanisms that influence the location and intensity of the Angola Low and westerly wave determine the establishment of cloud bands and hence rainfall over southern Africa (Mulenga *et al.* 2003).

Tropical cyclones of the southwest Indian Ocean basin are an important feature of the mid-late summer climate of southeast Africa. Southeast Africa is the only region on the African continent directly affected by tropical cyclones (Chikoore *et al.* 2015). On average, about 9 tropical cyclones form over the SW Indian Ocean every season (Buckle 1996; Tyson and Preston-Whyte 2000) usually within the ITCZ or some existing Mesoscale Convective Complex (MCC). Some tropical cyclones form over the warm Mozambique Channel under the influence of warm ocean eddies which may also influence their propagation characteristics. However, only about 5% of tropical cyclones make landfall over the east coast of southern Africa (Lindesay 1998; Reason and Kiebel 2004), recurving southwards before reaching land (Vitart *et al.* 2003). Even fewer cyclones penetrate inland due to the high and dry plateau and weak steering flow (Reason and Kiebel 2004; Mudenda and Mumba 2004).

Madagascar and Mozambique are vulnerable to tropical cyclone landfall whilst neighboring countries such as Zimbabwe, South Africa and Swaziland are also at risk when a landfall occurs. Coastal storm surges, strong damaging winds, excessive rainfall and flooding often accompany tropical cyclone landfalls. Tropical cyclones are therefore an important source of rainfall variability over southeast Africa at seasonal and inter-annual time scales.

Another weather system that produces floods over subtropical southern Africa is the cut-off low which is a mid-tropospheric low pressure system that has been "cut-off" from the basic westerly flow. Even though cut-off lows may occur throughout the year, they are most common during March to May and with a secondary peak during September to November (Singleton and Reason 2007). An average of 11 cut-off lows occur every year and are characterized by deep moist convection which results in heavy rainfall. They are persistent weather systems due to the presence of a blocking anticyclone over the Indian Ocean (Tyson and Preston-Whyte 2000). They are often accompanied by bitter cold weather and account for most of the snowfalls over South Africa.

Apart from infrequent flood events, prolonged droughts are a recurrent feature of the summer climate of southern Africa (Lindesay 1998; Rouault and Richard 2005; Manatsa *et al.* 2007) and bring serious threat to vulnerable communities of the region. Droughts have shown an increasing trend in recent decades (Rouault and Richard 2005) with prolonged periods of widespread drought affecting southern Africa throughout much of the 1960s, 1980s and 1990s (Jury and Levey 1993; Lindesay 1998). The most extensive drought on record over the region occurred during the 1982-84 season (Sheffield *et al.* 2008) whilst the most severe drought occurred in 1992.

This thesis seeks a detailed understanding of the processes that inhibit rainfall and produce meteorological drought over southern Africa, establishing the character of drought within a regional context. An understanding of the development and spread of recent droughts might indicate their evolution in future and improve our understanding of

the dynamic processes in the climate system of the region. An evaluation of the impact of drought on surface water resources and food production systems is essential for the formulation of appropriate mitigation and adaptation strategies for the future.

1.5 Background and motivation

Droughts occur with high frequency and severity over southern Africa (Manatsa *et al.* 2007) and have resulted in loss of lives and economic damage (Lyon 2009). It is widely held that climate change has altered the character of drought over the subcontinent with the most devastating drought events occurring in the past 35 years. Our weak understanding of drought is compounded by its evolving character due to climate change and environmental degradation.

The occurrence of extreme drought may increase in future (e.g. Sheffield *et al.* 2012) with drying projected over subtropical Africa, especially during the dry season (IPCC 2013). The southwest Cape winter rainfall region may experience the greatest impact due to expansion of subtropical highs and the associated retreat of cold fronts. Substantial drying is projected over South Africa during the spring, suggesting a delayed onset of the rainy season (IPCC 2013). Whilst the number of rainy days may decrease, the intensity of rains may increase implying heavy rainfall of short duration. Hence even longer dry spells and more frequent droughts are likely in future (Hoerling *et al.* 2006).

The annual cycle, intra-seasonal oscillations and behavior of rain bearing systems over southern Africa are fairly well understood but there are limited studies on drought characteristics (e.g. Richard *et al.* 2001). Meteorological research on droughts has focused mainly on localized domains (e.g. Matarira 1990; Jury and Levey 1993; Jury and Mwafulirwa 2002; Dube and Jury 2003; Mulenga *et al.* 2003; Kabanda 2005; Manatsa *et al.* 2008; Hoffman *et al.* 2009). Some research has evaluated drought policy and management (e.g. Msangi 2004; Dube 2008; Stringer *et al*. 2009) while others have investigated adaptation strategies for coping with drought (Gandure 2005; O'Farrell *et al.* 2009).

Several previous studies have focused on the oceans, particularly the El Niño Southern Oscillation (ENSO) phenomenon as the primary cause of drought events over southern Africa (e.g. Ropelewski and Halpert, 1987; Jury *et al.* 1994; Rocha and Simmonds 1997; Vogel 2000; Anyamba *et al.* 2002). It is long established that the ENSO phenomenon accounts for only 30% of variance of seasonal rainfall over the subcontinent (Tyson and Preston-Whyte 2000; Unganai and Mason 2002). Thus, the causes or modulation of other non-ENSO induced droughts require further investigation. Fewer studies have considered the relative contribution of changes in precipitation versus changes in evapotranspiration in understanding drought (e.g. Cook *et al.* 2014).

Not much research has been done on land-surface atmosphere couplings in modulating drought over the subcontinent. An assessment of the role of soil moisture, vegetation and land surface temperature is critical in such a process. This research employs land surface temperature datasets which have become available only recently (e.g. Moderate Resolution Imaging Spectroradiometer 8 km land surface temperature). High land surface temperature characterizes the Namib, Kalahari and the Karoo in South Africa resulting in enhanced evaporation during summer.

New and improved reanalysis datasets have also become available in recent years such as the Climate Forecast System Reanalysis (CFS-R) generated by the National Centers for Environmental Prediction – National Center for Atmospheric Research (NCEP-NCAR) and the ERA-Interim Reanalysis from the European Center for Medium-Range Weather Forecasts (ECMWF). These datasets allow for higher resolution analyses of climate and land surface parameters than was previously possible. New technologies, methods and improved interactive climate models for different kinds of analyses have become widely available and accessible to the climate research community (e.g. Royal Netherlands Meteorological Institute Climate Explorer; National Aeronautics and Space Administration Giovanni).

With recurrent droughts affecting the region, analyses of different aspects of drought are critical. A comprehensive understanding of drought processes should enhance the resilience of communities of southern Africa to plan and respond to drought in future.

1.6 Thesis aim, objectives and research questions

1.6.1 Aim

The aim of this thesis is to map, quantify and analyze the nature and impacts of meteorological drought events over southern Africa using satellite observations and reanalysis models during the period from 1979-2012.

1.6.2 Objectives

Specifically, the objectives of this thesis are to:-

a) Define a drought index for southern Africa and identify drought events during 1979-2012 using a precipitation minus evapotranspiration (P-E) anomaly index;
b) Investigate the meteorological causes and structure of drought over the subcontinent;
c) Determine the remote influence of El Niño, the South Atlantic and Indian Oceans on the atmospheric circulation and drought severity;
d) Map and quantify the spatial extent and impact of drought on crop yields, vegetation and surface streamflow.

1.6.3 Research questions

a) What are the dominant modes of drought spatial and temporal variability in southern Africa?
b) Which large-scale atmospheric circulation and thermodynamic anomalies inhibit rain and are precursors to meteorological drought in southern Africa?
c) How do ENSO and phenomena in the Atlantic and Indian Oceans affect Tropical-Temperate-Troughs and rainfall over southern Africa?
d) To what extent are climate signals related to soil moisture, crop yields and streamflow during drought?

1.8 Selection of study area

Interannual rainfall variability over southern Africa maximizes in an area covering Zimbabwe, southern Zambia, northern South Africa and eastern Botswana and the effects of ENSO events are important here (e.g. Reason and Rouault 2002). The deep tropics are excluded from the analysis, and the extreme west of the subcontinent may be considered arid (Karoo and Namib) such that the concept of drought is not meaningful there (Palmer 1965). The narrow coastal belt is excluded because of adiabatic warming under berg wind conditions (Foehn or Chinook type of wind) whilst Mozambique is left out due to its low altitude and humid conditions.

This thesis deals with southern Africa (south of 10°S) and the adjacent South Atlantic and Southwest Indian Oceans. Much of the analyses focus on an area on the plateau bounded by latitudes 15-28°S and longitudes 22-32°E. This region covers Botswana, northern South Africa, southern Zambia and Zimbabwe, and includes three major river basins of the subcontinent – Zambezi River, Limpopo River, Vaal River and the Orange River. It is a region of agricultural importance as the bulk of the staple crop (maize) are grown here (Figure 1.3). It is therefore appropriate to focus on this area for a study of southern Africa drought. The remote influence of the tropical Pacific Ocean is also investigated.

The Zambezi focus is on hydrology and run-off, whilst the Vaal-Orange focus is on vegetation cover and crop yield. It is hypothesized here that many droughts spread from the Limpopo basin (which is water-deficit).

1.9 Thesis structure

This thesis consists of 7 chapters.

Chapter 1 introduced the background to this thesis, including an overview of the geography, hydrology and vegetation of southern Africa. The chapter outlined the aspects to be dealt with in the thesis through sections on background and motivation, research

aims and objectives and research questions. The selection of study area was also justified.

Chapter 2 provides an extensive review of the literature on the causes, structure and impacts of drought from a global perspective. The role of the oceans is critically analyzed in this review. Research on drought over southern Africa and trends in global drought including climate change influences are also reviewed in this chapter.

In Chapter 3, the datasets employed in this research are described in detail, alongside the methods and approaches used to analyze them. The datasets from various global and regional centers are classified as atmospheric, terrestrial and ocean. A drought index based on an anomaly of the surface water balance (P-E anomaly) is defined and justified, and used to identify drought events in this study.

The mean state of rainfall and its trends, variability and vulnerability to drought are detailed in Chapter 4. Evapotranspiration and potential evapotranspiration which are key variables of the surface water balance are investigated here and related to surface heat fluxes. High potential evaporation is related to high land surface and maximum air temperatures which are then analyzed with a focus on summer drought over southern Africa.

Chapter 5 presents the causes and meteorological structure of drought over southern Africa. Composite circulation and moisture anomalies during drought are analyzed for the drought events identified in Chapter 3. This chapter also details the meteorological structure of the Botswana High which is a key transmitter of the drought signal. Prolonged historical dry spells are used as case studies. The global remote mechanisms of drought such as ENSO and the adjacent oceans are investigated and related to spatial modes of rainfall variability.

The impacts of drought on surface soil moisture, crop yields and agricultural productivity over the subcontinent are dealt with in Chapter 6. Normalized Difference Vegetation Index

(NDVI) anomaly images are employed to show the aerial extent and intensity of drought impacts. Long-term impacts of meteorological drought on streamflow and lake levels are also analyzed.

All chapters conclude with a short summary highlighting important findings, but a synthesis of key findings and conclusions of this PhD thesis are presented in the final chapter. The implications of the findings of this thesis are discussed in a wider context, whilst additional research questions arising from this study are recommended for future studies. Some solutions to drought management are proffered at the end.

Chapter Figures

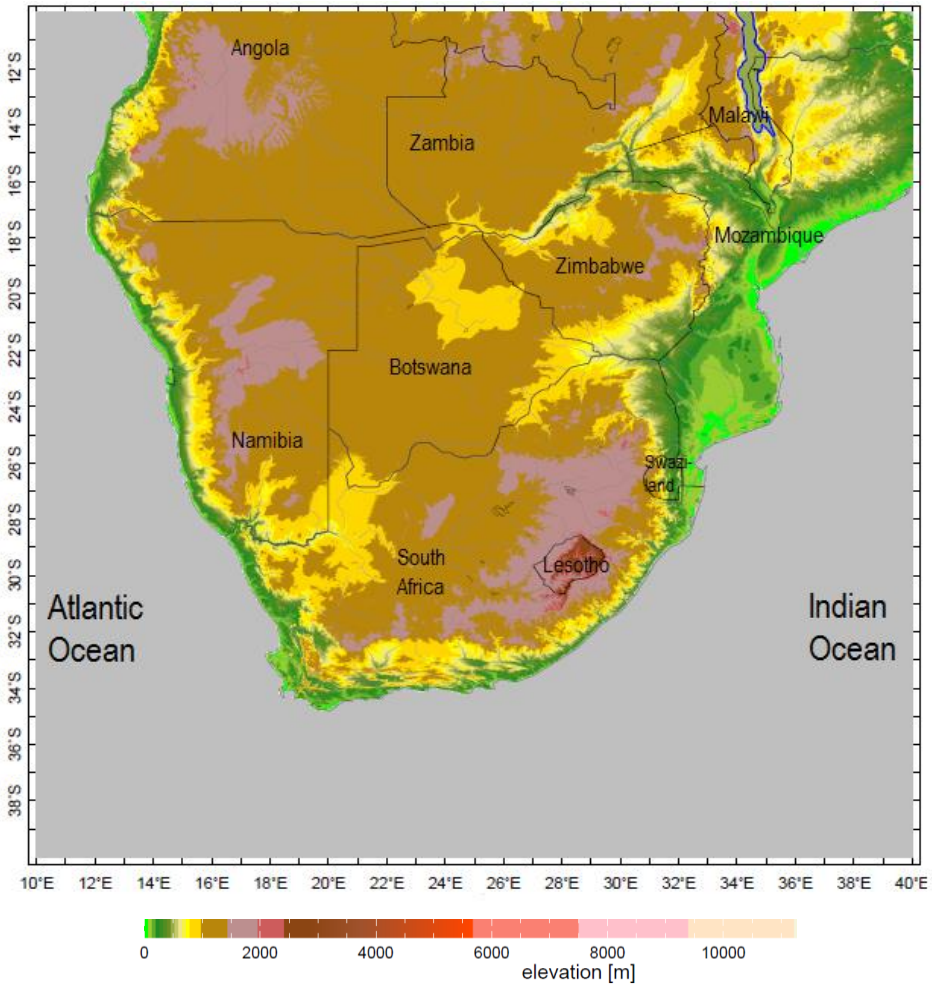

Figure 1:1 The southern African study area and the countries involved, with the elevation (meters Above Mean Sea Level (AMSL) indicated in shading colours

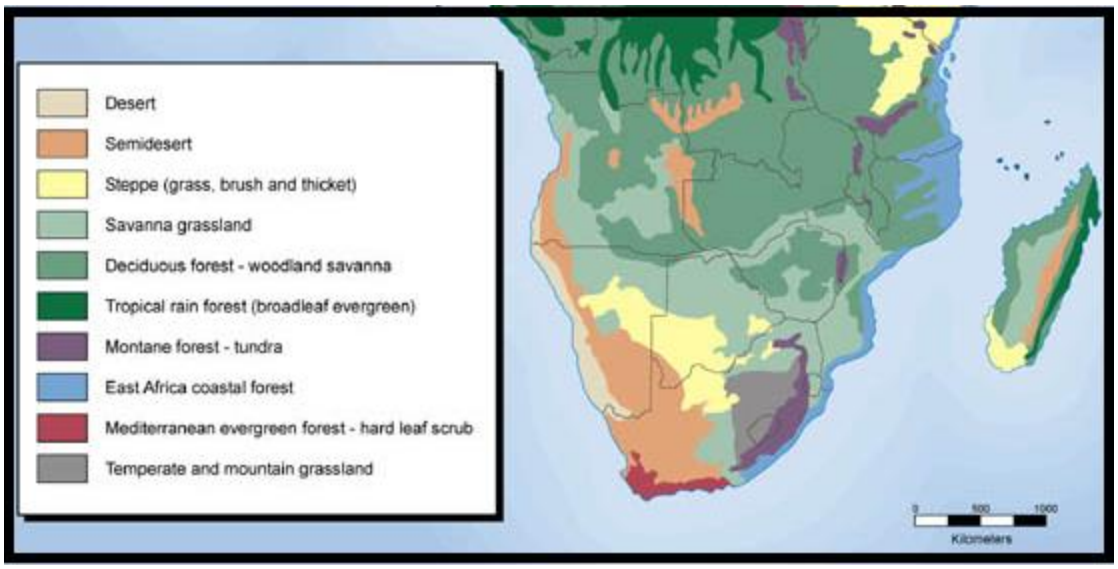

Figure 1:2 The vegetation biomes of southern Africa (adapted from http://exploringafrica.matrix.msu.edu/map-three/)

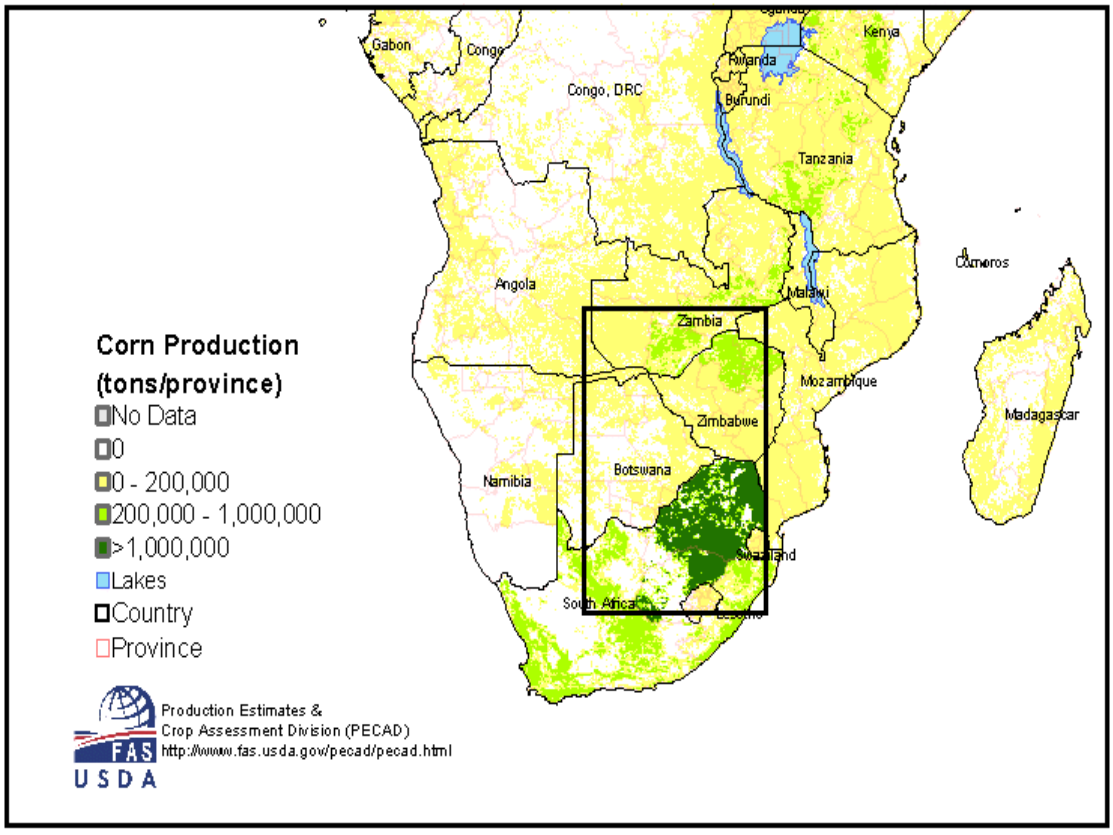

Figure 1:3 Corn/maize production (ton/province) in southern Africa shown in shading. The inset shows the main focus of this study which is an important region for agriculture (adapted from http://fas.usda.gov/pecad/pecad.html)

Chapter 2

A LITERATURE REVIEW

2.1 Introduction

Droughts are a recurring and inevitable global phenomenon with varying spatial and temporal characteristics from region to region, often threatening food systems and water resources management in several regions of the world. The first humans to migrate out of Africa around 70 000 years ago (toward Israel) were affected by severe drought (http://news.bbc.co.uk/2/hi/science/nature/4505516.stm). Droughts are also cited in biblical times (e.g. Deuteronomy 8:15; Jeremiah 2:6), and have thus been a subject of enquiry for longer than many aspects of the climate system.

Byun and Wilhite (1999) have summarized and classified studies of drought into four main categories. Some studies deal with meteorological causes of drought; while others examine the frequency and intensity of drought to determine the probability of recurrence. A third category of drought studies deals with costs and impacts of drought whilst the fourth group analyzes drought responses including mitigation and preparedness, and coping with drought. Most studies that have analyzed drought frequency and severity have also analyzed drought impacts (Byun and Wilhite 1999). This study covers the first three categories of drought studies.

The aim of this chapter is to present a comprehensive review of literature on the drought phenomenon from a global perspective and from a southern Africa perspective. It is important to discuss droughts in their climatological context as drought characteristics vary with region (Stahl and Hisdal 2004). The review is divided into the categories proposed by Byun and Wilhite (1999). Classification methods, definitions and drought indices are reviewed at first whilst knowledge on southern Africa drought and global trends are considered at the end.

2.2 Drought classification

Droughts may be classified as meteorological, hydrological or agricultural (Byun and Wilhite 1999; Hayes *et al*. 2012; WMO 2012) although they are all primarily caused by a sustained deficiency of precipitation. Thus, meteorological drought leads to other types of drought (Dai 2011b). In terms of timescales, short-term dryness reflects meteorological drought which impacts on soil moisture (agricultural drought) in the medium term and on stream flow and ground water (hydrological drought) at longer timescales (Hayes *et al.* 2012; WMO 2012) of 6 months to years, or longer (Rouault and Richard 2005). The propagation of drought across sectors is illustrated in Figure 2.1.

A meteorological drought results from a negative deviation from long-term mean rainfall usually over monthly or seasonal timescales. However, the arithmetic long-term mean rainfall depends on the time span used in the analysis of drought (Dube 2008). Meteorological drought may also result from consecutive dry days or from consecutive days with little precipitation (Bryun and Wilhite 1999). The definitions of 'consecutive days' and 'little precipitation' are not always straight forward. However, it is agreed a meteorological drought is established following the persistence of anticyclonic circulation unfavorable for cloud development.

An agricultural drought is often regarded as a soil moisture drought (Tallaksen and van Lanen 2004) and considered as probably the most significant (Palmer 1965). A soil moisture drought occurs when soil moisture levels are insufficient to support crop production (Tallaksen and van Lanen 2004). It reflects agricultural drought through controls on evapotranspiration and vegetation health (Sheffield and Wood 2008). The amount of soil water available becomes insufficient to support crop transpiration and evaporation (Murthy *et al*. 2009). An agricultural drought also occurs when there are insufficient water requirements for livestock grazing. The effects of a meteorological drought on agriculture and hydrology can be immediate or delayed (Palmer 1965) depending on prior water storage. An agricultural drought may occur in the absence of a hydrological drought but usually the agriculture sector is the first sector of the economy to be impacted by drought.

A hydrological drought results from reduced runoff and a shortage of streamflow and groundwater (Tallaksen and van Lanen 2004) and may result in dry river beds (Shaw 1994; Hisdal et al. 2004). Streamflow is also influenced by factors other than rainfall. For example, vegetation cover reduces streamflow and promotes infiltration and human influences such as diversions and abstractions of surface water and irrigation can influence the quantity of streamflow (Tallaksen and van Lanen 2004). Even so, a hydrological drought may persist long after the cessation of a meteorological drought (Heim 2002).

Other types of droughts include groundwater drought, surface water drought, and a socio-economic drought. A man-made drought has also been identified, caused by increased demand for water due to economic development, population growth and urbanization (Palmer 1965) and is referred to as a human-induced hydrological drought (Tallaksen and van Lanen 2004). The persistence of moisture deficits and negative impacts on society and natural resources are central to defining drought.

Aridity is sometimes confused for drought. Aridity is a permanent state of dryness whereas drought refers to a period of temporary dryness (Dai 2011b). Most arid climates are found in subtropical regions under the influence of the descending limb of the Hadley Cell. They are also affected by subtropical anticyclones and nearby cold ocean upwelling zones. Thus, the majority of the world's deserts lie on the western side of continents between 15-30°N and S of the equator (Kusky 2009). Sometimes arid zones are classified into hyper-arid, arid and semi-arid. Potential evapotranspiration can exceed precipitation by up to two orders of magnitude in these regions and the concept of drought is meaningless there.

There is no universal definition of drought as several definitions exist in the literature (Wilhite and Glantz 1985: Wilhite *et al.* 2007; WMO 2012). Wilhite and Glantz (1985) found more than 150 definitions of drought and this thesis also adds a new way of defining drought in southern Africa. Drought monitoring and analysis have been affected by the

absence of an adequate definition of drought due to its complexity and widespread impacts (Heim 2002). Drought definition may differ between different climatic regimes, location and application. The presence of drought may depend on its definition, so it is important to study drought within its climatological context. While there may be many definitions of drought, the preferred definition in this thesis is based on an anomaly of the surface water balance.

Tallaksen and van Lanen (2004) define drought as persistent and widespread below normal availability of water and therefore deviation from average of variables such as rainfall, soil moisture and streamflow. The development and persistence of drought is often defined by precipitation deficits (Lloyd-Hughes and Saunders 2002) over an extensive area over long periods (Tallaksen and van Lanen 2004).

It is also noted that different methods of analyzing drought may lead to different results. For example an analysis of mean annual rainfall or mean discharge may not depict drought, whereas an analysis of intra-seasonal rainfall may show midseason drought. This occurs often in regions affected by extreme rainfall events such as tropical cyclones which can drop unseasonal amounts of rainfall in just a few days resulting in very high seasonal totals for seasons which were otherwise dry. For example, tropical cyclone Domoina dumped more than 800 mm of rainfall over South Africa's east coast in a few days in January 1984 (Jury *et al.* 1993b) amidst a drought event. It is argued that mixed interpretations of drought hinder the study of drought (Tallaksen and van Lanen 2004).

2.3 Drought monitoring using drought indices

Significant advances in real time monitoring of drought have occurred over the past five decades, allowing for early warning (Hayes *et al.* 2012) and natural disaster reduction. Droughts generally affect large areas and are therefore difficult to monitor effectively using ground based observations (Kogan 1997). Since the 1980s, satellite remote sensing products have become increasingly available to compliment ground-based climate and hydrologic observations for crop and drought monitoring (Anyamba and

Tucker 2012; Hayes *et al.* 2012). These include remote sensed products of rainfall and vegetation condition.

Remote sensing techniques have evolved from just estimates of rainfall and vegetation condition to more environmental parameters such as evapotranspiration and surface soil moisture enabling a more complete analysis of the drought situation (Hayes *et al.* 2012). Remote sensing products enable earlier detection of drought compared to traditional in-situ indicators (Hayes *et al.* 2012).

Numerous drought indices have been developed and applied to monitor and quantify drought (Heim 2000; Keyantash and Dracup 2002; Tsakiris and Vangelis 2005; Dai 2011b; WMO 2012). A drought index is used to determine the deficiency of precipitation or water below a certain threshold which is usually a long-term mean. Some drought indices are derived from ground based observations whilst others are satellite derived. There are drought indices that are based on precipitation deficits only and also those that consider soil moisture and other variables such as evaporation and temperature. Some of the most widely used drought indices are detailed here and in section 3.3.1.

2.3.1 Palmer Drought Severity Index

The Palmer Drought Severity Index (PDSI) was among the first drought indices developed to determine drought severity in the United States (Wells *et al.* 2004; Hayes *et al.* 2012) in the 1960s. The PDSI is derived from a water balance model incorporating precipitation, temperature, potential evaporation and soil moisture content (Mika *et al*. 2004). The PDSI is relatively complex to evaluate (Glad 2010) and varies between -10 and +10 (Dai 2011a; Hayes 2011) where strong positive values represent extremely wet conditions and strong negative values indicate extreme drought. It is applicable to agricultural and water resources management.

Several limitations to the use of the PDSI in drought monitoring were identified (Alley 1984; Hayes *et al.* 1999, Heim 2002) including inconsistency across different climatological regions (Wells *et al.* 2004). The PDSI was designed specifically for the

semi-arid and dry sub-humid regions of the United States and may not produce realistic results for other regions (Palmer 1965). In response, a self-calibrating Palmer Drought Severity Index (scPDSI) was developed from the PDSI to make it more spatially comparable (Wells *et al.* 2004). The Precipitation < Potential Evapotranspiration climate of southern Africa is suited to the use of the scPDSI which is also more effective with longer duration droughts than with short-term droughts.

2.3.2 Standardized Precipitation Index

The Standardized Precipitation Index (SPI) is one of the most widely used drought measures which only requires precipitation data and is simple to calculate. The SPI was also developed in response to criticism of the PDSI (McKee *et al.* 1993). In turn, the SPI has also been criticized for neglecting the effects of temperature, evaporation and soil moisture. The SPI is based on standardized precipitation anomalies about a long-term mean with positive values reflecting wet conditions whilst negative values indicate drought. SPI values range from about -3 to +3 and may be used to compare drought in different climatic regions (Rouault and Richard 2005).

The SPI can be used to establish the temporal evolution of drought events including the onset, duration, cessation (Hayes et al. 1999) spatial extent and severity (Rouault and Richard 2005). It is also used operationally in drought monitoring when real time precipitation data are available. However, the SPI cannot identify locations that are more prone to drought than others and in regions where precipitation is highly seasonal, large SPI values can result from small deviations from normal precipitation (Glad 2010). It has been recommended by the World Meteorological Organization (WMO) for use by National Meteorological and Hydrological Services worldwide to define meteorological drought, in addition to existing methods (WMO 2012).

2.3.3 Vegetation indices

Since drought is naturally related to land surface characteristics, vegetation cover and vegetation health, several Vegetation Indices (VIs) have been developed and applied for drought monitoring (Karnieli *et al.* 2009). The most common VI is the Normalized

Difference Vegetation Index (NDVI) which is a measure of vegetation colour and fractional cover, and thus chlorophyll content and photosythesis rate. It has been used to monitor drought since the 1980s. The mean spatial patterns for vegetation NDVI have a high correspondence to mean rainfall (Lewis and Berry 1988; Richard and Poccard 1998) and may be used as an indicator for drought monitoring, agricultural production and classification of land cover (Anyamba and Tucker 2012).

The NDVI sensitivity to interannual rainfall variability is generally weak on the west (arid) and east of southern Africa (humid) but high sensitivity is found over semi-arid Botswana along the Kalahari transition zone (Richard and Poccard 1998; Chikoore and Jury 2010). Recent research suggests strong coupling exists between the land surface and the atmosphere along the eastern edge of the Kalahari (Chikoore and Jury 2010) where the mean summer NDVI is in the range 0.3-0.5 (along 25°E).

NDVI anomalies have also been widely used as an indicator for drought (Chikoore and Jury 2010) as they depict the difference between the current NDVI with long-term mean for the same period (Anyamba and Tucker 2012). Persistent negative NDVI anomalies are associated with drought conditions. Distinct differences in vegetation anomalies were found between the 1997/98 El Niño event and the La Niña of 1999/2000 over east and southern Africa (Anyamba *et al.* 2002).

The Enhanced Vegetation Index (EVI) is derived from and is an improvement of the NDVI and corrects for distortions which arise due to reflection by air particles and ground cover beneath the vegetation. Several other vegetation indices such as the Vegetation Condition Index, Soil Adjusted Vegetation Index, the Standardized Vegetation Index and the Vegetation Health Index have been derived from the NDVI (Kalma *et al.* 2008; Anyamba and Tucker 2012; Hayes *et al.* 2012).

2.3.4 Percent of normal rainfall index

The percent of normal rainfall index is the most used drought index by National Meteorological and Hydrological Services in southern Africa (Unganai and Bandason

2005). This may only be used in hindsight computed as total seasonal rainfall as a percentage of the long-term mean. Seasons with rainfall totals falling below 75% of long-term mean are considered as drought seasons. The percent of normal index assumes a symmetrical Gaussian distribution of seasonal rainfall received such that the mean and median have a central tendency. The mean precipitation is not always the same as median precipitation which is a value exceeded by 50% of the long-term record. However, an arithmetic 'normal' does not necessarily imply normal weather conditions (http://drought.unl.edu/Planning/Monitoring/ComparisonofIndicesIntro/PercentofNormal.aspx).

2.3.5 Other drought indices

Numerous other drought indices have been derived and applied and can be found in the literature. They include a Rainfall Anomaly Index (van Rooy 1965), deciles (Gibbs and Maher 1967), a Crop Moisture Index (Palmer 1968), a Surface Water Supply Index (Shafer and Dezman 1982), a Soil Moisture Drought Index (Hollinger *et al.* 1993) and a Crop Specific Drought Index (Meyer *et al.* 1993). The Standardized Precipitation and Evapotranspiration Index (SPEI) has been derived from the SPI. A Weighted Anomaly Standardized Precipitation Index (WASP) has also been derived and applied in drought studies. WASP and SPI are highly correlated (Lyon 2009).

A history and review of drought indices has been detailed in Heim (2000), Heim (2002), Hayes (2011), and others. While there are many drought indices and definitions, a P-E anomaly index is preferred in this thesis and is defined in Chapter 3.

2.4 Causes and prediction of drought

There is no single cause of drought (Namias 1983; AMS 1997). However, it is agreed that the primary cause of drought is a lack of rainfall over a large area for an extended period (Tallaksen and van Lanen, 2004) coupled with high evaporative losses due to persistent large scale circulations that inhibit rainfall e.g. lasting anticyclonic subsident circulation (Gustard *et al.* 2004).

Drought may result from local forcings (such as soil moisture and vegetation) or remote forcings (such as the tropical oceans) which may also act in combination (AMS 1997). Thus, causes of drought may be classified into those due to changes in atmospheric circulation; due to changes in temperature of the lower boundary (sea and land) or due to changes in moisture content of surface soils over land areas (Trenberth and Guillemot 1996; Mo *et al*. 1997).

Examples of studies dealing with causes of drought globally include Namias (1983), Lockwood (1986), Trenberth and Branstator (1992), Byun (1996), Schubert *et al.* (2004) and Cook *et al.* (2007). However, it is noted here that by far the majority of research on drought causes has focused on drought in the United States.

2.4.1 Atmospheric circulation

Globally, the immediate cause of drought is persistent subsidence which warms up the atmosphere and lowers the relative humidity (Namias 1983). Dry or drought conditions over southern Africa are mainly associated with large scale intense anticyclones over the subcontinent (Lindesay 1998) and the Botswana High is the most persistent. The Botswana High is a mid-tropospheric (400-600 hPa) anticyclone usually centered over Botswana/Namibia inducing widespread subsidence and it is most intense during late-summer (Reason 2016). The Botswana High coincides with the descending limb of the Hadley cell. Upper-level highs such as the Botswana High are thermally induced by condensational heating with a warm core largely the result of subsidence (Lenters and Cook 1996). The tropical high rainfall Congo basin northeast of the Botswana High is the main source of condensational heating (Reason 2016).

In many regions such as southern Africa, the rainy season is characterized by wet and dry spells. Drought events develop initially from prolonged dry spells which result from the establishment of anticyclonic circulation over southern Africa inhibiting vertical cloud development. Although most frequent during winter (Lindesay 1998) sub-tropical anticyclones also prevail during summer and are the major cause of intra-seasonal dry spells. Persistent anticyclones often cause the retreat of the ITCZ from the Zambezi valley

toward the Congo basin. The Angola Low is weakened during this time. The Angola Low is a thermally induced heat low which is persistent over southeast Angola (Biè Plateau) during summertime and is an important feature modulating moisture convergence over southern Africa (Mulenga 1998). It is an anchor point for the ITCZ and cloud bands.

Drought processes act to inhibit convection and displace the main rain bearing systems such as cloud bands away from the subcontinent (Mulenga *et al.* 2003). In an investigation of wet and dry spells over South Africa, Cook *et al.* (2004) established that dry summers were associated with an equatorward displacement of the ITCZ. They also determined that during drought seasons tropical-temperate troughs and attendant cloud bands tend to locate over the warm ocean east of the subcontinent, near Madagascar.

In a study of dry spells over southern Africa, Usman and Reason (2004) found the highest frequency of dry spells occurs in December over the west and southwest of the subcontinent, which are largely arid. The lowest dry spell frequency was found in the area of the ITCZ. A significant result of their analysis was the coincidence between El Niño events and high dry spell frequencies.

2.4.2 Land-surface temperatures

Drought events are often accompanied by above normal surface to air temperatures and heat waves (Madden and Williams 1978; Namias 1983; Chang and Wallace 1987; Trenberth and Shea 2005; Lyon 2009; Dai 2011b) and thus high land surface temperatures may be a good indicator of drought conditions. However, heat waves have a typical timescale of a week whereas major droughts are of the order of months. Heat waves may occur during summers with high soil moisture (Chang and Wallace 1987) and can feedback to upper level anticyclones which further enhance drought conditions (Chang and Wallace 1987).

It is well established that terrestrial summer air temperatures are negatively correlated with rainfall (e.g. Trenberth and Shea 2005). Dry periods result in soil moisture deficits, increased sensible heat flux and consequently high surface air temperature (Lyon 2009).

Measurements of Land Surface Temperature (LST) derived from satellite observations in the thermal infrared have been used to depict drought (Karnieli *et al.* 2009) and may be used as an indicator for soil moisture, evapotranspiration and vegetation.

A strong negative correlation has been found between LST and NDVI (Goward *et al.* 2002; Yue *et al.* 2007; Karnieli *et al.* 2009). However, this relationship is not always negative and varies with vegetation type and latitude. The NDVI-LST relationship is negative when vegetation growth is limited by water and positive when limited by energy/temperature (Karnieli *et al.* 2009). It appears vegetation growth in tropical rainforests or in high latitudes is largely influenced by energy (Karnieli *et al.* 2009). It is also noted that droughts are most likely in the low latitudes where a negative relationship between LST and NDVI exists. Variations in correlations between LST and NDVI have also been observed between seasons and time of day hence the use of daytime LST (Sun and Kafatos 2007) and maximum temperature observations to characterize drought.

2.4.3 Sea surface temperatures

In addition to LST, droughts over southern Africa have been related to remote oceans and phenomena such as the El Niño Southern Oscillation (ENSO), the Indian Ocean Dipole and the Subtropical Indian Ocean Dipole. Whilst ENSO results from variation of Sea Surface Temperature (SST) between the east and west equatorial Pacific Ocean, the Southern Oscillation drives a 'see-saw' of surface atmospheric pressure and circulation (Behera and Yamagata 2003). The ENSO phenomenon is a dominant factor in the variability of summer rainfall over southern Africa (Matarira 1990; Reason *et al*. 2000; Makarau and Jury 1997; Matarira and Jury 1992; Richard *et al.* 2000) and warm ENSO events have been linked to dry weather and droughts particularly over the central and southeastern sector of subcontinent (Ropelewski and Halpert 1987; Nicholson *et al.* 1988; Jury *et al.* 1994; Rocha and Simmonds 1997; Richard *et al.* 2000; Reason and Rouault 2002). The most severe droughts have occurred in southern Africa during the mature phase of ENSO (Rouault *et al.* 2005) when warmer than normal sea temperatures are observed over the central and eastern equatorial Pacific Ocean and the western tropical Indian Ocean (Nicholson *et al.* 2001).

Through a reorganization of the Southern Oscillation via the Walker cells, El Niño acts to displace convection and major rain producing systems to lie eastwards over the Indian Ocean (Lindesay 1998). Anticyclonic circulation anomalies become established through a deep layer over the subcontinent during this time. The upper-level (300-200 hPa) circulation over the subcontinent is characterized by enhanced westerly anomalies from the Atlantic Ocean. Warm ENSO events are associated with intense heating and above average temperatures over southern Africa during the austral summer (Ropelewski and Halpert 1987; Lyon and Mason 2007). The length of the maize growing season is shortened as a result of the early cessation of the rains (Moeletsi *et al.* 2011) as El Niño favors lower yields.

Most, but not all abnormal climate events over southern Africa occur during El Niño or La Niña. However, ENSO alone cannot account for all drought events in southern Africa (Rocha and Simmonds 1997; Lindesay 1998; Richard *et al.* 2000; Manatsa *et al.* 2007). The most intense El Niño event of 1997/98 did not result in the expected widespread severe drought over southern Africa (Reason and Jagadheesha 2005; Harrison *et al*. 2008; Lyon and Mason 2009). The rainfall deficits of 1997/98 were mild and of smaller aerial extent compared to other ENSO related droughts of the 1980s and 1990s (Anyamba *et al.* 2001; Anyamba *et al.* 2002; Reason and Jagadheesha 2005; Lyon and Mason 2007; Lyon and Mason 2009). Unlike during 1991/92 and 2002/03, the Angola low and cloud bands were strengthened during 1997/98 resulting in more rainfall than was expected considering the magnitude of the Southern Oscillation Index (Reason and Jagadheesha 2005).

There are some drought events such as the 1967/68 drought that were not related to El Niño - strengthening the argument that other mechanisms also cause droughts over the subcontinent. Thus, the relationship between ENSO and the regional rainfall is non-linear and 'partial' accounting for about 30% of rainfall variability at seasonal time scales (Tyson and Preston-Whyte 2000). It is also suggested that the ENSO relationship with rainfall

over southern Africa is dynamic and evolves over time (e.g. Richard *et al.* 2000; Reason 2002; Manatsa and Matarira 2009).

Several earlier studies on drought have focused on their predictability (e.g. Matarira 1990; Manatsa *et al*. 2007; Manatsa *et al*. 2008). Given the strong influence of ENSO on the rainfall of southern Africa, the ENSO phenomenon is a widely used predictor not only for droughts, but also for seasonal rainfall over the region. The ENSO impact is typical during the late summer i.e. JFM (Lindesay 1998; Sheffield *et al.* 2008) which coincides with critical stages of growth for the maize staple crop. Two of the worst droughts over southern Africa were associated with the ENSO events of 1982/83 and 1991/92 (Rouault and Richard 2003).

Recent research suggests that there exist several 'flavors' of ENSO and identified Modoki events (Ashok *et al.* 2007; Ratnam *et al.* 2012b). Modoki is Japanese to mean "similar but different" (Ashok et al. 2007) such that El Niño/La Niña Modoki occurs when the central equatorial Pacific Ocean (international dateline) is anomalously warmer/cooler and flanked by cooler/warmer STT anomalies on the west and east creating a zonal tripole pattern (Ashok *et al.* 2007). Significantly lower rainfall is experienced over southern Africa during El Niño than during El Niño Modoki (Ratnam *et al* 2014).

It has also been found that SSTs in the Indian Ocean and tropical Atlantic Ocean have an important role on rainfall anomalies in southern Africa (Walker 1990; Mason 1995; Reason 1999; Reason 2002; Reason and Mulenga 1999). The tropical Atlantic Ocean and the southwest Indian Ocean are important sources of low level moisture over the subcontinent (Cook *et al*. 2004). An increase of SSTs in the tropics leads to enhanced evaporation and convection and a low pressure anomaly at the surface. Previous studies have shown that a warm SST anomaly has a greater influence on the atmospheric circulation than a cold SST anomaly (e.g. Lau 1997).

It was suggested that the Indian Ocean might play a bigger role in the climate of southern Africa than was previously thought (Behera and Yamagata 2001). An Indian Ocean Dipole

(IOD) of ocean temperatures (Saji *et al*. 1999; Webster *et al.* 1999; Behera *et al.* 1999; Iizuka *et al.* 2000; Yamagata *et al.* 2002) was found to have significant correlation with rainfall variability over the region (Manatsa *et al.* 2007). The IOD was discovered by Saji *et al.* (1999) following anomalous summer weather in Asia in 1994 (Yamagata *et al.* 2003). The IOD is a coupled ocean-atmosphere mode affecting rainfall variability at seasonal to interannual timescales.

A study by Manatsa *et al.* (2008) suggests that the ENSO effect on reducing rainfall over Zimbabwe is tied to the positive phase of the IOD. El Niño onset is also significantly impacted by an extreme positive IOD (Yamagata *et al.* 2016). A positive (negative) IOD occurs when the western tropical Indian Ocean is warmer (colder) than the east side (Figure 2.2). A positive IOD is generally associated with high rainfall over East Africa and drought conditions in southern Africa. Reason (2002) found the abnormally wet 1970s and abnormally dry 1980s to be strongly related to cycles of ENSO. Reason (2002) also argues that the SST anomalies in the Pacific Ocean associated with the Southern Oscillation have also become more extensive since 1970. In a more recent paper, Manatsa and Matarira (2009) have suggested that the IOD had a more dominant role than ENSO on the regional rainfall from 1960 to 1996, whilst ENSO became more significant after 1996.

An important region of ocean-atmosphere interactions is the southern Indian Ocean. A southwest-northeast dipole of SSTs was first described by Behera and Yamagata (2001) and termed the Indian Ocean Subtropical Dipole (IOSD). Similar southwest-northeast dipole patterns have also been observed over the South Atlantic (Faucherau *et al.* 2003) and South Pacific (Morioka *et al.* 2013a). The Antarctic Oscillation (AAO) plays an important role in the generation of the IOSD even when tropical SST variations are weak (Morioka *et al.* 2014) whilst anomalies in the Mascarene High induced by ENSO may also help generate the IOSD (Morioka *et al.* 2013b). A positive (negative) IOSD event occurs when the southwestern (southeastern) Indian Ocean is anomalously warm (cold) in the austral summer (Behera and Yamagata 2001). Positive IOSD events are associated with higher than normal rainfall over southeastern Africa due to the anomalous low pressure

created by warm SST anomalies in the southwest Indian Ocean (Reason 2001a, Reason 2002). The IOSD has also been found to influence the strengthening/weakening of the Mascarene High.

2.4.4 Soil moisture content

In the hydrological system, soil moisture is usually the first affected by drought (Byun and Wilhite 1999). Soil moisture is the water used for evapotranspiration and is critical in the partitioning of energy at the surface (Oglesby and Erickson III 1989). Surface and root-zone soil moisture also acts as an integrator between rainfall and crop yields.

The occurrence of drought events in some continental regions has been linked to conditions at the lower boundary such as soil moisture and vegetation fraction. Surface soil moisture content modulates drought over long timescales. Conversely, drought may act to sustain itself through negative feedbacks between the land surface and the overlying boundary layer (AMS 1997)

Even though soil moisture volume is small compared to other components of the hydrological cycle, it still exerts an important influence on atmospheric processes. Soil moisture provides a positive feedback to precipitation through an increased moisture flux in the atmosphere (Cook *et al.* 2006). A soil moisture flux may also act to enhance moisture convergence. However, this relationship is not straightforward (Cook *et al.* 2006).

In contrast, New *et al.* (2003) argue that soil moisture may exert a negative feedback on precipitation over southern Africa. Wet soils result in reduced sensible heat flux and increased stability in the lower atmosphere. Cook *et al.* (2006) also found that an increase in soil moisture results in a reduction in precipitation over southern Africa. This is done through increased stability and reduced moisture convergence. Surface pressure was found to be anomalously high with enhanced upper level subsidence.

Soil moisture deficits have also been used as a drought index (e.g. Sheffield and Wood 2008). Until recently, long-term observed soil moisture data has been largely unavailable over southern Africa (Cook *et al*. 2006). Many studies have employed reanalysis soil moisture estimates to determine the onset and development of drought. Gravity Recovery and Climate Experiment (GRACE) satellites which were launched into orbit in 2002 by the National Aeronautics and Space Administration (NASA) use gravity measurements to estimate soil moisture content at the surface and in the root zone.

2.4.5 Other causes of drought

The Quasi-Biennial Oscillation (QBO) has been found to influence rainfall over southern Africa (Mason and Lindesay 1993; Jury *et al.* 1994; Lindesay 1998). QBO is a cycle of stratospheric (typically 30 hPa) equatorial zonal winds between easterlies and westerlies. The east phase of the QBO has been related to below average rainfall (drought) over the subcontinent. The QBO and SOI have a strong statistical correlation during the west phase of the QBO (Lau and Sheu 1988; Mason and Lindesay 1993) which has been found to influence climate variability in several regions of the tropics and subtropics. Jury *et al.* (1994) illustrated through a conceptual model how the west phase of the QBO triggers an overturning circulation that supports wet conditions over southern Africa. The ENSO-rainfall relationship over southern Africa appears to be also modulated by the QBO (Mason and Tyson 1992; Richard *et al.* 2000).

Solar activity or the sunspot cycle has been linked to variability of rainfall at decadal timescales and droughts in southern Africa. Sunspots are cooler areas on the sun's photosphere which appear darker and result in variability of solar output. The quasi-decadal oscillation in rainfall over southern Africa has been linked to the 11-year sunspot cycle (e.g. Jury and Mwafulirwa 2002).

Sometimes extended periods of dry weather are experienced over southern Africa as a result of active cyclogenesis over the southwest Indian Ocean and the Mozambique Channel. The 1983/84 and 2011/12 seasons experienced rainfall deficits largely due to subsidence on the west side of tropical cyclones in the Mozambique Channel (Chikoore

et al. 2015). Thus, drought seasons derive from several different climatic influences on the circulation (Lindesay 1998).

2.5 Characteristics of drought

Droughts are not similar in character and their impacts are not the same either (Palmer 1965) and may be considered dynamic in nature. A drought event may be determined by one or a combination of characteristics, including duration, severity/intensity (Shefield and Wood 2008) and spatial extent (area covered by drought). Drought indices such as those defined in section 2.3 are used to determine the various characteristics of drought.

Some key characteristics of the drought phenomenon are its intensity, spatial extent and temporal evolution. Spatial and temporal characteristics of drought may vary from region to region (Tallaksen and van Lanen 2004) and from time to time. Some droughts are extensive covering large areas whilst others may be considered as regional or localized.

2.5.1 Drought severity or intensity

The intensity or severity of a drought event is arguably the most important drought dimension (Tsakiris and Vangelis 2005). Drought severity is the extent to which deficits occur in precipitation, soil moisture and water storage (Dai 2011b) and may be determined by departures from some threshold which may be a long-term mean. Drought severity may also refer to the degree of severity of impacts (AMS 1997). It depends upon precipitation, potential evapotranspiration (PET), soil characteristics, vegetation cover (Tsakiris and Vangelis 2005) and air temperature. Vegetation cover, soil moisture and precipitation have locally intermittent and heterogeneous properties, while PET is governed by the regional climate (Tsakiris and Vangelis 2005).

2.5.2 Drought duration

In contrast to other natural hazards such as floods, earthquakes and tsunamis, drought is a creeping phenomenon that evolves much more slowly such that it may remain unnoticed for long periods (Tallaksen and van Lanen 2004; Glad 2010). Thus the onset, duration and cessation of drought are difficult to determine accurately whilst drought

cycles and interannual variability are also of considerable interest. The magnitude of drought is a combination of drought intensity and duration.

Quantifying drought duration and intensity presents a significant problem (Bryun and Wilhite 1999). A difficulty with drought duration is that the onset of a drought is often slow, making it difficult to determine its start accurately (Eden 2012). The SPI defines the onset of drought as that period when SPI values become negative and drought conditions persist until the SPI becomes positive again.

Droughts can occur over several timescales, ranging from midsummer droughts to prolonged multi-year droughts. Meteorological droughts are mostly defined over monthly and seasonal timescales (Byun and Wilhite 1999) resulting from extended periods of dry weather. Thus, monthly datasets are often preferred over daily data for studies of drought.

The frequency and duration of dry spells in a season are critical for the development and propagation of a drought event. Drought conditions could prevail for several years in one region (Hayes *et al*. 2012) as happened over southern Africa throughout much of the 1960s, 1980s and 1990s. It is established that drought duration and intensity have gradually increased since the 1970s particularly in tropical and subtropical regions (IPCC 2007).

2.5.3 Aerial extent of drought

The intensity of a drought event is also related to its aerial extent. The more intense the drought event, the more likely it will be widespread whilst a moderate drought tends to be more confined in extent.

Some drought indices track variability within an affected area and recurrent spatial patterns (Stahl and Hisdal 2004). It was found that the spatial extent of droughts over southern Africa has increased since the 1970s (Rouault and Richard 2005). The SPI, SPEI and NDVI have been used to map the spatial extent and intensity of drought.

Lyon (2004) found a significant relationship between the spatial extent of drought in the tropics and the strength of El Niño. He highlighted the importance of separating the ocean from land areas when analyzing the El Niño impact in the tropics, as it is not uniform. The land area affected by drought in a strong El Niño is significantly larger than that affected by a weak El Niño.

2.6 Drought impacts

Communities are affected by droughts in different ways (Calow *et al*. 2010). Of all natural disasters, drought impacts are ranked among the most costly (Hayes *et al*. 2012), significantly affecting rural livelihoods and agro-based economies. However, drought impacts are non-structural and difficult to quantify (Heim 2002; Murthy *et al*. 2009) as they may be environmental, economic or social. They occur at different spatial scales such as the national level or household level (Vogel 2000; Wilhite *et al.* 2007). Drought impacts depend on its intensity and duration (Rouault and Richard 2005). Even so, drought events of similar intensity may produce different impacts at different times (Wilhite *et al.* 2007) over different regions.

Drought impacts are often categorized as either direct or indirect (Byun and Wilhite 1999; Wilhite *et al*. 2007) and may range from reduced water levels, lower crop yields, increased veld fires, limited grazing, decline in livestock production to food insecurity. Impacts of drought are dynamic and complex in nature due to interactions of supply and demand (Vogel 1994, Wilhite *et al.* 2007). They can be severe in semi-arid regions where availability of water is low even under normal conditions (Tallaksen and van Lanen 2004). The impacts of drought may be more severe when multi-year droughts occur such as in the early 1980's and early 1990's in southern Africa.

The impacts of drought also depend on vulnerability and social inequalities (some due to non-climatic factors) and may vary with ability to cope and build resilience (Dai 2011b). In countries with developing economies, droughts can trigger severe famine and loss of human lives (Hayes *et al*. 2012). Impacts of drought may be experienced in a region outside the area affected by drought (Wilhite *et al.* 2007) and can be compounded by

societies that increase the demand for water e.g. by overdeveloping an area (Wilhite *et al.* 2007). In addition, impacts of a meteorological drought may also persist long after normal weather has returned (Palmer 1965).

Drought impacts have been comprehensively detailed in reviews by Wilhite (1992), Bradford (2000), and Wilhite *et al.* (2007), and others.

2.6.1 Environmental impacts

Droughts result from reduced rainfall and enhanced evaporation losses which impact negatively on surface and underground water resources (Vogel 1994; 2000). These may be worsened by the simultaneous occurrence of high temperatures or heat waves (Lyon 2009).

Whilst a soil moisture drought results from recent precipitation deficiency, deficits in water resources are caused by precipitation deficits over much longer time scales (Bryun and Wilhite 1999). Therefore long-lasting drought results in reduced streamflow, lower groundwater and dam levels (Tallaksen and van Lanen 2004). During the 1991/92 drought in southern Africa, about 90% of small dams dried up in Botswana, Namibia, South Africa and Zimbabwe (Jury and Mwafulirwa 2002). Drought impacts on surface water resources lag meteorological and agricultural drought (AMS 1997).

Some research has considered the impact of drought on groundwater in rural areas as boreholes may dry out (e.g. Calow *et al*. 2010) even though there are limited observations of groundwater in southern Africa. Droughts may also affect the quality of water, in addition to quantity (Tallaksen and van Lanen 2004). Stagnant water which is associated with drought is more likely to cause disease than flowing water.

Due to the international nature of major rivers of Africa, water resources of a country depend on the inputs and consumption upstream. In addition to water supply, lakes are also used for fishing, tourism and recreation and these activities are significantly affected

during drought episodes which may result in conflict over shared water resources. Tate *et al.* (2000) have detailed the drought impact on streamflow in southern Africa.

When combined with population growth and human activities such as over cultivation and overgrazing, drought impacts may lead to environmental degradation and desertification (Msangi 2004; Tallaksen and van Lanen 2004).

2.6.2 Economic impacts

The droughts of the 1980s and 1990s had wide ranging impacts on economies of southern Africa (Vogel 2000). Direct economic impacts of drought result from reduced crop yields and increased surface and groundwater abstraction. Impacts of drought on water resources may also result in reduced hydropower generation for example on Lake Kariba and Lake Cahora Bassa (along the Zambezi River) with far reaching economic consequences. Water rationing and load shedding of electricity often result. Soil moisture is usually the first to be impacted by drought since deficiency of water affects the soil first (Bryun and Wilhite 1999) and hence crop growth and rain-fed agriculture are affected early. The impact of drought on crop yields depends on the type and variety of crop cultivated (Murthy *et al*. 2009).

Maize is the staple food in Africa south of the equator. Maize yields were significantly reduced during the droughts of the 1980s (Vogel 2000) declining to 10% of normal during 1982 to 1984 (Makarau 1995). Comparisons of rainfall and maize yields have shown a statistically significant positive correlation in many maize growing areas of the subcontinent (Vogel 1994). Drought impacts on crops also depend on economic factors and operational farm management practices (Vogel 1994). Those may include the cropped area and the time of planting. Small grains such as sorghum and millet are more drought resistant but are less preferred because of their lower nutritional and market values. The contribution by agriculture to the Gross Domestic Product (GDP) is also reduced by recurrent droughts over southern Africa (Vogel 2000).

Drought may have direct or indirect impacts on agricultural production (Vogel 1994). National herds of cattle in Botswana, Lesotho, Mozambique, Zambia and Zimbabwe were decimated by 70% during the early 1990s (Vogel 2000) and by up to 80% during the 1982-84 drought (Makarau 1995).

General circulation models such as the General Large Area Model (GLAM) for annual crops have been used to investigate the impact of weather and climate on crop yields for annual crops such as maize, groundnuts and wheat (e.g. Challinor *et al*. 2003; Challinor *et al.* 2005).

2.6.3 Social impacts

Long-term effects of drought may lead to poverty, famine and unemployment (Msangi 2004). Due to low socio-economic status of communities of southern Africa (annual per capita income < $5000), droughts often turn into natural disasters (Manatsa *et al.* 2007) and may lead to human mortality.

Some secondary industries obtain and process raw materials from agriculture and their performance is significantly affected by agricultural droughts. These may include maize millers, abattoirs, cotton ginneries, tobacco firms, breweries and others. Drought may also affect employment levels and therefore livelihoods of workers in these sectors. It was estimated that about 250 000 jobs were affected by the severe droughts of the early 1990s (van Zyl 1993). Unemployment and retrenchments often led to increased crime levels (Vogel 2000) and social unrest.

2.7 Drought preparedness, mitigation and response

Different approaches to the drought hazard are cited. Reactive response crisis management involves responding to drought impacts whilst proactive risk management involves early warning and preparedness for drought (Hayes *et al*. 2012). Drilling boreholes to exploit groundwater is also used as a means to cope with drought.

Mason *et al.* (1994) demonstrated the potential for drought events over southern Africa to be predicted using global climate models with SSTs from the adjacent Indian and Atlantic Oceans. Drought predictions are often linked to seasonal climate predictions. Since 1997, climate experts from National Meteorological Services in southern Africa convene every year in August to generate a consensus forecast based on statistical approaches. The Southern Africa Regional Climate Outlook Forum (SARCOF) has been criticized for being subjective and not employing dynamical approaches to seasonal prediction. Drought prediction can provide advance early warning to governments and affected communities and reduce the risk of natural disasters.

The Global Forecasting Center for Southern Africa (GFCSA) is a platform where seasonal predictions generated by research institutions in southern Africa are shared. Model forecasts from the University of Cape Town and the Council for Scientific and Industrial Research (CSIR) and the South African Weather Service (SAWS) are also available to augment output from global centers and the SARCOF process.

More recently, an ocean-atmosphere general circulation model was developed in South Africa – the first to be developed in the country (Beraki *et al*. 2014). The ECHAM4.5-MOM3-SA model was developed for seasonal climate prediction and was skilled to predict El Niño and La Niña with up to 8 months lead time. The skill was comparable to coupled models run by global centers such as the International Research Instititue for Climate and Society (IRI), National Centers for Environmental Prediction (NCEP) and the European Center for Medium Range Weather Forecasting (ECMWF). Model forecasting systems and long range prediction in South Africa have been detailed in Landman *et al.* (2012).

Many regions have developed early warning systems. In the Southern Africa Development Community (SADC), early warnings of hydrometeorological hazards are coordinated by the Famine Early Warning Systems Network (FEWS NET). Risk of droughts turning into disasters is determined by exposure, vulnerability and response to the drought hazard (AMS 1997).

2.8 Drought in southern Africa

Droughts occur regularly in southern Africa (Rouault and Richard 2005; Manatsa *et al.* 2008) and this section reviews some of the most significant contributions to knowledge on drought in various regions of southern Africa, beginning with the earlier studies up to the most recent studies.

The influences of Atlantic Ocean and Indian Ocean SSTs and their interactions with the Southern Oscillation (1953-1989) on South African rainfall were analyzed in Mason *et al.* (1994). Typical circulation changes associated with summer droughts were also detailed. A 4-level, mixed layer (Slab Ocean) Commonwealth Scientific and Industrial Research Organization (CSIRO) general circulation climate model was used to simulate drought over South Africa with regional SST anomalies as boundary conditions. Principal Components Analysis (PCA) of SSTs was done to account for variance in summer rainfall through correlations. Warming of the equatorial western Indian Ocean and the Agulhas system was found to have significant correlations with the occurrence of drought in southern Africa. The simulated circulation showed cyclonic anomalies over the Indian Ocean northeast of Madagascar and increased upper westerly flow over southern South Africa.

In one of early studies to employ vegetation indices over southern Africa, Unganai and Kogan (1998) investigated the application of the Vegetation Condition Index and the Temperature Condition Index in monitoring drought during 1985 - 1994. The vegetation anomalies were related to atmospheric circulation anomalies at 500 hPa. The 1992 and 1995 droughts were identified using NDVI and associated with positive geopotential height anomalies at 500 hPa. Their study concluded that Advanced Very High Resolution Radiometer data could be used to map the spatio-temporal behavior of drought in southern Africa. Subsequently, Anyamba *et al.* (2001) and Anyamba *et al.* (2002) employed NDVI anomalies to analyze southern Africa's vegetation response patterns to the warm and cold ENSO events of 1997/98 and 1999/2000.

Nicholson *et al.* (2001) studied the relationship between El Niño and drought over Botswana during the period 1946–1992. SST anomalies in the south Atlantic and Indian Oceans were also analyzed. In the agriculture region northeast of Botswana, rainfall was below normal for 17 of 22 ENSO episodes. They compared composites of dry seasons with those of wet seasons under ENSO episodes. The rainfall response to ENSO appeared to be modulated by the influence of the Atlantic and Indian Oceans. For ENSO wet seasons, it appeared anomalously cool SSTs in the tropical Atlantic Ocean promote rainfall over Botswana whilst warmer SSTs in these sectors trigger drought. They found that the ENSO-rainfall relationship was strongest during the late summer and not so strong in early summer.

The spatial and temporal variability of 20th Century droughts over southern Africa and their teleconnections with the oceans and atmospheric circulations were analyzed by Richard *et al.* (2001). They didn't find significant trends in late summer (JFM) rainfall during the 20th century. However, the interannual variability showed varying amplitudes. They showed that SST and atmospheric anomaly patterns associated with droughts before 1970 were dissimilar to those after 1970. They found the tropical oceans and atmospheric circulation linked to ENSO becoming more dominant after 1970. This is in agreement with Reason (2002). During most drought, the jet stream at 200 hPa was strengthened and displaced northward, tropical inflows were diminished resulting in fewer tropical-temperate troughs. Richard *et al.* (2001) also found a strengthening of the north-south temperature gradient over southern Africa during drought events.

Jury and Mwafulirwa (2002) analyzed climate variability and dry summers in Malawi during the period 1962-1995. They found rainfall cycles at 2.4, 3.8 and 11.1 years corresponding to cycles of QBO, ENSO and Sunspot activity. It was also found that the ENSO influence is more significant in the south of the country. Rainfall over southern Africa was positively correlated with SSTs over the Agulhas current and the tropical east Atlantic Ocean – the oceans immediately adjacent to the subcontinent. The west Indian Ocean was found to be negatively correlated suggesting that warm SSTs in that region result in drought in southern Africa.

Mulenga *et al.* (2003) analyzed circulation anomalies associated with ENSO and non-ENSO droughts over northeastern South Africa (Limpopo) separately during the period 1921-2000. Severe drought occurred nearly in all cases of strong ENSO events. A composite of ENSO events reveals that convection is suppressed by high pressure anomalies and low level divergence coupled with increased upper westerlies over southern Africa. The ascending limb of the Walker cell shifts to the warm ocean east of Madagascar. They found dry ENSO summers to be linked to a significant re-organization of tropical circulation whilst dry non-ENSO summers were linked to mid-latitude influences. There seems to be enhanced advection of cold and dry southwesterly airflow in the low levels.

Dube and Jury (2003) used NCEP-NCAR reanalyses to investigate the precursors of drought in KwaZulu-Natal, South Africa via a case study of the 1992/93 event. This drought was not widespread across southern Africa. The equatorial Pacific Ocean was neutral but cooler SSTs were observed in the Mozambique Channel, coupled with warmer conditions in the south Indian Ocean. The Indian Ocean appeared to exert a greater influence on the drought in KwaZulu-Natal in the absence of significant influence from ENSO and QBO. In a north-south section along 30°E, enhanced uplift was found over the Zambezi valley with strong subsidence over KwaZulu-Natal due to a westerly downslope airflow. The local winds had a dominant influence in producing and sustaining drought conditions.

In a study of intra-seasonal dry spells over the subcontinent, Usman and Reason (2004) defined a ‘drought corridor’ between 20-25°S covering northern South Africa, southern Zimbabwe, southern Mozambique and Botswana. This corridor forms the drainage basin of the Limpopo River and is a focus of this study.

Rouault and Richard (2005) applied the SPI to analyze the intensity and aerial extent of droughts over southern Africa (south of 10°S) from 1901 – 1999. They employed the SPI at time scales of 3, 6, 12 and 24 months using Climate Research Unit (CRU) and Global

Precipitation Climatology Center (GPCC) datasets. Out of 12 most severe droughts in the study, eight coincided with El Niño events. The period from 2001-2004 was characterized by droughts at several timescales. They also found an increase in recent drought at the two year timescale over the subcontinent. Similar results were found in a related earlier study by Rouault and Richard (2003) which used SPI to study drought intensity and spatial extent in South Africa from 1921 – 2002.

Manatsa *et al*. (2008) investigated the influence of the IOD on droughts in Zimbabwe for the period 1940-1999. In a departure from a widely held hypothesis, the study found that when compared against each other, the positive IOD mode exerts a greater influence on seasonal rainfall (or drought) over Zimbabwe compared with the ENSO phenomenon. However, some droughts occurred in the absence of a positive IOD mode. It was hypothesized in their study that ENSO may have an indirect influence on Zimbabwe rainfall via teleconnections from the Pacific Ocean to the Indian Ocean. In their paper, Manatsa *et al.* (2008) used statistical composite and partial correlation analyses, but did not employ dynamical models to investigate if a physical relationship really exists.

Lyon (2009) considered heat waves and summer droughts over southern Africa (south of 15°S) in the period 1961-2000. It was found that impacts of drought are exacerbated when dry spells and heat waves coincided. The study compared three Coupled Model Intercomparison Project (CMIP3) models with observations and simulated the future evolution of heat waves and drought under the A1B greenhouse gas scenario. Daily maximum temperature and monthly precipitation during DJF were used to investigate drought characteristics, heat waves and their co-occurrence over southern Africa. The coupled models simulated drought and heat wave relationships similar to those found in the observations. The study also found large interannual variations in GPCC precipitation observations over southern Africa. The models projected an increased frequency of heat waves and droughts during DJF over southern Africa in the 21st century.

This review shows that nearly half of the studies on droughts in southern Africa have focused on regional droughts mainly in South Africa. This may be related to the paucity

of observations over much of the subcontinent outside South Africa and also the distribution of population centers and universities. Instead, this research deals with a larger scale, focusing on the geographical domain of southern Africa extending from the Zambezi to the Limpopo basins and across to the subtropics (15-28°S). This thesis also employs some of the latest range of datasets which have only become available in recent times.

2.9 Temporal trends of drought

Several studies have analysed drought across global land areas, mainly investigating trends in drought frequency and area covered by drought. Global warming and climate change scenarios are also used to project future drought. However, some more recent studies appear to have reached conflicting results on how drought will evolve under climate change (e.g. Dai 2012 and Sheffield *et al.* 2012). Trenberth *et al.* (2014) argue that this may be due to the various forms of the PDSI and different datasets used to define evapotranspiration.

Dai (2012) found increasing trends of drying in observations of global precipitation and drought indices from 1950-2010. Streamflow in the world's major river basins also shows a similar drying trend from a different dataset. The models in Dai (2012) project an increase in drought risk and severity from 2010-2099 due to either a decrease in precipitation or enhanced evaporation. However, significant differences were found between observed and modelled drying and this may be due to variations in tropical SSTs which are not well represented in the models.

On the other hand, Sheffield *et al.* (2012) formulated and evaluated trends in PET based on Thornthwaite and Penman-Monteith and found the two methods in disagreement on trends of drought in many regions. They found a declining trend in the PDSI based on Thornthwaite (increasing drought) but no significant trend in the PDSI based on Penman-Monteith. The Thornthwaite method calculated a significant increase in the area affected by drought but there was mixed signal with the Penman method suggesting a small and insignificant increase. They argue that previous estimates which suggest an increase in

global drought may have been overestimated, and conclude that little change has occurred in global drought.

Trenberth *et al.* (2014) investigated the link between global warming and changes in drought. It is thought that global warming may not cause drought but may lead to more intense droughts when they occur.

Cook *et al.* (2014) employed General Circulation Model (GCM) output from CMIP5 models and focused on atmospheric response to greenhouse gas warming. The study was aimed at investigating how precipitation and PET will change by 2090. They simulated and compared output from both the PDSI and SPEI drought indices and found that increased surface temperatures will result in increased PET. An increase in PET causes an amplification in drying, expanding the spatial extent of drought across sub-tropical zones such as southern Africa.

2.10 Summary

Globally, the drought phenomenon has attracted extensive research since several regions of the world are affected by various forms of drought. Most research on drought have dealt with drought in the United States. The following summarizes what is known about meteorological drought in southern Africa:-

a) Numerous drought indices have been developed and used in the analysis of drought to represent its complex nature (Hayes *et al.* 2005). However, it may be optimal to use a combination of drought indices (Hayes *et al.* 2012). P-E anomaly is the preferred index used to quantify drought in this thesis, where P is the observed rainfall and E is the calculated potential evaporation.
b) ENSO related droughts appear to be associated with low-level divergence and enhanced subsidence over the subcontinent. The ascending limb of the Walker cell is displaced eastwards to the Indian Ocean as upper westerlies are strengthened.

c) Several areas of the Indian Ocean have differing influence on the regional rainfall. It appears the ocean east of Madagascar exerts the strongest influence on seasonal rainfall over southern Africa.
d) The Indian Ocean or the Quasi-Biennial Oscillation modulate the ENSO-drought relationship over southern Africa.
e) Many studies of drought in southern Africa have focused on regional domains, or provinces of South Africa. These localized droughts appear to be caused by localized perturbations within the large scale.
f) The future of drought under climate change is blurred, partly because evaporation losses may be described in a number of ways.

Despite these advances in understanding drought, it is also known that the drought phenomenon and its impacts are evolving with time due to climate change, population growth and environmental degradation.

Chapter Figures

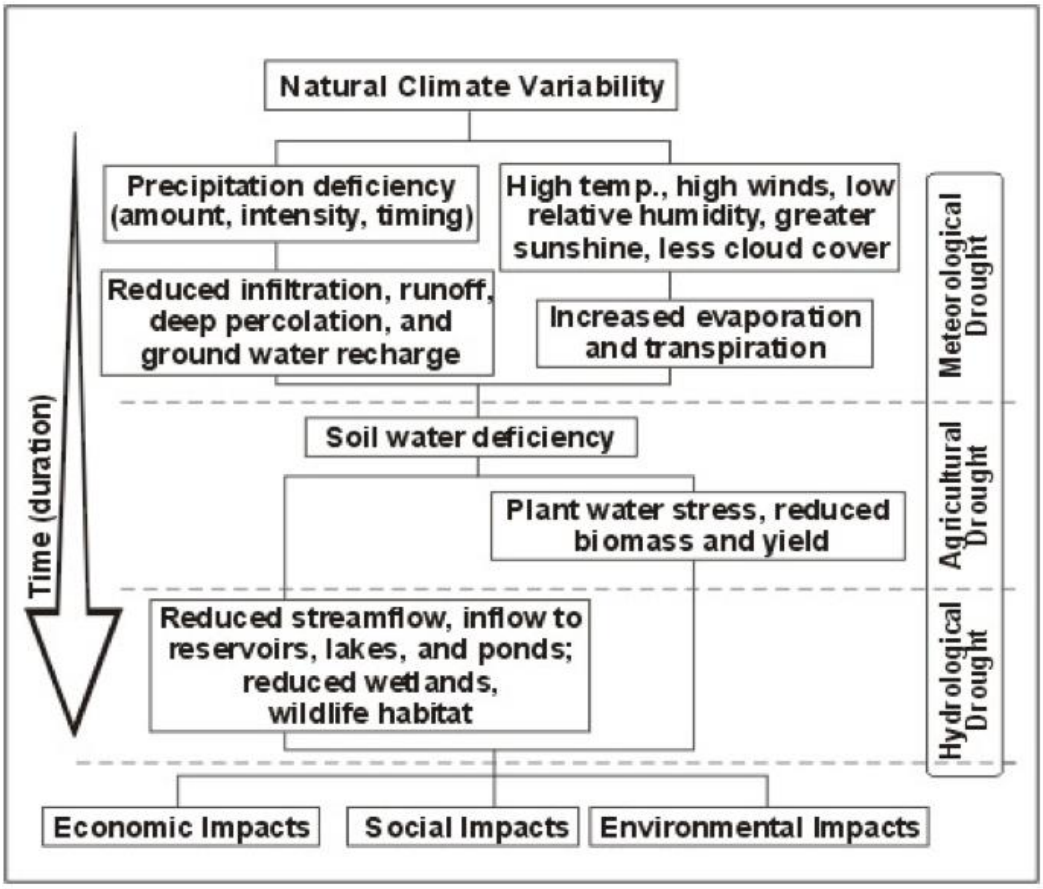

Figure 2:1 Propagation of drought in the climate system (after Wilhite 2000a)

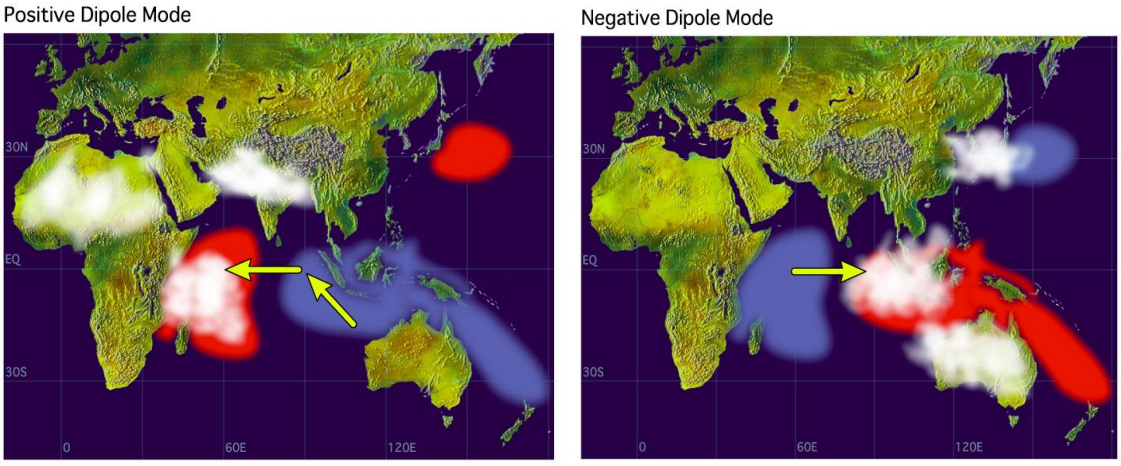

Figure 2:2 Positive and negative modes of the Indian Ocean Dipole (source: JAMSTEC 2015). The red color represents warmer SSTs whilst blue indicates colder.

Chapter 3

DATA AND METHODOLOGY

3.1 Introduction

Climate datasets have become more widely accessible to the climate research community since satellite data and model reanalyses became available in the past 20 years. Before that, National Meteorological and Hydrological Agencies were the sole custodians of in-situ weather, climate and hydrological data.

Historically, rain gauge station data have been widely used in drought research studies but several limitations have also been noted. For example, different types of rain gauges have been used in different regions (Kidd 2001). The distance between gauges also varies widely and may not be representative of aerial rainfall due to high spatial variability of rainfall particularly in semi-arid regions. Rain gauges are also sparse in remote areas such as mountainous regions or the vast oceans. In cases of severe weather and extensive flooding, rain gauges may be inundated for several days such that surface rainfall observations are not possible. Rain gauge observations are also discontinuous and incomplete in many regions of southern Africa (Unganai and Kogan 1998), often containing gaps which occur due to non-climatic factors such as political instability (Kidd 2001; Reason *et al.* 2006) and inadequate funding of meteorological services (Reason and Jagadheesha 2005; Glad 2010).

Some sudden changes in observations occur due to relocation of a station, new instruments or changes in observer (von Storch and Zwiers 1998). Hence, some quality control is required with gauge observations. Wars and civil strife have also disrupted meteorological observations in some countries. In cases where the data are available, station data access is restricted and sometimes the data are sold at high cost. There is a trend in many weather services to privatize; they do not report their observations to global networks in real-time or later.

The vertical structure of the atmosphere during drought events is studied using upper air observations which are also sparse over much of the African continent. Observations of temperature, humidity, geopotential height and wind in the upper air at various pressure levels are done using radiosonde weather balloons. Radiosondes transmit observations to a ground based station via radio signal. They are expensive to procure and for this reason upper air observations are mostly unavailable and sparse over southern Africa.

In the absence of reliable and continuous station observations, satellite estimates of meteorological parameters become critical as they are continuous in time and space, at least since 1979. Meteorological parameters that can be retrieved from satellite information include clouds and precipitation, surface temperature and reflectance, winds, radiation and lightning and vertical profiles of temperature and humidity. Satellites record monochromatic radiance (signal) which is detected by a radiometer within specific electromagnetic bands including visible, infrared and microwave.

Observations of land surface characteristics and other environmental variables such as vegetation health (greenness), fraction of photosynthetically active radiation, surface soil moisture, evapotranspiration and albedo have also been made possible by satellites since about 1979.

Climate Reanalysis datasets refer to historical observations that use Numerical Weather Prediction (NWP) models to analyze and interpolate into a gridded field. Retrospective analyses “reanalyses” provide data products which are widely used in climate research, including meteorology, oceanography, hydrology and other geophysical sciences. They are a combination of observations and simulations such that where the observations are sparse, the reanalyses are dominated by simulations.

Crop yields and river flow data have also become widely available in recent years. Historically, national grain collecting centers were the most reliable sources of agricultural crop yields. Today, several credible sources of crop yield (e.g. Food and Agriculture Organization of the United Nations Statistics Division (FAOSTAT), Agricultural Research

Council (ARC) and river flow data (SA hydrological service) and soil moisture (e.g. GRACE satellite) exist.

The aim of this chapter is to define the datasets employed in this thesis, their sources and to describe and justify the methods used to analyze them.

3.2 Description and sources of data

To achieve the aims of this thesis, several datasets were obtained from global and regional centers and analyzed. In some cases, the climate hubs allowed for online interactive manipulation and investigation of the data. The datasets used may be classified under their climatic domain as atmospheric, ocean or terrestrial (land surface) as indicated in Table 3.1. The variables in the atmosphere are specified as either surface or at pressure levels, being of higher spatial resolution at the surface than aloft. Some variables are observed whilst others are derived therefrom. Some of the data are observed at the surface, remotely sensed by satellites or derived from model reanalyses.

The datasets analyzed in this thesis mainly span the period from 1979-2012 whilst a few are more recent (e.g. MODIS LST data). Rainfall, moisture parameters, surface heat fluxes and circulation are presented first, whilst ocean and land surface parameters are presented later. The data for drought impacts on maize yields and surface hydrology span much longer periods. Some of the data are centralized (or standardized) using the following equation

$$Z = \frac{(x_i - \bar{x})}{\sigma} \tag{3.1}$$

where x_i is a discrete data point, $\bar{x}$ is the historical mean whilst σ represents the standard deviation.

3.2.1 Rainfall

The focus of this study is a region of limited observations (especially over Botswana) such that an analysis of gauge observations alone will not provide an adequate spatial

representation of the rain field (Figure 3.1). In addition, there are not many real-time operating automatic stations in southern Africa and therefore rain gauge observations are combined with satellite estimates to monitor and analyze the rainfall of the region.

The prime rainfall datasets employed here are the Global Precipitation Climatology Project (GPCP) version 2.3 which uses multiple observing platforms including satellite and surface observations. Local rain gauge observations are merged with passive microwave rain rates from polar orbiting meteorological satellites and estimates from IR sensors on geostationary satellites (Huffman *et al.* 2009). The data are interpolated to a 2.5° x 2.5° resolution at monthly timescales from 1979 to 2013. The rain gauge observations in the GPCP are obtained from the Global Precipitation Climatology Center version 7 (GPCCv7; Schneider et al. 2013).

The GPCCv7 dataset is an optimal gauge interpolation, whilst the University of East Anglia's Climate Research Unit (CRU) datasets are similarly based on gauge observations over land areas. Other satellite based rainfall products that extend over land and oceans include the Climate Prediction Center Merged Analysis of Precipitation (CMAP).

The GPCP rainfall dataset over southern Africa (averaged over 22-32E; 15-28S) exhibits a well-defined annual cycle which is also found in the GPCCv7, the European Center for Medium-Range Weather Forecasts's (ECMWF) Interim Reanalysis (ERA-Int) rainfall datasets and the National Centers for Environmental Prediction (NCEP) Climate Forecast System Reanalysis (CFS-R) rainfall dataset (Saha *et al.* 2010) which is drier (Figure 3.2). The GPCPv2.3 dataset are obtained via the KNMI Climate Explorer Tool (climexp.knmi.nl) and the NCEP PSD Interactive climate analysis and plotting webtools (https://www.esrl.noaa.gov/psd/cgi-bin/data/getpage.pl).

3.2.2 Relative humidity

Relative Humidity (RH) is a measure of the amount of water vapor in the atmosphere. It is the ratio of the mass of water vapor in the air relative to what the air can hold at the

same temperature and is usually presented as a percentage. While RH varies according to temperature, monthly averages provide useful information particularly in vertical section, as analyzed from the NCEP Reanalyses in Chapter 5. The data are obtain at 2.5° x 2.5° resolution and are available online from https://www.esrl.noaa.gov/psd/data since 1948.

3.2.3 Outgoing longwave radiation

Outgoing Longwave Radiation (OLR) data are used to analyze variations in convection over southern Africa. OLR refers to the radiation that is emitted by the earth's surface and its atmosphere, undergoing attenuation as it escapes upward to be detected by satellites. In the tropics, regions of high OLR are regions of high surface temperature, clear skies (or few clouds) and dry weather. Conversely, regions of low OLR are regions of deep convection, frequent cloud and high rainfall. Thus, OLR has been widely used as a proxy for cloud, convection and precipitation in several studies (e.g. Levey 1993; Levey and Jury 1996; Pohl *et al.* 2009; Macron *et al.* 2014; Ratnam *et al.* 2015). NOAA Interpolated OLR are analyzed here at 2.5° x 2.5° at the top of the atmosphere. Jury *et al.* (1993b) found a strong negative correlation (-0.93) between rainfall and OLR over southern Africa. Strong positive OLR anomalies can therefore indicate persistence of drought conditions.

3.2.4 Circulation parameters

The immediate cause of drought is a subsiding atmospheric circulation around a persistent anticyclonic cell. Circulation anomalies are investigated at important levels in the atmosphere (e.g. surface, 850 hPa, 500 hPa and 200 hPa). Mean Sea-Level Pressure (MSLP) are analyzed over the oceans but in some cases the 850 hPa level is preferred over Mean Sea Level (MSL) to represent the surface because of the high plateau over the southern Africa landmass. The strength and location of surface highs and lows is an important determinant for areas of uplift and subsidence.

Geopotential (Φ) refers to the work done to lift a unit mass to a height z from mean sea level and is given by

$$\Phi = \int_0^z g dz \approx gz \qquad (3.2)$$

where g is gravity and dz is the geometric height z. Whereas, geopotential height (Z) is an approximation of the actual height in the free atmosphere of a pressure surface above mean sea level and is given by

$$Z = \frac{\Phi}{9.80665} \tag{3.3}$$

Geopotential height therefore represents ridges and troughs in the upper air, the equivalent of surface anticyclones and cyclones. Geopotential height anomalies at various levels (850 hPa, 500 hPa and 200 hPa) are a useful indicator of stability and uplift of moisture, clouds and precipitation. The middle level (~500 hPa) geopotential height anomalies during drought conditions are analyzed and related to NDVI, river flows and remote influences such as ENSO. Vertical sections of geopotential height anomalies are also mapped, averaged by longitude and latitude over southern Africa.

Composite zonal (u), meridional (v) and vertical (w converted to ω) components of the wind vector and anomalies are also analyzed over southern Africa and the adjacent oceans from the surface to the upper levels. Vertical velocity ω is given by

$$\omega = \frac{Dp}{Dt} \tag{3.4}$$

where p is pressure and t is time.

Since pressure decreases monotonically with height, ω is negative for rising motion (uplift) and positive for subsidence. Therefore, dry or drought conditions are consistently associated with strong positive values of ω over large areas.

Vertical motion (uplift and subsidence) is closely related to divergence (or convergence) of the horizontal wind (Barry and Chorley 2003). Divergence is composed of transverse (directional) divergence and downstream (velocity) divergence. The geostrophic wind is non-divergent (Holton 2004) and therefore the divergence of the actual wind may be determined from the divergence of the ageostrophic wind. The downstream component of the divergence ($\nabla . u$) field of the horizontal wind is given by

$$\nabla . u = \frac{\partial u}{\partial x} + \frac{\partial v}{\partial y} \tag{3.5}$$

where (∂v) and (∂u) represent horizontal change in meridional and zonal velocities while (∂x) and (∂y) represent horizontal change in distance in the x and y directions. Negative values of velocity divergence represent convergence. In this thesis, divergence is analyzed during drought at the surface and in the upper air.

Vorticity is a measure of rotation or angular velocity in the circulation (Barry and Chorley 2003). This maybe planetary vorticity (due to earth rotation) or relative vorticity (due to wind shear or curvature). The shear component of relative vorticity (ζ) is given by

$$\zeta = \frac{\partial v}{\partial x} - \frac{\partial u}{\partial y} \tag{3.6}$$

and planetary vorticity may be given by the Coriolis parameter (f)

$$f = 2\Omega sin\phi \tag{3.7}$$

where $\Omega = 7.292 \text{ x } 10^{-5}\, rads^{-1}$ represents the angular velocity of the earth and ϕ is the latitude which is negative in the Southern Hemisphere. Cyclonic vorticity is negative and clockwise in the Southern Hemisphere whilst anticyclonic vorticity is positive and counterclockwise. Relative vorticity and divergence are analyzed in the lower levels from 850-700 hPa and in the upper air from 250-200 hPa. The 500 hPa surface is important as it is considered the level of non-divergence (Barry and Chorley 2003) separating areas of divergence from convergence.

Instead of pressure levels, some model derived circulation variables are analyzed at sigma levels. The sigma (σ) coordinate system is defined as

$$\sigma = \frac{P}{P_s} \tag{3.8}$$

where P is the pressure level at which the variable is being analyzed and P_s is the surface level pressure. Therefore, values of σ vary from nearly 0.2101 in the upper air to 1 at the surface. Sigma levels follow the terrain and may represent continuous fields better.

The circulation parameters analyzed here are obtained mostly from the NCEP/NCAR Reanalysis Project (Kalnay *et al.* 1996) and NCEP-DOE Reanalysis 2 (Kanamitsu *et al.* 2002) and analyzed in the Grid Analysis and Display System (GrADS). The NCEP/NCAR reanalysis have a global coverage at 2.5° x 2.5°, T42 Gaussian, T62 spectral grid

available at daily and monthly time steps, with 17 pressure levels and a coverage from 1948-present.

3.2.5 Surface heat fluxes

Energy gained by the earth's surface which is not lost through radiation may be used for evaporation (and converted to latent heat), to raise the temperature of the air (and converted to sensible heat through conduction and convection) and to raise the temperature of the surface (soil or water). Therefore the surface energy balance is given by

$$F^* = F_{SH} + F_{LH} + F_{GS} \tag{3.9}$$

where F_{SH} represents sensible heat flux, F_{LH} is latent heat flux and F_{GS} is the ground storage. The partitioning of energy into latent and sensible heat fluxes depends largely on surface soil moisture and also vegetation cover which is important for creating microclimates.

Sensible Heat Flux (SHF) and Latent Heat Flux (LHF) that are analyzed here are obtained from ECMWF ERA-Int, NCEP CFS-R and NASA Modern-Era Retrospective Analysis for Research and Applications (MERRA). A comparison of LHF over southern Africa from MERRA, ERA Int and CFS-R reanalyses shows a well-defined annual cycle with a peak in the late summer (February) and a minimum in the dry season (Figure 3.3). The annual cycle for SHF also minimizes during the winter but reaches a maximum in the late spring (October) prior to the onset of the rainy season (Figure 3.4). In both cases, the MERRA LHF and SHF are consistent and are therefore selected for further analysis in this thesis. The data are multiplied by 0.0345 to convert Wm^{-2} to mm/day for comparison with rainfall data.

The MERRA heat fluxes are calculated from the bulk aerodynamic formulas

$$LHF = \rho C_e L_v (Q_s - Q_a)(U_{10}) \tag{3.10}$$

$$SHF = \rho C_h C_p (T_s - T_a)(U_{10}) \tag{3.11}$$

where ρ is air density, C_e and C_h are exchange coefficients of moisture and heat, C_p is specific heat capacity of water, L_v is the latent heat of vaporization, Q_s and Q_a are specific humidity for the surface and air respectively, T_s and T_a are surface and air temperature respectively and U_{10} is the wind speed at 10 m.

3.2.6 Evapotranspiration and potential evapotranspiration

Evapotranspiration (ET) is a key variable of the surface water and energy balances. It represents surface water loss from the soils, water bodies and vegetation to the atmosphere via the processes of evaporation and transpiration (Kalma *et al.* 2008). ET is an important component after precipitation in the surface water balance (Sheffield *et al.* 2010). Transpiration may decrease during a drought especially in agricultural areas as crops may die. High evaporation rates coincide with high land surface temperature, sunny and windy weather.

Ground based observations of ET are essentially not available (Sheffield *et al.* 2010) and therefore ET is mostly modelled. ET data used here are generated by the Global Land Data Assimilation System version 1 (GLDAS-1) and version 2 (GLDAS-2) using the monthly 0.25 x 0.25° NOAH model experiment. The version 2 data are available from 1948-2000 and version 1 from 2000 to present.

Potential evapotranspiration (PET) is an expression of the atmospheric demand for water vapour, and is usually greatest over the arid regions. PET may be derived from the Penman (or Penman-Monteith) formula or using a more simplified method by Thornthwaite (1948). The PET calculation of Penman takes into account solar radiation, humidity and wind. Since ET and PET are directly related, PET is preferred here because it represents the atmospheric demand for water vapour (Matsoukas *et al.* 2011) which should be high during drought conditions.

PET analyzed in this thesis was obtained from CRU via the International Research Institute for Climate and Society (IRI) climate data library.

A CRU self-calibrating PDSI (scPDSI) is used in this thesis for comparisons with the drought index derived in section 3.3.1 and also with variables such as runoff in the Limpopo. The scPDSI (Wells *et al.* 2004) is a variation of the original PDSI described by Palmer (1965). The scPDSI was aimed at allowing comparisons between drought analyses from different climatic regimes and is also computed from time series of temperature and precipitation. It is calibrated using local soil/surface conditions which are better than the fixed coefficients in the original PDSI (Dai 2011a).

3.2.7 Land-surface and maximum air temperature

Land surface temperature (LST) data are also used to characterize drought over the subcontinent. LST may also be considered as a form of declouded OLR. United States Geological Survey (USGS), Land Distributed Active Archive Center (DAAC), Moderate Resolution Imaging Spectroradiometer (MODIS) LST data at 1 km resolution obtained via the International Research Institute for Climate and Society (IRI) web portal (http://iridl.ldeo.columbia.edu/) are used in this analysis. The MODIS LST data are available since 2000 and have been detailed by Huete *et al.* (2002) and Vancutsem *et al.* (2010). LST data may also be used to estimate air temperature (e.g. Vancutsem *et al.* 2010) and also to detect the risk of spontaneous combustion and fire.

Due to the limited nature of the LST data, summer LST are used to identify intense dry spells during the drought of 2003 as a case study. After ranking, the hottest are considered to represent intense dry spells (drought).

Maximum air temperature data from 1960 - 2009 are analyzed over southern Africa using the CRU data. The maximum temperature is the highest temperature of the day recorded at 2 m above ground level and which usually occurs in the late afternoon (~3pm) on a fine day in the subtropics. Some studies have found a link between high surface and air temperatures, heat waves and drought in southern Africa (e.g. Lyon 2009).

3.2.8 Sea-surface temperatures

Sea-surface temperature (SST) anomalies over the Niño regions (Figure 3.5) of the equatorial Pacific Ocean are analyzed for remote forcing on the regional rainfall. SST anomalies in the Indian Ocean and tropical Atlantic Ocean are also analyzed for relationships with seasonal rainfall and drought events. The influences of El Niño Southern Oscillation (ENSO) events, the Indian Ocean Dipole (IOD) and the Indian Ocean Subtropical Dipole (IOSD) may be shown in phase or out of phase using SST anomaly maps. The NOAA Optimum Interpolated SST (OISST) version 2 (v2) data are obtained from NOAA/OAR/ESRL PSD, Boulder, Colorado, USA from their website at http://www.esrl.noaa.gov/psd/ and analyzed here.

The OISST (v2) data are assimilated using satellite and in-situ SSTs including sea-ice simulated SSTs. The data are available at a spatial resolution of 1.0° latitude x 1.0° from 1979-2014 and have been detailed by Reynolds *et al*. (2002).

3.2.9 ENSO indices

Several indices have been developed to measure the strength of ENSO. Some are based on SST anomalies whilst others are based on Sea-Level Pressure (SLP) anomalies. One measure of ENSO is the Southern Oscillation Index (SOI) which is a standardized difference of SLP between Tahiti (eastern Pacific Ocean) and Darwin (northern Australia). It measures fluctuations of SLP between the west and central equatorial Pacific Ocean. Prolonged negative values of SOI indicate El Niño whilst sustained positive values reflect the presence of a La Niña event/episode in the equatorial Pacific Ocean.

There are several formulas used to calculate the SOI but the data used here calculated as follows:-

$$SOI = \frac{P_{diff} - P_{diffav}}{SD(P_{diff})} \qquad (3.12)$$

where $P_{diff} = Average\ Tahiti_{MSLP} - Average\ Darwin_{MSLP}$

P_{diffav} is the long-term average of the pressure difference P_{diff}

$SD\ (P_{diff})$ is the long-term standard deviation of P_{diff}

The SOI data employed here are obtained from the NOAA Climate Prediction Center (CPC). SST anomalies in the Niño regions are also used to show statistical correlations with circulation parameters.

3.2.10 Indian Ocean indices

The Indian Ocean Dipole may be measured by the Dipole Mode Index (DMI). The DMI is an anomaly between SSTs in the western (50°E-70°E, 10°S-10°N) and eastern (90°E-110°E, 10°- equator) (Saji *et al.* 1999, Behera and Yamagata 2003). SSTs used in the determination of the DMI are derived from HadSST1 and obtained via the Royal Netherlands Meteorological Institute (KNMI) Climate Explorer. The IOD can also be represented in terms of SLP and OLR.

As with the DMI, the IOSD Index is calculated from an anomaly difference of SSTs between the western (55°E-65°E, 27°S-37°S) and eastern (90°E-100°E, 18°S-28°S). The IOSD are also computed from HadSST1 data.

3.2.11 Surface soil moisture

A farmer, a soil scientist, a hydrologist and a meteorologist may all have a different perception of soil moisture. Surface soil moisture data is analyzed here for variability as well as its response to meteorological drought. Some drought indices are based on soil moisture anomalies. Satellite estimates of soil moisture have become available recently through passive microwave sounding even though only a few centimeters can be estimated. Soil moisture data are obtained from NASA Gravity Recovery and Climate Experiment (GRACE) beginning in 2002. The data are derived from satellite observations of changes in gravity which result from changes in ground water, surface water (lakes, dams) and surface soil moisture. The data are obtained via http://geoid.colorado.edu/grace/.

Climate Prediction Center (CPC) surface soil moisture v2 reanalysis data are also used to show the spatial patterns of soil moisture anomalies during drought. The data are interpolated at 0.5 x 0.5 degree resolution and available from 1948 and have been detailed by Fan and van den Dool (2004).

3.2.12 Normalized Difference Vegetation Index

Satellite Normalized Difference Vegetation Index (NDVI) is a measure of vegetation greenness and has been widely used in climate research and drought monitoring. The NDVI is highly correlated with rainfall and ET in semi-arid regions. The NDVI detects reflectance of vegetation in the visible bands of the electromagnetic spectrum (Chikoore and Jury 2010) and may be calculated as follows:

$$NDVI = \frac{NIR-VIS}{NIR+VIS} \tag{3.13}$$

where VIS and NIR are spectral measurements of vegetation reflectance in the VISIBLE (Red) and NEAR-INFRARED bands of the electromagnetic spectrum. The NDVI calculates the differences between reflectance in the NIR and absorption in the Red bands. The wavelengths average 0.67 µm (VIS) and 0.86 µm (NIR) whilst vegetation reflectance peaks at about 0.8 µm, such that the NIR band is more sensitive (Tucker 1979). Typically, NDVI values on the earth's surface range from -0.1 for water bodies to 0.9 for dense vegetation (Tucker 1979). NDVI below 0.3 indicates little or scarce vegetation with bare soils (Jury *et al*. 1997b) whilst negative values reflect clouds, water and snow (Wang *et al.* 2003). Anomalously low values of NDVI observed over the eastern coast of southern Africa may be an artifact of averaging with ocean pixels.

With more than 30 years of observations now, the NDVI may be used to analyze the extent and frequency of drought (Anyamba and Tucker 2012). In an earlier study, Unganai and Kogan (1998) have also shown that the spatial aspect and temporal evolution of droughts in southern Africa can be mapped using NDVI data.

NDVI datasets are employed in this thesis to map and quantify the spatial extent and temporal evolution of drought events over the subcontinent. Several versions of NDVI data are available but the datasets used in this study are obtained from the United States Geological Survey (Tucker *et al.* 2005) and MODIS (Didan 2015).

3.2.13 Crop yield and value of agricultural production

Crop yield data are obtained from FAOSTAT and South Africa's ARC. The data are obtained at monthly resolution from 1961 to 2012 (FAOSTAT, faostat3.fao.org) and from 1981-2010 (ARC). Maize yields from the ARC are for South Africa's Free State Province which is the main maize growing region in the country. When compared against the national yield from FAOSTAT a high correlation of R = 0.95 (90% significance) is noted. Combined maize yields for the study region are analyzed and correlated with rainfall, NDVI and ENSO. The bulk of maize yields in the Southern Africa Development Community (SADC) is from South Africa, but the FAOSTAT maize yield data for Botswana and Zimbabwe are also analyzed separately in Chapter 6.

The value of agricultural production is also obtained from FAOSTAT at annual resolution from 1961-2012. It is a measure of the market value of agricultural products at the time they were produced and converted to the US dollar (http://faostat.fao.org/site/613/default.aspx#ancor).

3.2.14 Hydrological data

The study area is dominated by two major river systems i.e. the Zambezi in the north and the Limpopo in the south. Station data are obtained and analyzed for 2 stations on the 2 basins which have a long record of observations.

In South Africa, hydrological data are limited in supply and are also inconsistent in terms of reporting periods (Olivier *et al.* 2013). A review of gauging in South African rivers is given by Wessels and Rooseboom (2009). The main river flow data analyzed here are obtained for the Limpopo catchment from the South Africa's Department of Water Affairs (Hydrological Information System). Verified hydrological data are obtained for the

Limpopo River at Botswana A5H006 (22.9°S, 28.0°E) for the period from 1971-2012. Monthly peak flows are obtained online from www.dwaf.gov.za and analyzed.

For the Zambezi catchment, river flow data is obtained from the Zambezi River Authority (ZRA) at monthly resolution from 1948-2010. Zambezi River flow data is analyzed for the station at Victoria Falls (25.9°E, 17.9°S). Natural flows are recorded at both stations as there are no dams or diversions upstream. River flow data does not necessarily represent point data, but conditions in the catchment upstream of the gauging station (Rees *et al.* 2004).

Some problems associated with river flow data may be missing data or missing data entered as zero flows (Rees *et al.* 2004). However, it is also argued that in drought conditions, river flows are low and may even drop to zero (Hisdal *et al.* 2004). To deal with missing data entered as zero flows for Limpopo River at Botswana during the dry season, only the summer flows are averaged and analyzed for the peak months of February and March.

Reservoir level data for Lake Kariba for 1961-2012 are obtained from the ZRA. Lake Kariba was impounded in 1958 as a collaboration between Northern Rhodesia (now Zambia) and Southern Rhodesia (now Zimbabwe). The recorded end-of-month levels (meters) are analyzed. The data is provided starting from 1961, but the period from 1963 is considered when the dam had reached a minimum operating level.

3.3 Research Methods

By definition, climate is a statistical average of daily weather and may be studied as a time series spanning several decades. Therefore, several time series analysis techniques are employed in the analysis of drought in southern Africa. The approach is to consider the long-term mean climate (1979-2012) and then to identify drought events using a P-E anomaly drought index. The focus shifts to the drought events identified and investigation of meteorological structure and circulation over southern Africa and the adjacent oceans,

and how they may be related to cycles of ENSO and other remote forcings. The spatial extent, and impacts of drought on maize yield, vegetation and runoff are then determined.

3.3.1 Drought index

Drought may be quantified using absolute measures such as determining soil moisture levels or in relative terms such as the PDSI, or the two approaches may be compared (Trenberth *et al.* 2014). Precipitation alone is not the only control on surface water resources such as streamflow and soil moisture (Cook *et al*. 2014). The atmospheric demand for evaporation is also determined by temperature, humidity and wind which are also important variables.

The drought index employed in this research is based on an anomaly of the surface water balance. Precipitation falling in a catchment is either stored in the soils, leaves the system as runoff and groundwater or returns to the atmosphere via evaporation. The surface water balance is given by:

$$\Delta S = P - E - R - I \tag{3.14}$$

where ΔS (changes in storage) are related to the balance of gains by P (precipitation) and losses by E (evapotranspiration), R (runoff) and I (infiltration). Using scale analysis, and assuming that R and I are a < 10% fraction of P, the main drivers of the surface water balance are then $P - E$. The drought index is an expression of the anomaly in supply (precipitation) minus demand (potential evapotranspiration). This demand is frequently not met, particularly in water limited situations such as drought. In the $P - E$ anomaly drought index, GPCP precipitation and CRU PET are the main variables. It is found that PET exhibits a closer relation with SHF than with LHF (Figure 3.6) and is therefore a useful indicator of losses in the surface water balance.

The annual cycle of $P - E$ peaks in DJF coinciding with the rainfall maximum (Figure 3.7). A comparison of the $P - E$ anomaly index with the CRU scPDSI shows good agreement (Figure 3.8). The P-E index exhibits a weak upward trend (R^2=0.2192) whilst the PDSI is neutral (R^2=0.02) despite the severe droughts of 1992 and 1995.

A $P-E$ anomaly index is used to identify drought events over the study area during the satellite era from 1979-2012. Strong negative P-E anomalies indicate drought conditions. A number of drought periods are identified using this definition during 1979-2012 as shown in Figure 3.8. It is found that 1992 was the most severe drought to affect southern Africa during the study period (1979-2012). Consecutive multi-year droughts have occurred during 1982-84 and droughts were also most frequent during the 1980s according to this classification. A total of seven drought events (1982, 1983, 1984, 1987, 1992, 1995 and 2003) were identified using the $P-E$ anomaly index. They are classified as moderate, severe and extreme in Table 3.2.

3.3.2 Climatologies and anomalies

Long-term mean climatologies of several variables are presented as background to understanding the drought phenomenon. Long-term mean (1979-2012) spatial patterns of meteorological, ocean and land surface characteristics are mapped over southern Africa and the adjacent oceans as some climate drivers lie outside the domain of the study.

Temporally, climatologies are determined through time series analysis techniques. Long-term averages, seasonal means and annual cycles, standard deviations and trends are analyzed. Climatologies are presented either as Y-T graphs or as spatial maps generated using the GrADS interactive tool.

Anomalies are also an important climatological descriptor as they refer to deviations of observations from long-term climatologies or simply an exaggeration of the annual cycle. Standardized anomalies may also be determined by dividing anomalies with the long-term standard deviation. The base climatology against which the anomalies are computed is the WMO recommended 1981-2010. It is important that the same scales, color palate, contour intervals and wind vector scales are used to allow for inter-comparisons between seasons. The circulation (dynamic) and thermodynamic anomalies that cause drought are investigated to determine the meteorological structure of drought.

3.3.3 Correlation and trend analysis

Time series of seasonal rainfall and P-E over southern Africa are regressed onto SSTs and correlations are calculated between indices and fields. The analysis focuses on:

- time (leads and lags)
- space (spatial correlation, teleconnections)
- between 2 time series (cross-correlations)

Linear and 2nd order co-variance and trends are analyzed between several time series datasets used in this research. Correlations of ENSO indices such as SOI and Niño 3.4 SSTs with rainfall and circulation variables such as geopotential height, vector winds and omega are also made at 90% significance.

Typically, a time series (y_t) consists of a trend (T), cyclical component (C), seasonal cycle (S) and a random component (R) and may be given by

$$y_t = T + C + S + R \tag{3.15}$$

Trends may be linear or non-linear (polynomial) and simple linear regression is widely employed to determine linear trends whilst the statistical significance of those trends is required (typically using a student-t test). Trends in long-term rainfall, surface fluxes, PET, key drought characteristics as well as impacts data are analyzed.

Problems with linear trends are that sometimes long-term trends have shorter term trends embedded within them. Thus, it may be necessary to detrend a time series in order for subtrends and fluctuations to be determined. In this research, time series which exhibit a clear trend (e.g. maize yields) are detrended to remain with a seasonal cycle and fluctuations over time.

3.3.4 Wavelet analysis

While Fourier decomposition identifies cycles in time series data, wavelet analysis transforms a one-dimensional timeseries into a time-frequency domain (two-dimensional

image) portraying the time evolution of frequencies and scales (Lau and Weng 1995). The wavelet transform represents the signal at a number of scales. Dominant modes of variability are identified using wavelet analysis including how they evolve and when they occur (Torrence and Compo 1998). Wavelets are important in processing non-stationary climate signals.

Different wavelet functions may be used such as Morlet, Paul and DOG which may be continuous, orthogonal or non-orthogonal. Orthogonal wavelets are preferred for data compression whilst continuous wavelets perform better for scale analysis (Lau and Weng 1995).

The Morlet wavelet consists of a plane wave with amplitude modulated by a Gaussian and is defined as

$$\psi 0(\eta) = \pi^{-1/4} e^{i\omega 0\eta} e^{-1/2\eta^2} \qquad (3.16)$$

where $\omega 0$ is non-dimensional frequency (taken as 6 here) and η is non-dimensional time. The Morlet wavelet is suitable for feature extraction as it allows a balance between frequency localization and time (Grinsted et al. 2004). A cone of influence in a wavelet transform defines a region in which edge effects become significant (Torrence and Compo 1998).

Wavelet analysis has become widely used in climate research. Torrence and Webster (1999) used wavelet analysis to determine dominant periods of ENSO-Monsoon (Indian Monsoon) variability from 1871 to 1994. The AAO and ENSO influence on Baltic Sea ice conditions was also studied using a wavelet approach by Jevrejeva (2003). In this study, the Morlet wavelet is used to identify evolving cycles in the GPCP precipitation data following the approach of Torrence and Compo (1998).

3.3.5 EOF analysis

Dominant spatial and temporal modes of variability of geophysical phenomena may be analyzed using Empirical Orthogonal Function (EOF) analysis or Principal Component Analysis (PCA). The spatial regionalization of drought may be achieved through EOF

analysis (Cai *et al*. 2015). EOF analysis is a statistical method of data clustering which is widely used in the geophysical sciences for factor analysis. It reduces the dimensions in the data, computing new variables (EOFs) which are orthogonal in decreasing order of significance (Cai *et al.* 2015). Eigenvalues and eigenvectors are estimated from a characteristic equation. Most of the variance is represented through the first EOF (EOF1 or PC1).

The number of EOFs should be as many as the data being analyzed but only a few modes characterize substantial variance in the data. In order to determine the number of modes to retain for rotation and discussion a scree plot is made for eigenvalues against each EOF mode (e.g. EOF1, EOF2 etc). A scree plot allows for visual inspection of the important modes in the data which are found on the steep part of the plot. The varimax method of orthogonal rotation was used in this study.

EOF analysis has been widely used to analyze rainfall over southern Africa (e.g. Mulenga 1998; Jury 1999; Unganai and Mason 2001, Chikoore and Jury 2010). In this research, GPCP rainfall and SSTs are analyzed using EOF analysis to determine dominant drought modes in southern Africa. It should be remembered when interpreting results that EOF analysis is based on statistical principles and not on physical principles.

3.3.6 Composite analysis

In addition to case studies, drought events are also studied as part of a composite. Common characteristics of drought are identified using this technique. Composite analysis is a technique widely used in the geophysical sciences to analyze pattern similarity on several time scales (e.g. daily, monthly and seasonal). Composite analysis is sometimes referred to as a “selective climatology” as it provides a climatology of selected periods of time with a common “characteristic” e.g. periods of drought. Composites depict historically repeating patterns and trends better than individual events (Levey 1993; Mulenga 1998). Prominent characteristics of the selected drought events are highlighted whilst the noise of individual events is largely removed (Manatsa *et al.* 2011).

Mulenga *et al*. (2003) used composite analysis techniques in a study of droughts in northeastern South Africa (Limpopo). Several other studies have employed composite analysis in climate research in southern Africa (e.g. Levey 1993; Kabanda 2005; Mulenga 1998; Chikoore and Jury 2010; Manatsa *et al.* 2011).

In this study, the drought events of 1982, 1983, 1984, 1987, 1992, 1995 and 2003 are included in composites of the anomalies of various fields such as rain, relative humidity, soil moisture, geopotential heights and circulation parameters. The period of time averaging is mainly the summer months (DJF), with less attention to the dry season. The dynamic influences of the Atlantic and Indian Oceans and the ENSO phenomenon on drought characteristics over southern Africa are analyzed as drought composites by season. This technique is used throughout the thesis.

3.3.7 Event scale analysis

Whilst composite analysis techniques are useful, they sometimes group together potentially diverse events (Chikoore 2005). Drought events in a composite may have different spatial extent and different propagation characteristics (Chikoore and Jury 2010). In addition, each drought event has equal contribution to a composite despite differences in severity and also differences in the magnitude of the forcing mechanism (e.g. ENSO or non-ENSO droughts). In response to this, a case study approach is also used to study the major drought events as individual events during the 34 year period from 1979-2012. The cases of drought are identified and categorized by severity after McKee *et al*. (1993) highlighting that droughts are not the same in character. The 2003 case is also selected because several ‘new’ datasets only start at 2000 (e.g. GRACE soil moisture).

3.4 NOAA Earth System Research Laboratory

The Physical Sciences Division of the Earth Systems Research Laboratory (ESRL) allows for weather and climate research from local to global scales. The ESRL is used to map in vertical and plan views, the meteorological structure of drought over southern Africa and the adjacent oceans. A significant proportion of the composite analysis in this thesis is

done in this laboratory. Composites of monthly and seasonal NCEP Reanalysis relative humidity; MSLP; geopotential heights; zonal, meridional and vertical velocity; vector winds and OLR are analyzed there. Mean climatologies and anomalies from long-term mean are calculated. The new climate normal is 1981-2010 and therefore anomalies are calculated with respect to the 1981-2010 long-term mean. The NCEP Reanalysis data are available from 1948, but most of this thesis focuses on the satellite era post-1979.

3.5 KNMI Climate Explorer

The KNMI Climate Explorer is an interactive web-based climate analysis tool used to extract climate data and perform powerful statistical analyses. Surface and upper air variables available on KNMI include those from NCEP (CFS-R), ECMWF (ERA40 and ERA Int.) and NASA (MERRA). Statistical analyses performed include mean plots, seasonal cycles, difference plots, EOFs, and correlations with a field or other time series. Daily or monthly mean time series are investigated, including relationships between them. The Climate Explorer allows users to upload their own timeseries and investigate them; display, detrend or correlate them with a prescribed timeseries or climate indices. The KNMI Climate Explorer may be accessed online using a standard browser at climexp.knmi.nl and was used to perform some of the analyses.

3.6 IRI Climate Data Library

The IRI's data library (http://iridl.ldeo.columbia.edu/) contains a wide range of station, satellite and reanalysis datasets from different sources. The data library allows for users to download, view and map data, and perform complex statistical analyses such as EOF analysis. NDVI images, LST, regional elevation maps and the distribution of GPCC rain gauges in the study area are all generated via the IRI data Library. The N-S and E-W vertical structure of the circulation shown in Chapter 5 is also analyzed there. The library is accessible via iridl.ldeo.columbia.edu.

3.7 Grid Analysis and Display System (GrADS)

Some of the ocean and atmospheric variables displayed in this thesis are generated through the use of the Grid Analysis and Display System software. GrADS is an

interactive software platform that allows manipulation and visualization of earth system data. Monthly means and anomalies and other derived variables from the NCEP/NCAR Reanalysis I (1948-present) and the NCEP-DOE Reanalysis 2 (1979-2015) datasets in netCDF format are manipulated and displayed through GrADS. Most of the interactive websites and data portals mentioned above also use GrADS to display data.

3.8 Summary

This chapter has described the datasets employed in this research alongside the methods used to analyze them. In the process of justifying datasets and methods, some important results have also been revealed in this chapter and are summarized here

a) Rain gauge and other weather observations are sparse in southern Africa. The rainfall datasets preferred here are the GPCP v2 which compare favorably with rainfall datasets from other major centers. The primary period spans the period from 1979-2012. Sometimes analysis is done for periods prior to 1979 and also beyond 2012 to put the period within context.
b) Several statistical research methods and climate models are employed to investigate various fields.
c) A drought index based on the P-E anomaly is employed to identify droughts in this thesis. GPCP acts as the precipitation reference and seasonal cycle whilst the MERRA sensible heat flux denotes potential evapotranspiration.
d) This drought index identifies extreme drought events during 1992 and 1982, severe drought during 1983 and 1995, and moderate drought conditions during 1984, 1987 and 2003. Subsequent analyses will focus on these events.
e) Drought events were most frequent and more severe during the 1980s, but fewer compared to the 2000s. Successive droughts occurred during 1982-1983.
f) Whilst it was thought that PET would correlate with LHF, it is found that SHF reflects PET better such that SHF may be a useful drought indicator.
g) The annual cycle of P-E anomaly peaks in DJF coinciding with precipitation whilst soil moisture peaks in JFM.
h) The P-E index exhibits a weak upward trend whilst the PDSI is neutral despite the multiyear droughts that characterized the first half of the study period.

Chapter Tables and Figures

Table 3-1 Summary of the variables, parameters and fields obtained and analyzed in this thesis

DOMAIN	**VARIABLES**	
ATMOSPHERE	Surface	GPCP precipitation, P-E, latent heat flux, sensible heat flux, ET, PET, SLP, u and v wind components, 2 m air temperature, RH, Divergence
	Pressure Level	500 hPa geopotential heights, u, v, ω wind components, RH, OLR
OCEAN	Nino 3.4 Index, SOI, Indian Ocean and Atlantic Ocean SSTs	
TERRESTRIAL	LST, surface soil moisture, NDVI, Zambezi flow, Kariba lake levels, maize crop yields, value of agricultural productivity	

Table 3-2 Ranked drought events identified by a P-E anomaly index over southern Africa

	Drought category			
	Moderate	**Severe**	**Extreme**	**Successive**
Drought Season	1984	1983	1992	1982-3
	1987	1995	1982	
	2003			

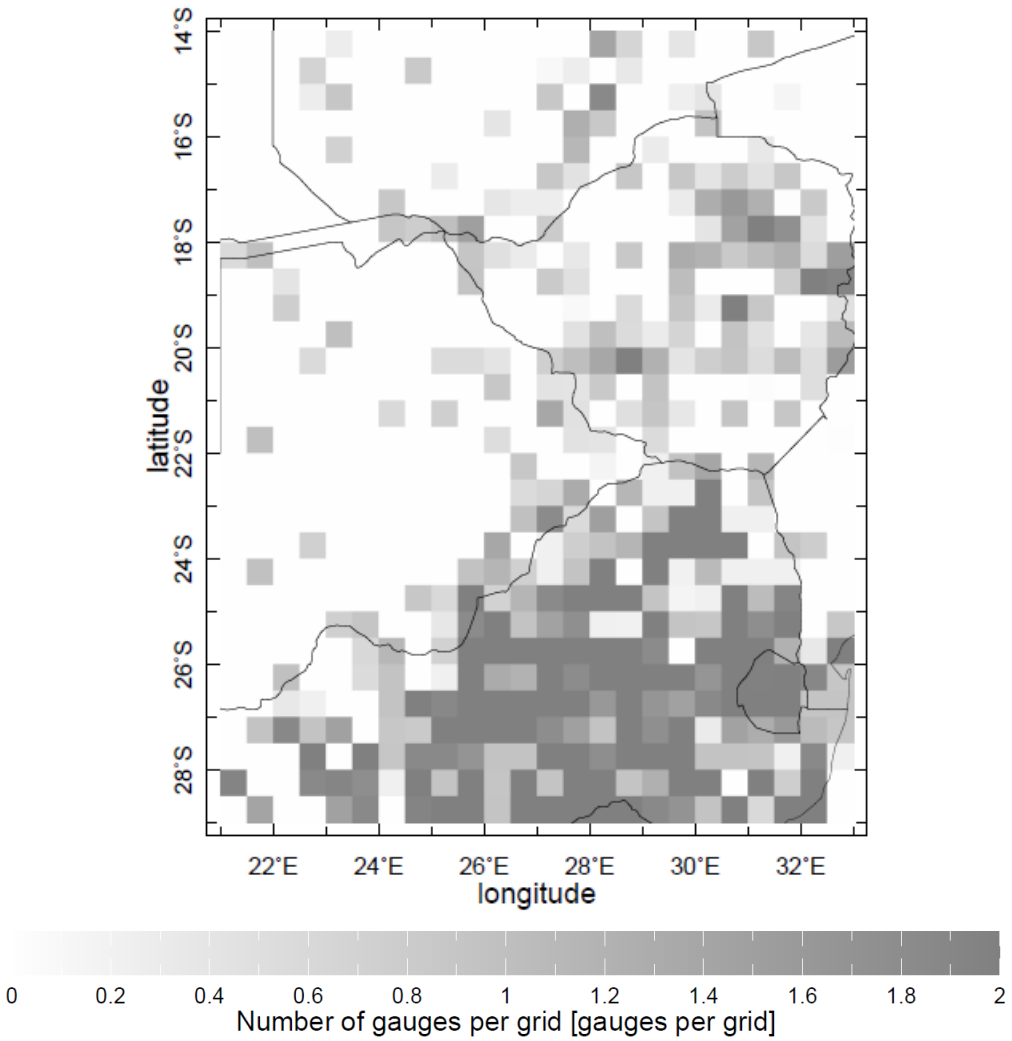

Figure 3:1 Distribution of GPCC rain gauges over the study area indicated by shading. The white spaces indicate no rain gauges in those gridboxes.

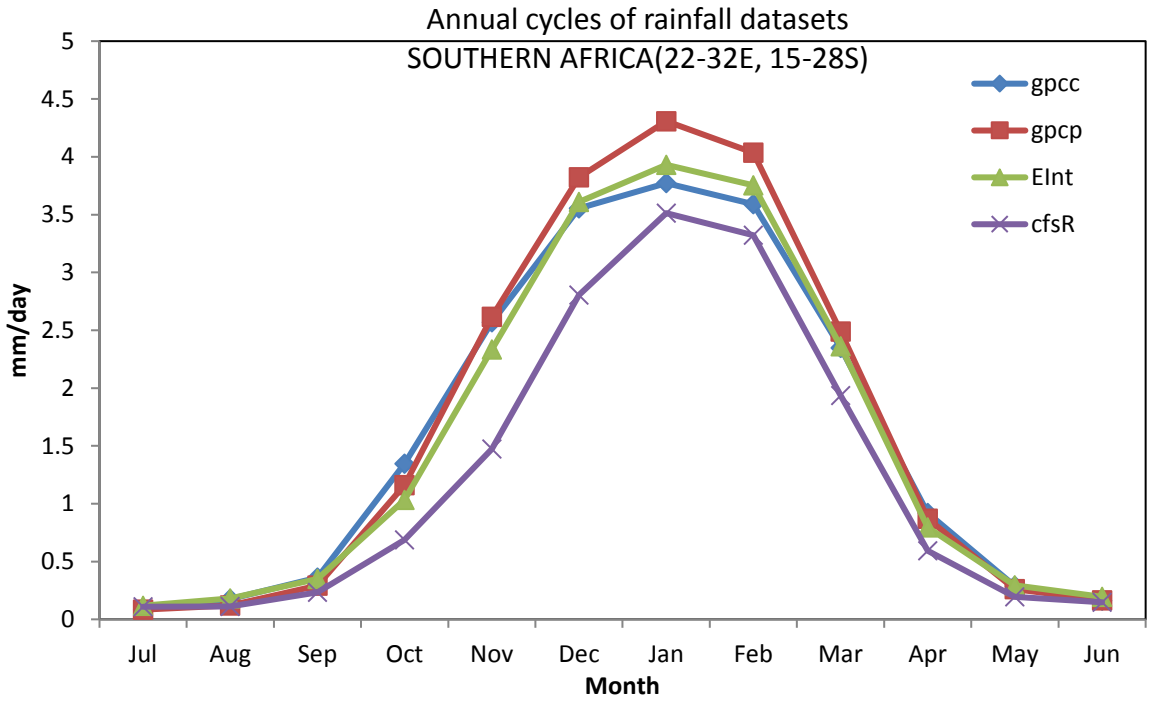

Figure 3:2 Mean annual cycles of GPCC, GPCP, ERA-Int and CFS-R rainfall datasets over the southern Africa region

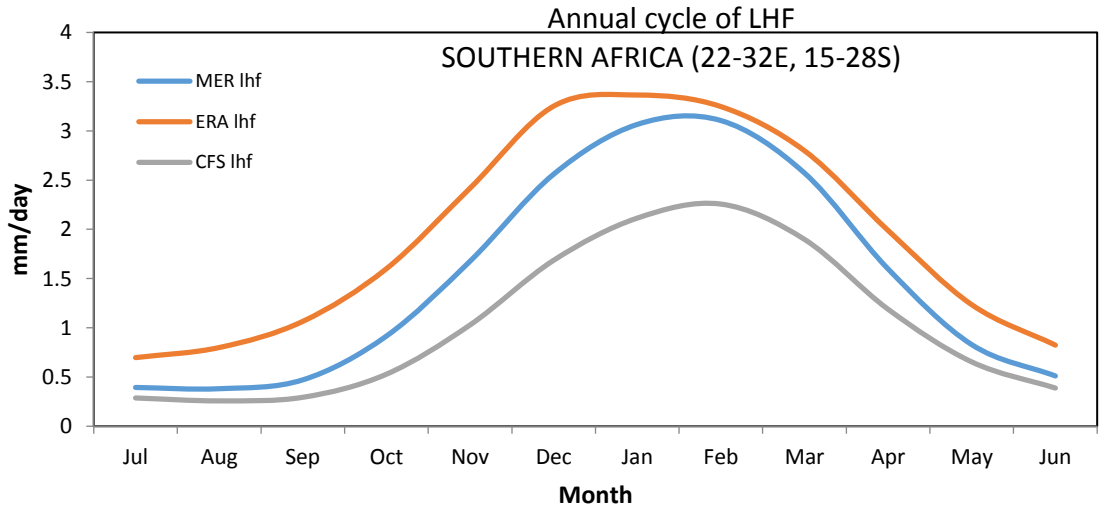

Figure 3:3 Mean annual cycles of LHF from MERRA, ERAInt and CFS-R reanalyses for the southern Africa region

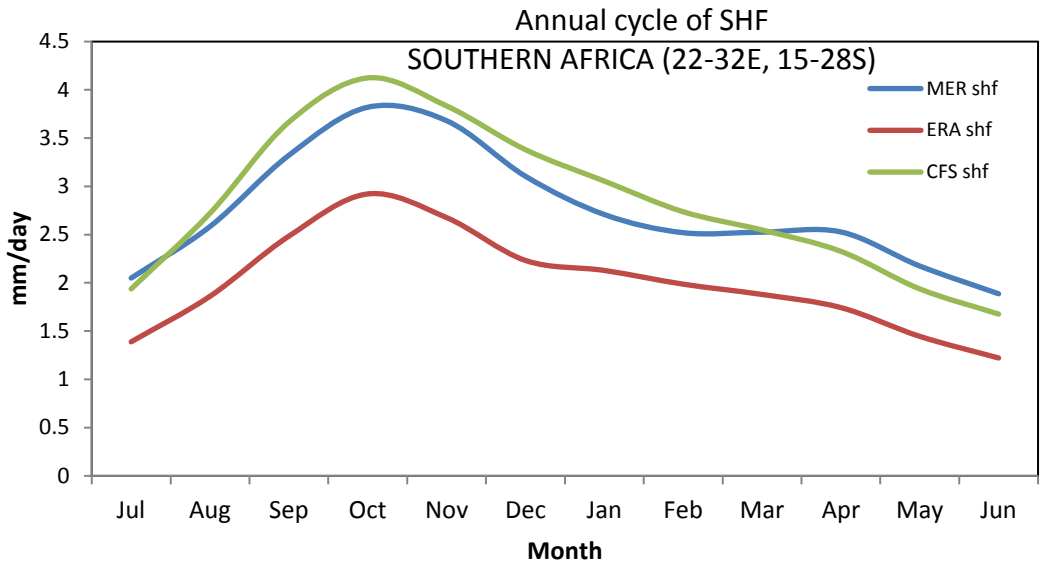

Figure 3:4 Annual cycle of SHF from MERRA, ERAInt and CFS-R reanalyses.

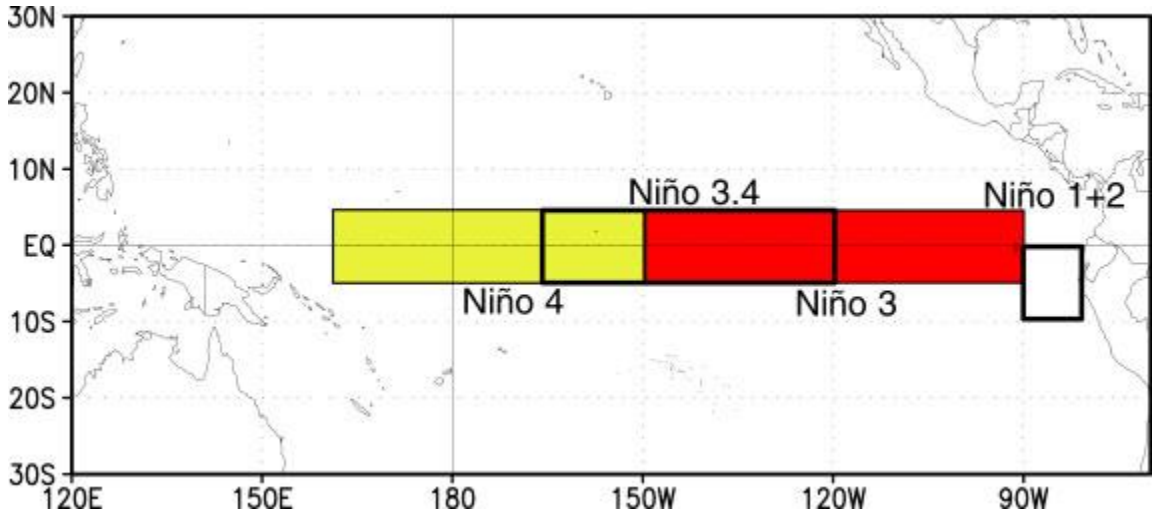

Figure 3:5 El Niño regions used to measure the strength of El Niño over the equatorial Pacific Ocean (source: Climate Prediction Center www.cpc.noaa.gov)

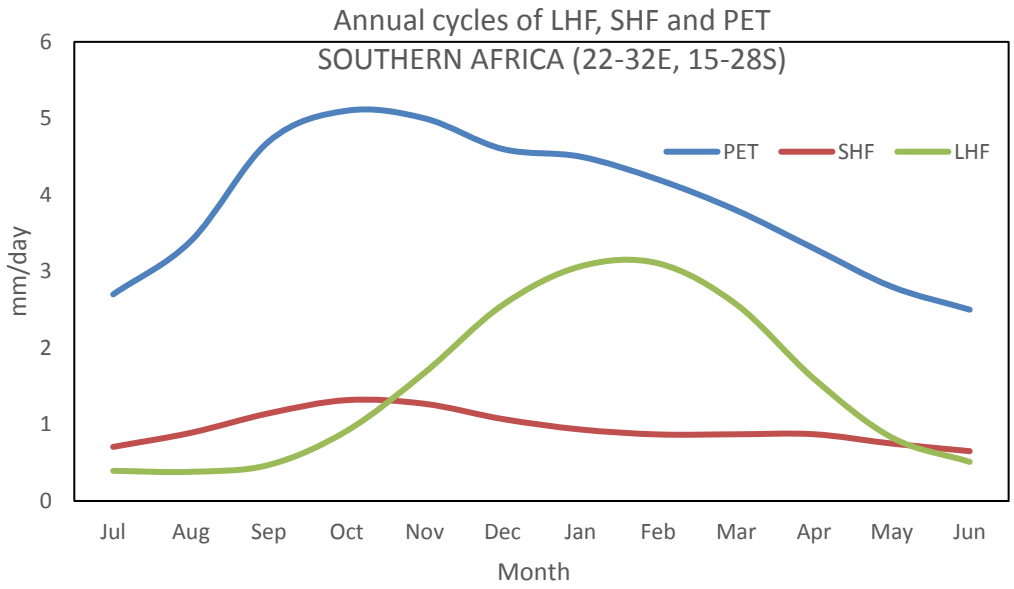

Figure 3:6 Mean annual cycles of LHF, SHF and PET over the southern Africa region

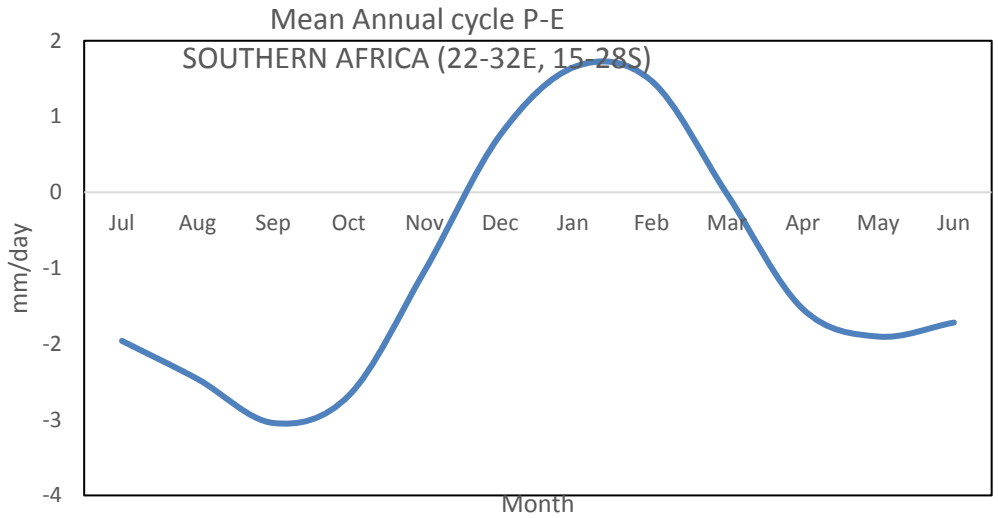

Figure 3:7 Mean annual cycle of P-E over southern Africa

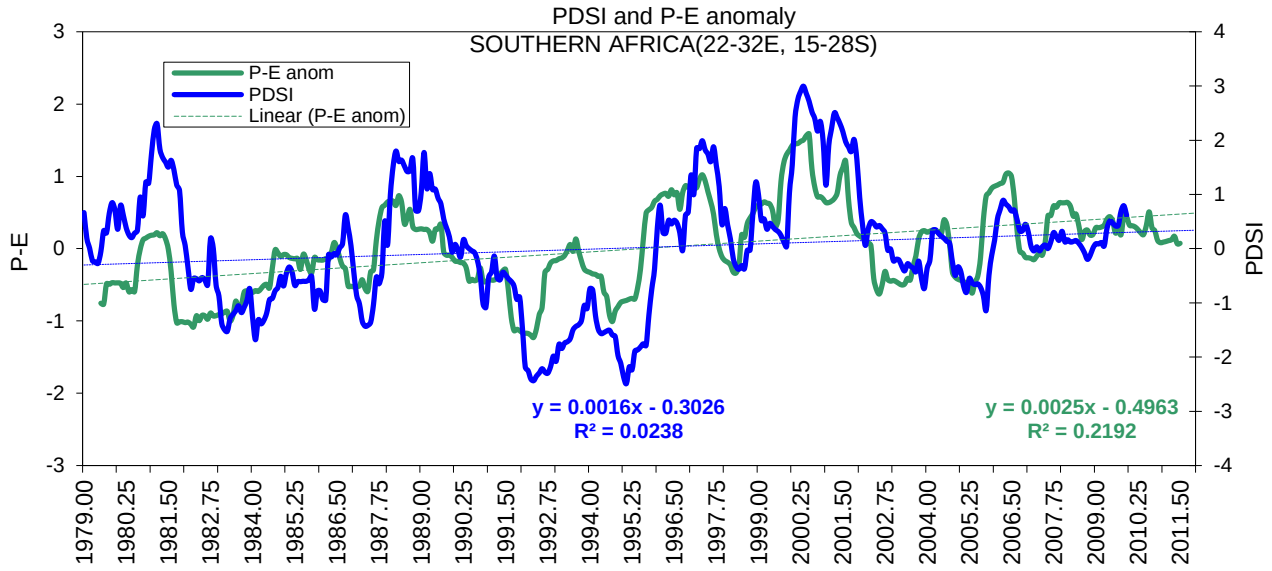

Figure 3:8 Interannual variability of PDSI and P-E anomaly over southern Africa. The P-E index exhibits a weak upward trend (R^2=0.2192) whilst the PDSI is neutral (R^2=0.02)

Chapter 4

DROUGHT AND THE SURFACE WATER BALANCE IN SOUTHERN AFRICA

4.1 Introduction

Meteorological droughts may have different characteristics and consequences in a range of climate zones with greater impact in the semi-arid regions. The duration of drought and intraseasonal distribution of the little rainfall during drought may also differ considerably from season to season. Other important characteristics of meteorological drought include the spatial patterns (area covered by drought) and its intensity. Spatial patterns may also be deduced from the drought impact (e.g. NDVI), in addition to meteorological variables.

The aim of this chapter is to present a climatology of key variables related to the surface water balance in southern Africa. As determined in the previous chapter, P and E are the main components of the surface water balance. Precipitation is critical as most socio-economic activities and rural livelihoods in southern Africa depend on its consistent supply. PET represents atmospheric demand whilst ET is the actual evaporation that took place and will be close to PET under energy limited conditions but can be far from PET under water limited conditions. Annual cycles and inter-annual variability of PET are also investigated whilst the mean climate variables of southern Africa are also presented alongside the analyses of drought. Anomalies induced by drought events identified in the previous chapter are analyzed and discussed.

This research focuses on the austral summer season, and therefore much less analysis refers to the long dry season from May to September.

4.2 Rainfall

4.2.1 Spatial patterns

Mean spatial patterns of summer rainfall over southern Africa show strong gradients from west to east with higher rainfall experienced over the north east, part of the Zambezi basin

(Figure 4.1). Annual rainfall maximizes over the Zambezi (~15°S) valley in the north, coinciding with the dominance of the ITCZ. Low rainfall is found in the Limpopo valley (~21-23°S) and increases out of that region to the northeast and southeast. The west of the region is arid, covering the Kalahari of Botswana and the Karoo of South Africa and so the study of drought over arid regions is meaningless.

The influence of a range of the west-east Soutpansberg Mountains over the southeast of the study area (northern Limpopo, South Africa) is discernible in the mean pattern. However, due to the resolution of the GPCP data, orographic effects due to isolated mountains may not be distinct. The eastern escarpment which extends from the Drakensberg in South Africa to eastern Zimbabwe (Figure 1.1) allows for mechanical lifting of moist air from the Indian Ocean steered by a ridging high over South Africa's KwaZulu-Natal coast. It has been found that some stations on the eastern escarpment record annual rainfall totals exceeding 1500 mm regularly (Malherbe *et al.* 2012; Hart *et al.* 2013).

Long-term averages of annual rainfall may be misleading especially in regions where rare extreme events can influence them. The 1981-2010 rainfall averages over eastern southern Africa have a component of rare tropical cyclone landfalls such as the heavy rainfalls of February 2000 due to cyclone tropical cyclone Eline which produced 25% of the January to March mean rainfall (Reason and Keibel 2004). However, climate extremes such as tropical cyclones do not significantly influence patterns of variability in the multi-decadal oscillation (~18 year cycle) which influences rainfall over southern Africa from 20-30°S (Tyson *et al*. 2002; Malherbe *et al*. 2012).

There exists high variability between extreme wet and extreme dry seasons over central southern Africa, suggesting vulnerability of the study area to extreme events (Figure 4.2), including floods and droughts (Mulenga *et al*. 2003). The highest variability is found in the Limpopo valley (20-25°S) consistent with Usman and Reason (2004) and Kabanda (2005). A zone of high dry spell frequencies was found between 20-25°S, and defined as a "drought corridor" (Usman and Reason 2004) whilst Reason *et al.* (2005) determined

that increased frequency of dry spells in the Limpopo is associated with El Niño. Drought seasons were found to be associated with high dry spell frequencies. In addition to high dry spell frequency, most land falling tropical cyclones follow the Limpopo valley onto the interior plateau (Malherbe *et al.* 2012) suggesting significant variability between drought and floods in this region.

However, a composite rainfall anomaly for anomalously dry years identified in Chapter 3 shows strong negative departures of rainfall mainly in the northeast of the study area, with a minimum over central Zimbabwe (Figure 4.3). It appears patterns of rainfall anomaly during drought affect Zimbabwe more than the Limpopo valley, perhaps because the Limpopo receives lower mean rainfall. Each of the seven drought seasons analyzed in this study has affected Zimbabwe.

An analysis of rainfall anomalies by season shows that drought tends to be a widespread phenomenon over the study area. However, no drought is similar to another, with significant heterogeneity in the intensity of drought over the region (Figure 4.4). This may suggest that predictability of area covered by drought is a difficult task for seasonal climate forecasters. The 1991/92 season is clearly the most severe, whilst the 1982/83 drought also had significant rainfall departures. The more intense a drought is, the wider the areal coverage of strong negative anomalies. This result is consistent with Kabanda (2005) in a study of drought over northern Limpopo in South Africa.

Though widespread, the 1983/84 drought was punctuated by landfall of tropical cyclones Domoina (January 1984) and Imboa (February 1984) which resulted in positive rainfall anomalies over the southeast of the study area (Figure 4.4). Tropical cyclone Domoina dumped up to 800 mm of rain from 28-31 January 1984 in some mountain areas of South Africa's KwaZulu-Natal (Jury *et al*. 1993b). These rainfall anomalies by season are further analyzed together with surface wind anomalies in Chapter 5.

EOF analysis of GPCP precipitation over southern Africa shows important spatial loadings over Zimbabwe in EOF1 (24% variance), EOF2 (16% variance) and EOF3 (9%

variance). The eigenvalues, variances explained by EOF1 to EOF4 and the accumulated variances are shown in Figure 4.2 but only the first three spatial loadings are retained for further discussion. A dipole mode (EOF1) is the most dominant mode of rainfall variability over southern Africa with negative spatial loadings over Zimbabwe and positive loadings over the northeast, extending from East Africa through northern Madagascar with a northwest-southeast orientation (Figure 4.5a). Another drought mode is also found in EOF3 (Figure 4.5c) with a wet mode over Zimbabwe in EOF2 (Figure 4.5b).

4.2.2 Annual cycle and intraseasonal variability

As shown in Chapter 3 (Figure 3.2), the rainfall distribution over the study area is strongly seasonal, with the bulk of the rainfall experienced during the austral summer from November to March. Rainfall amounts of up to 100 mm/month are recorded during December to February. Sometimes the rains have an early onset (September/October) and in fewer cases the rainy season may extend well into April. Surface convergence is enhanced during the summer months with the establishment of the equatorial trough across the Zambezi (~15°S). The rest of the year is predominantly dry with little rainfall, dominated by a subsiding circulation and low level divergence.

At intraseasonal timescales, the rainy season over southern Africa is characterized by alternating wet and dry spells (Makarau 1995). The duration of dry spells within a season may determine the success or failure of rain-fed agriculture in a given season. Prolonged dry spells or high frequency of dry spells in a season may develop into meteorological droughts (e.g. Usman and Reason 2004) and are of considerable interest to this research as droughts initially develop from extended dry spells.

Drought seasons are typically characterized by erratic rainfall distribution within the rainy season and longer dry spells. Whilst there is no significant variability of onset between drought and non-drought seasons, the cessation is significantly early during drought resulting in a shorter duration of the rainy season. This character may have significant consequences on rain-fed agriculture. In addition, climate change has resulted in a general delay in the onset of the summer rainy season in southern Africa.

4.2.3 Inter-annual variability

From season to season, rainfall is also highly variable and therefore unreliable over southern Africa (Figure 4.6). There is no significant trend (R^2= 0.001) in the rainfall time series despite the low rainfall that characterized the 1980s and the early 1990s. Kabanda (2005) found a declining rainfall trend through the 1980s and the early 1990s in a study of drought in South Africa's Limpopo Province. Previously, it was shown that rainfall in South Africa exhibits some decadal oscillations with a period of about 18-20 years (e.g. Tyson 1990; Kruger 1999). This quasi-decadal oscillation (~ 11 yr) may account for the droughts of the 1980s and early 1990s and the above normal rainfall of the 2000s. Some studies have found conflicting results on rainfall trends in southern Africa from different datasets (e.g. Jury 2013; MacKellar *et al.* 2014). The temperature trends are more robust.

Departures from mean rainfall also show high inter-annual variability with drier years (negative departures) during the 1980s and 1990s. There appears to be a critical turning point in rainfall anomalies from about 1995. Thus, the regional rainfall was on a partial recovery since the minimum of the 1990s such that a continued drying trend envisaged in some studies (e.g. New *et al.* 2006) is not supported here. This is an important finding of this thesis. Muchuru *et al.* (2015) also did not find any significant positive/negative trends in rainfall of the Zambezi catchment in Zimbabwe. It is shown that the driest year in the time series corresponds to the 1991/1992 season whilst the wettest season occurred in 2000 largely due to floods induced by multiple landfalls of tropical cyclones Eline, Gloria and Hudah from the SW Indian Ocean in February-March. It appears the frequency of extremely dry seasons has declined in the latter part of the study period (1979-2012).

Oscillations longer than the annual cycle in the rainfall data are also investigated. Wavelet analysis of 1979-2012 monthly precipitation shows significant cycles of rainfall variability at 2.5 and 4.5 years (Figure 4.7). Within the cone of influence is a strong signal at period 2.5 year during 1990-1997 and another at period 4.5 year during 1997-2005. These cycles may be related to phases of the Quasi Biennial Oscillation (QBO) and El Niño

Southern Oscillation (ENSO) respectively which have similar cycles. However, due to the rather short timeseries analyzed, longer cycles such as decadal oscillations cannot be determined here. An example is the multi-decadal ~18 year cycle in rainfall over southern Africa (south of 15°S and most distinct across 20-30°S) determined by Tyson *et al.* (2002). Morioka *et al.* (2015b) found a link between decadal variability over southern Africa and local air–sea coupling in the South Atlantic Ocean which may be significant for the transmission of a SLP anomaly to the southwestern Indian Ocean.

4.3 Outgoing longwave radiation

Outgoing longwave radiation (OLR) is a measure of convection in the tropics. Deep convective clouds act to block and decrease OLR escaping to space. OLR is therefore a useful proxy for convection and rainfall in tropical regions. The annual cycle of OLR exhibits double maxima over southern Africa – with a major peak during September and a secondary peak during May just prior and just after the main rainy season (Figure 4.8). OLR is at a minimum during DJF, coinciding with the presence of deep cumulonimbus convection in the ITCZ.

OLR is also a useful proxy for drought events. Droughts are characterized by prolonged periods of clear skies such that strong positive OLR anomalies prevail. Composite anomalies of OLR for drought seasons display the strongest signal over Zimbabwe (> 13 Wm^{-2}; Figure 4.9). High OLR over the subcontinent suggests that convection is supressed with reduced cloudiness and high surface temperatures. Positive anomalies over central southern Africa support the focus of this study of drought on this region. At the large scale, convection is enhanced over the Indian Ocean north and east of Madagascar extending northwest to the East African Rift Valley (Figure 4.9).

Over the period 1979-2012, OLR anomalies are more pronounced with negative anomalies which are associated with wet seasons (Figure 4.10). This is typical in semi-arid regions.

4.4 Land surface temperature

Mean spatial patterns of Land Surface Temperature (LST) over the study region show high values over the Limpopo valley extending into Botswana (Figure 4.11). The LST patterns do not only reflect the climate but also the elevation of the region. Highest LST values are associated with the lowest elevation in the Limpopo valley. The annual cycle of LST values is at a minimum during the austral winter (June-August) and peaks from early- to mid-summer (OND; Figure 4.12).

LST may also be used to identify intense dry spells. Strong positive anomalies of February LST are identified and ranked and the 90^{th} percentile are classified as dry. The maximum temperature anomalies are shown and discussed in the next section. It is argued that the hottest periods during February correspond to extended periods of dry weather and therefore meteorological drought. Ideally, the hottest periods during midsummer (e.g. February) should correspond to the worst droughts. The most widespread drought over the subcontinent was the 1991/92 drought. It was also the most intense.

4.5 Maximum temperature

Summer heat waves have been found to have a strong positive relationship with the occurrence of drought in southern Africa (Lyon 2009). Often heat waves occur during severe drought and therefore an analysis of maximum temperatures (Tmax) is important for studies of meteorological drought.

Mean spatial anomaly patterns of Tmax closely resemble patterns of LST (not shown). Whilst the annual cycle shows a minimum in June-July with temperatures rising to a plateau (> 31°C) from October to January (Figure 4.13). Due to area averaging across the study domain, some areas of the upper Limpopo valley (Botswana) experience much higher maximum temperatures during this period. Tmax is phase-locked to LST over southern Africa.

Tmax anomalies associated with drought appear greatest over the western Limpopo valley in Botswana (Figure 4.14) and this may be related to adiabatic warming induced

by subsidence under the mid-tropospheric Botswana High. These warm anomalies result in a strengthening of the north-south temperature gradients, consistent with Richard *et al.* (2001).

It is found that maximum temperatures are inversely correlated with the P-E index over the study area at R = -0.47 (90% significance) which is similar to the OLR argument. Ranked Tmax (Februaries only) show that all seven drought events identified in this study were among the 10 hottest temperatures during the study period (Table 4.1). However, not all extremely hot seasons are drought seasons, as evidenced by the 1998, 2005 and 2007 seasons.

A slight warming trend (R^2=0.18) is observed during the latter part of the study period perhaps consistent with a global warming and climate change signal (Figure 4.15). The warming trends have also been found in earlier studies by Kruger and Shongwe (2004), New *et al.* (2006), and Jury (2013). Kruger and Shongwe (2004) found a stronger warming trend during the 1980s compared to a slower rate of increase during 1990-2003. In another study on heat waves and drought, Lyon (2009) projected an increase in the frequency of heat waves in southern Africa from 2000-2100.

4.6 Potential evapotranspiration, sensible heat flux and net radiation

It has been determined in Chapter 3 that the main components of the surface water balance equation are precipitation (P) and evapotranspiration (ET). It is estimated that up to 91% of precipitation received over southern Africa returns to the atmosphere via evapotranspiration (Martyn 1992), higher than the Africa average of 80% (UNEP 2008).

It is useful to analyse P-E as the drought index in a region such as southern Africa where ET exceeds P most of the time over a large part of the study area.

ET is the water lost from the surface to the atmosphere but actual evaporation declines during drought in the absence of water for evaporation (e.g. Figure 4.16) due to a lack of precipitation. However, a regression trend of sensible heat flux using the ensemble of all

CMIP5 models with RCP2.6, southern Africa has a positive value > 0.1 Wm^{-2}/yr in the period 1980-2050.

The mean annual cycle of potential evapotranspiration (PET) over southern Africa peaks during October-November before the onset of the main rainy season and declines during the austral winter (Figure 4.17). PET is in good agreement with SHF (Figure 4.17). Significant spatial patterns of PET anomalies show strong positive anomalies (> 80 Wm^{-2}) over the western Limpopo valley in Botswana (Figure 4.18) similar to anomalies of maximum temperature.

4.7 Summary and discussion

The climate of southern Africa is largely semi-arid with high variability at intraseasonal, seasonal and inter-annual time scales. Droughts are a distinct and recurring feature of the summer climate over the region. This chapter has investigated the spatial and temporal evolution of drought events over southern Africa. The focus for most of the droughts is the Limpopo River valley, spreading northwards and southwards as the season progresses. A prolonged period of dry seasons in this study occurred during much of the 1980s and the early 1990s, which may be part of a quasi-decadal cycle. The satellite GPCP datasets begin in 1979 and do not allow determination of longer cycles in the data such that decadal oscillations are not covered in this thesis.

Rainfall anomalies by drought season show significant spatial variability such that no drought is similar to another, but consistently with greatest impact over Zimbabwe. It is found that the 1992 drought was the most severe drought over southern Africa during 1979-2012. A decline in the frequency and intensity of drought is observed after 1995. Perhaps the trends are influenced by the severe droughts that characterized the start of the study period.

It appears the most significant trend in the rainfall time series in southern Africa is the slow oscillation characterized by prolonged periods of declining rainfall followed by a similar period of recovery. A continued drying trend is not supported by this analysis. The

seven droughts analyzed in this study are among the ten hottest summers in southern Africa. However, not all hottest summers are drought periods. SHF represents drought better than LHF as it exhibits a strong correlation with PET which is an expression of atmospheric demand for water vapour.

A slight upward trend in SHF indicates increased evaporation losses over southern Africa. While the rain and OLR composite anomalies are greatest over Zimbabwe, potential evaporation and air temperature anomalies are greatest over the western Limpopo valley.

Chapter Tables

Table 4-1 Ranked Tmax (°C) for February from 1979-2012. The definitive selection of drought seasons identified in Table 3.2 with the most negative P-E anomalies are shown with an asterisk.

Rank	February Year	Tmax (°C)
1	1992*	33.7
2	1987*	32.4
3	1983*	32.4
4	2005	32.1
5	1995*	32.1
6	2007	31.9
7	1998	31.9
8	2003*	31.8
9	1984*	31.7
10	1982*	31.4

Table 4-2 Eigenvalues, percentages of variance explained (%) by EOF1 to EOF4, and accumulated variance (%)

EOF	Eigenvalue	Variance (%)	Accumulated variance (%)
1	523.7	23.8	23.8
2	349.4	15.9	39.7
3	193.9	8.8	48.5
4	161.8	7.4	565.9

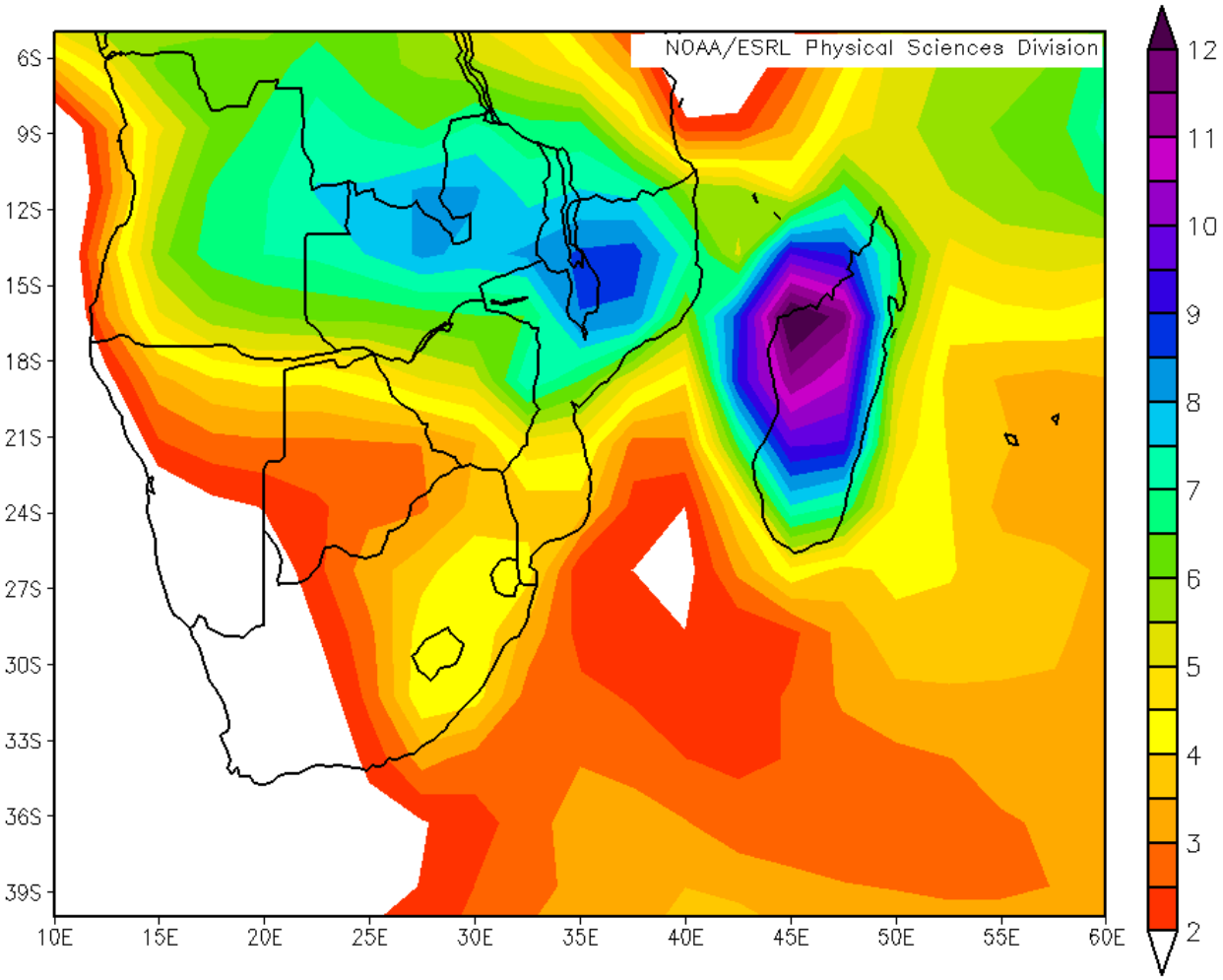

Figure 4:1 Long term (1980-2012) mean summer (DJF) GPCP precipitation (shaded in mm/day) over southern Africa and the adjacent oceans

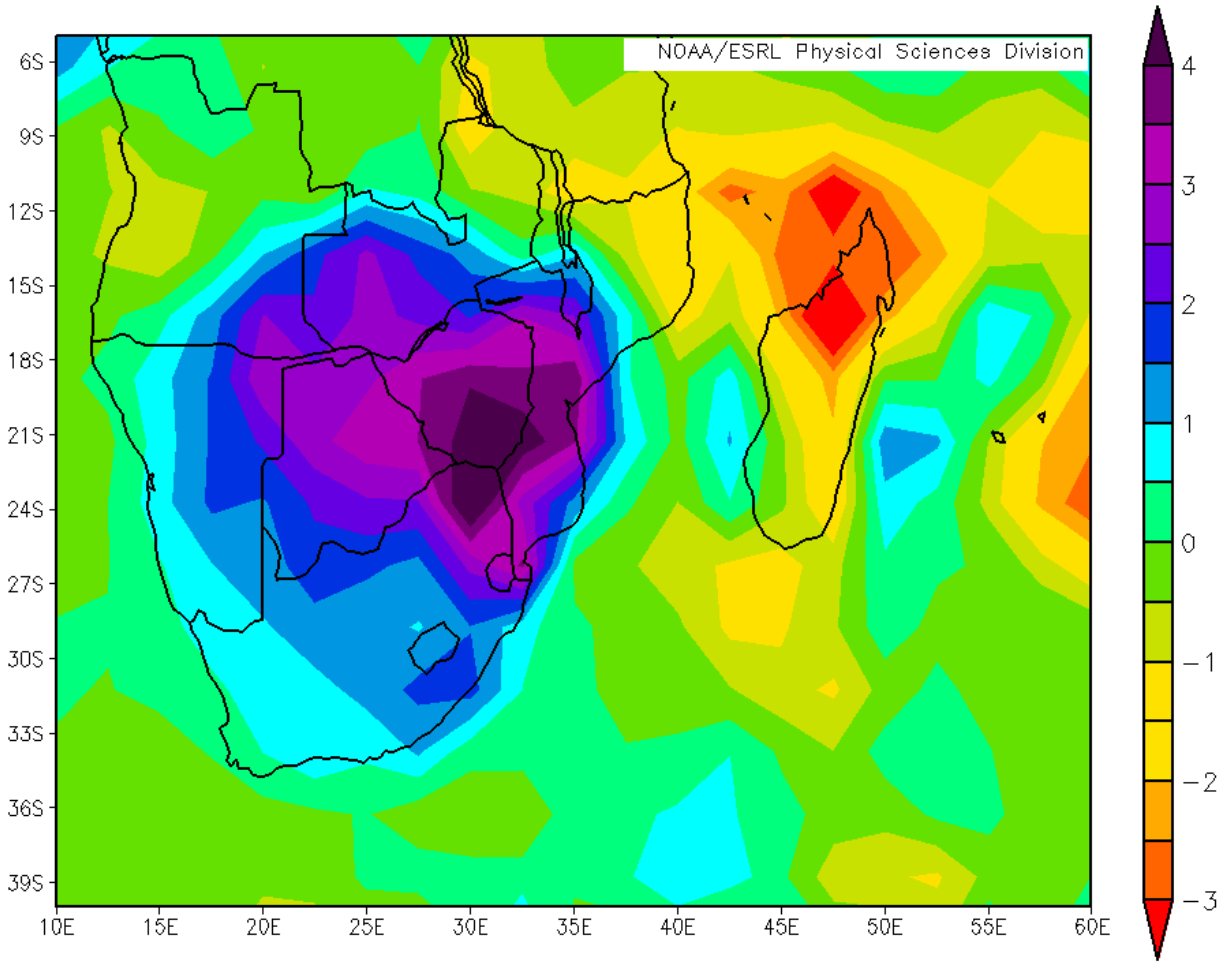

Figure 4:2 Mean GPCP Precipitation (mm/day) for wet years minus dry years over southern Africa and the adjacent oceans

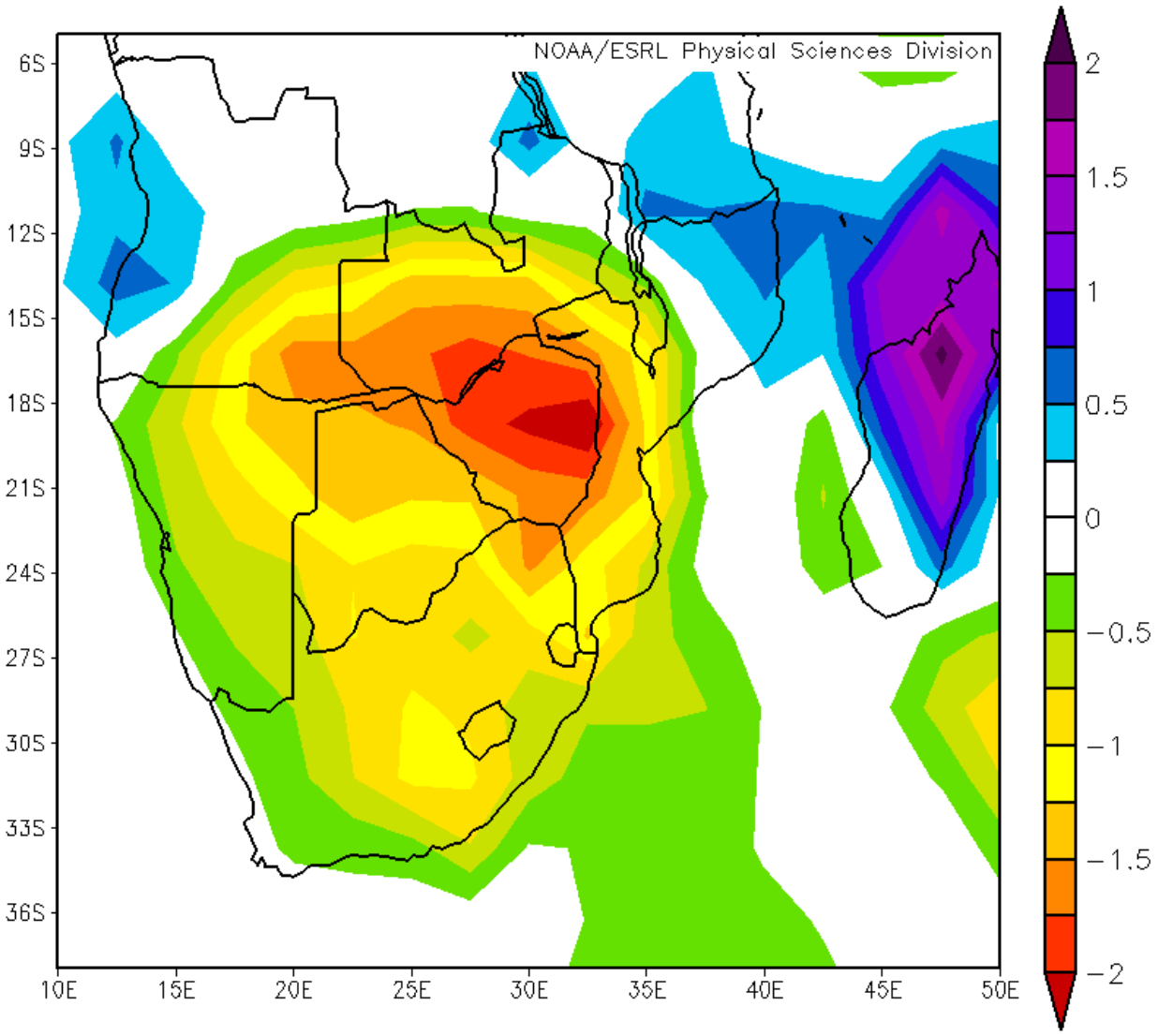

Figure 4:3 Composite mean GPCP precipitation anomaly (shaded in mm/day) for droughts over southern Africa and the adjacent oceans

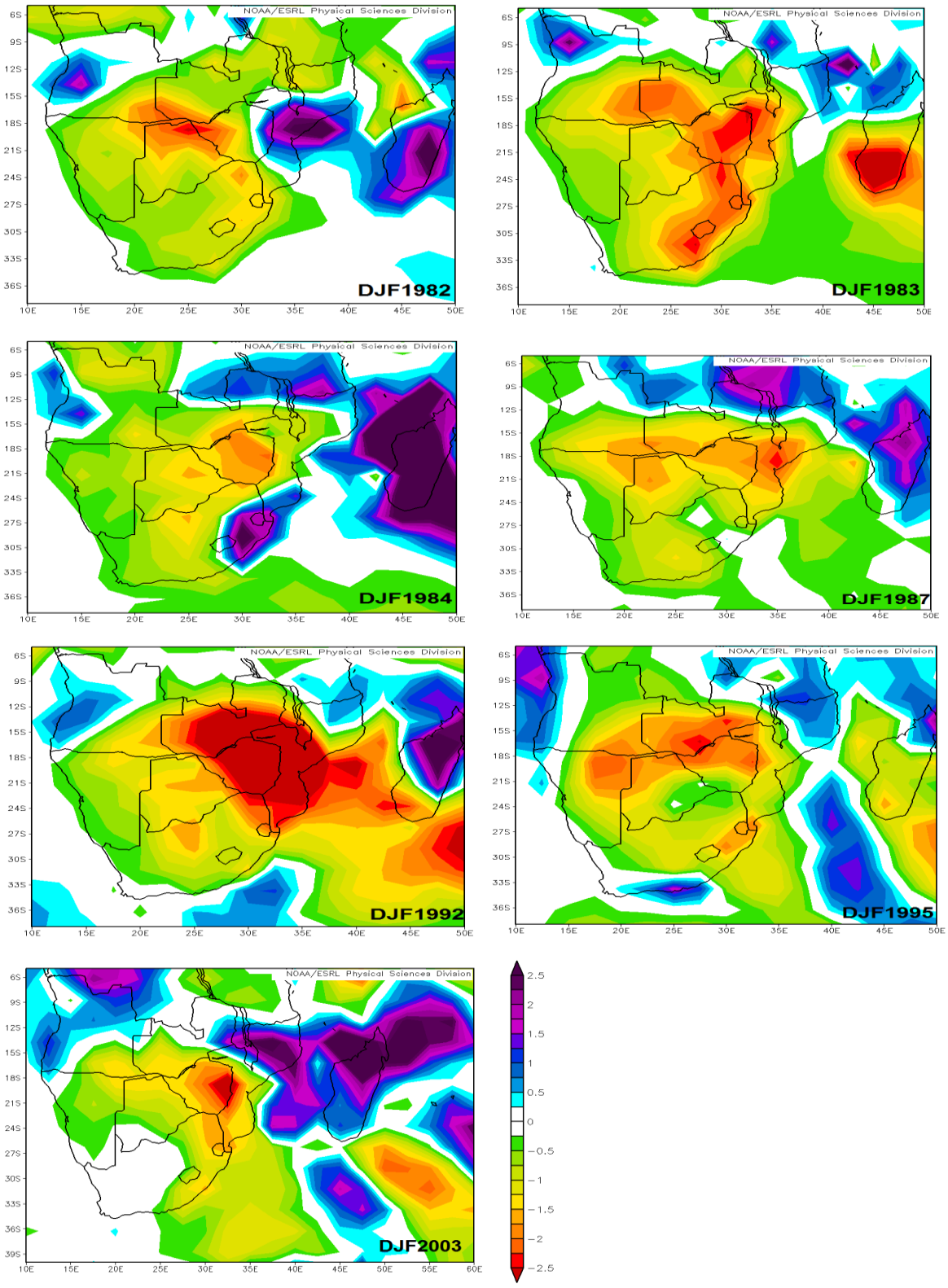

Figure 4:4 Summer (DJF) GPCP precipitation anomalies (shaded in mm/day) over southern Africa and the adjacent oceans during the seven drought seasons identified in this study. The same scale is used for comparisons.

(a)

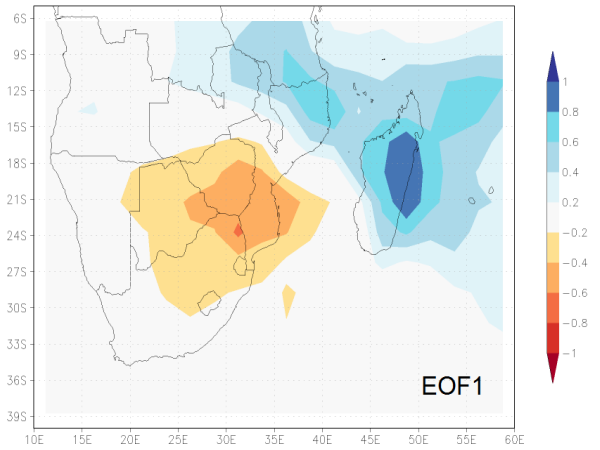

(b)

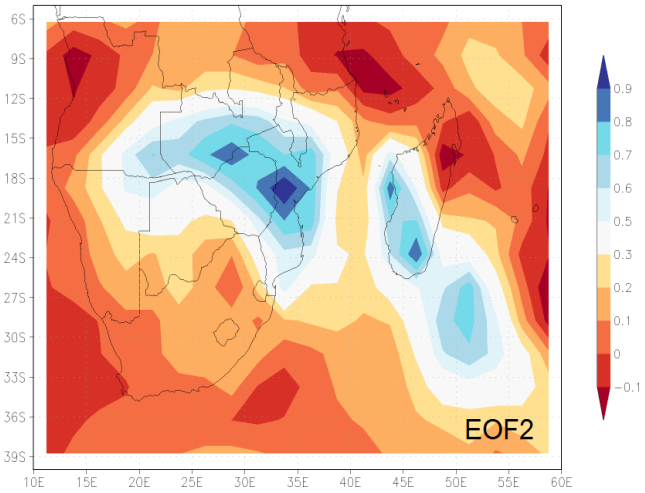

(c)

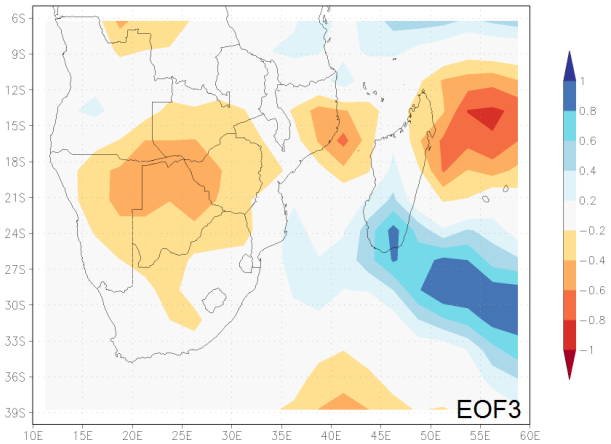

Figure 4:5 (a) EOF1 (24% variance) (b) EOF2 (16% variance) and (c) EOF3 (9% variance) of summer (DJF) rainfall over southern Africa

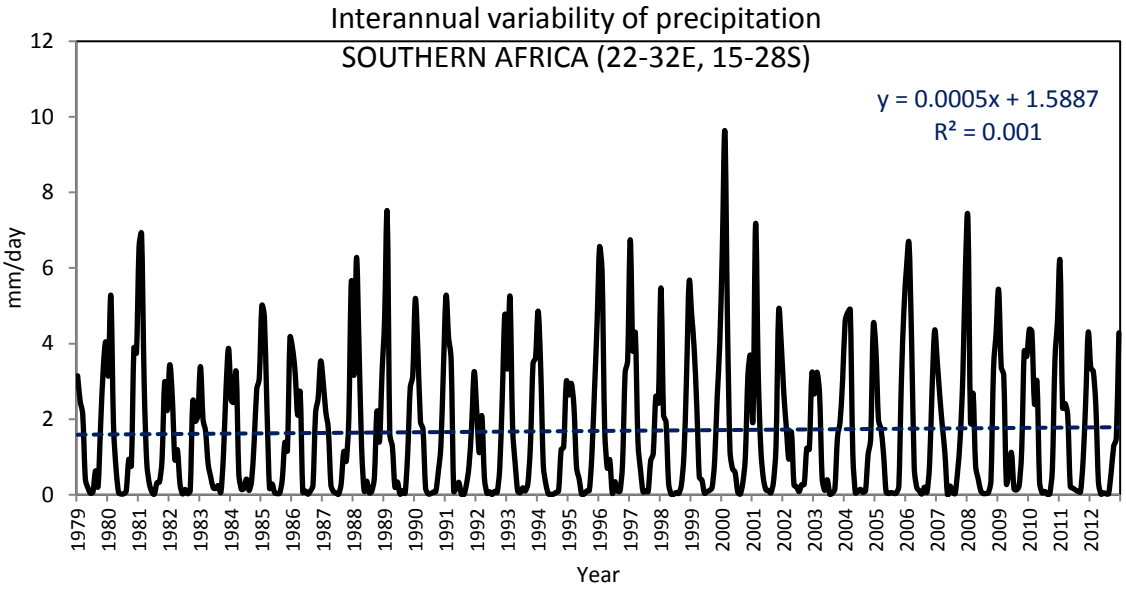

Figure 4:6 Interannual variability of GPCP precipitation (mm/day) over southern Africa (averaged over 22-32E; 15-28°S): 1979-2012

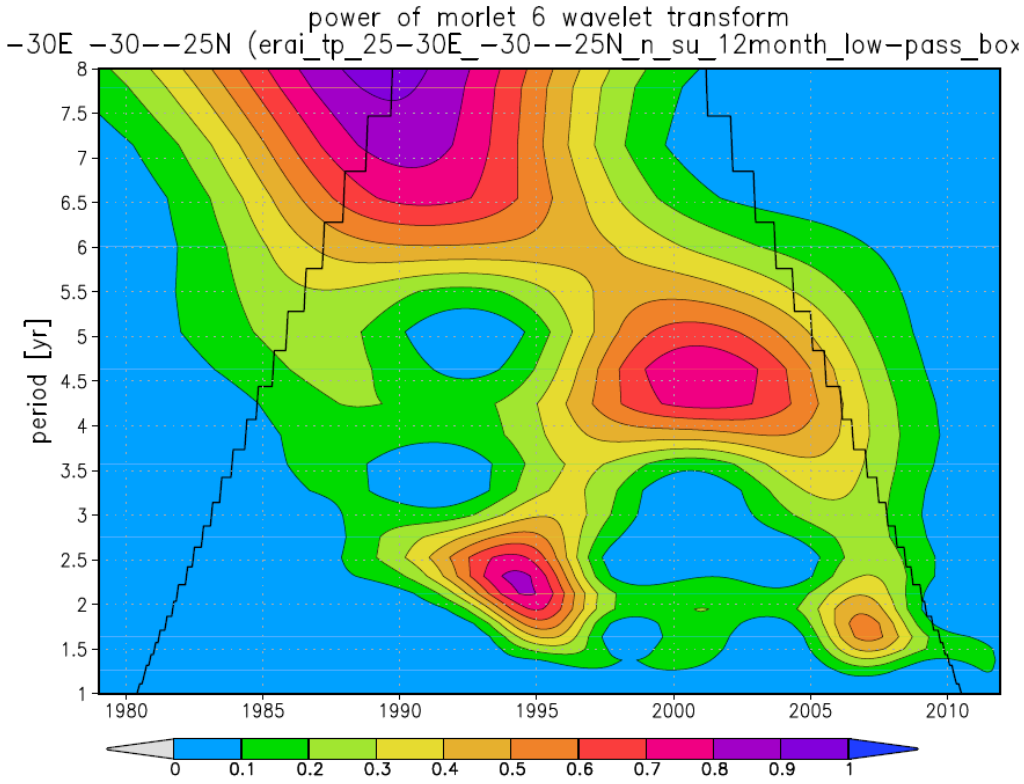

Figure 4:7 Morlet wavelet analysis of GPCP precipitation for the southern Africa region (averaged over 22-32E; 15-28°S)

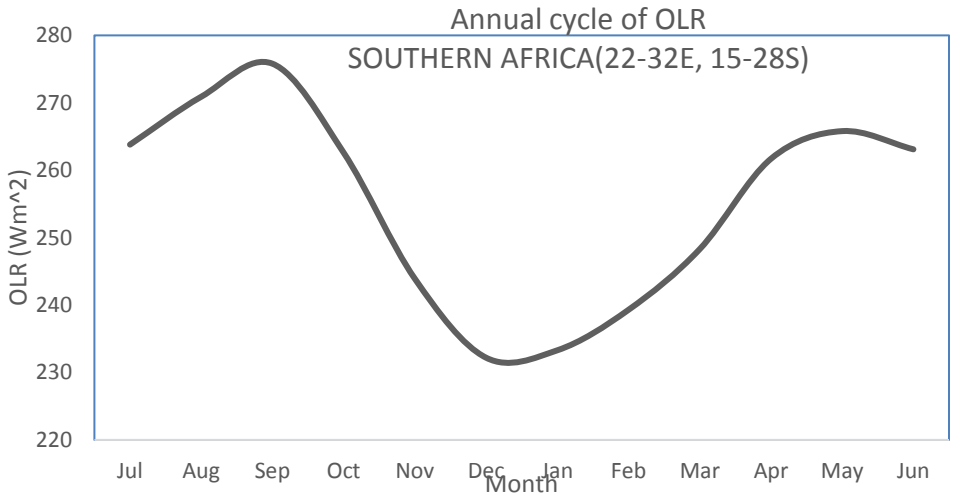

Figure 4:8 Mean annual cycle of NCEP OLR (Wm^{-2}) over southern Africa (averaged over 22-32E; 15-28°S): 1979-2012

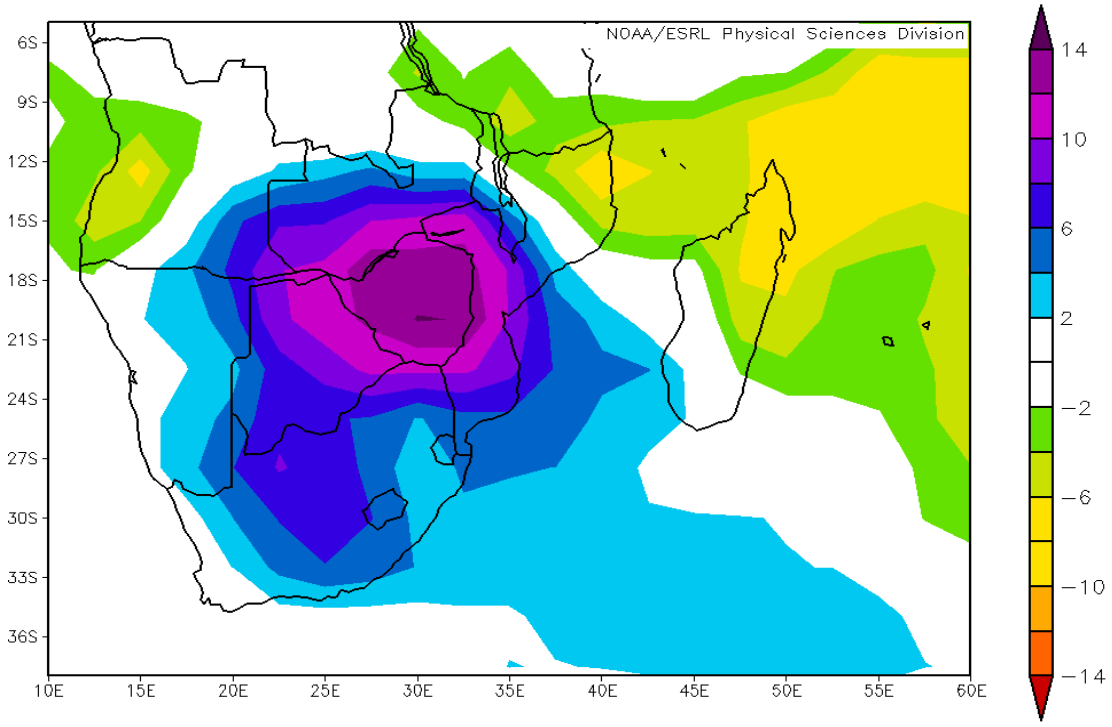

Figure 4:9 Composite mean NCEP OLR anomalies (shaded in Wm^{-2}) for the seven drought seasons over southern Africa and the adjacent oceans

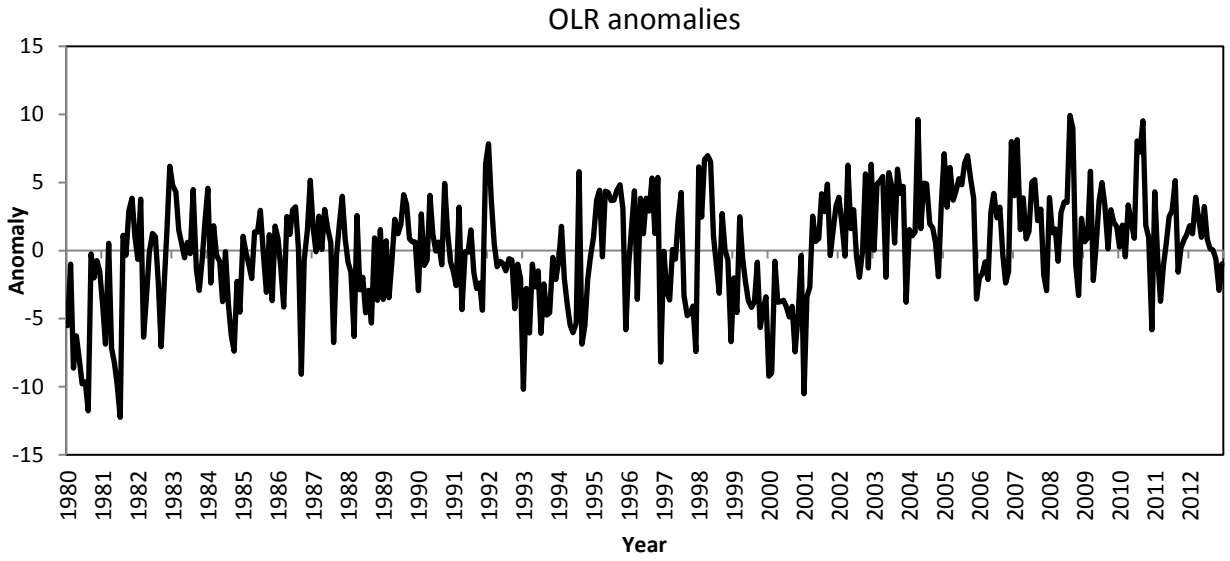

Figure 4:10 Interannual variability of NCEP OLR anomalies (Wm^{-2}) over southern Africa (averaged over 22-32E; 15-28°S): 1979-2012

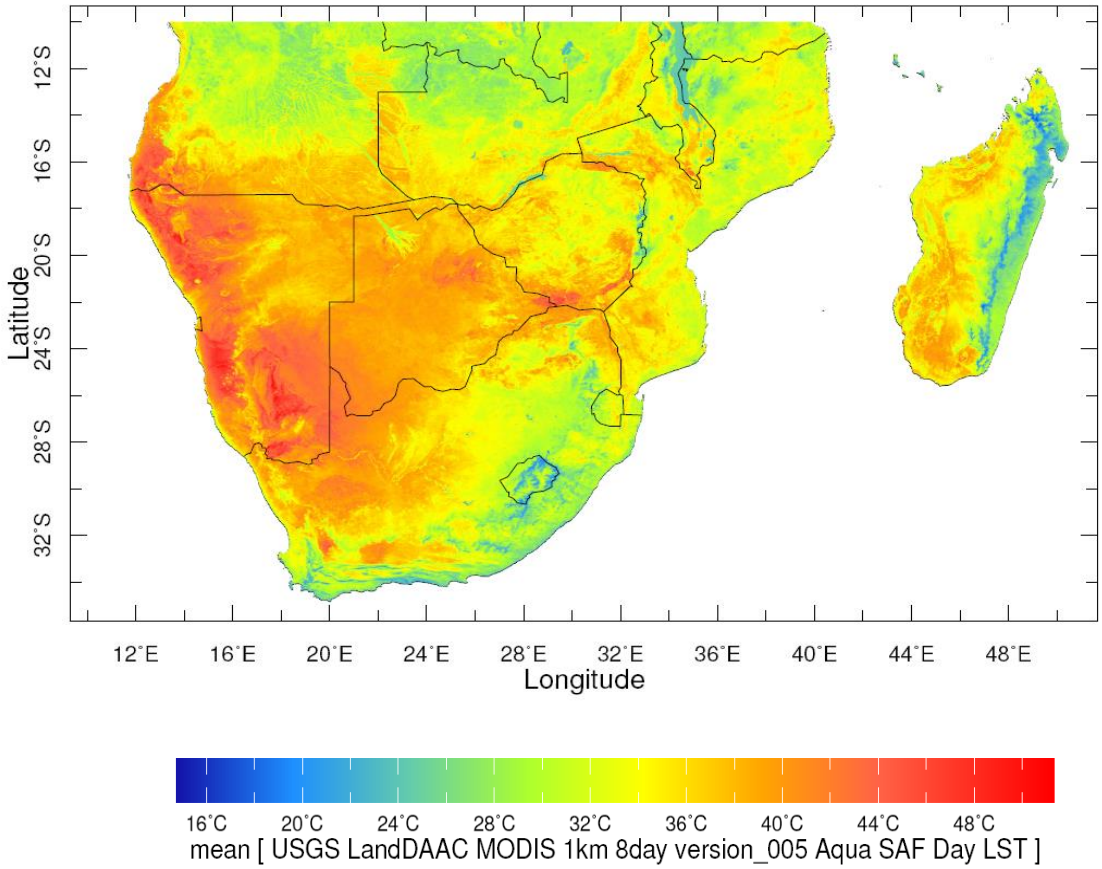

Figure 4:11 Spatial patterns of long-term mean daily MODIS land surface temperature (shaded in °C) over southern Africa during summer (DJF)

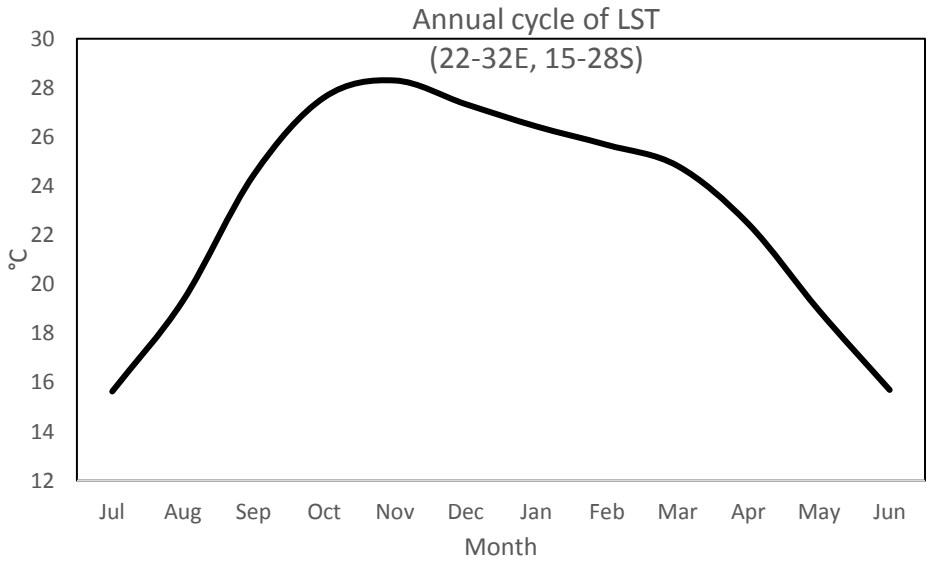

Figure 4:12 Mean annual cycle of MODIS land surface temperature (°C) over southern Africa (averaged over 22-32E; 15-28°S)

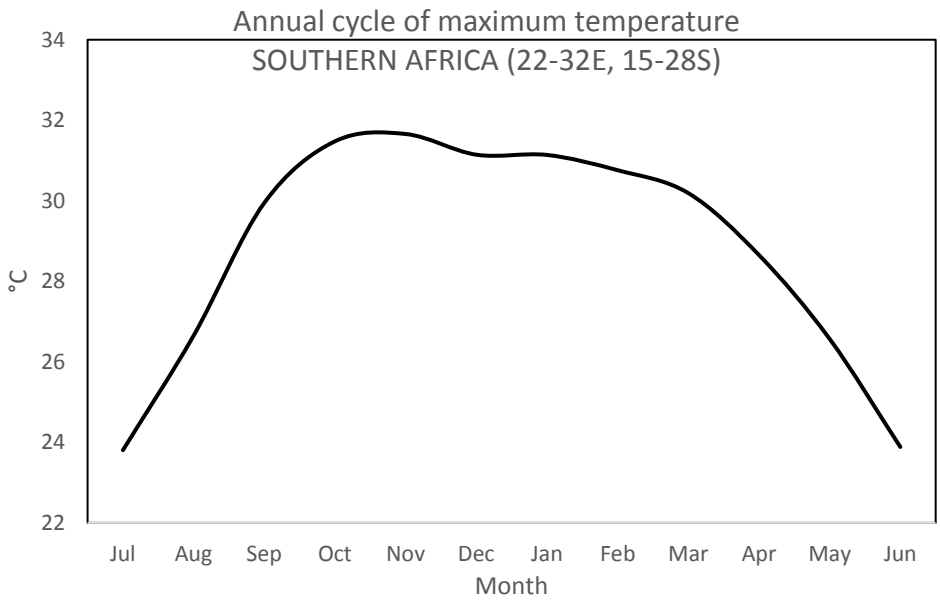

Figure 4:13 Mean annual cycle of NCEP maximum air temperature (°C) over southern Africa (averaged over 22-32E; 15-28°S)

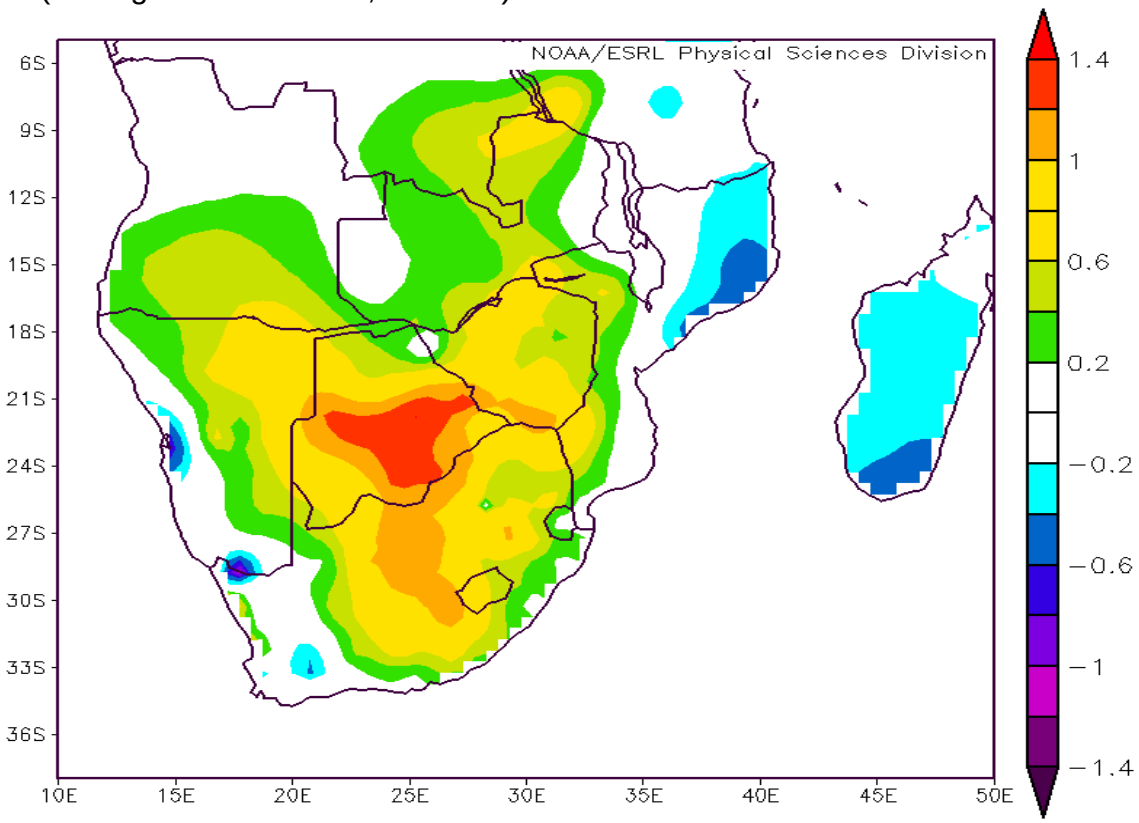

Figure 4:14 Composite mean NCEP maximum air temperature (shaded in °C) anomaly for drought over southern Africa

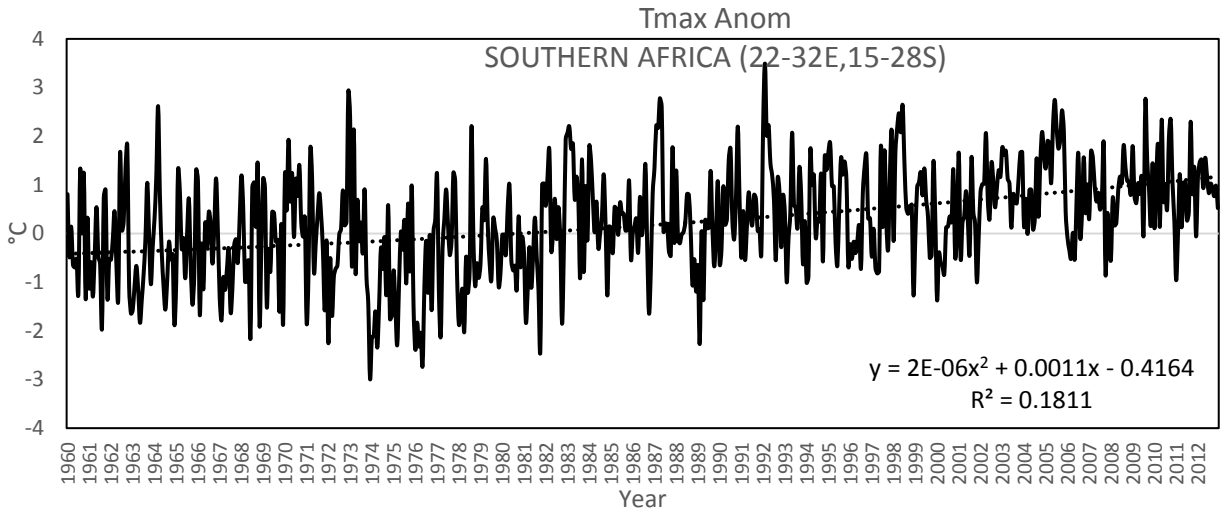

Figure 4:15 Long-term (1960-2012) NCEP maximum air temperature (°C) anomalies over southern Africa (averaged over 22-32E; 15-28°S)

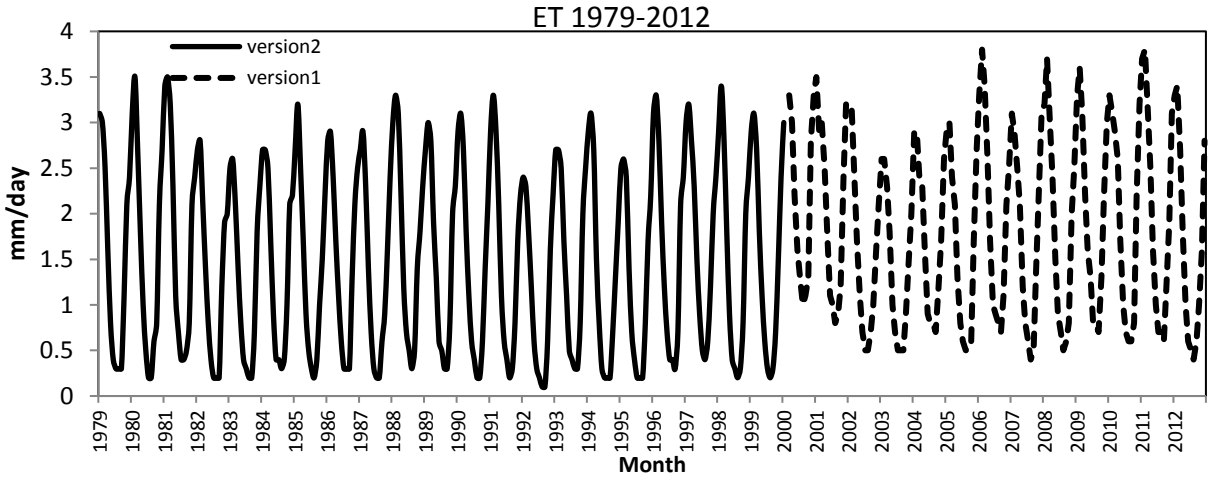

Figure 4:16 Interannual variability of surface evaporation (mm/day) over southern Africa (averaged over 22-32E; 15-28°S)

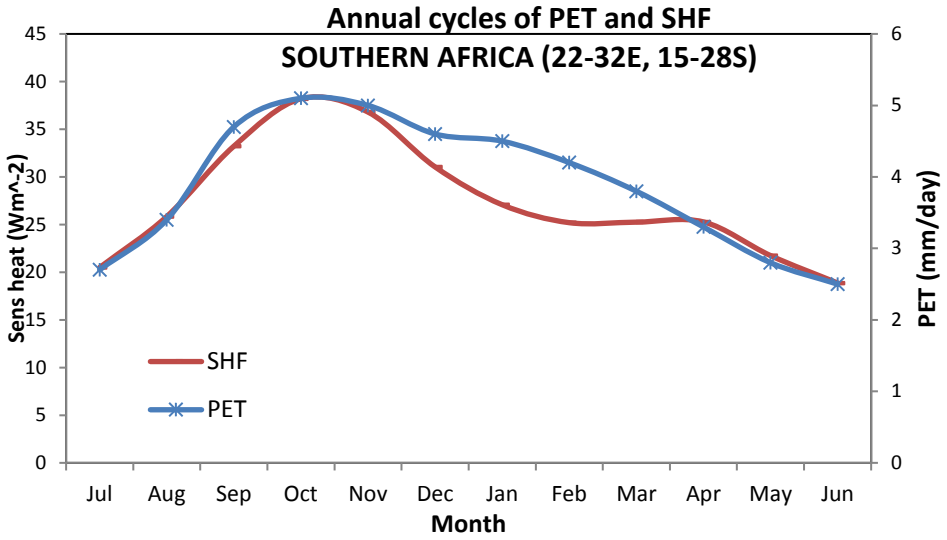

Figure 4:17 Mean annual cycles of PET (mm/day) and MERRA SHF (Wm^{-2}) over southern Africa (averaged over 22-32E; 15-28°S)

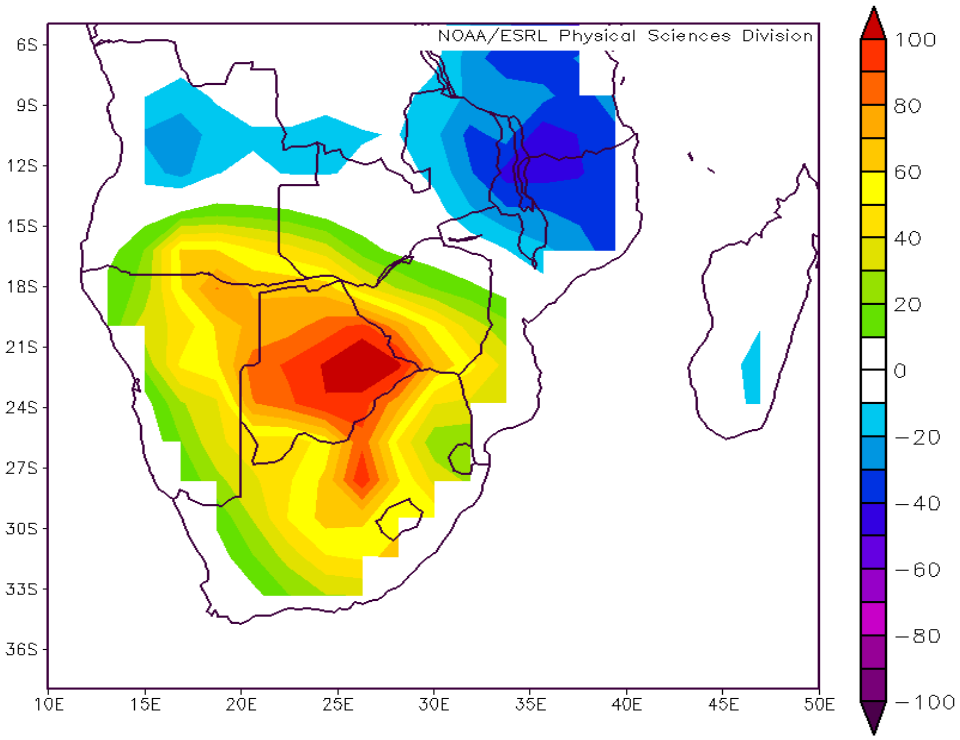

Figure 4:18 Composite mean anomalies of NCEP PET (shaded in Wm^{-2}) over southern Africa during drought periods

Chapter 5

METEOROLOGICAL STRUCTURE OF DROUGHT OVER SOUTHERN AFRICA

5.1 Introduction

The immediate cause of drought is the failure of rainfall following the establishment of anticyclonic and subsiding circulation over a region (Gustard *et al.* 2004). This leads to prolonged dry spells during the summer season which may result in meteorological drought. However, it is generally accepted that dry spells are essential during the rainy season to allow for crop development and prevent water logging and leaching of nutrients.

In southern Africa, dry spells are consistently associated with the establishment and intensification of the mid-tropospheric Botswana High. At the event scale, it is essential to establish the meteorological drivers of drought and to understand the behavior of the Botswana High and how it is influenced by remote phenomena such as ENSO and anomalies in the Indian Ocean. The circulation anomalies that cause drought are often a reflection of remote global scale forcing mechanisms.

The aim of this chapter is to identify the main drivers of drought over southern Africa during the period 1979-2012. Important features of the climate system that inhibit rainfall and promote drought over the subcontinent are analyzed and discussed. The analyses presented here focus on the austral summer (DJF) whilst important historical drought events identified in Chapter 3 are cited as case studies for illustration.

Since this thesis focuses on the anomalies induced by drought, annual mean (and composite mean) circulation patterns are presented as a background to this chapter.

5.2 Mean circulation

Being largely in the subtropics, the mean circulation over southern Africa is predominantly anticyclonic (Tyson and Preston-Whyte 2000). Subtropical anticyclones are found in the

descending limb of the Hadley Cell in regions around 30°N and S of the equator. Two anticyclones influence the climate of southern Africa on either side of the subcontinent (Figure 5.1). The South Atlantic Ocean anticyclone (St Helena High) in the west is associated with offshore flow and equatorward subsiding air masses whilst the south Indian Ocean anticyclone (Mascarene High) drives onshore easterlies (trade winds) onto the subcontinent which advect moisture from the Indian Ocean (Figure 5.2). The south-north pressure gradient determines the strength of the southeast trade winds (Manatsa and Behera 2014) and therefore the extent of moisture intrusions. Thus, the influences of the two subtropical anticyclones are distinctly unique. At intraseasonal timescales, the St Helena High ridges along the south and east coasts, driving cool and moist south/southeasterlies onto the interior plateau. The Cape south coast receives a significant proportion of annual rainfall (~46%) from these ridging highs (Engelbrecht *et al.* 2015).

During summer, southern Africa is mostly under the influence of onshore tropical easterlies from the SW Indian Ocean which is the major source of low level moisture over the subcontinent (Figure 5.2). Prevailing winds are offshore over the west coast. Surface ocean currents (Figure 5.3) are driven by the large scale wind stress curl, which in turn is related to the distribution of subtropical highs, the circumpolar trough and the ITCZ, and their seasonal changes. Thus, in addition to surface ocean currents, the St. Helena and Mascarene Highs act to enhance the spatial gradients of rainfall from west to east over southern Africa. It is now thought that the Mozambique Current which feeds into the Agulhas takes the form of three large anticyclonic gyres and is rarely continuous (Lutjeharms *et al.* 2012).

As the thermal equator moves south during the austral summer, tropical lows develop over the Zambezi valley. The most persistent low is the Angola heat low which forms over the Bie Plateau region of Angola (Figure 5.1). The Angola low modulates low-level moisture convergence over southern Africa (Mulenga 1998). Southeast trade winds off the Atlantic Ocean recurve to become northwesterlies (Congo Air) converging in the ITCZ over the Zambezi (Figure 5.2). The Mascarene High drives easterly trade winds towards

the Angola Low, and the wind strength depends on their intensity. Manatsa *et al*. (2013) found a link between the ozone hole and deepening of the Angola low increasing the south-north pressure gradient from the subtropical Mascarene High. A low in the Mozambique Channel forms part of the equatorial trough and the ITCZ during the austral summer (Figure 5.1). Thus, the main sources of low-level moisture over southern Africa during the austral summer are the SW Indian Ocean and the Congo basin.

Aloft, the mean circulation is dominated by a large subtropical anticyclone with a center over Botswana/Namibia (Figure 5.4) called the Botswana High which is a reflection of the Mascarene High as surface anticyclones tilt to the NW with height. Once established, the Botswana High is associated with subsidence and dry weather over much of the subcontinent. The Botswana High is the most intense of the three mid-tropospheric anticylones over continents in the Southern Hemisphere (Reason 2016). It drives dry air from the south increasing atmospheric stability over southern Africa. The persistence of the Botswana High is therefore a primary cause of meteorological drought in southern Africa.

During summertime, Tropical-Temperate Troughs (TTTs) form in the mid-troposphere over southern Africa with a northwest-southeast orientation allowing for transfer of tropical moisture and energy to the mid-latitudes. The TTTs involve interactions between micro- or mesoscale convection in tropical Africa to synoptic scale mid-latitude westerly waves (Hart *et al*. 2013). The strength of the Angola Low is key to the formation of TTTs. They contribute a significant (30-50%) amount of summer season rainfall over southern Africa (Hart *et al.* 2013). Therefore, the formation and frequency of TTTs and cloud bands may be key to determining whether a season is affected by drought or not.

In the upper levels (~200 hPa), a strong/gale westerly flow characterizes much of the subcontinent with easterlies over the deep tropics (Figure 5.5). Using thermal wind arguments, winds over the mid-latitudes and subtropics become stronger and more westerly in the upper air (Lutgens and Tarbuck 2010). The baroclinic subtropical jet stream is situated near 35°S during the austral summer.

Changes in day to day weather over southern Africa occur as a result of perturbations to large scale patterns and the passage of transient easterly/westerly waves to the north/south. Cumulus convection is also a key process in tropical southern Africa such that localized or mesoscale showers and thunderstorms are common during the austral summer when there is sufficient moisture, instability and Convective Available Potential Energy (CAPE).

Equatorward and poleward of the subtropical anticyclones are transient perturbations in the easterlies and westerlies respectively. High amplitude westerly waves may result in the development of cut-of low pressure systems in the mid-troposphere. Cut-off lows may produce heavy falls of rainfall in short periods (Singleton and Reason 2007). They tend to be more common during the March to May season even though they can occur throughout out the year. Cut-off lows are often accompanied by a ridging high at the surface in the presence of a blocking Mascarene High in the Indian Ocean such that they become persistent.

Cold fronts are also found in westerly waves largely affecting the subtropical latitudes of southern Africa including South Africa's Western Cape and Cape South Coast. They shift equatorward during the austral winter producing a Mediterranean type of climate characterized by winter rainfall. This thesis focuses on the summer circulation and drought in the summer rainfall region of southern Africa.

5.3 Large scale circulation anomalies inducing drought

In this section, composite analysis is used to analyse the anomalies in the mean circulation which are typically associated with drought events over southern Africa. The results begin with the plan view whilst the vertical sections are also shown. The composites are made up of DJF summers for the drought seasons 1982, 1983, 1984, 1987, 1992, 1995 and 2003. Whilst composite analysis highlights important common features, variability in individual events is also presented and discussed.

5.3.1 Low level circulation

High pressure anomalies are observed during drought over the southwest Indian Ocean south of Madagascar and over much of the subcontinent (Figure 5.6a). As a result, anticyclonic wind anomalies are established in the low levels (850-700 hPa) with a center over Botswana (Figure 5.6b). The Angola Low is shallow and weakened during drought periods. A trough east of Madagascar causes a westerly wind anomaly over the SW Indian Ocean. The zone of convergence retreats equatorward to lie over the Congo basin (~8°S).

An analysis of surface wind vectors and precipitation anomalies for each of the seven drought seasons shows four main patterns that are recurring. In most cases (1981/82, 1982/83 and 1986/87) westerly wind anomalies from the adjacent Atlantic Ocean are quite distinct (Figure 5.7). Weak trade winds over the greater Agulhas Current region which may be associated with either a weakened Mascarene High or Angola Low (or both) are observed during 1986/87, 1991/92 and 1994/95. In some cases (1982/83, 1986/87 and 1991/92), a difluence of the trade winds which become southerly towards a trough east of Madagascar is dominant. The influence of vortices in the Mozambique Channel is observed during 1981/82, 1983/84 and 2002/03. Mason *et al.* (1994) also found a cyclonic anomaly east of Madagascar during drought. Tropical cyclogenesis in the Mozambique Channel appears to have a significant influence on drought over southern Africa and so the influence of tropical cyclones on dry weather is discussed separately in section 5.6. The 1994/95 drought has a unique pattern, with enhanced easterlies over Botswana (Figure 5.7) whilst Cook et al. (2004) found a weakened moisture flux over the Agulhas region of the Indian Ocean in analysis for the same season.

5.3.2 Vorticity and divergence

Composite mean vorticity in the low levels and in the upper air for drought seasons over southern Africa are shown in Figure 5.8. The blue area in the Mozambique Channel is cyclonic and guides the upper anomalous flow equatorward over southern Africa, which must sink according to conservation of absolute vorticity. In the low levels anticyclonic

vorticity is dominant across the subcontinent centered around 20°S, in the drainage basin of the Limpopo River (Figure 5.8).

The vorticity anomaly is triple the strength of the divergence anomaly. Clearly, the upper divergence shows a connection to the Indian Ocean (dipole), and indicates upper convergence over central South Africa and Botswana, hence sinking motion (Figure 5.9). Low level divergence also extends across the subcontinent in an area co-located with anticyclonic vorticity. Some upper level divergence along the west coast suggests some uplift and hence wet anomalies which may affect the extreme west coast and the Namib when drought is widespread over the rest of the subcontinent. The influence of Benguela Niños on west coast rainfall is discussed in section 5.5.5.

5.3.3 Middle level circulation

At 500 hPa, a composite mean for drought events shows positive geopotential height anomalies over the subcontinent particularly over the southwest covering Botswana and Namibia (Figure 5.10a). Positive geopotential height anomalies are consistent with a warmer atmosphere that usually characterizes drought. These positive anomalies imply mid- to upper level convergence and therefore sinking down the atmosphere and warmer temperatures at the surface. An intensification of the Botswana High causes displacement of tropical rain belts and TTTs away from southern Africa. The Botswana High was found to be the most intense of the three semi-permanent mid-tropospheric anticyclones that form over landmasses in the Southern Hemisphere (Reason 2016). Troughs of negative geopotential height anomalies are observed over the Indian Ocean (Figure 5.10a). This pattern suggests that TTTs and attendant cloud bands are relocated to lie over the warm ocean east of Madagascar extending to East Africa during drought periods.

An extensive anticyclonic circulation is established causing subsidence and inhibiting uplift over much of the subcontinent (Figure 5.10b). This circulation pattern suggests that drought tends to be widespread (rather than regional) over southern Africa, a result anticipated by the large area average used to define composite summers. While it is

accepted that subsidence is a prevailing characteristic of the subtropics (Tyson and Preston-Whyte 2000), it is enhanced during drought.

As the middle levels are dominated by anticyclonic wind anomalies for every drought season, some variability may be observed from one drought to another (Figure 5.11). The Botswana High is most intense during the 1983 and 1987 drought seasons. In all cases, the middle level airflow across the study area is stable and dry from the south (southeasterly or southwesterly). During wet seasons, cloud bands which bring signficant rainfall to southern Africa are associated with northwesterlies, advecting moisture and convective energy from the deep tropics. Tropical cyclone activity in the Mozambique Channel is evident during 1984, 1995 and 2003.

5.3.4 Upper level winds

At the large scale, upper level (250-200 hPa) winds show a strengthening of upper westerlies over the subcontinent around 15-25°S over the Zambezi and Limpopo (Figure 5.12). The upper westerlies also accelerate southwest of Africa. These represent the subtropical jet stream which is strengthened and displaced equatorward, a large scale pattern related to ENSO. Mulenga *et al*. (2003) also found anomalous upper westerlies in a study of circulation anomalies associated with ENSO-induced droughts.

A cyclonic circulation anomaly is observed south of the Mozambique Channel associated with the cyclonic vorticity observed in Figure 5.8. A low pressure system in the upper air is an indication of convergence there, and therefore subsidence according to the continuity equation.

5.3.5 Vertical structure

In vertical section, positive geopotential height anomalies are observed over southern Africa throughout the depth of the atmosphere over the longitudes 10-20°E (averaged over 15-30°S), with maxima in the middle levels from 700-400 hPa (Figure 5.13a). Positive anomalies are also found during drought in the middle levels over southern Africa

from about 15-35°S (Figure 5.13b). Hence, the establishment and strengthening of the Botswana High is a primary trigger of drought in southern Africa.

A composite analysis of the zonal wind and vertical velocity for all the drought periods from 1000 -100 hPa shows strengthening of upper tropospheric westerlies over southern Africa. The composites show strong subsidence in the area between longitudes 20-30°E (averaged over 15-30°S) with a greater impact over the eastern sector (Figure 5.14a). Subsidence is greater over the eastern side of an anticyclone as the airflow is equatorward and descending along an isentropic (constant θ) surface. The analysis of meridional wind and vertical velocity (averaged 22-32°E) shows pronounced subsidence between latitudes 10-20°S (Figure 5.14b) which corresponds to the drainage basin of the Zambezi River. This is consistent with intensification of the Botswana High which is found at these levels over this area and is an important finding of this thesis.

The drought situation is associated with a strengthening and an equatorward displacement of the subtropical jet stream.

5.4 Atmospheric moisture

A favorable circulation, instability, surplus moisture and high CAPE are critical for deep convection, cloud formation and rainfall. The southwest Indian Ocean is a major source of low-level moisture over southern Africa (Cook *et al.* 2004). Another important source of middle-level moisture is the Congo Basin. An intrusive mid-tropospheric westerly trough allows for moist northwesterly winds originating in the Congo basin to affect southern Africa. This tropical moisture rises along isentropic surfaces (conveyor belt), resulting in bands of cloud and precipitation in a northwest-southeast direction over the subtropics.

During drought conditions, significant drying occurs throughout a column of atmosphere from the surface to the top of the atmosphere. Drying is most pronounced over longitudes 15-30°E (averaged over 15-30°S; Figure 5.15a) and latitudes 15-35°S (averaged over

22-32E; Figure 5.15b). This also supports the weakening and retreat of the tropical rain belts (ITCZ) to the Congo Basin.

5.5 Global remote mechanisms of drought

In this section, influences of global remote phenomena are examined. The focus is on ocean-atmosphere interactions and how they influence the occurrence, extent and intensity of drought in southern Africa. A correlation of PC1 of a southern Africa rain index with SST anomalies shows strong signals in several areas of the tropical oceans at 90% significance (Figure 5.16). The eastern and central equatorial Pacific Ocean and the western equatorial Indian Ocean show negative correlations with rainfall over southern Africa. The subtropical Indian Ocean and the tropical Atlantic Ocean are positively correlated with rainfall over the region.

The occurrence of El Niño and La Niña events may be determined using several indices and the more commonly used Southern Oscillation Index (SOI) and a Niño 3.4 index are preferred in this study. The Dipole Mode Index (DMI) is the preferred index for the Indian Ocean Dipole whilst the IOSD index represents the Indian Ocean Subtropical Dipole. Case studies of the circulation associated with El Niño and non-El Niño droughts are also presented.

5.5.1 Sea-surface temperature anomalies

As with the meteorological structure, spatial patterns of global sea-surface temperature (SST) anomalies associated with each of the seven drought seasons identified in this study are mapped and analyzed. The Pacific Ocean El Niño signal is dominant in 5 drought seasons – 1983, 1987, 1992, 1995 and 2003 even though at varying intensities (Table 5.1; Figures 5.17). 1982 is ENSO neutral whilst 1984 is a weak La Niña. Thus, the successive droughts of the 1980s were forced by different mechanisms as 1982 was ENSO neutral, 1983 strong El Niño whilst 1984 was a weak La Niña.

The Indian Ocean is important during 1987, 1992 and 1995. A positive IOD event coincided with the 1992 drought whilst negative phases of the IOSD prevailed during the

1987 and 1995 droughts. Cold SST anomalies over the tropical Atlantic Ocean adjacent to Africa have occurred during the 1982, 1987 and 1992 droughts whilst warm anomalies have occurred during the 1995 drought (Figure 5.17).

5.5.2 El Niño Southern Oscillation

The Southern Oscillation refers to a seesaw of sea-level pressure between the central and eastern equatorial Pacific Ocean and the western Indo-Pacific Ocean (Behera and Yamagata 2003). This variation of atmospheric pressure has been linked to variability of SSTs in the equatorial Pacific Ocean, and the combined effect is termed the El Niño Southern Oscillation (ENSO). A time series of the SOI from 1979-2012 shows fluctuations from positive (La Niña) to negative (El Niño) phases, punctuated by neutral conditions (Figure 5.18). SOI values between -1 and +1 are mostly considered as near neutral. Thus, Table 5.1 shows the El Niño and La Niña events during the study period. Of the seven droughts identified in Chapter 3 using the P-E anomaly index, five droughts (1982/83, 1986/87, 1991/92, 1994/95 and 2002/03) have occurred during the presence of El Niño conditions. However, the 1983/84 drought occurred during weak La Niña whilst the 1981/82 event occurred under ENSO neutral conditions.

Whilst their occurrence appears random, the SOI exhibits cycles of between 2-7 years. Typically, an El Niño/La Niña event begins in May-June and may persist until the austral autumn. ENSO peaks during December – February, coinciding with the summer rainfall season over southern Africa. At times, successive ENSO events have occurred such as the El Niños of 1986-1988 and 1992-95 and also the prolonged La Niña episodes of 1998-2001. In addition, there appears to be increased frequency of La Niña events since 1999/2000. The correlation between the SOI timeseries and the P-E index is R = +0.2 over southern Africa, significant at 95% confidence level. For the entire southern Africa region, previous research has determined that El Niño accounts for about 30% of rainfall variability (e.g. Tyson and Preston-Whyte 2000).

A correlation of the SOI and rainfall over southern Africa shows positive values (at 90% significance), with a stronger association over the east, covering Zimbabwe, southern

Zambia, southern Mozambique and South Africa's Limpopo (Figure 5.19). Strong negative SOI values are significantly related to major drought events over southern Africa (20-35°E; 15-25°S). Negative SOI values have been linked to sustained subsidence in the mid-troposphere over southern Africa (Jury *et al* 1994). The Niño 3.4 index shows a similar signal but with a negative correlation over much of southern Africa such that warm ENSO events result in rainfall deficits particularly over the eastern sector (Figure 5.20). However, the strong ENSO event of 1997-98 was associated with only mild departures from normal rainfall (Figure 5.21) as the Angola Low and cloud bands were strengthened resulting in higher than expected rainfall (Reason and Jagadheesha 2005).

A positive correlation (at 90% significance) occurs between the NDJ Nino 3.4 index and DJF geopotential height at 500 hPa over southern Africa (Figure 5.22). As SSTs rise in the central equatorial Pacific Ocean, high pressure is established over southern Africa and the Botswana High intensifies. Vertical velocity (DJF) at 500 hPa is also positively correlated (90% significance) with NDJ Niño 3.4 with higher association over the eastern sector (Figure 5.23). Warm SSTs in the Niño 3.4 region indicate positive omega values implying subsidence over southern Africa. At the surface, pressure rises occur over much of the subcontinent including the tropical SW Indian Ocean and the Mozambique Channel with positive Niño 3.4 (Figure 5.24). These pressure rises may account for fewer tropical cyclones forming over the SW Indian Ocean during warm ENSO events.

Strong positive surface temperature anomalies occur during El Niño events. Thus, heat waves are more likely during El Niño, and this finding is consistent with Lyon (2009).

Due to the significance of the ENSO signal over the study area, early signs of El Niño/La Niña may provide useful indicators for seasonal climate prediction in southern Africa.

5.5.3 El Niño and non-El Niño droughts: 1984 and 1992 events

In this section, a comparison is made of a typical El Niño drought and a typical non-El Niño drought. According to the P-E anomaly drought index, the 1992 drought is the most severe drought to affect southern Africa since records began in 1860. The 1992 drought

occurred under strong El Niño conditions whereas the 1983/84 drought occurred during the presence of a weak La Niña in the eastern equatorial Pacific Ocean (Table 5.1). Some of the results discussed here have already been presented in an earlier section.

Significant differences are observed in the circulation patterns for the two drought seasons. Positive anomalies of 500 hPa geopotential heights are observed mainly to the west of southern Africa during 1984 with negative anomalies over the east and Mozambique Channel (Figure 5.11). The 1992 event is much more widespread, with omega anomalies at the same levels extending to the Mozambique Channel. The upper level winds exhibit strong positive anomalies over the Zambezi during 1992 whilst easterly anomalies are widespread during 1984. Easterly wind anomalies helped drive tropical storms westward, accounting for the uplift observed over the Mozambique Channel. Mulenga *et al.* (2003) also found enhanced upper westerlies over South Africa during El Niño drought which restricted the formation of TTTs whilst mid-latitude influences characterized non-ENSO droughts.

In a few cases, successive El Niños and La Niñas have occurred but with different impacts on seasonal rainfall and this may be due to differences in the state of the Indian Ocean.

5.5.4 Indian Ocean influences

The Dipole Mode Index (DMI) is widely used to measure the phase and strength or intensity of the Indian Ocean Dipole (IOD). The time series of DMI index with P-E is shown in Figure 5.25. Most, but not all positive DMI events are linked to drought over southern Africa, whilst the severe and extreme droughts of 1995, 1992 and 1983 occurred in the presence of positive IOD, in addition to warm ENSO conditions. However, the dominant positive IOD event of 1997 did not result in severe drought. Warm SSTs in the tropical Indian Ocean extending to the east of Madagascar support a relocation of the cloud bands from southern Africa to the Indian Ocean as far as East Africa. It has been shown earlier that the positive phase of the IOD is linked to the upper level convergence found over South Africa and Botswana. The Mascarene High also affects the characteristics of the IOD (Manatsa and Behera 2014). It is argued that a positive phase of the DMI coupled

with warm ENSO act to produce severe drought over southern Africa. The two co-occurred during 1982/83, 1986/87, 1987/88, 1991/92, 1994/95 and 1997/98.

The Indian Ocean Subtropical Dipole (IOSD) Index and P-E index are shown in Figure 5.26. It appears cooler SSTs (in the west) near Africa in the subtropics promote drought perhaps through reduced moisture supply from the SW Indian Ocean. Thus, five of the seven droughts in this study coincided with negative phases of the IOSD i.e. 1983, 1984, 1992, 1995 and 2003. This is consistent with Manatsa and Behera (2014) who showed that TTTs and attendant cloud bands shift to the SW Indian Ocean during warm ENSO phase.

The IOD and IOSD result from fluctuations in SST anomaly patterns which affect tropical cyclone genesis, intensity and propagation characteristics in the SW Indian Ocean (e.g. Ash and Matyas 2012, Manatsa and Behera 2014). However, it is not the scope of this research to investigate how Indian Ocean indices affect tropical cyclone characteristics in the SW Indian Ocean.

The Indian Ocean seems to exert more influence on southern African rainfall patterns in the absence of a strong ENSO signal from the Pacific Ocean.

5.5.5 Atlantic Ocean influences

The influence of the South Atlantic Ocean on seasonal rainfall over southern Africa has received less research attention as most research has focused on the Pacific Ocean and the Indian Oceans. The warming or cooling of the surface ocean water near Africa may affect sea level pressure which modulates moisture convergence over southern Africa. The trade winds recurve to become north westerlies over the equatorial Atlantic Ocean bringing moisture from the Congo Basin (Congo Air). Composite of drought seasons over the tropical Atlantic Ocean shows a significant area of interest. An area of the Atlantic Ocean adjacent to Africa between 5-15°S is related to changes in sea-level pressure over the adjacent interior Figure 5.27. A cooler/warmer ocean results in anomalously higher/lower SLP over the ocean and adjacent interior (Figure 5.26). Higher pressure anomalies associated with a cooler Atlantic Ocean result in a weakening of the Angola

Low whilst cloud band formation is inhibited. Similar results were found in a study of Vaal river discharge by Jury (2016).

Sometimes warm water from the north intrudes south resulting in unusual warming of the Atlantic Ocean in the area of the Benguela Current, analogous to warming in the Peruvian Current (eastern Pacific Ocean). These intrusions of warm water have been termed Benguela Niños and tend not to occur together with Pacific Ocean Niños (e.g. Florenchie *et al.* 2003). Big Benguela Niño events occurred during the 1984 and 1995 drought seasons. In a study relating Benguela Niños to rainfall over southern Africa, Hansingo (2008) determined that warming over the southeast Atlantic Ocean may rigger anomalously wet conditions over western Angola or farther inland depending on the magnitude of warming. SST anomalies in this region may also influence circulation anomalies over the southwest Indian Ocean and the Mozambique Channel (Hansingo 2008).

Benguela Niños alone can influence regional rainfall along the Angola/Namibia coast through enhanced evaporation and moisture convergence over the SST forcing (Hansingo and Reason 2009). The Atlantic Ocean exerts significant influence on rainfall variability over a large area of southern Africa via a connection between zonal wind stress over the equatorial Atlantic Ocean and Benguela Niños (Reason *et al*. 2006). The influence of warm SST events over the southeast Atlantic Ocean is most significant during February to April when the SSTs are at a peak (Rouault *et al.* 2003). During the austral summer, a mid-latitude mode over the South Atlantic Ocean was related to variability in the St Helena High, meridional shifts in the ITCZ and weakening/strengthening of the Angola Low (Vigaud *et al.* 2008).

5.6 Tropical cyclones and drought

Tropical cyclones in the SW Indian Ocean are predominantly influenced by the east-west IOD (Saji *et al*. 1999; Webster *et al*. 1999; Xie *et al*. 2001; Behera *et al.* 2005; Yeshanew and Jury 2007; Luo *et al*. 2010; Izumo *et al*. 2010). On some occasions, enhanced cyclogenesis near Madagascar or in the Mozambique Channel may bring dry weather or

extended dry spells over central areas of southern Africa. This occurs as a result of enhanced subsidence over the western flanks of the storms (Reason 2007) and diffluent flow at the surface. Westerly surface wind anomalies are observed west of the Mozambique Channel with easterly anomalies over the east resulting in convergence and uplift around 40°E (Figure 5.28a). This is consistent with Mudenda and Mumba (2004) in a study of cyclone Bonita 1996 and more recently Chikoore *et al.* (2015) in a study of an active 2012 tropical cyclone season.

On the other hand, tropical cyclone landfalls can also produce unseasonal rainfall amounts for seasons that are otherwise dry. A typical example occurred during the drought of 1984 when landfalls of tropical cyclones Domoina and Imboa resulted in high rainfall in southern Mozambique, Swaziland and South Africa's eastern province (Figure 5.28b, Jury *et al*. 1993b). Intense rainfall from tropical cyclone landfalls may result in seasonal rainfall totals in an area exceeding long-term normals. Tropical cyclone Eline affected southern Africa during February 2000 and dumped about 25% of the mean for January to March in just a few days (Reason and Keibel 2004). This highlights one of the limitations of the per cent of normal method of determining drought.

5.7 Summary and discussion

This chapter has discussed the meteorological structure of drought in southern Africa including the influence of remote oceans on drought. The establishment, strengthening and persistence of the Botswana High is a primary cause of drought in southern Africa. Positive geopotential height anomalies were found in the middle levels over southern Africa with enhanced subsidence between 20-30°E and 10-20°S.

Most droughts during the study period have occurred during the presence of an El Niño in the equatorial Pacific Ocean. El Niño is positively correlated with high surface pressure, an intensification of the Botswana High, a strengthening and equatorward displacement of upper westerlies and enhanced subsidence mainly over the eastern sector of the subcontinent. The Indian Ocean acts to modulate drought through co-occurrences of positive DMI and negative IOSD with warm ENSO.

The drought signal appears to be greatest over Zimbabwe. The 1992 drought, being the most severe occurred during a strong El Niño, a positive phase of the IOD and cold SST anomalies over the tropical Atlantic Ocean adjacent to Africa. Tropical inflows of moisture are reduced as westerly wind anomalies become dominant over the Indian Ocean. The persistence of tropical cyclones over the Mozambique Channel east of 40°E may result in extended dry spells and drought during the late austral summer. This may explain why dry periods were experienced during the late summers of 1983/84 and 2011/12 under weak La Niña conditions.

Chapter Tables and Figures

Table 5-1 ENSO events during 1979-2012 based on the SOI

El Niño seasons			La Niña seasons		
Weak	**Moderate**	**Strong**	**Weak**	**Moderate**	**Strong**
2004/05	1986/87	1982/83	1983/84	1998/99	1988/89
2006/07	1987/88	1997/98	1984/85	2007/08	1999/2000
	1991/92		1995/96		2010/11
	1994/95		2000/01		
	2002/03		2005/06		
	2009/10		2008/09		
			2011/12		

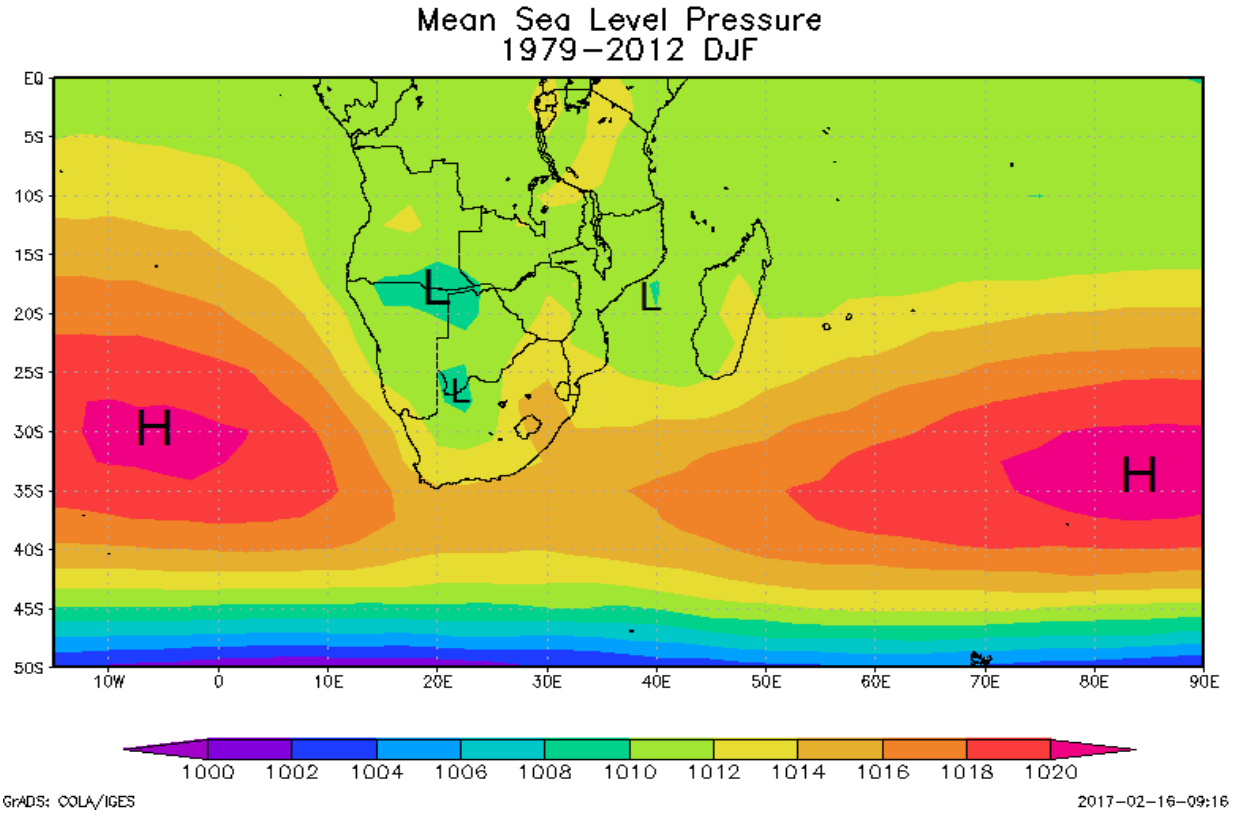

Figure 5:1 Composite mean summer (DJF) NCEP sea level pressure (shaded in hPa) over southern Africa and the adjacent oceans: 1979-2012

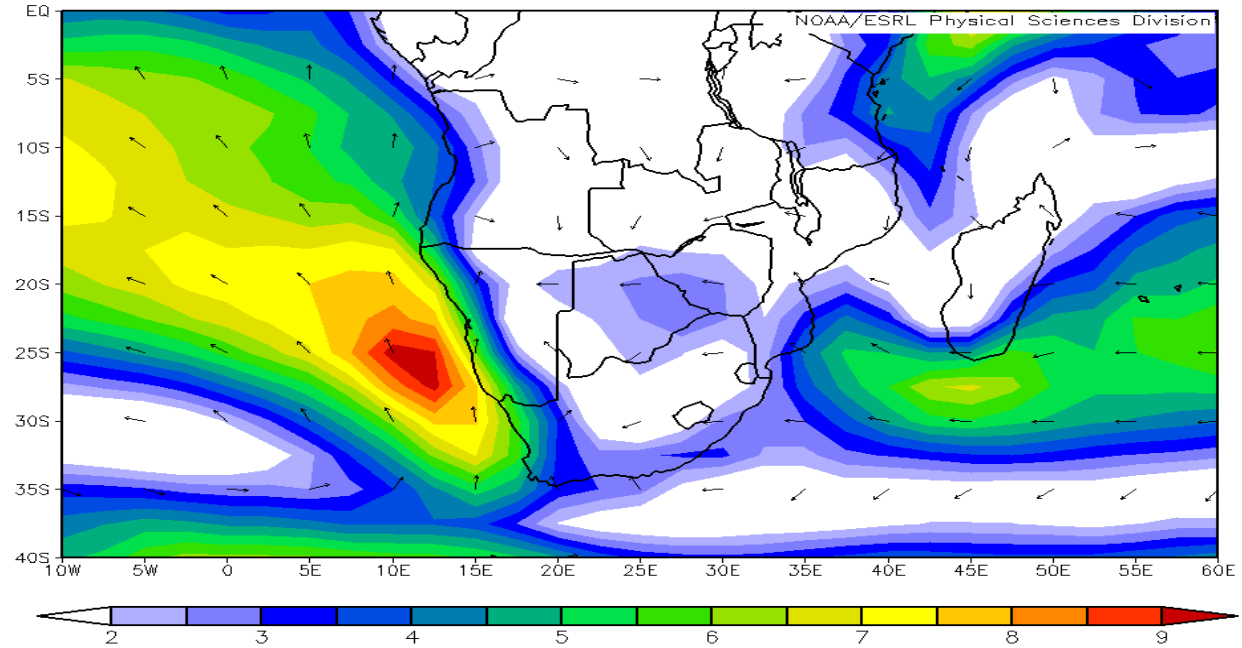

Figure 5:2 Mean summer (DJF) NCEP surface winds (vector) and wind speed (shaded in m/s) over southern Africa and the adjacent oceans

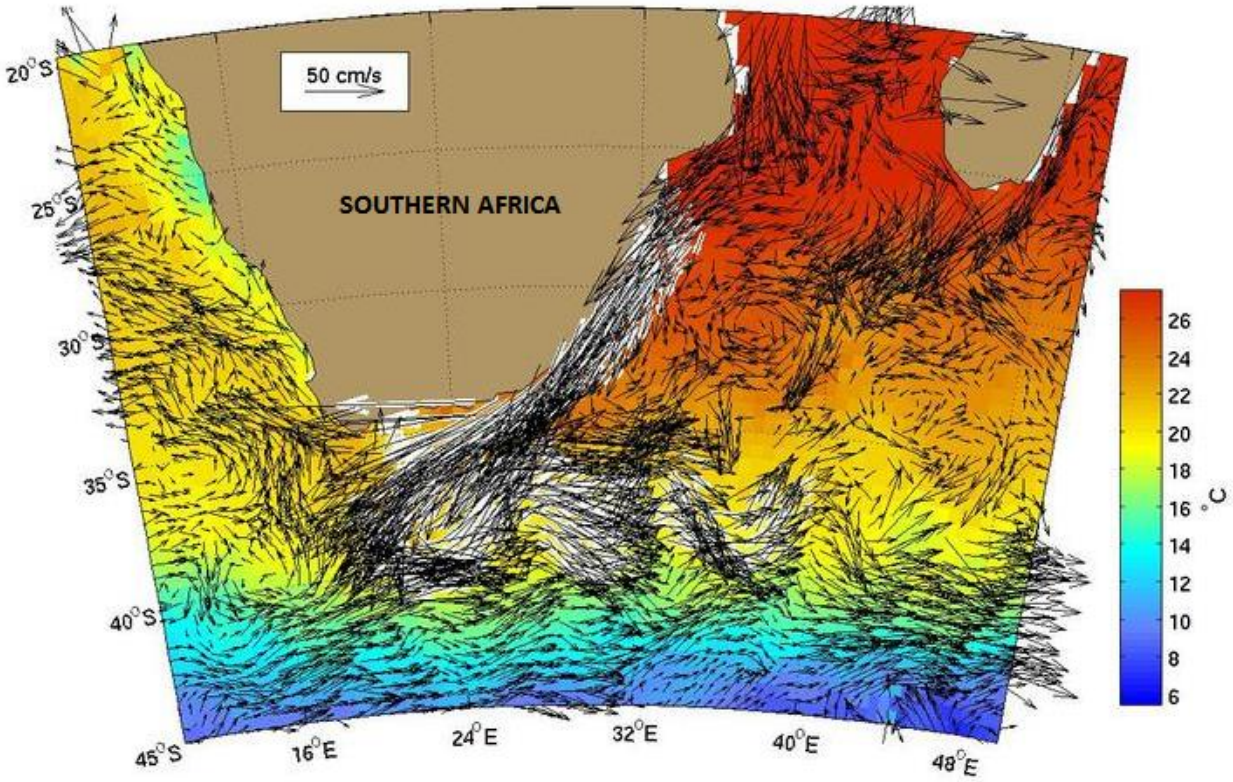

Figure 5:3 Mean summer sea surface temperature (shaded in °C) over the southeast Atlantic Ocean and the southwest Indian Ocean showing ocean currents adjacent to southern Africa (Adapted from http://oceancurrents.rsmas.miami.edu)

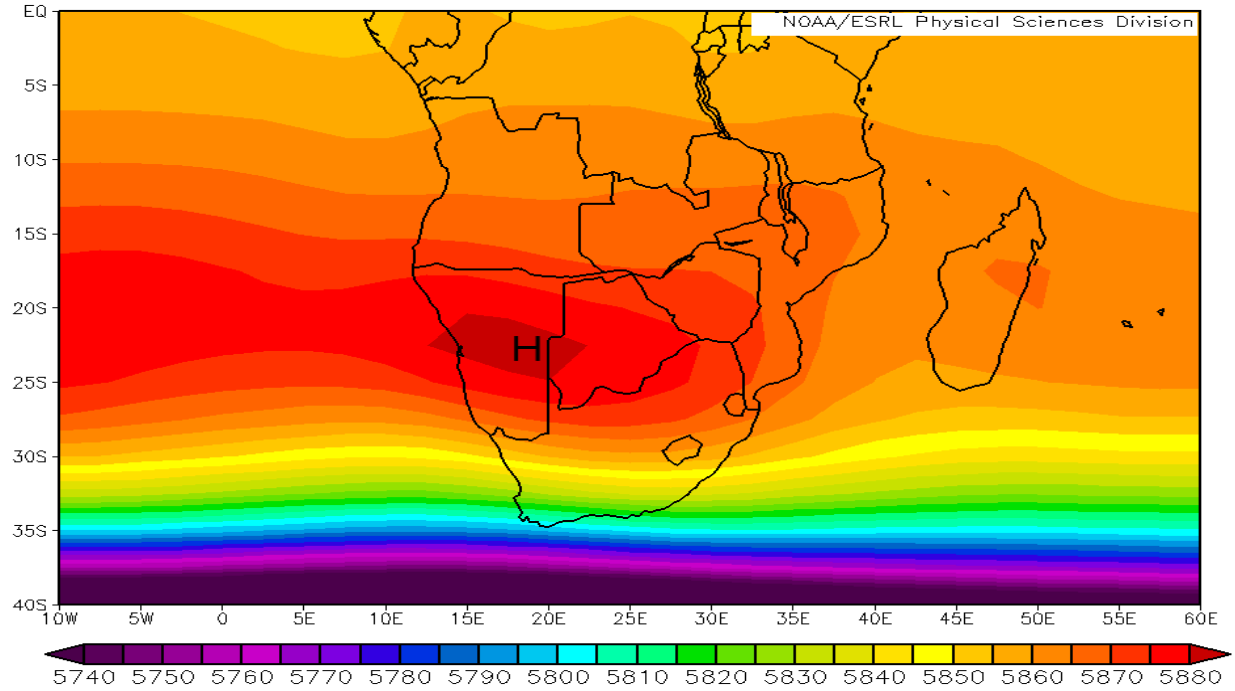

Figure 5:4 Mean summer (DJF) NCEP geopotential height (shaded in m) at 500 hPa over southern Africa and the adjacent oceans

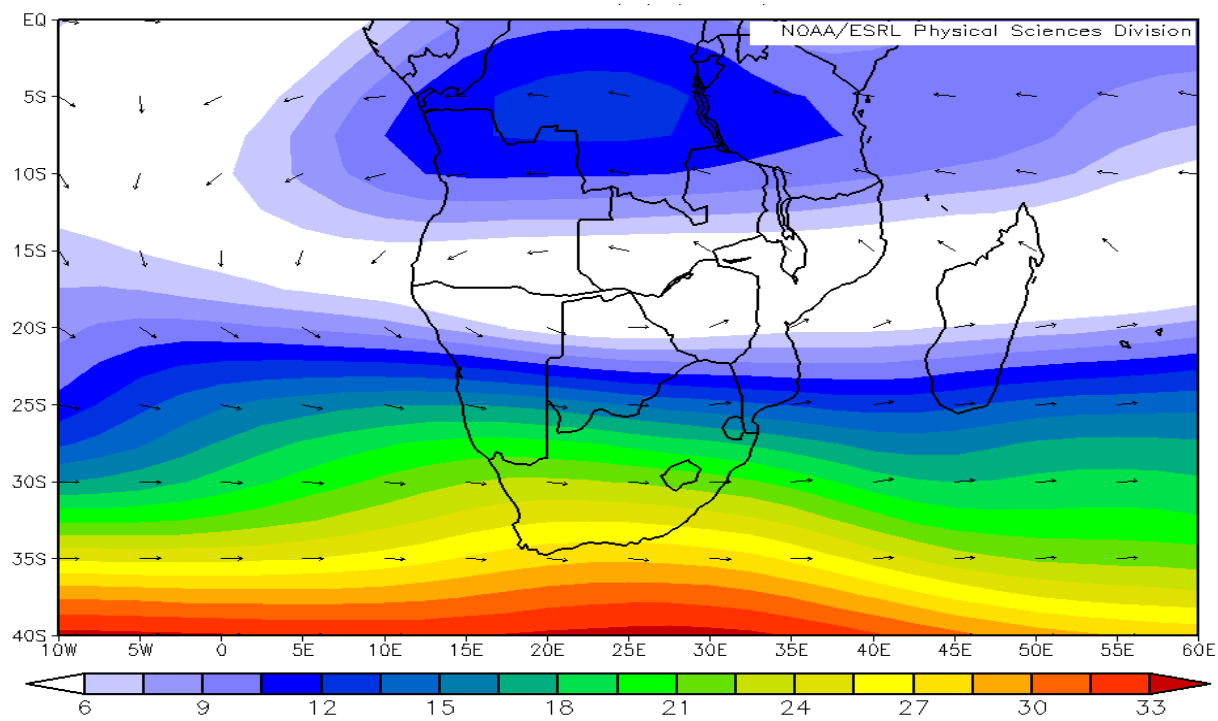

Figure 5:5 Mean summer (DJF) upper level (200 hPa) NCEP vector winds over and wind speed (shaded in ms^{-1}) southern Africa and the adjacent oceans. The jet stream is in shades of red

(a)

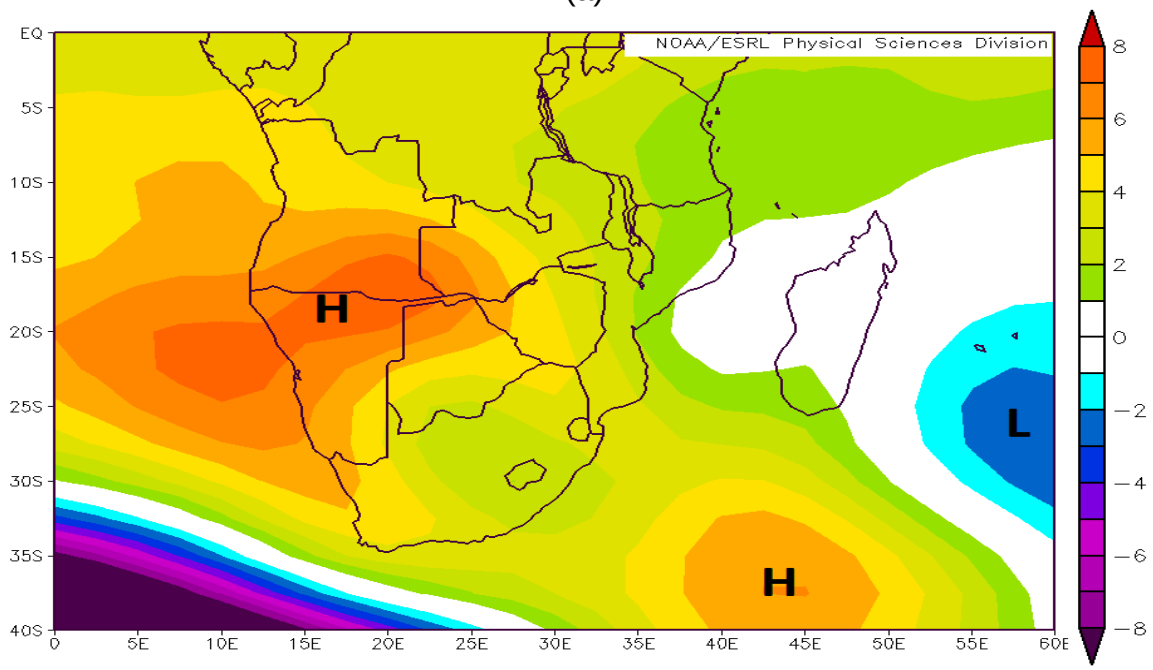

(b)

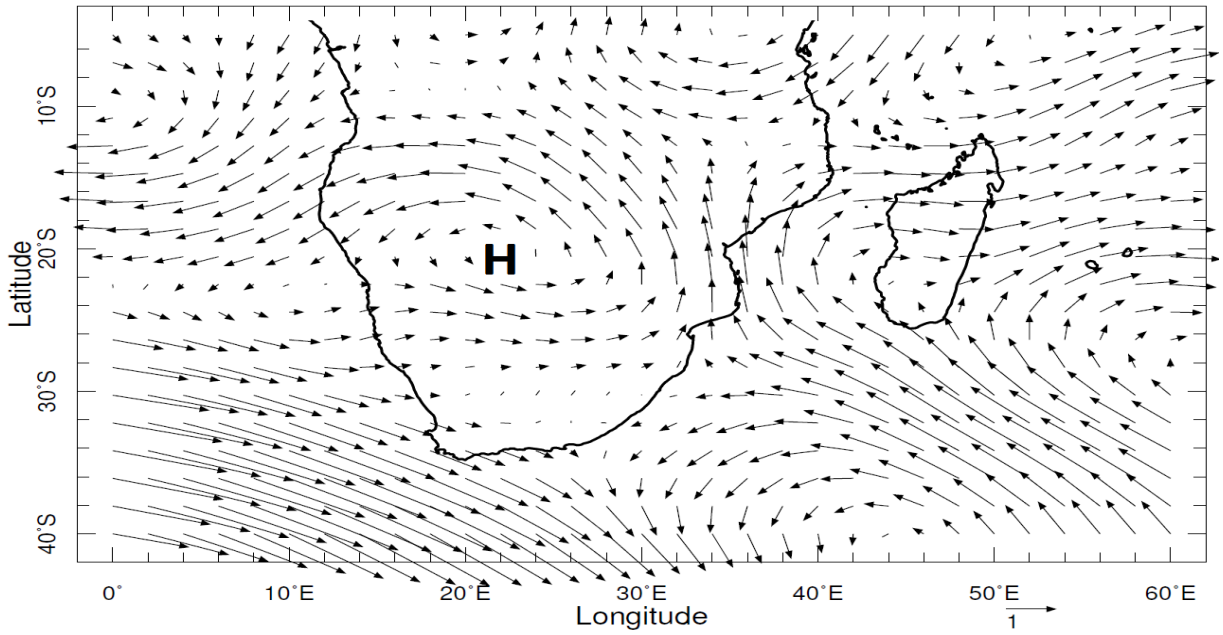

Figure 5:6 Composite mean (a) NCEP geopotential height (shaded in m) anomalies at 850 hPa and (b) associated low level (850-700 hPa) NCEP wind (vector) anomalies for drought periods over southern Africa and the adjacent oceans. A wind scale vector is shown.

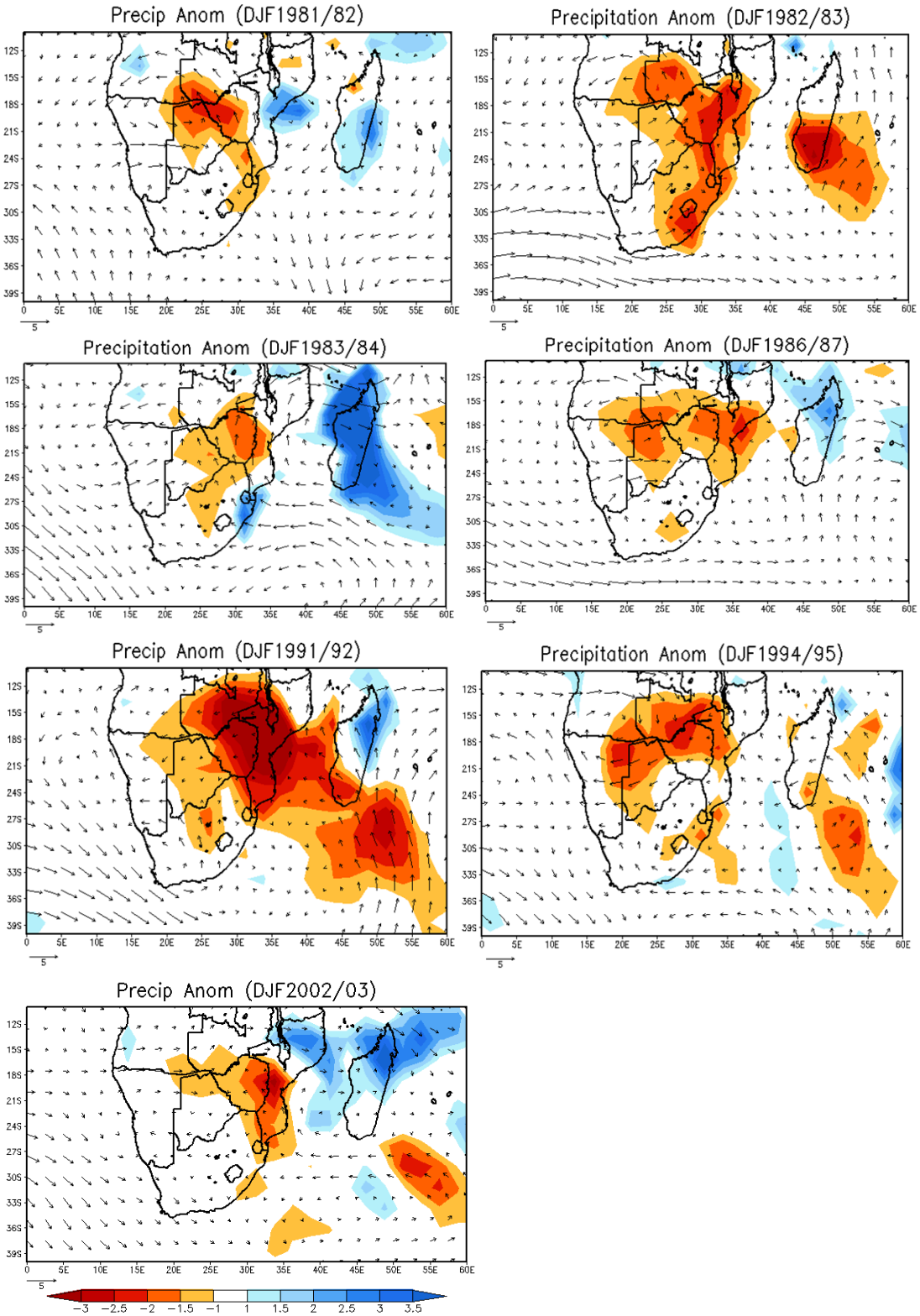

Figure 5:7 Composite mean NCEP surface wind (vector) and GPCP precipitation (shaded in mm/day) anomalies over southern Africa and the adjacent oceans for drought seasons. A wind scale vector is shown.

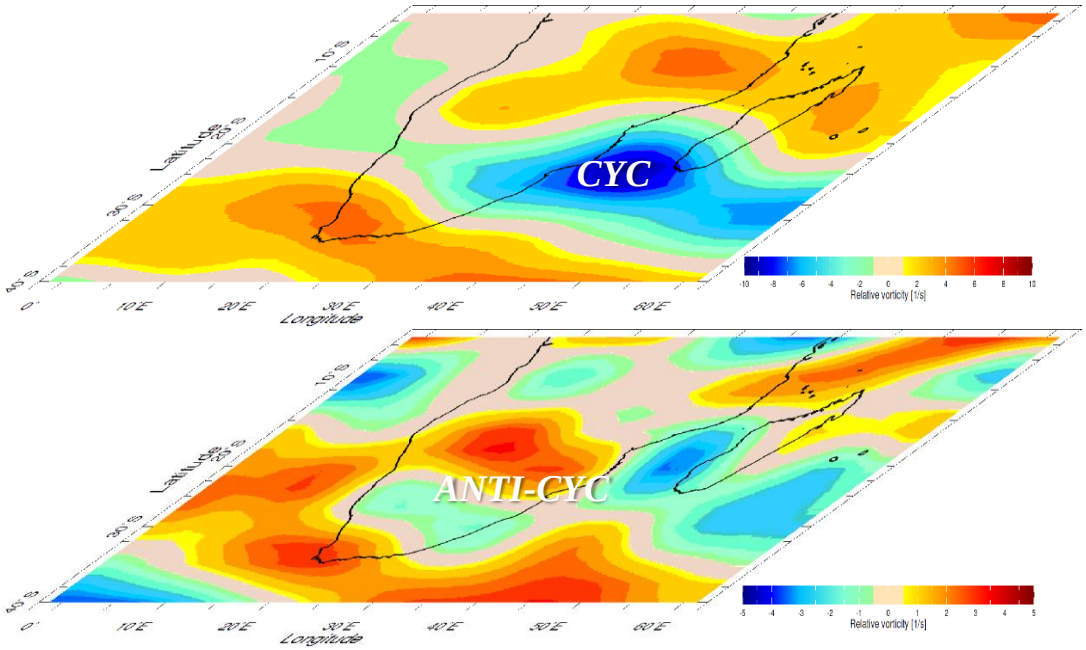

Figure 5:8 Composite mean NCEP relative vorticity (shaded in s^{-1}) for 250-200 hPa (above) and for 850–700 hPa (below) over southern Africa and adjacent oceans for drought seasons (each with its own scale x 10^{-5}).

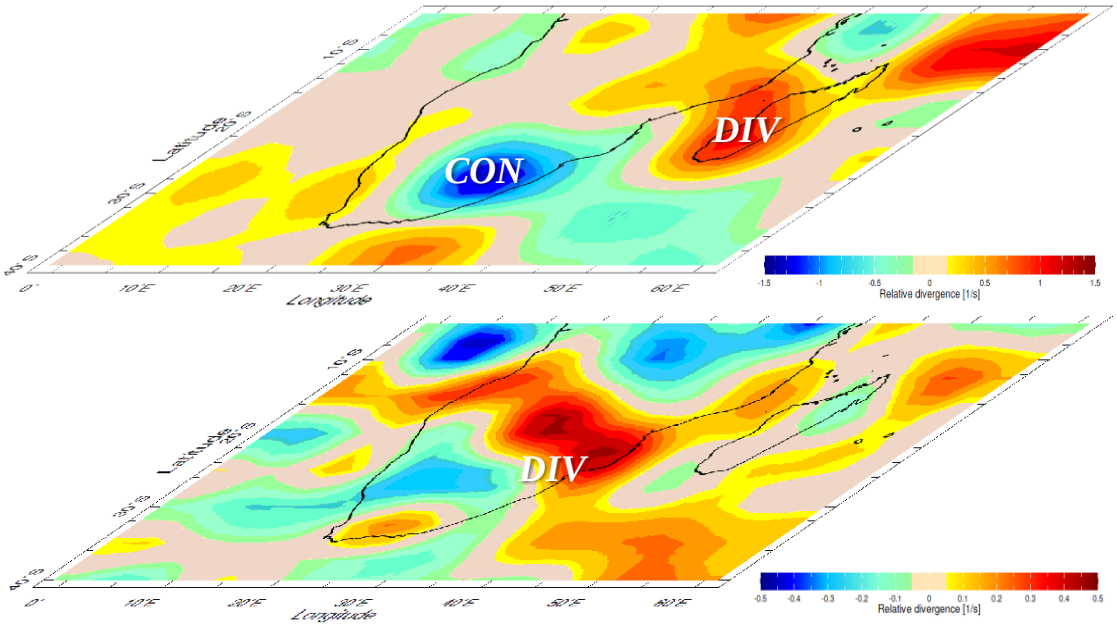

Figure 5:9 Composite mean NCEP divergence for 250-200hPa (above) and for 850-700 hPa (below) during drought seasons over southern Africa and adjacent oceans (each with its own scale x 10^{-5}).

(a)

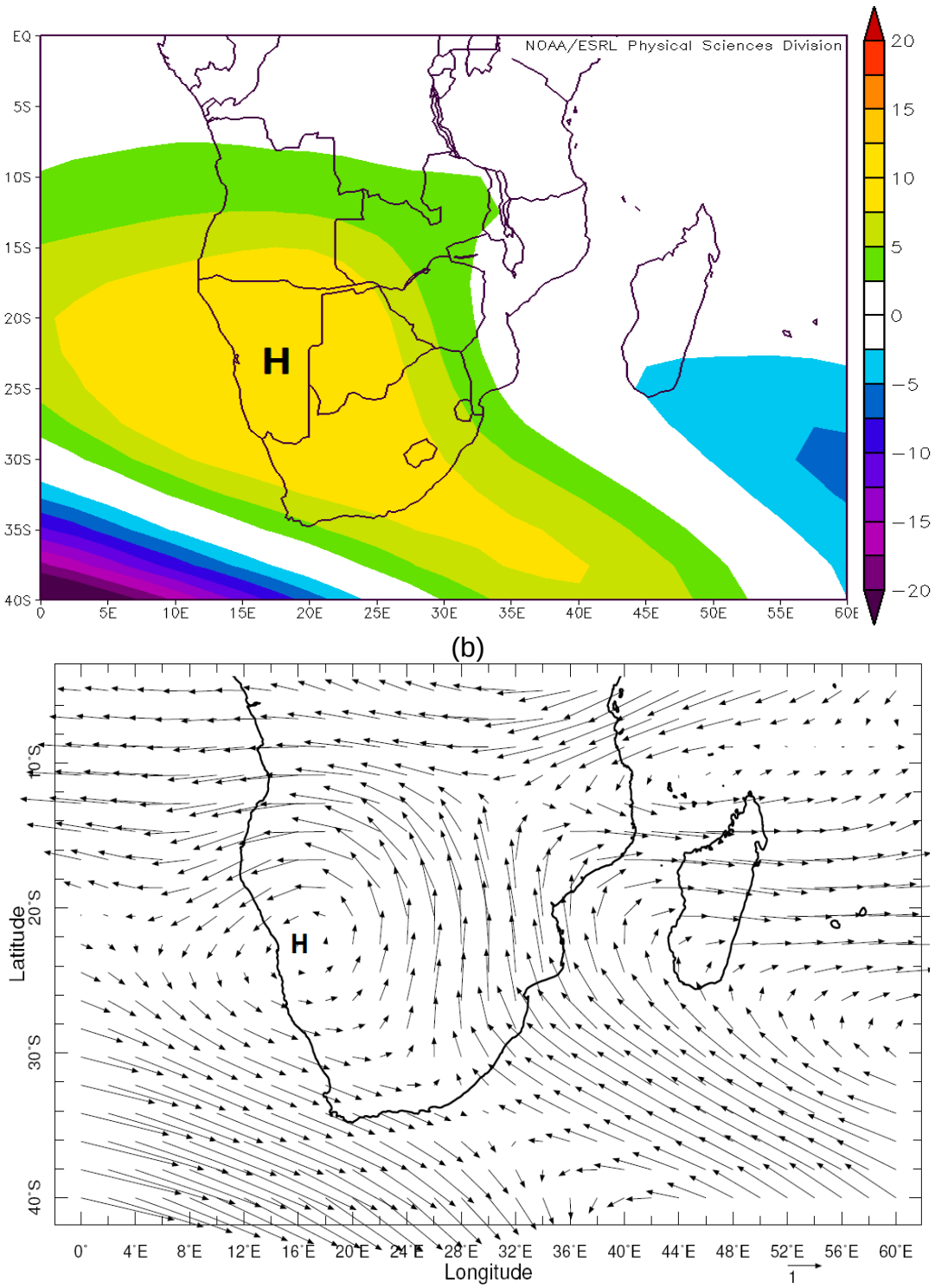

Figure 5:10 Composite mean summer (DJF) NCEP (a) geopotential height (shaded in m) and (b) associated wind vector anomalies at 500 hPa over southern Africa and the adjacent oceans during drought seasons. A wind scale vector is shown in (b).

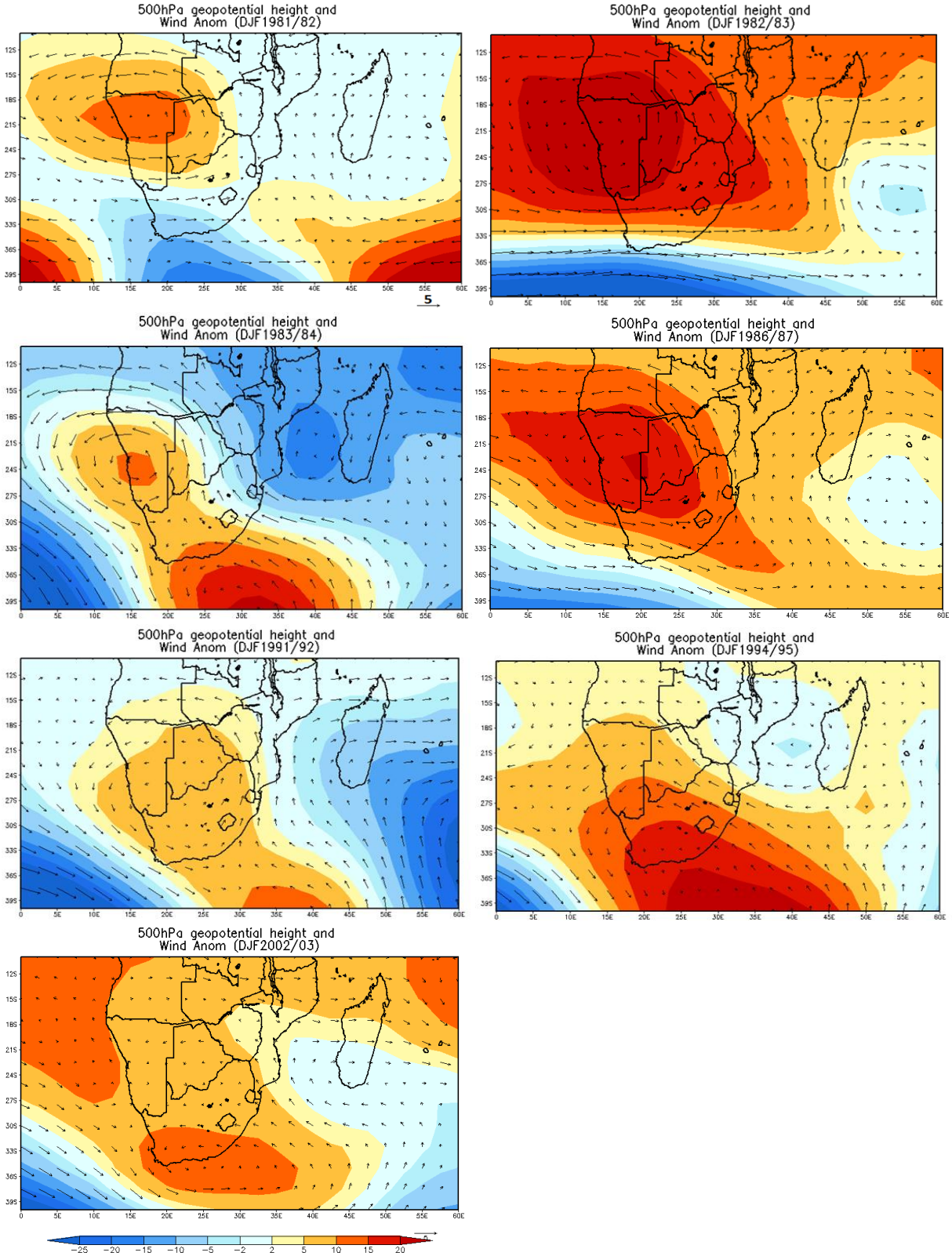

Figure 5:11 Composite summer (DJF) mean NCEP geopotential height (shaded in m) and wind vector anomalies at 500 hPa over southern Africa for each of the seven drought seasons. A wind scale vector is shown.

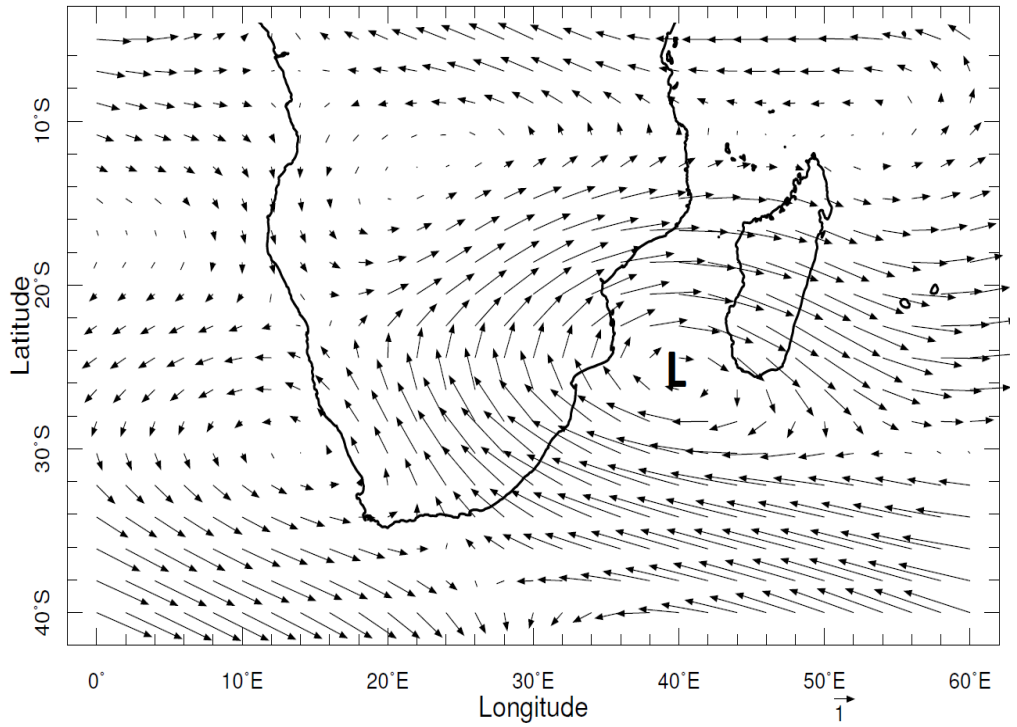

Figure 5:12 Composite mean upper level (250-200 hPa) NCEP wind (vector) anomalies over southern Africa and adjacent oceans for drought seasons. A wind scale vector is shown.

(a)

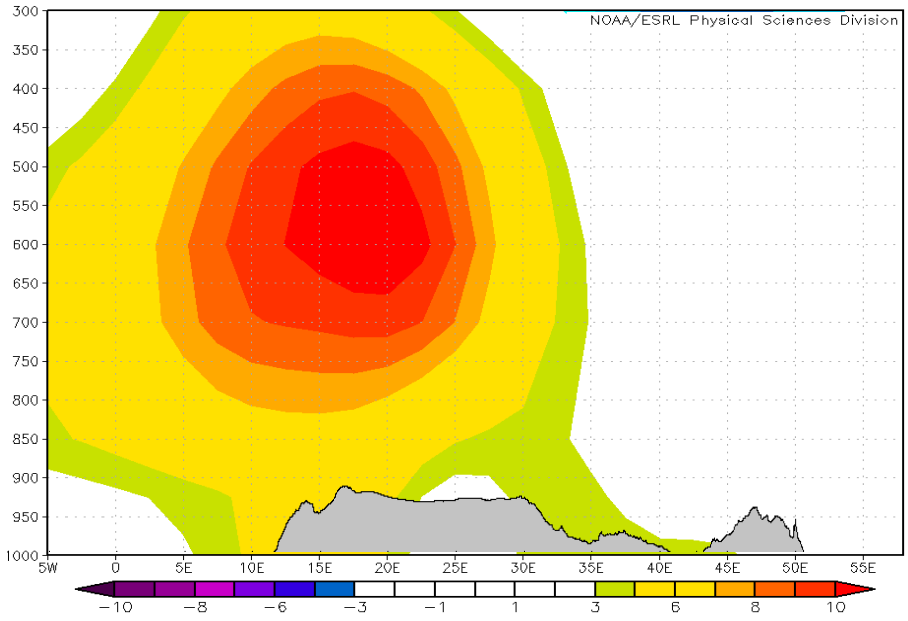

(b)

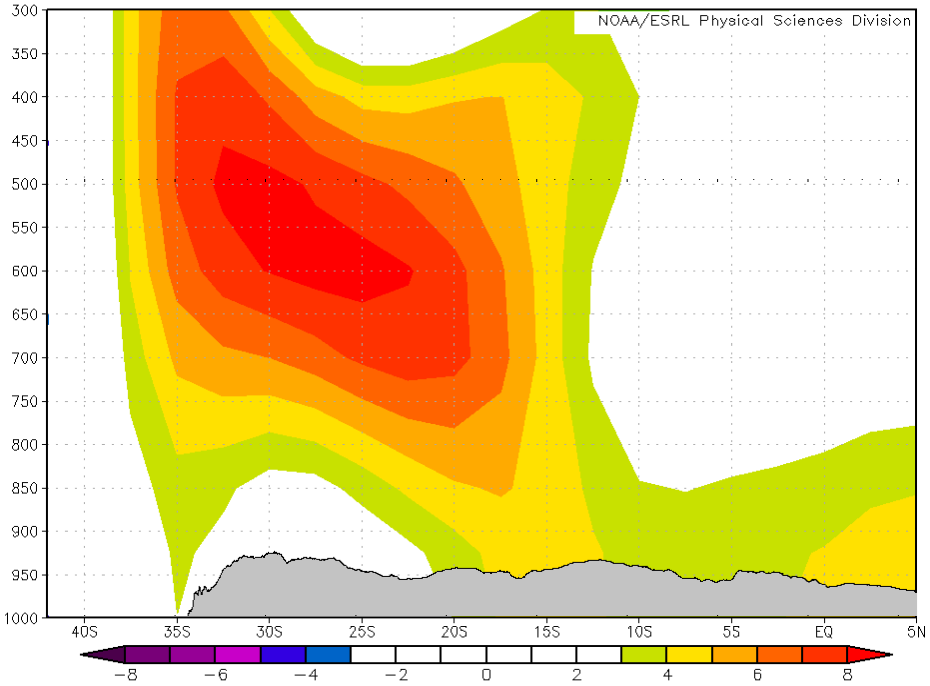

Figure 5:13 Composite mean vertical NCEP geopotential height (shaded in m) anomalies over southern Africa (averaged for 22-32°E; 15-28°S) during drought seasons from (a) west-east and from (b) north-south

(a)

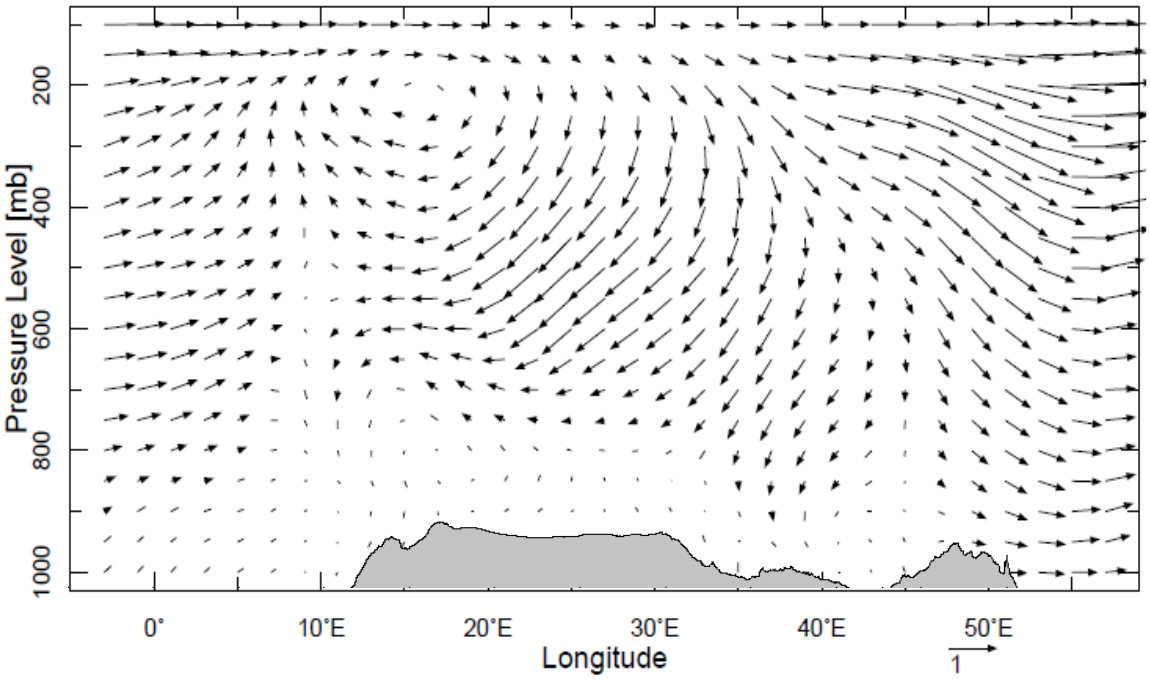

(b)

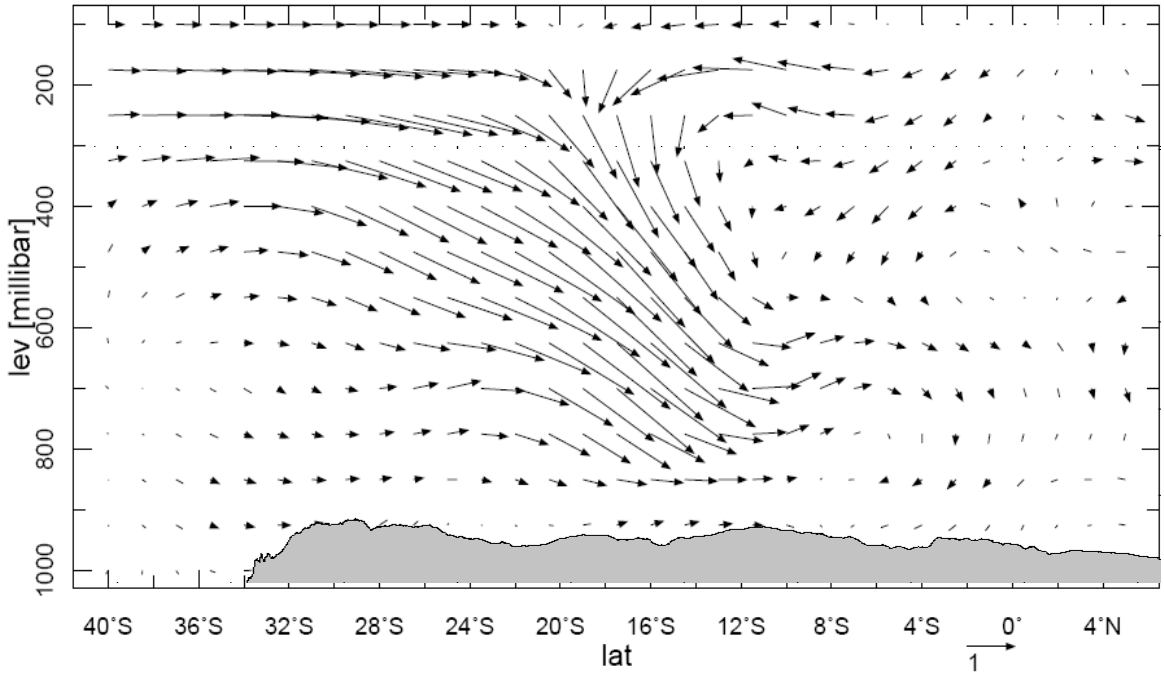

Figure 5:14 Composite mean vertical structure of NCEP circulation over southern Africa showing meridional, zonal and vertical wind (vector) anomalies from 1000-100 hPa during drought seasons from (a) west-east and from (b) south-north. A wind scale vector is shown.

(a)

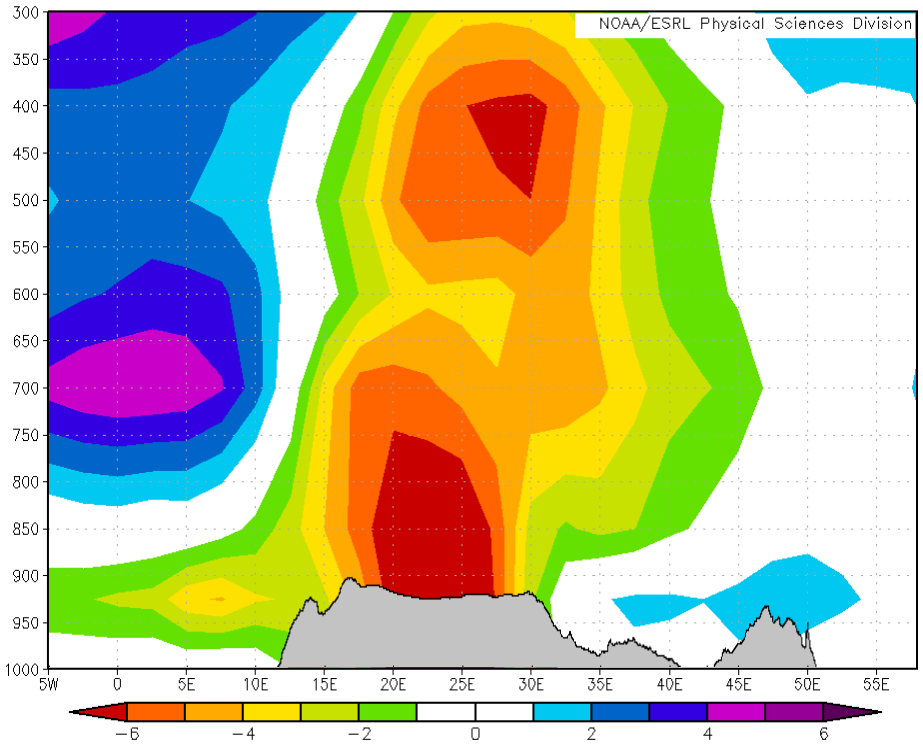

(b)

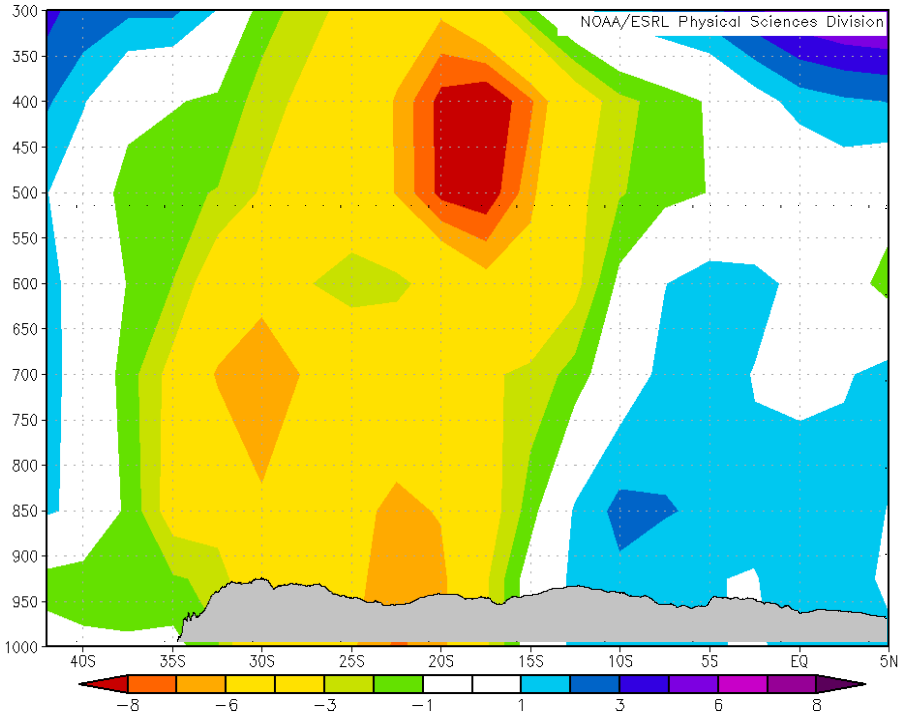

Figure 5:15 Composite mean NCEP relative humidity (shaded in %) anomalies over southern Africa (averaged over 22-32°E; 15-28°S,) vertically from 1000-300 hPa during drought periods from (a) west-east and from (b) south-north

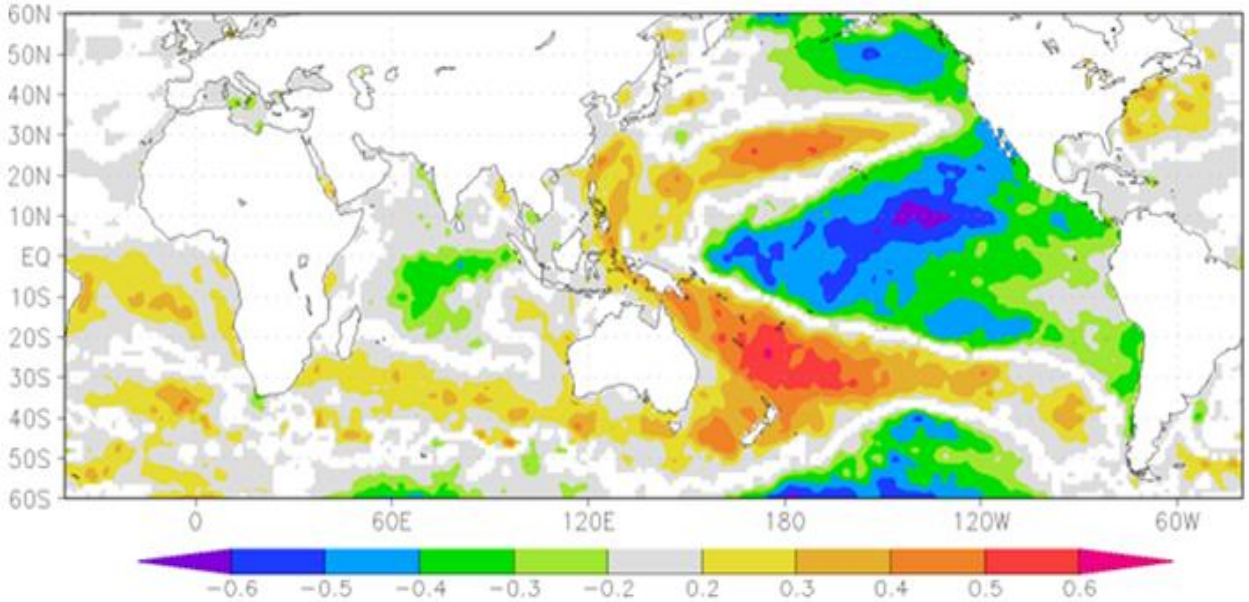

Figure 5:16 Correlation of PC1 of GPCP precipitation anomalies with HadISST1 anomalies (1960-2008). A southern Africa rain index is used. The shaded areas are significant at 90% or more.

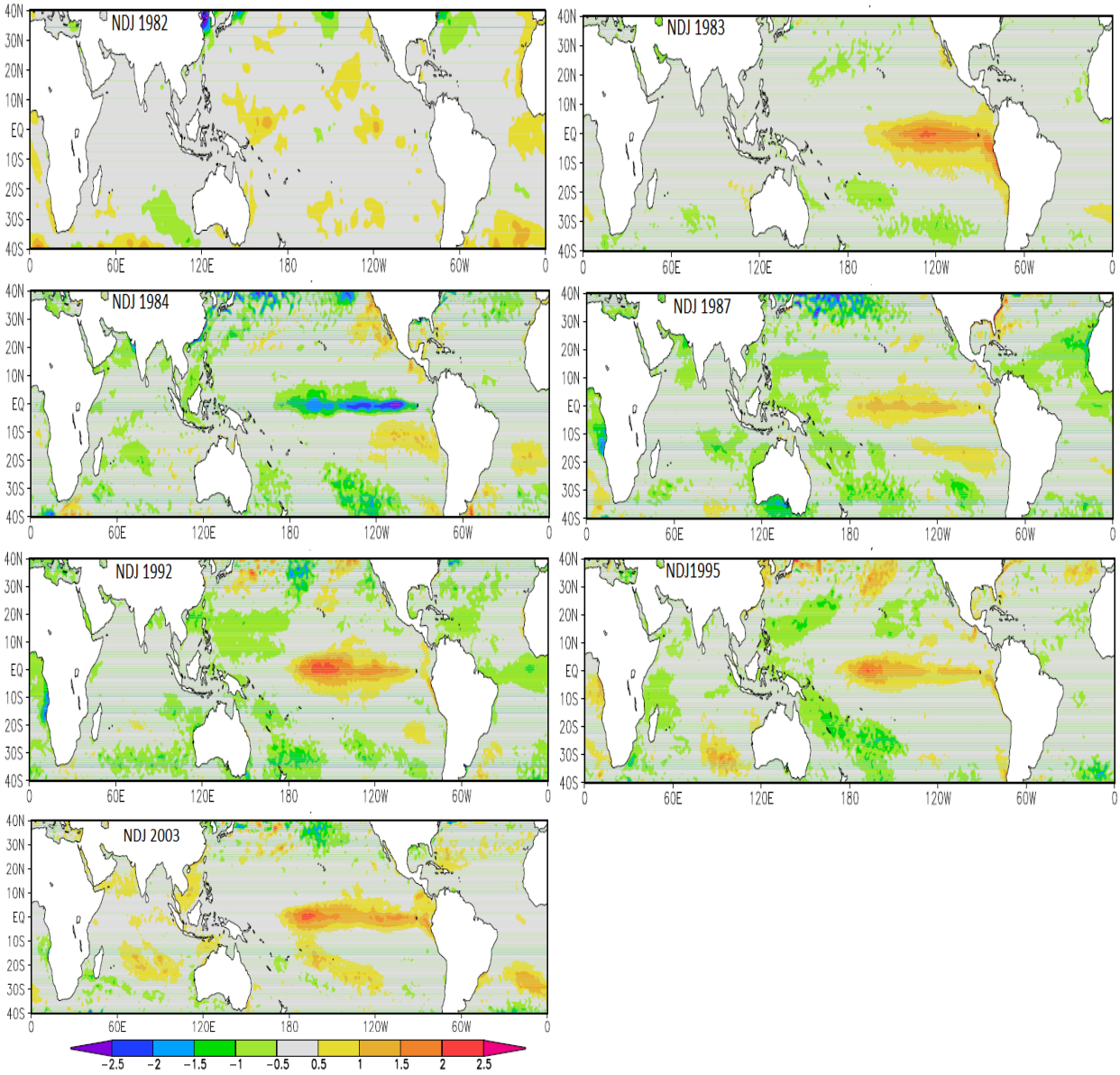

Figure 5:17 NOAA OISST sea-surface temperature (shaded in °C) anomalies over the tropical oceans during NDJ for the seven drought seasons analyzed in this study

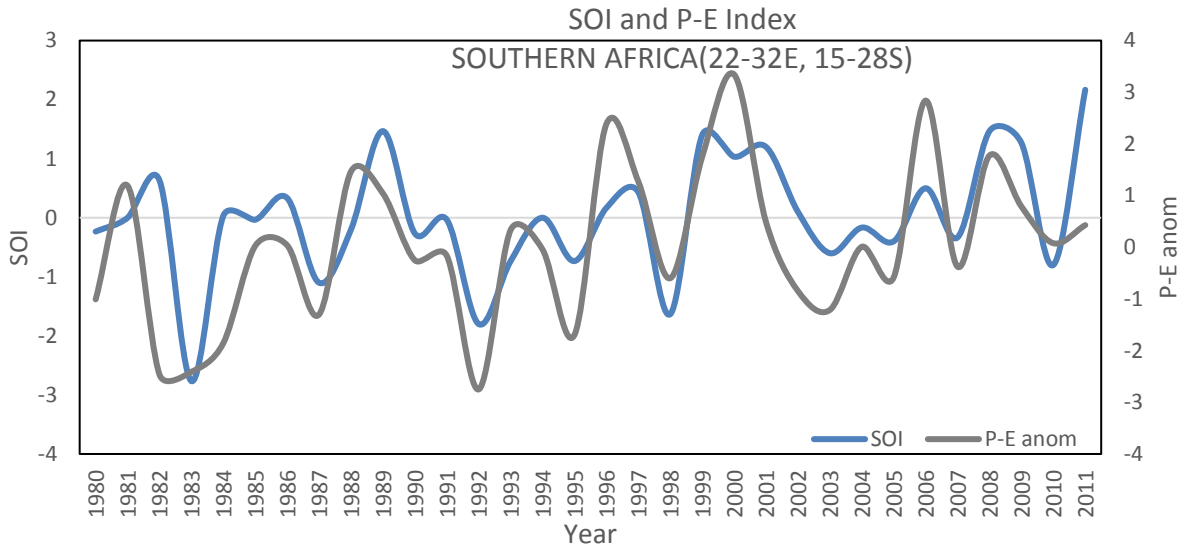

Figure 5:18 Variability of SOI and P-E anomalies over southern Africa (averaged over 22-32E; 15-28S): 1979-2012

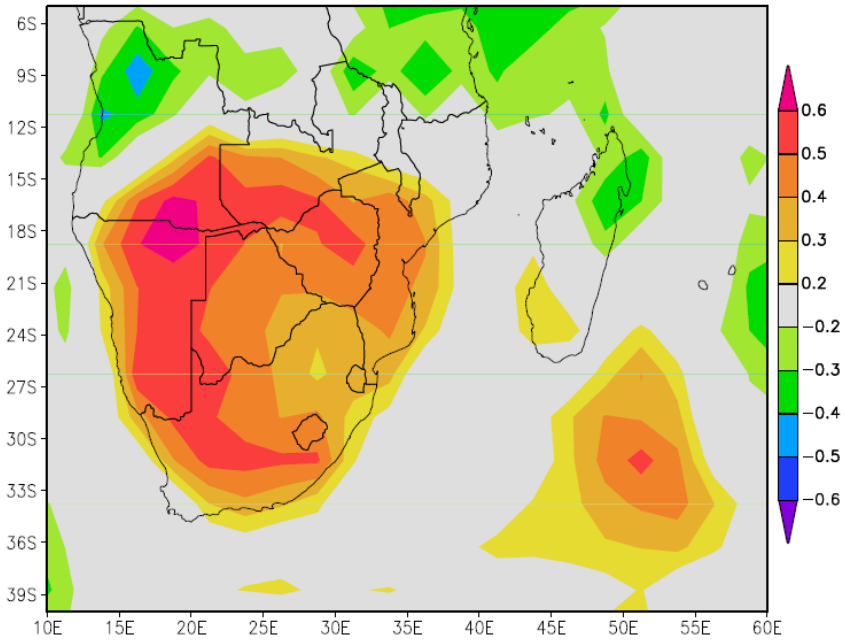

Figure 5:19 Correlation between NOAA CPC Southern Oscillation Index and GPCP precipitation during the austral summer over southern Africa and the adjacent oceans. The shaded areas are significant at 90% or more.

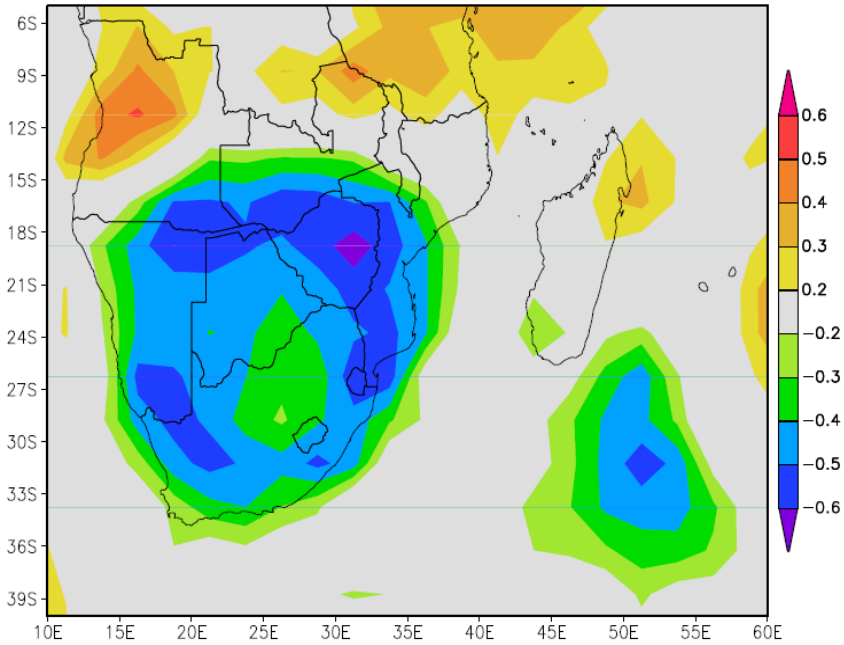

Figure 5:20 Correlation of summer DJF Niño3.4 index with GPCP precipitation over southern Africa and the adjacent oceans. The shaded areas are significant at 90% or more.

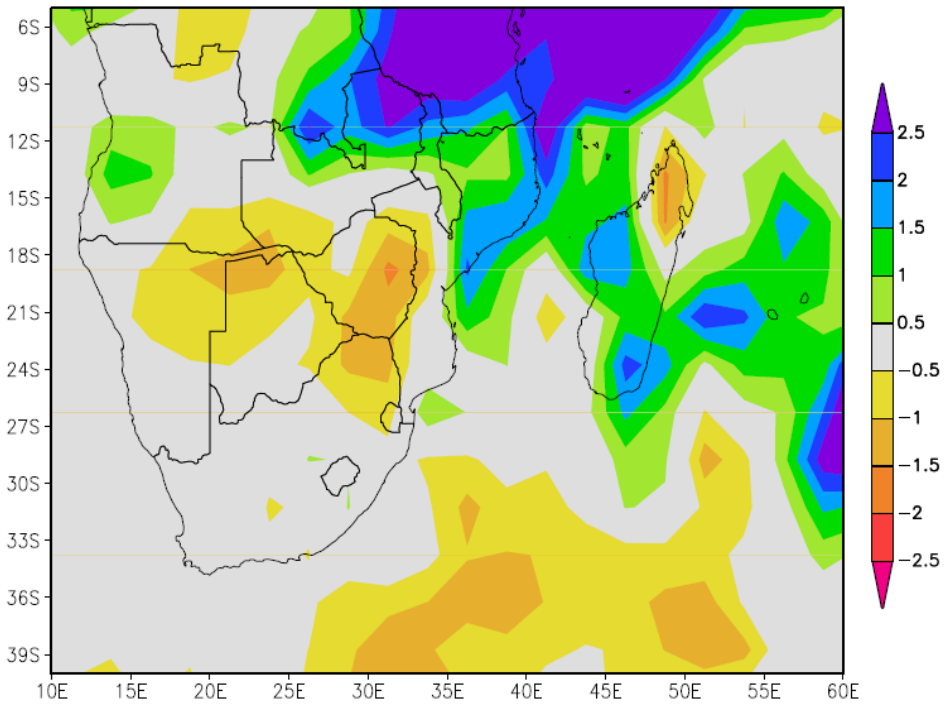

Figure 5:21 1997/98 summer (DJF) GPCP precipitation (mm/day) anomalies over southern Africa and the adjacent oceans

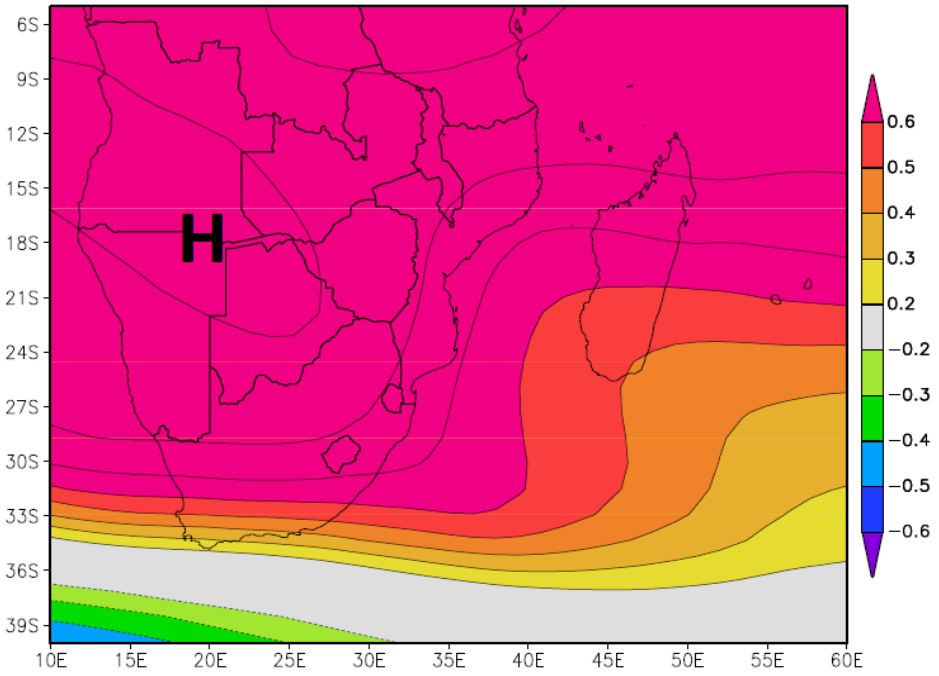

Figure 5:22 Correlation of summer (DJF) Niño 3.4 and NCEP geopotential height at 500 hPa over southern Africa and the adjacent oceans. The shaded areas are significant at 90% or more.

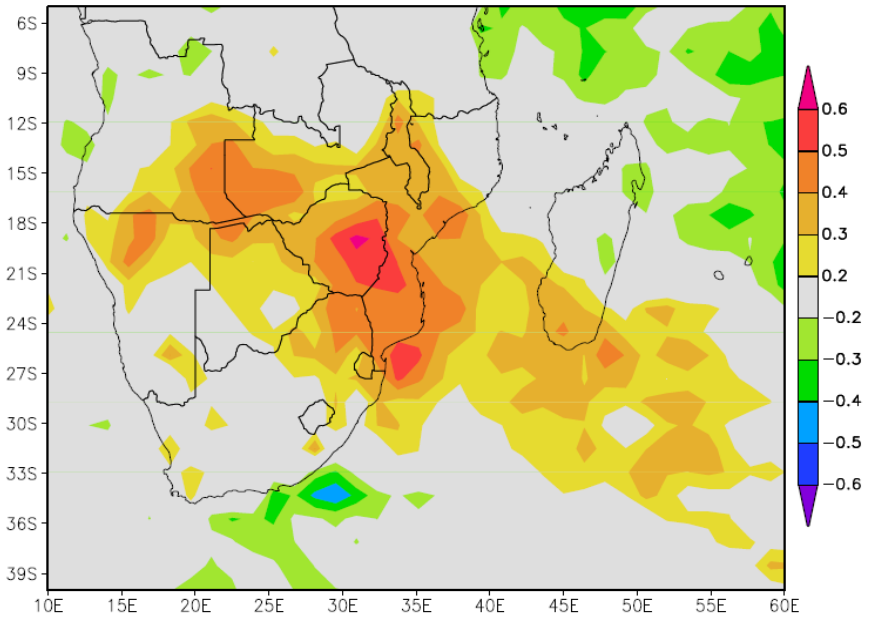

Figure 5:23 Correlation of summer (DJF) Niño 3.4 with NCEP omega at 500 hPa over southern Africa and the adjacent oceans. The shaded areas are significant at 90% or more.

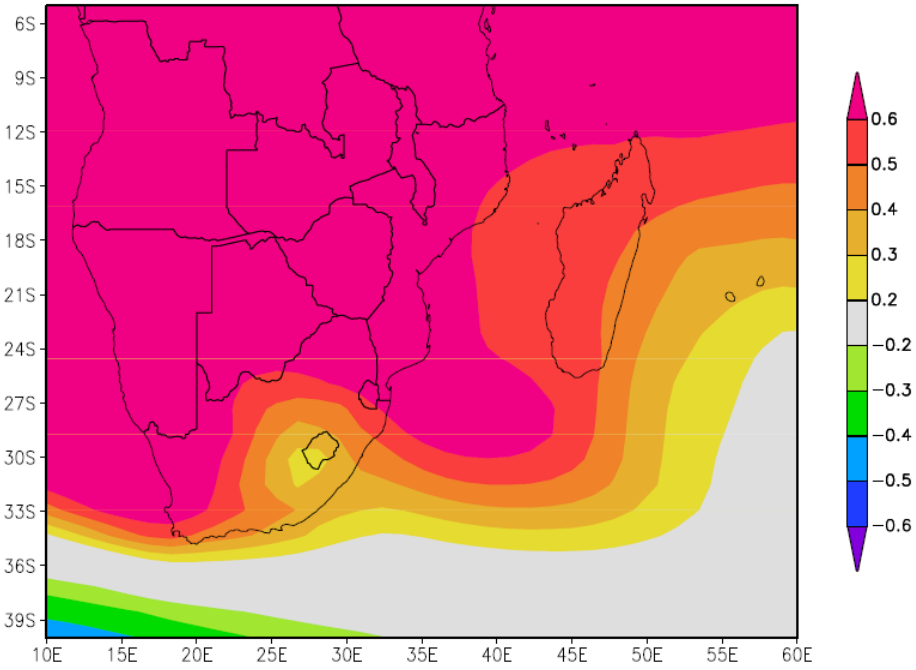

Figure 5:24 Correlation of summer (DJF) Niño 3.4 with 850 hPa geopotential height over southern Africa and the adjacent oceans. The shaded areas are significant at 90% or more.

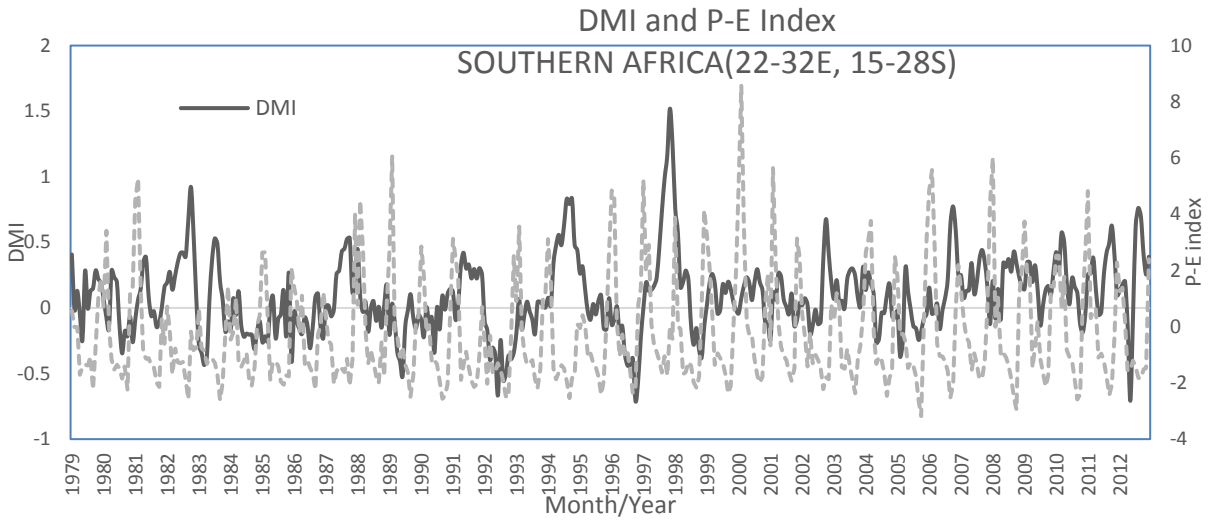

Figure 5:25 Variability of DMI and P-E index over southern Africa (averaged over 22-32E, 15-28S): 1979-2012

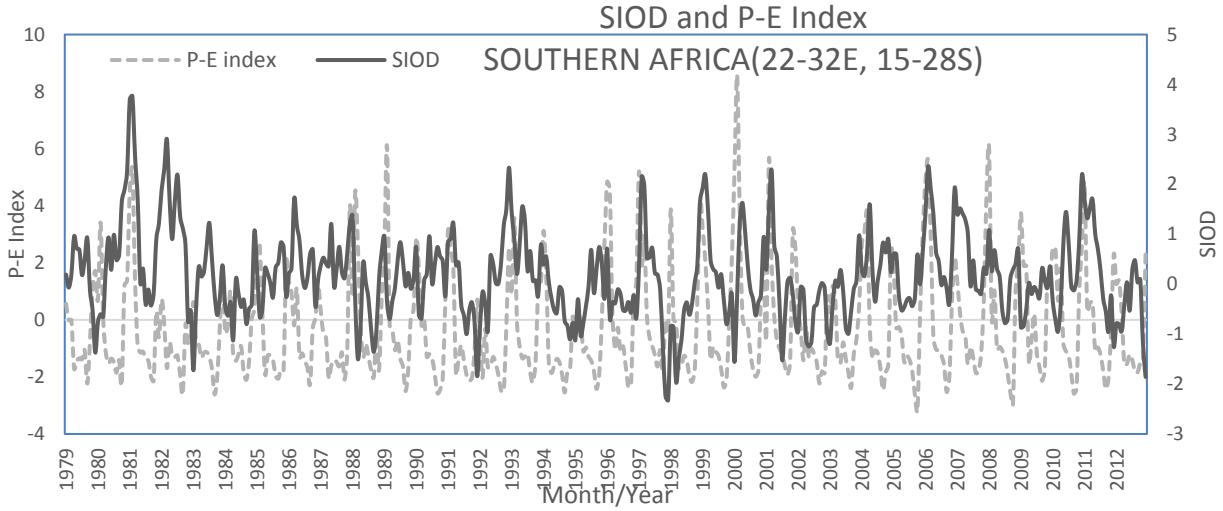

Figure 5:26 Variability of IOSD and P-E index over southern Africa (averaged over 22-32E, 15-28S): 1979-2012

s

(a) (b)

(a)

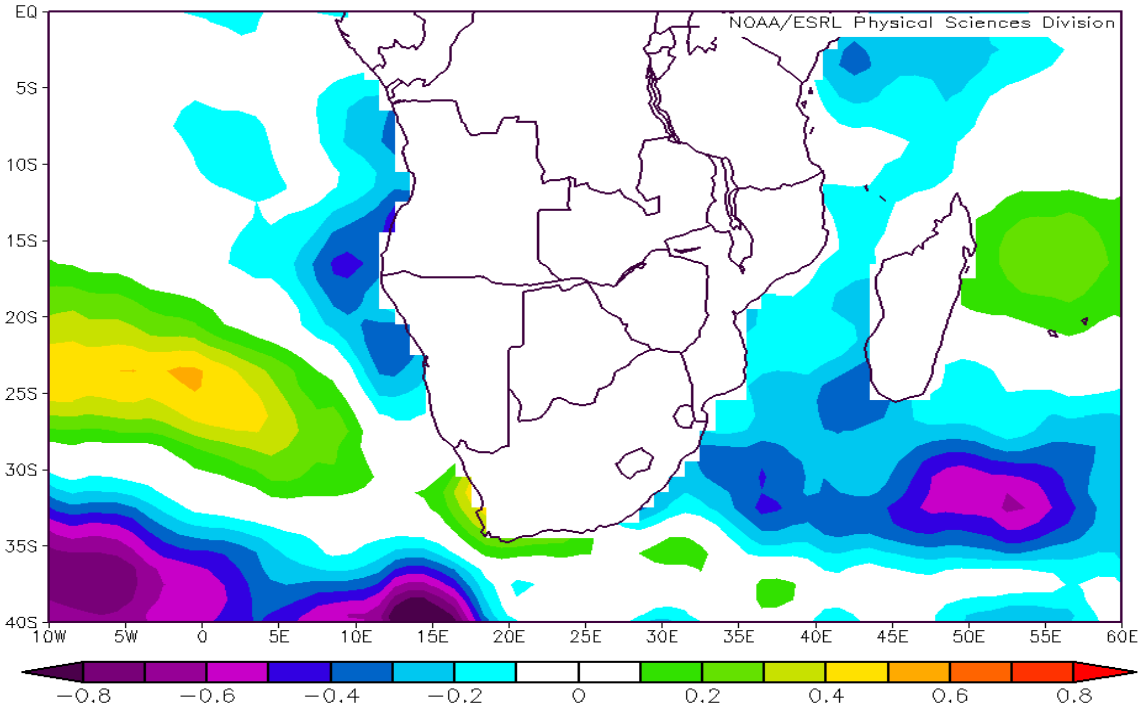

(b)

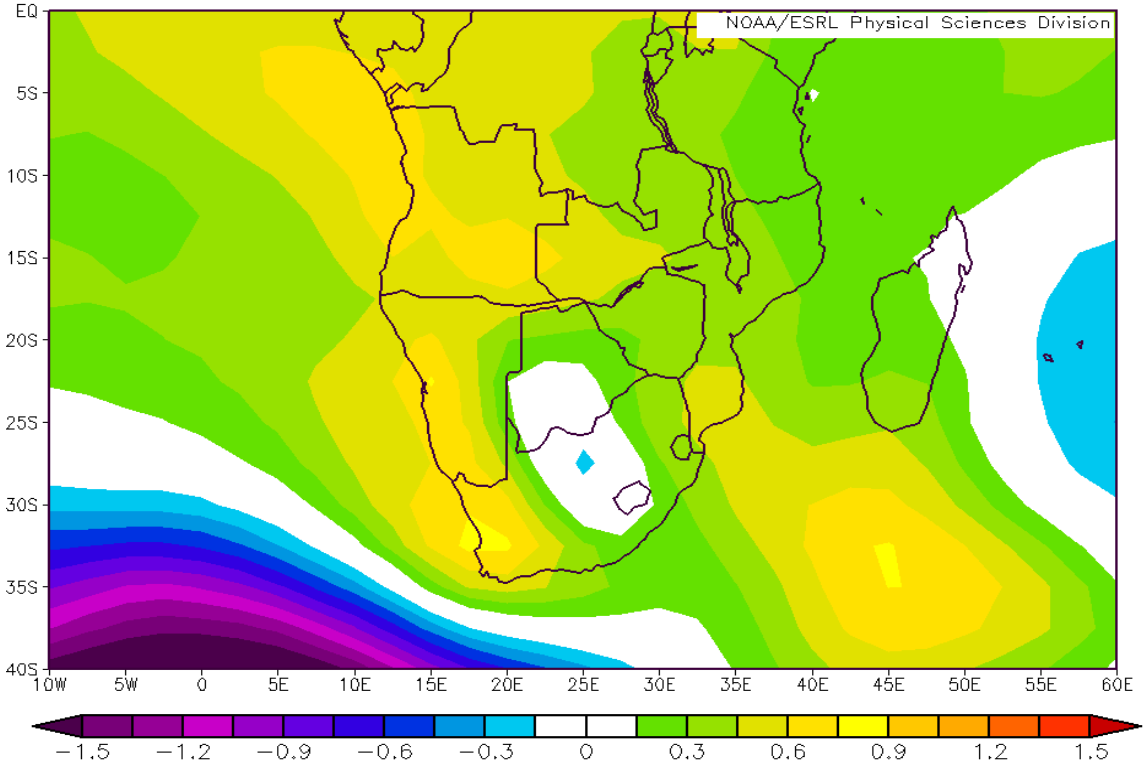

Figure 5:27 (a) Composite mean NOAA OISST sea-surface temperature (°C) anomalies for all drought seasons over the southeast Atlantic Ocean and the Southwest Indian Ocean near Africa and (b) associated NCEP SLP (shaded in hPa) anomalies

(a)

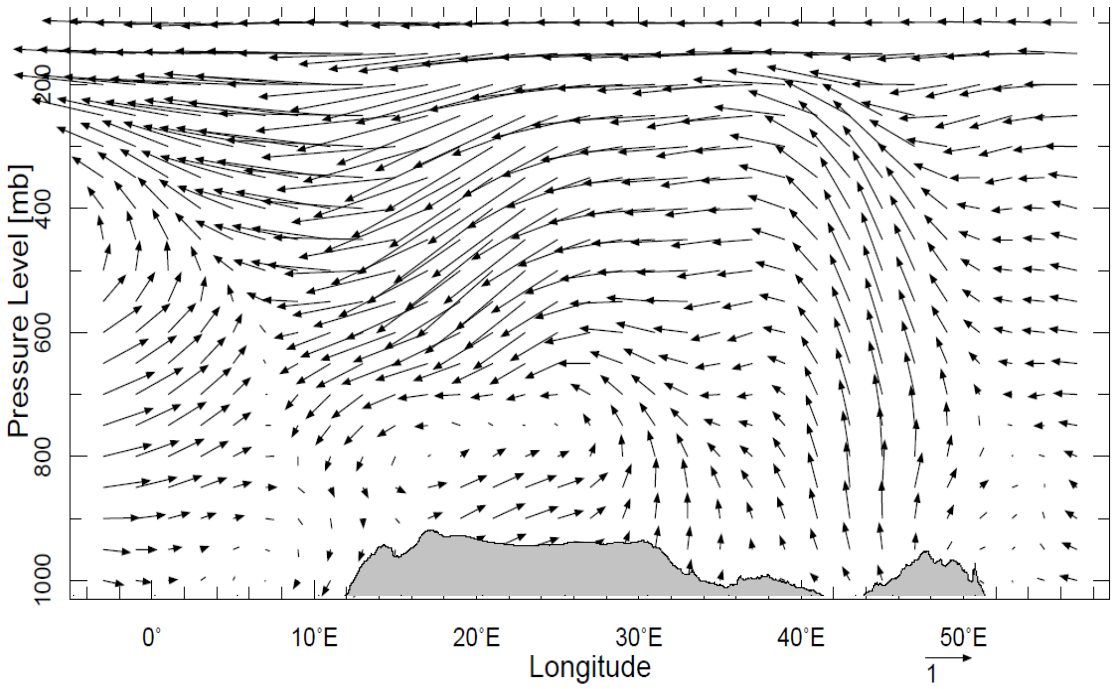

(b)

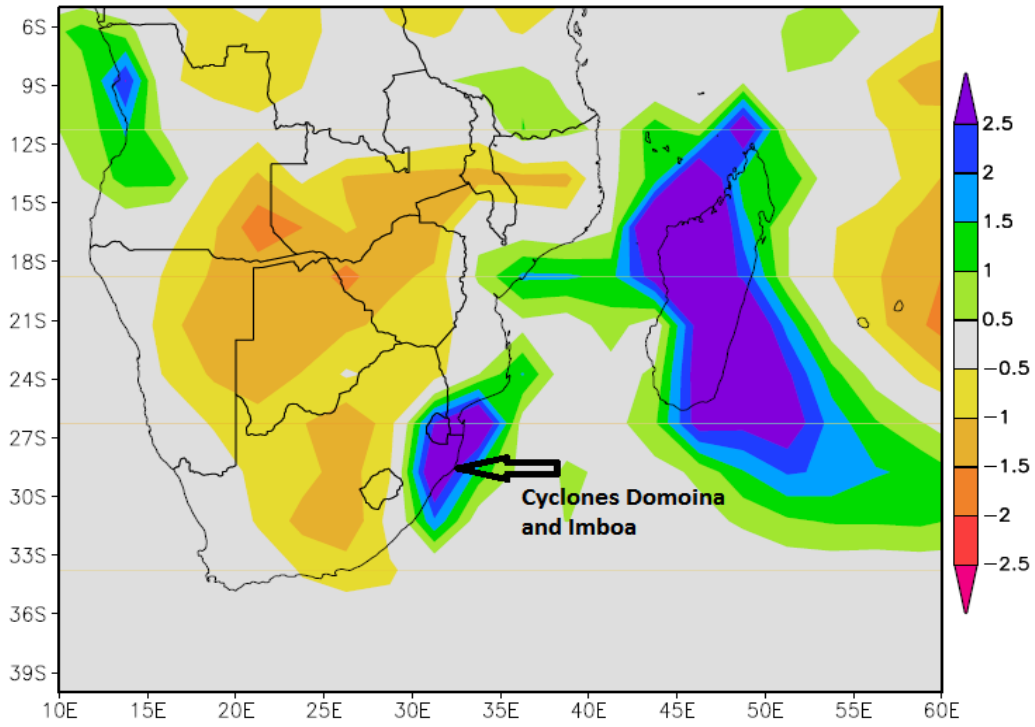

Figure 5:28 (a) Vertical structure of NCEP circulation (wind vector) and (b) composite mean GPCP precipitation (shaded in mm/day) anomalies during the Jan-Mar 1984 drought season over southern Africa and the adjacent oceans

Chapter 6

DROUGHT IMPACTS IN SOUTHERN AFRICA

6.1 Introduction

Drought lowers crop and livestock production when soils dry up and vegetation turns brown. Water levels drop in reservoirs whilst some rivers may run dry. Some impacts of drought are visible in the short-term whilst other impacts take longer to appear. Whereas surface water levels in rivers and streams may reflect the absence of rainfall in the short-term, groundwater levels may not fall until a year later.

Poor water management by Water Authorities may also lead to artificial shortages and demand for water in certain regions. Overgrazing and over cultivation cause land degradation which, in the long term, may lead to desertification. Thus, impacts of drought are a function of the vulnerability of a region to precipitation deficiency (AMS 1997) and other socio-physical variables.

Rainfall is a most important meteorological parameter in mainland African nations as it creates soil moisture and influences patterns and productivity of rain-fed agriculture and vegetation health. In addition, water resources of a region are heavily dependent on its rainfall climatology. Unavailability of water greatly impacts rain-fed agriculture and subsequent harvesting of staple grain crops (Schulze 1997). Thus, rainfall is critical in determining agricultural yields in a region such as southern Africa where irrigation is not extensive.

Drought reflects deficits of water in soils and hydrological systems (Trenberth *et al.* 2014) whilst surface soil moisture acts as an integrator such that an agricultural drought results from soil water deficits (AMS 1997). Thus, the intensity of a drought event can also be measured in terms of impacts of precipitation deficits (AMS 1997) and spatial patterns of vegetation anomaly may also be a measure of impact. Historically, soil moisture and streamflow have been used to depict agricultural and hydrological drought, respectively.

Whilst impacts of drought are many and varied, the focus of this chapter is on surface soil moisture, crop yields, vegetation condition and surface runoff over southern Africa. Drought impacts on economies are also explored to a lesser extent. As in previous chapters, event scale analysis is also employed here.

6.2 Soil moisture

Soil moisture is an important component of the hydrological cycle which regulates runoff and drought development. An agricultural drought occurs when soil moisture levels are insufficient to support crop growth. Water stress follows when the plant available water is inadequate to meet a plant's demand for water (Pinheiro *et al.* 2001). It has been argued that high evaporative losses coupled with low precipitation result in soil moisture deficits and therefore agricultural drought (e.g. Cai *et al.* 2009). Satellite and gravity based estimates and model reanalysis soil moisture are analysed and mapped.

The mean annual cycle of surface soil moisture shows a peak during the late austral summer from JFM decaying during September just prior to the onset of the rainy season (Figure 6.1). The soil moisture peak is therefore lagged to rainfall and to P-E by one month (Figure 6.1).

Interannual variability of surface soil moisture shows fluctuations of soil moisture with lower peaks during 2003, 2007 and 2012 (Figure 6.2). Declines in soil moisture are either associated with declines in precipitation or with an increase in evaporation (latent heat flux).

Soil moisture composite anomalies associated with drought are greatest over Zimbabwe (Figure 6.3) as with rainfall and OLR. However, the correlation of GPCP data with surface soil moisture shows positive correlation $R > 0.6$ (90% significance) mainly in the Limpopo valley (Figure 6.4). It appears that the soil moisture rainfall relationship is strongest in semi-arid regions. Chikoore (2005) also found high variability of surface soil moisture in the Kalahari transition zone. Some studies have investigated the feedbacks of soil

moisture on precipitation in southern Africa (e.g. Cook e*t al.* 2006). However, it is not the scope of this research to investigate soil moisture feedbacks to the atmosphere or the effect of soil moisture on the causation or perpetuation of drought.

Whilst it is recognized that other fixed fields such as soil type, orography and vegetation also influence soil moisture retention, these fields are incorporated at high spatial resolution in the CPC soil moisture dataset (Fan and van den Dool 2004). In semi-arid Botswana, soil type is also related to the vegetation cover (Nicholson and Farrar 1994). Farrar *et al.* (1994) found high soil moisture retention with the clayey vertisols whilst it was least in the sandy luvisols. It is also not the scope of this thesis to determine the influence of soil type on soil moisture during drought conditions in southern Africa.

In a study over southern Africa, Pinheiro *et al.* (2001) found a statistically significant correlation between surface soil moisture and soil temperature. Soil temperatures increased with a decline in soil moisture content on the basis that increased temperatures enhance evaporative losses of surface soils.

6.3 Maize

In Africa, South Africa is the largest producer and net exporter (Malherbe *et al.* 2014) of the maize crop, accounting for about 30% of the total production. The maize crop makes up about 70% of total grain production and is planted in about 60% of the cropping areas in South Africa. More than 90% of maize production is on the Highveld (> 1000 m) which includes parts of the Northwest, Free State, Mpumalanga and Gauteng Provinces as shown in Chapter 1 (Figure 1.3).

6.3.1 Climate requirements

Maize is the staple food for southern Africa (Moeletsi *et al.* 2011), grown in all the countries of the region at varying scales. White maize is grown in greater proportion relative to yellow maize which is predominantly for animal feed. The maize crop is mostly planted in summer as flowering occurs during DJF (Usman and Reason 2004). It is grown in semi-arid regions of the subcontinent and is highly vulnerable to changes in rainfall and

temperature. As a result, drought events have been associated with reduced maize yields and food shortages over southern Africa and sometimes famine. Agriculture also forms the basis of livelihoods for most of the region's rural communities.

Mean annual rainfall totals are not a particularly useful indicator for crop production (Lindesay 1998) as seasons with similar rainfall totals can have quite diverse characteristics (Tennant and Hewitson 2002). Thus, the performance of a given season with respect to crop growth and yields depends more on the spread of the rainfall over the growing season (Usman and Reason 2004) rather than seasonal totals. An agricultural season can fail due to a delayed onset, early withdrawal or intense rainfall of short duration followed by long dry spells (Camberlin *et al.* 2009). A flood induced by a tropical storm can destroy an entire crop which was otherwise healthy and promising.

Thus, seasonal rainfall predictions would be more valuable to smallholder farmers if they contained information about the spread of rainfall with time (Vogel 2000) beginning with the onset of the maize growing season (Tadross *et al*. 2005). A farmer should be concerned about the availability of sufficient soil moisture throughout the growing season (Tadross *et al*. 2005).

6.3.2 Maize yields

In most cases, maize is grown as an annual crop harvested once a year in southern Africa. In some southern Africa countries such as Zimbabwe, not all maize is delivered to grain collection centers as some is retained for subsistence or sold informally for better prices. The variability of maize yields combined for the countries in southern Africa from 1960-2012 is shown in Figure 6.5. There is a slight upward trend (R^2=0.18) in the maize output from southern Africa from about 1995 which may be a function of several factors. It may be a result of increased area under crop production, mechanization, better crop

varieties, increased irrigation, awareness of good farming practices or even increased uptake of seasonal climate predictions in agricultural management.

Whilst the combined regional maize production shows a slight upward trend, there are variations by country in trends of maize yield. South African maize yields dominates the trends. However, maize production in Zimbabwe reached a plateau during the late 1970s and has undergone a general decline since then (Figure 6.6). The Rhodesian bush war of the 1970s may account for a decline in yields then, whilst the droughts of the 1980s and 1990s have also contributed to the decline in maize yields there. The more recent decline (after 2000) may have resulted from land reform in which large commercial farms which were once productive were underutilized by new farmers who were inexperienced and underesourced. Botswana maize yields have also declined steadily throughout the period under investigation (Figure 6.6).

Despite an upward trend, the variability of total maize yields fluctuates with detrended regional rainfall even though the relationship is non-linear (Figure 6.7). The drought periods identified are also periods of low maize yields as indicated by significant negative anomalies (Figure 6.8). The lowest yields in the 53 year record occurred during the 1992, 1982-84 and 1995 drought seasons respectively. Even though the 1982-84 droughts were prolonged, the 1991/92 drought had the greatest impact on maize yields. In a study of maize yields over the Free State Province of South Africa, Moeletsi *et al.* (2011) found that the variability of yields was largely a result of rainfall variability. However, high rainfalls may also be associated with floods such as in February 2000 when some of the maize crop was inundated and washed away.

6.3.3 Value of agricultural production

Apart from diversified South Africa, the economies of most countries in southern Africa depend on agricultural output. The performance of those countries' economies is then tied to agricultural yields. The value of agricultural production is a measure of the market value of agricultural products at the time they were produced and converted to the US dollar (USD, http://faostat.fao.org/site/613/default.aspx#ancor). The total value of

agricultural production with respect to maize in southern Africa also shows an upward trend from 1960-2011 (Figure 6.9). The value of maize yield averages about USD 810 000 a year according to FAOSTAT data but may exceed USD 1 million in some wet seasons. During the 1992 drought, the value of agricultural productivity dropped drastically to only USD 752. Low values of agricultural productivity were also observed during the prolonged droughts of 1982-84 and 1995.

The rainfall over southern Africa is better correlated with value of agricultural productivity at R = 0.54 (90% significance) than with yields. The correlation is higher at R = 0.68 (90% significance) when considering the 1980-2001 period. Some previous studies have also found a weak, but statistically significant correlation between rainfall and agricultural production in South Africa (e.g. Vogel 1994; Lindesay 1998).

6.4 Normalized Difference Vegetation Index (NDVI)

The NDVI is an indicator of vegetation condition, including the health of grasslands, forests and agricultural fields such that spatial aspects of the NDVI anomaly may also be used to estimate impacts of drought on livestock herds and wildlife. NDVI anomaly images representing drought are presented here. While it has been shown earlier in the GPCP datasets that most drought is widespread in southern Africa, it is found here that each drought has unique spatial characteristics in impacts.

As with most climate parameters, the NDVI over southern Africa exhibits strong seasonality (Figure 6.10). However, unlike LST and Tmax which peak during the early summer, the NDVI over southern Africa peaks during the late austral summer from February-March and is at a minimum in the late spring September-October prior to the onset of the rainy season. The annual cycle of NDVI closely follows that of soil moisture (Figure 6.10). Peak NDVI values of 0.5 may be observed increasing to 0.6 during extremely wet seasons with minimum values of between 0.2 and 0.3 during the dry season. It has been found that the NDVI-rainfall relationship is complex and linear to an extent, such that NDVI rises to a threshold after which it increases very slowly with an increase in rainfall (Nicholson and Farrar 1994).

Since vegetation is most affected by drought through soil moisture, the NDVI anomaly has also been used to depict drought impact in several regions. NDVI anomalies show negative departures during drought periods identified in this study (Figure 6.11). Averaged over the entire southern Africa, the most negative NDVI anomalies occurred during March 1992, and also during 1987, 1984, 1985 and 1995 (Table 6.1). The months of March and February are key periods for drought impact analysis.

NDVI anomalies are mapped and analyzed for each of the seven drought events identified in Chapter 3 and shown in Figures 6.12. Whilst all drought seasons exhibit negative NDVI anomalies, the 1992 and 1995 drought seasons reveal the worst impact on biomass and food production. The departures from normal were minimal during the moderate 2003 drought. In all seasons, the area of greatest impact in southern Africa appears to be Botswana (Figure 6.12). South Africa's maize belt was also affected severely during 1983, 1984, 1987, 1992 and 1995.

It is found that late summer NDVI is positively correlated R = 0.63 (90% significance) with maize yields over southern Africa. In contrast, a strong inverse relationship R = -0.68 (90% significance) exists between NDVI and LST anomalies over southern Africa (Figure 6.13) suggesting periods of 'brown' vegetation (drought) are also periods of high LST, and perhaps heat waves over the study area.

For the 1997/98 El Niño, NDVI anomalies were found to be above normal during the summer season (Anyamba *et al.* 2001). The strong El Niño during the 1997/98 austral summer did not produce the severe drought that was expected, hence vegetation thrived. Instead, only moderate dry conditions were experienced over central southern Africa (Reason and Jagadheesha 2005). The Angola low was not weakened and so it allowed cloud bands to form producing higher rainfall than was expected for a strong El Niño season (Reason and Jagadheesha 2005). The Angola Low is an important factor in modulating rainfall in southern Africa during ENSO.

6.5 Surface hydrology

Mean surface runoff over the study area shows high runoff in two main areas – in the north on the Zambezi escarpment and also in the Drakensberg in the southeast between the Lesotho and Swaziland (Figure 6.14). Low runoff is found in the west (mainly Botswana) and in the Lowveld between Zimbabwe and South Africa. Area averaged surface runoff for the southern Africa region shows significant variability from season to season (Figure 6.15). The 2000 floods are distinct in the time series. The variation of river flows is analyzed along the Zambezi River at Victoria Falls and the Limpopo River at Botswana (Figure 6.16) and analyzed for drought impact. Reservoir levels for Lake Kariba

6.5.1 Annual cycles and interannual variability

The hydrological year in the Zambezi valley spans from October to September with peak flows of up to 3000 m^3s^{-1} at Victoria Falls during April at the end of the rainy season (Figure 6.17). Low flows occur during September - October prior to the onset of the rainy season. In comparison, the surface hydrology in the upper Limpopo basin peaks earlier with an annual cycle from September to the following August (Figure 6.18). Baroclinic westerly wave disturbances characterize the early summer circulation (D'Abreton and Lindesay 1993; Makarau and Jury 1997) and this result may reflect the influence of the Tropical-Temperate Troughs (TTTs) and cloud bands affecting the upper Limpopo drainage basin. TTTs affect the basin earlier than the Inter-Tropical Convergence Zone (ITCZ) which is the main source for the Zambezi River basin. TTTs provide between 30-60% of annual rainfall (Hart *et al*. 2013). An important finding is that the rainfall leads surface soil moisture which in turn leads the surface runoff at sub seasonal time scales.

The long-term mean variability of Zambezi flows at Victoria Falls show a marked decline from the 1960s to the mid-1990s when a minimum is observed (Figure 6.19). The lowest flows occurred during 1995-1996. This decline may be associated with the decline in rainfall over comparable time periods. In contrast, an earlier study by van Lanen *et al.* (2004) found that the lowest discharge on the Zambezi occurred during the 1980-1990 period. A recovery or partial recovery in flows is observed since the low flows of the 1990s

(Figure 6.19) which is consistent with the long-term variability in rainfall over the study area.

Inter-annual variability of late summer Limpopo flows shows distinct peaks associated with flood events in the Limpopo catchment (Figure 6.20). The tropical cyclone induced floods of 1996 and 2000 produce the dominant peaks in the time series such as cyclone Bonita which dumped heavy rainfalls and induced floods over the subcontinent during January 1996. Despite the paucity of hydrological data in the study area, the droughts of the early 80s and early 90s are also reflected by low flows.

6.5.2 Low flow and deficit characteristics

Low flow analysis deals with minimum flows in a river system occurring in the dry season (Tallaksen and van Lanen 2004). The lowest flows per year are selected to form a timeseries of low flow characteristics which may be analyzed (Hisdal *et al.* 2004). It has been shown here that the low flows over the Zambezi basin occur during September-October just prior to the onset of the main rainy season. A review of low flow hydrology is also detailed by Smakhtin (2001).

The mean annual minimum flow at Victoria Falls for 1948-2009 is 291 m^3s^{-1}. The annual minimum flows show a significant shift with a downward trend observed from about 1980 to 1995 and a slight recovery thereafter (Figure 6.21). The gradual decline of low flows may be a result of the prolonged periods of drought during the 1980s and 1990s. This decline of low flows may suggest beginnings of drying of small rivers and tributaries in the basin in future.

Whilst most impacts of drought are short-term, there are longer term impacts which may emerge only if drought persists for longer periods. The early 80s were characterized by three successive drought seasons from 1982-1984 whose impacts may have been carried forward from one season to the next.

6.5.3 Lake Kariba

Lake Kariba (Figure 6.16) was impounded along the Zambezi River in 1958 and reached minimum operating level in 1962. It is considered one of the largest man made reservoirs on earth (Muchuru *et al.* 2014). In addition to inflows from the Zambezi, major rivers such as the Gwayi, Sengwe, Sanyati and other smaller tributaries from Zimbabwe also empty into the reservoir.

The mean annual cycle of reservoir levels at Lake Kariba peaks during the May-July (Figure 6.22) and is lagged by one month to the peak flows at Victoria Falls upstream. The full supply level of the reservoir is 488.5 m whilst the minimum operating level is 475.5 m. Runoff into the reservoir is significantly reduced during drought. Thus, the impacts of drought on lake levels are clearly visible in the time series during the 1980s and 1990s (Figures 5.23 and 5.24). The lowest reservoir levels since Lake Kariba was impounded were recorded in December 1992 following the 1992 drought at 475.91 m about 6 m below the mean. Distinct peaks are discernible for the 2000 and 2011 seasons at 487.53 m and 487.67 m respectively. The two seasons are associated with an active ITCZ and severe tropical storms affecting the drainage basin of the Zambezi River. Tropical cyclone Eline (February 2000) traversed southern Africa from the Mozambique Channel and flooded several tributaries of the Limpopo, Zambezi and Orange River systems. During 2011, persistent heavy storms and floods affected large areas of the upper Zambezi basin in Zambia and Angola. The extreme rainfall and flooding of January 2011 and its predictability were analyzed by Muchuru *et al.* (2014).

Human influences on reservoir levels are not investigated here but it is assumed that dam releases are limited during times of drought to conserve water. The extent and impact of sedimentation on reservoir levels of Lake Kariba may also need further investigation. Information about river flows and lake levels is also important for those farmers with maize under irrigation. Prediction of seasonal river flows may assist irrigation farmers to plan for an upcoming agricultural season (Malherbe *et al.* 2014).

Positive correlations of R > 0.5 (at 90% significance) of rainfall upstream of Lake Kariba with lagged reservoir levels are found over Zambia and Angola and the reservoir catchment area in Zimbabwe (Figure 6.25). The ENSO signal also appears to influence inflows and reservoir levels as the Niño 3.4 index is negatively correlated at R= -0.27 (90% significance, Figure 6.26). In a study of long-term rainfall in the Lake Kariba catchment, Muchuru *et al.* (2015) found no significant seasonal shifts or positive/negative trends in the data.

6.6 Summary and discussion

This chapter has discussed the impacts of drought on soil moisture, agricultural production and surface water hydrology in southern Africa. It was found that strong negative soil moisture anomalies occur over the region with a maximum over Zimbabwe. Maize yields over southern Africa exhibit a clear upward trend, despite fluctuations which may be due to rainfall variability. There exists a stronger relationship between drought over southern Africa and value of agricultural productivity than with actual crop yields. Short-term drought impacts are lagged to rainfall by up to two months.

Severe droughts are generally those of long duration and having a large aerial extent such that the impacts are greatest. By far the worst drought in terms of rainfall anomalies and impacts was the 1992 event. It is found that drought impacts will vary depending on the rainfall patterns of the previous season as successive droughts have a compounding effect. The ENSO impact on maize, Lake Kariba reservoir levels and NDVI was also distinct. However, the impact of sedimentation on the accuracy of lake levels and long-term trends requires careful consideration.

Chapter Figures

Table 6-1 Ranked NDVI anomalies over southern Africa (averaged over 22-32E; 15-28S). The definitive selection of drought seasons identified in Table 3.2 with the most negative P-E anomalies shown with an asterisk.

Rank (low to high)	**Month/Season**
1	Mar 1992*
2	Mar 1987*
3	Mar 1984*
4	Feb 1985
5	Mar 1995*
6	Mar 1983*
7	Feb 1992*
8	Feb 1995*
9	Feb1987*
10	Jan 1995*

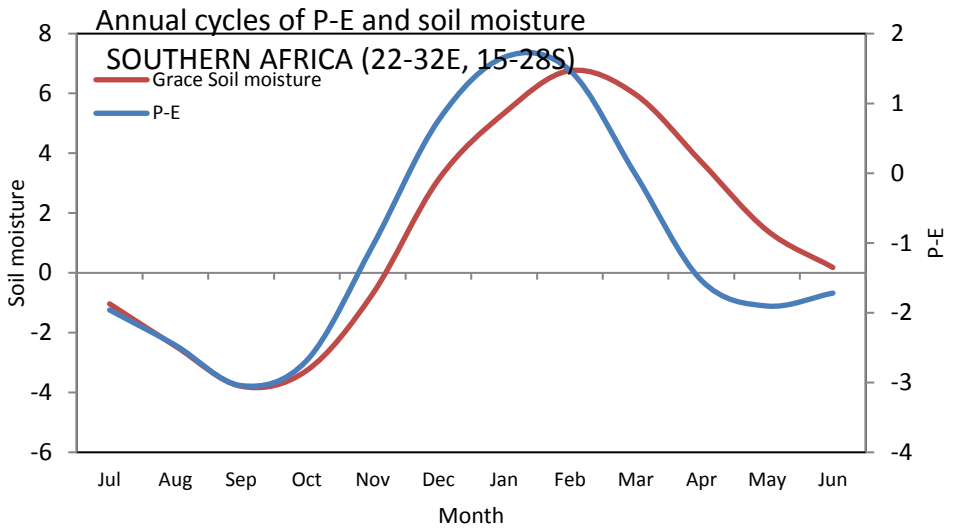

Figure 6:1 Mean annual cycles of GRACE soil moisture and the P-E index over southern Africa

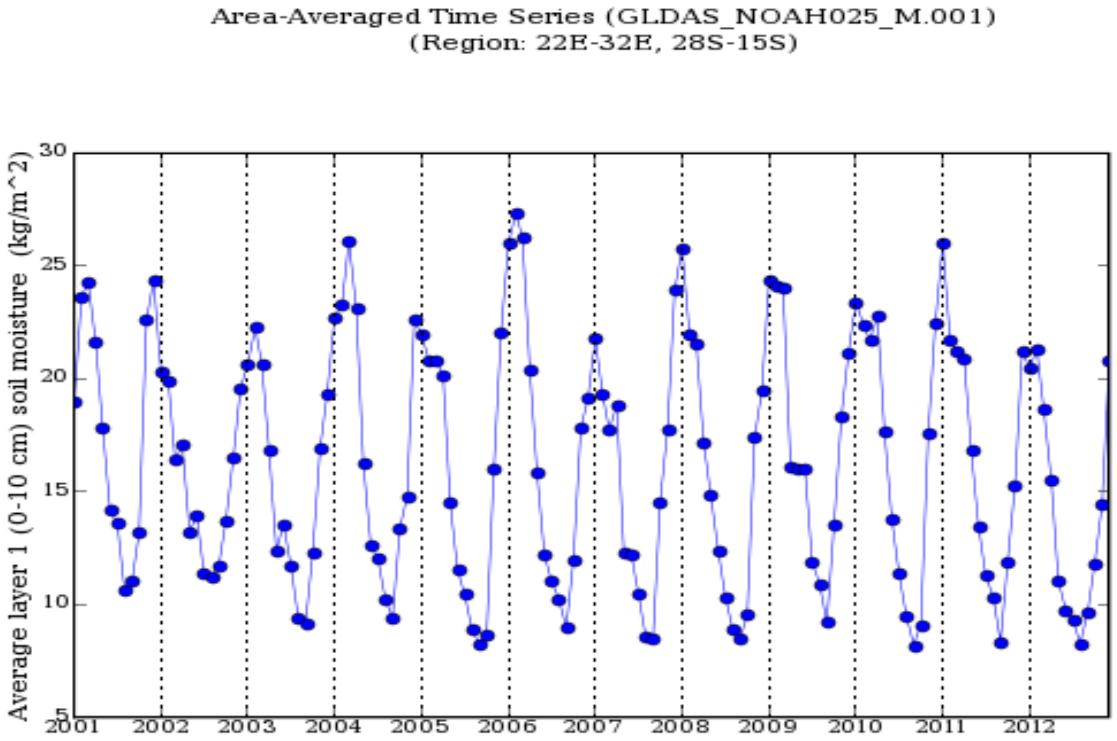

Figure 6:2 Interannual variability of surface GRACE soil moisture (kgm^{-2}) over southern Africa (2001-12)

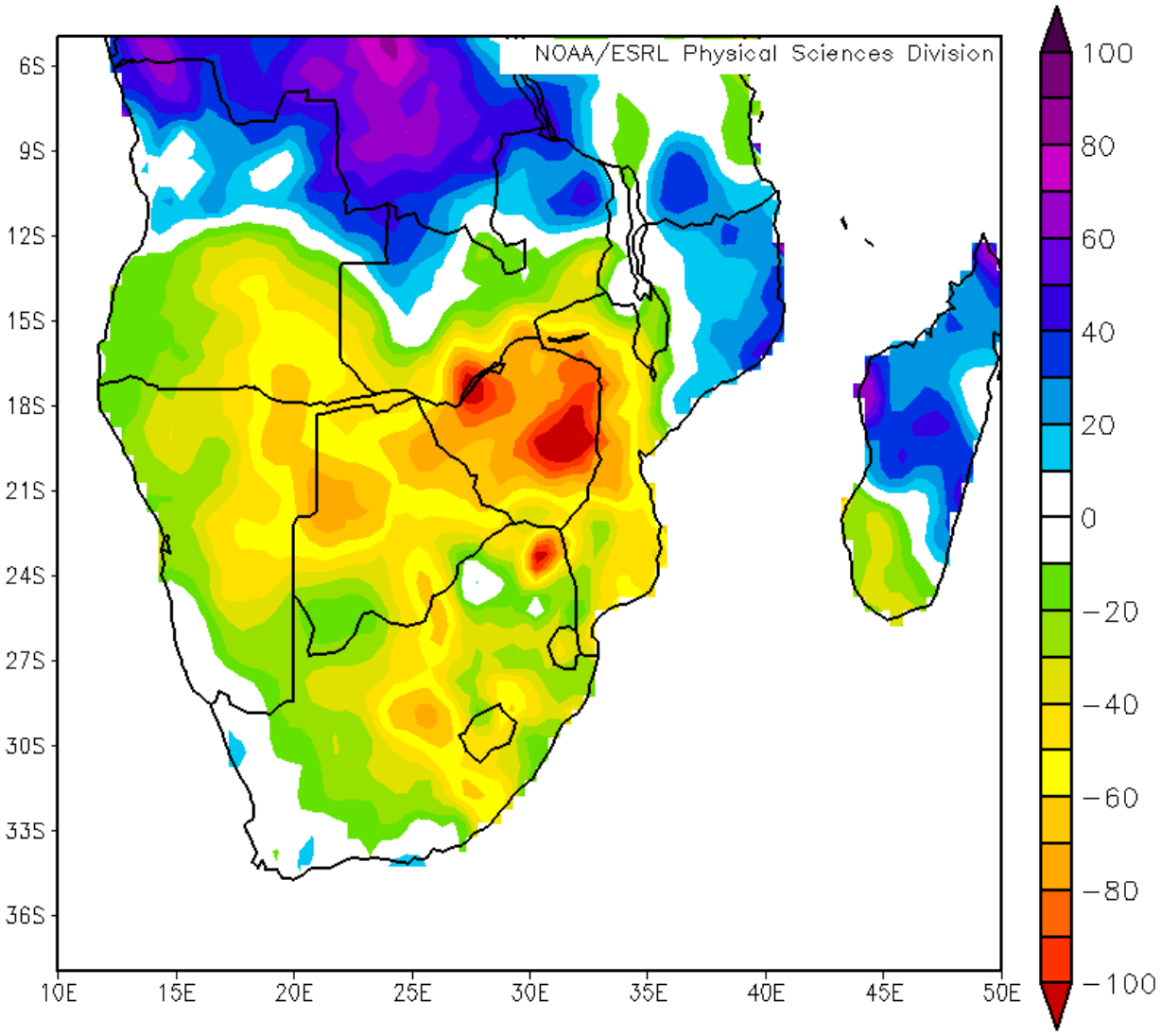

Figure 6:3 Composite mean CPC surface soil moisture (v2) anomalies during late summer to early autumn (February-April) over southern Africa for drought periods. Values are given in mm.

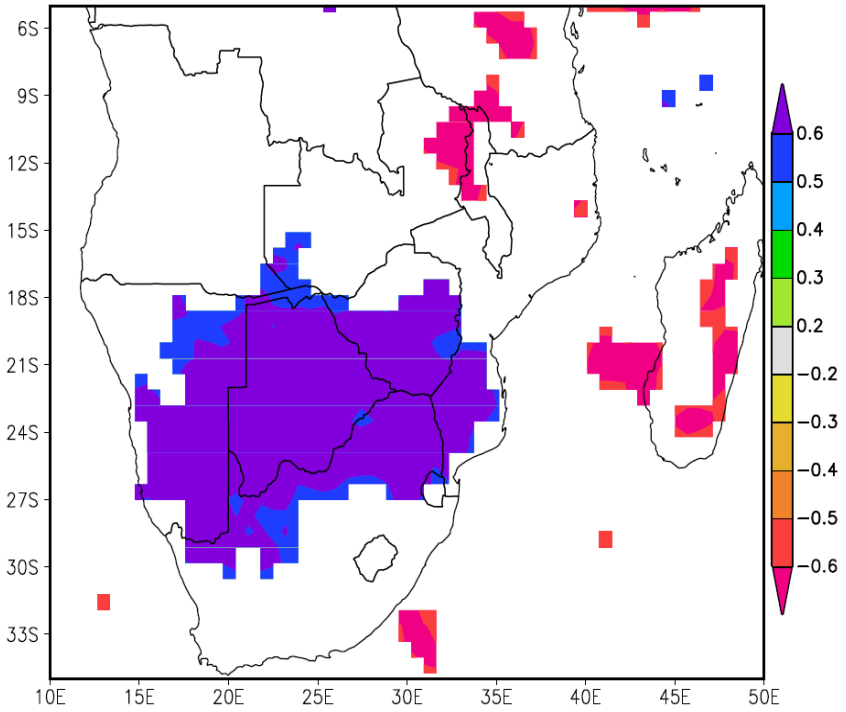

Figure 6:4 Correlation between CPC surface soil moisture (v2) and GPCP precipitation in southern Africa. The shaded grid boxes are significant at 90% or more.

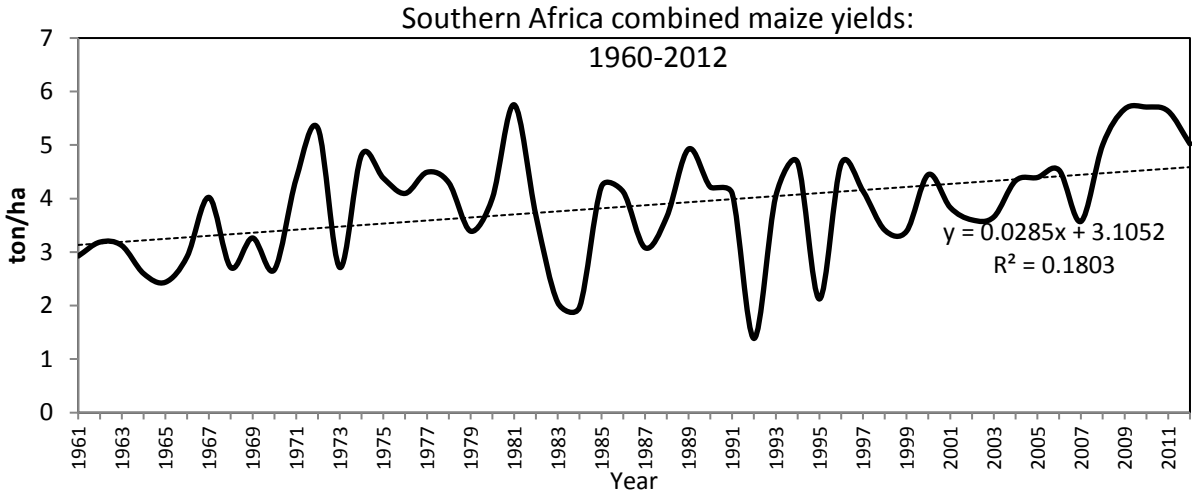

Figure 6:5 Interannual variability of combined FAOSTAT maize yields (ton/ha) for southern Africa (1961-2012). Trend is slightly upward despite the low yields of 1983-84, 1991/92 and .

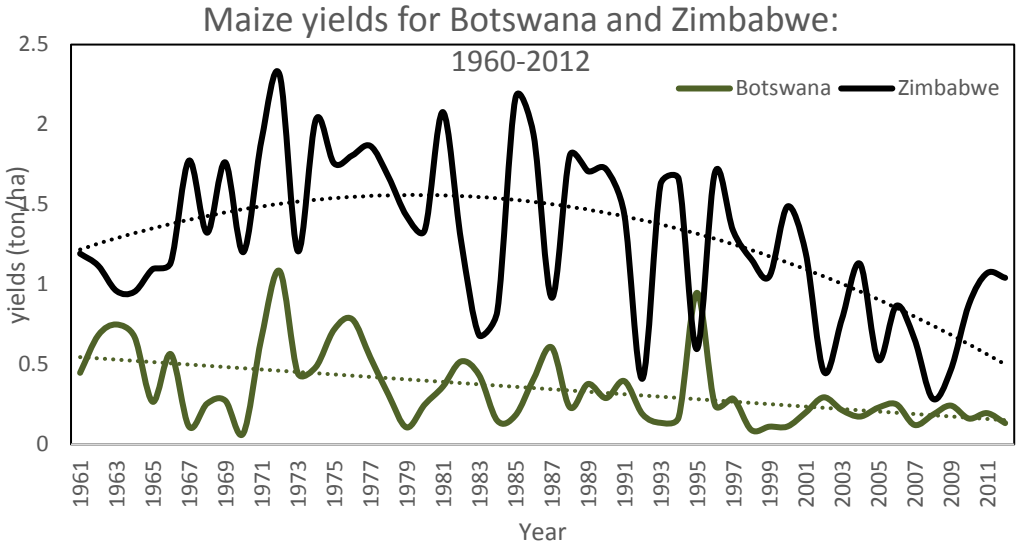

Figure 6:6 Variability of FAOSTAT maize yields (ton/ha) for Botswana and Zimbabwe: 1960-2012

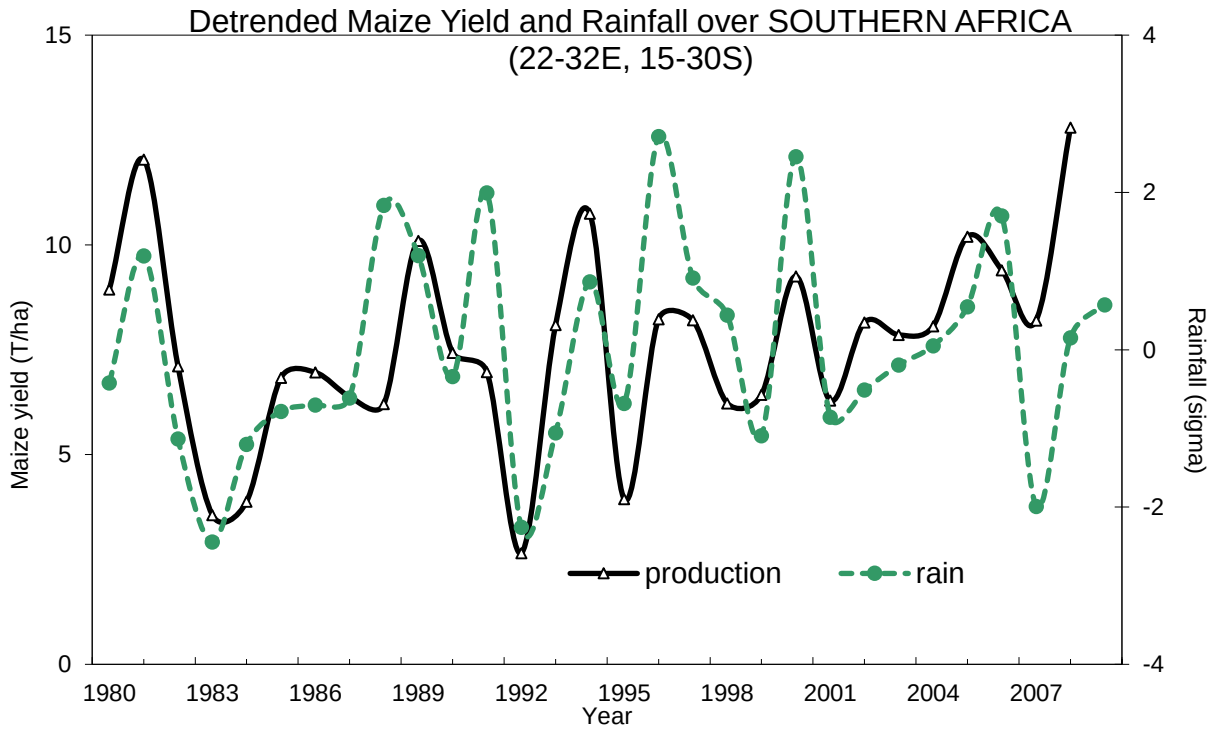

Figure 6:7 Detrended FAOSTAT maize yields (ton/ha) and seasonal rainfall (sigma) anomalies over southern Africa: 1980-2012

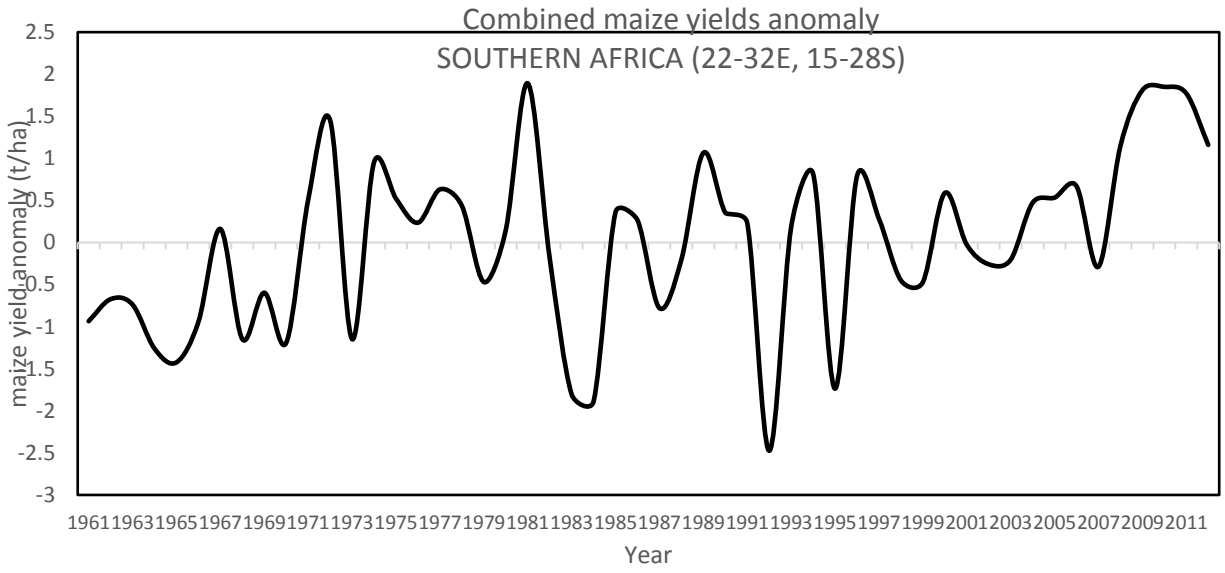

Figure 6:8 Combined FAOSTAT maize yields (ton/ha) anomaly for the southern Africa region

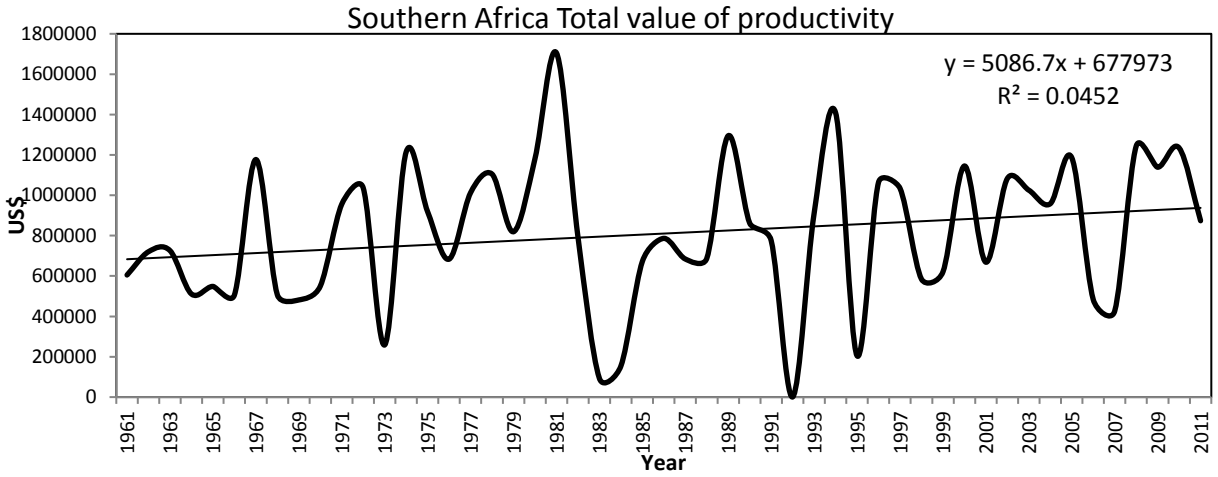

Figure 6:9 FAOSTAT value of agricultural productivity (for maize in US$) in southern Africa

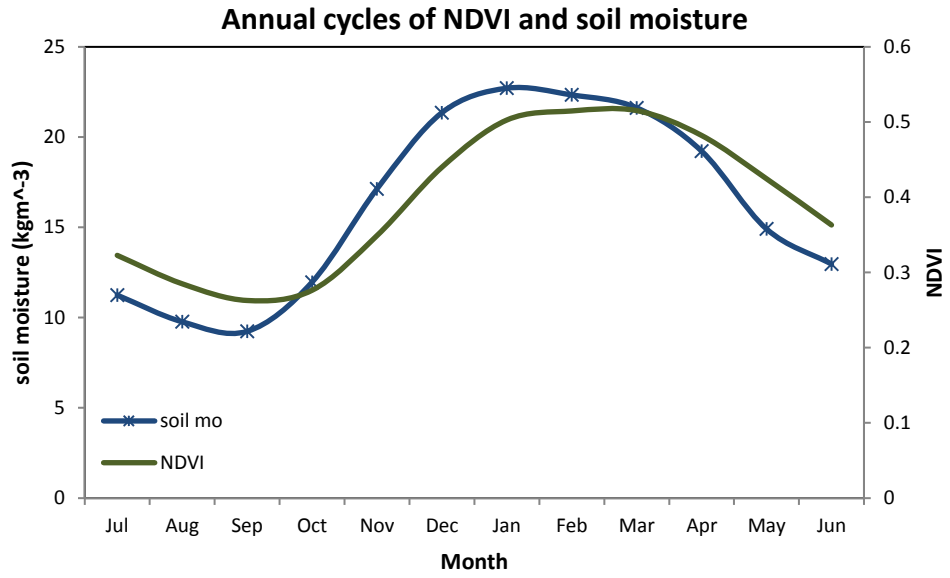

Figure 6:10 Mean annual cycles of NDVI and surface soil moisture (kg of water/m^3 of soil)

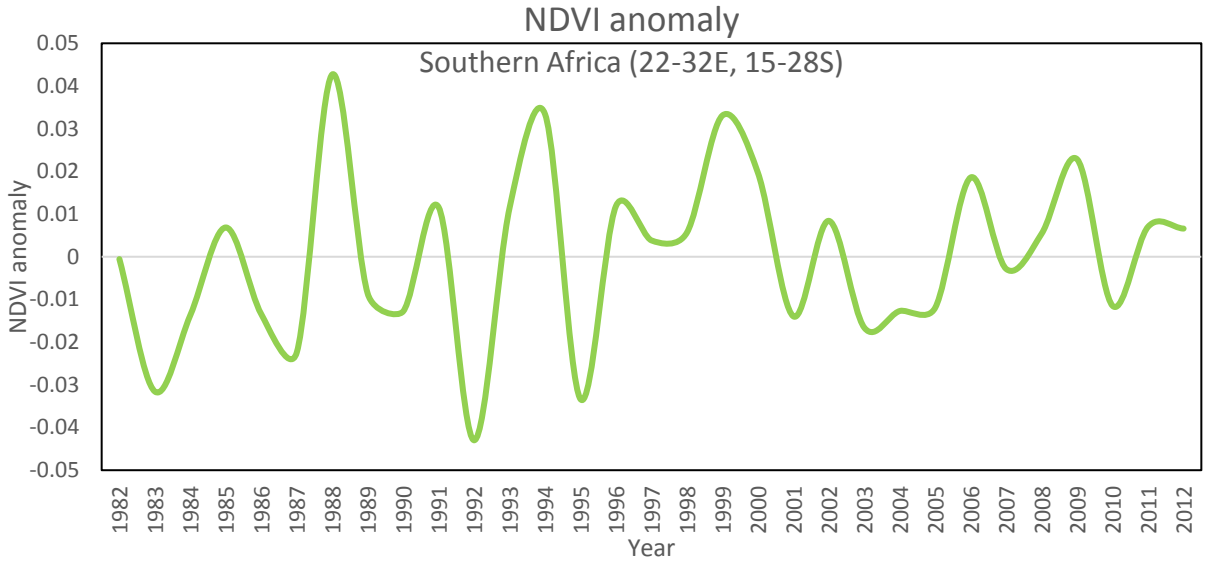

Figure 6:11 Anomalies of late summer mean NOAA NESDIS NDVI over southern Africa: 1982-2006

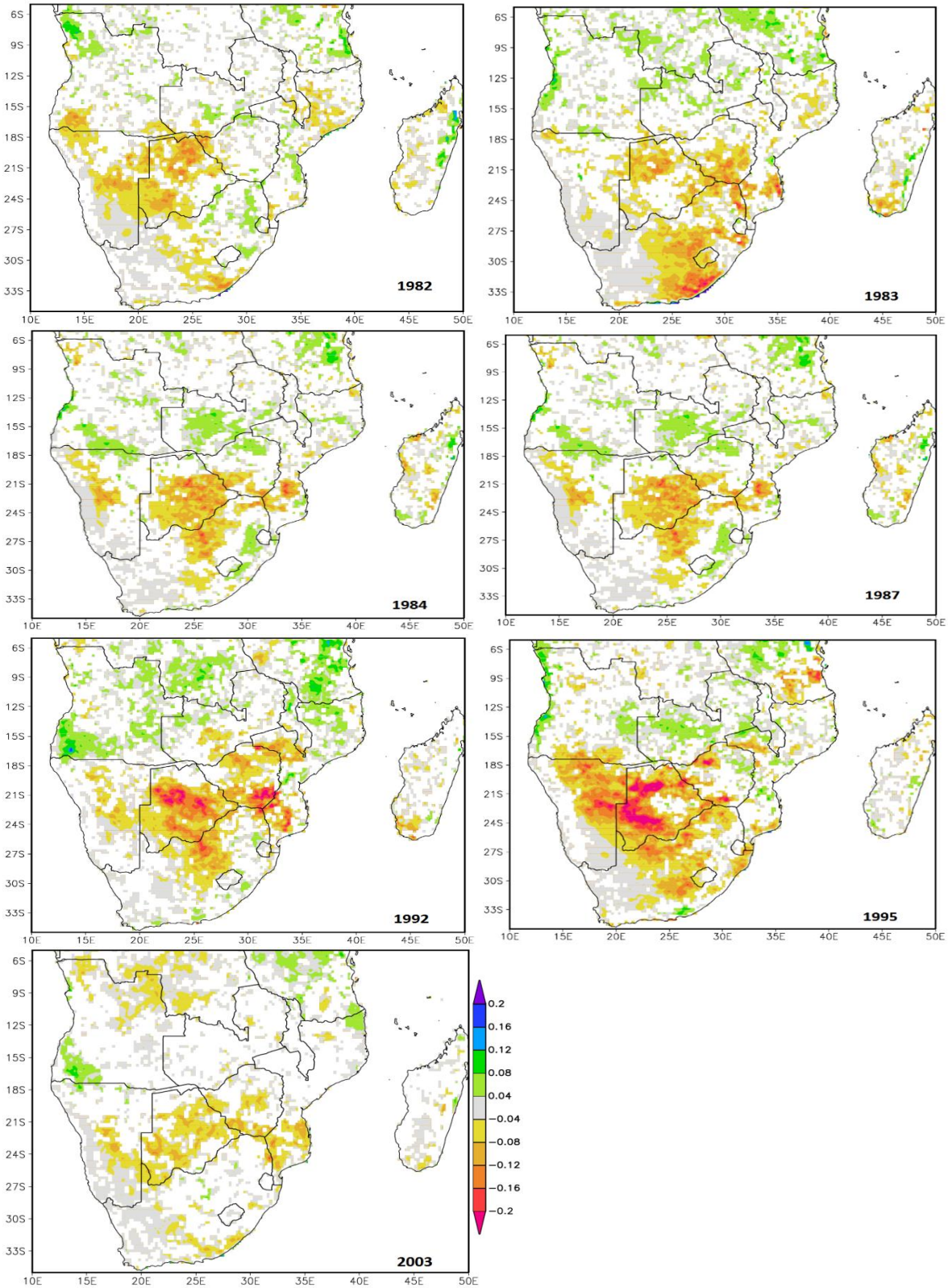

Figure 6:12 USGS NDVI anomalies over southern Africa for the seven drought seasons analyzed in this study

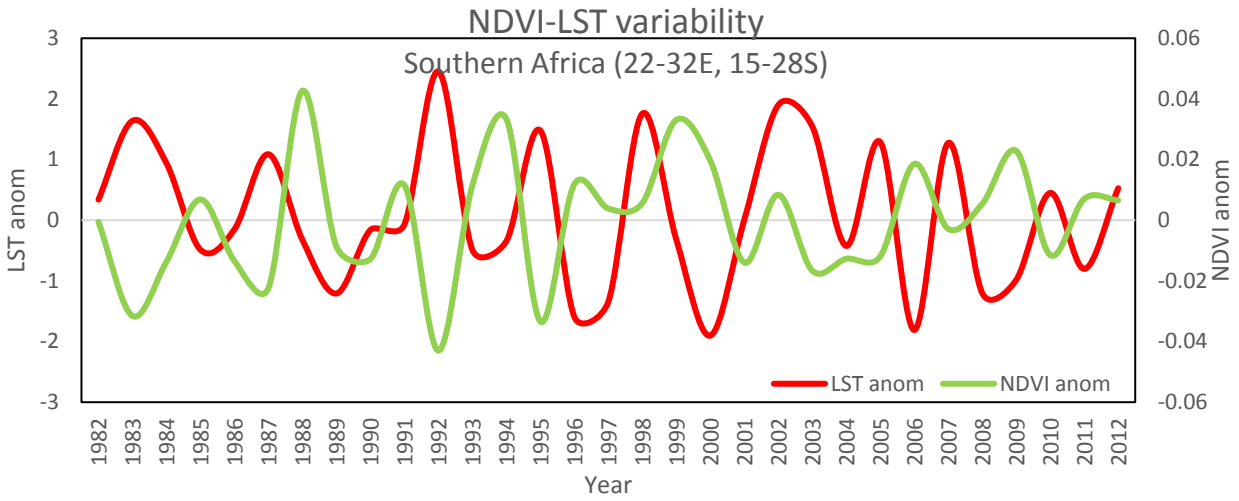

Figure 6:13 Variability of NDVI and MODIS LST (°C) anomalies over southern Africa (averaged over 22-32E; 15-28S): 1982-2012

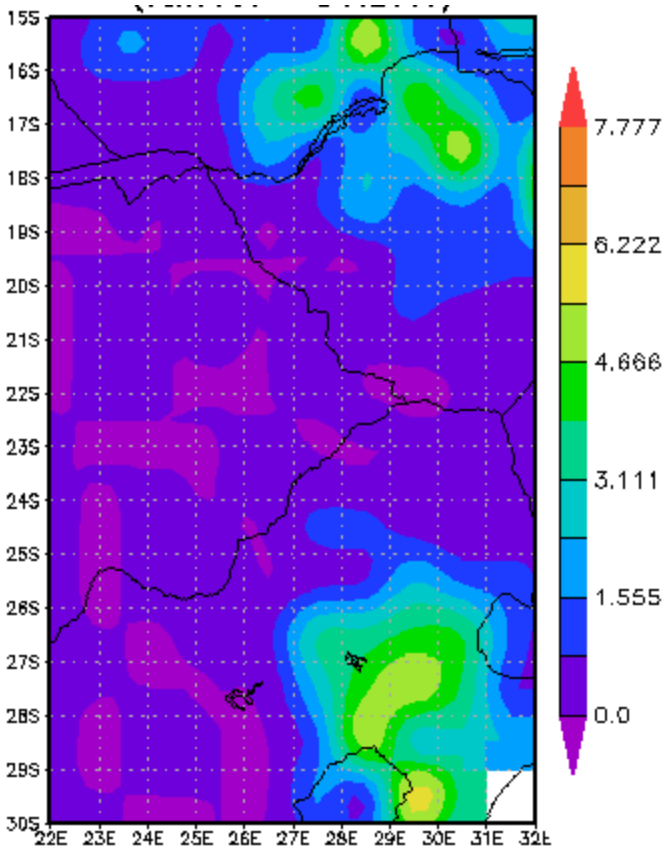

Figure 6:14 NASA Giovanni mean surface runoff over southern Africa (10^{-6}kgm^{-2}s^{-1})

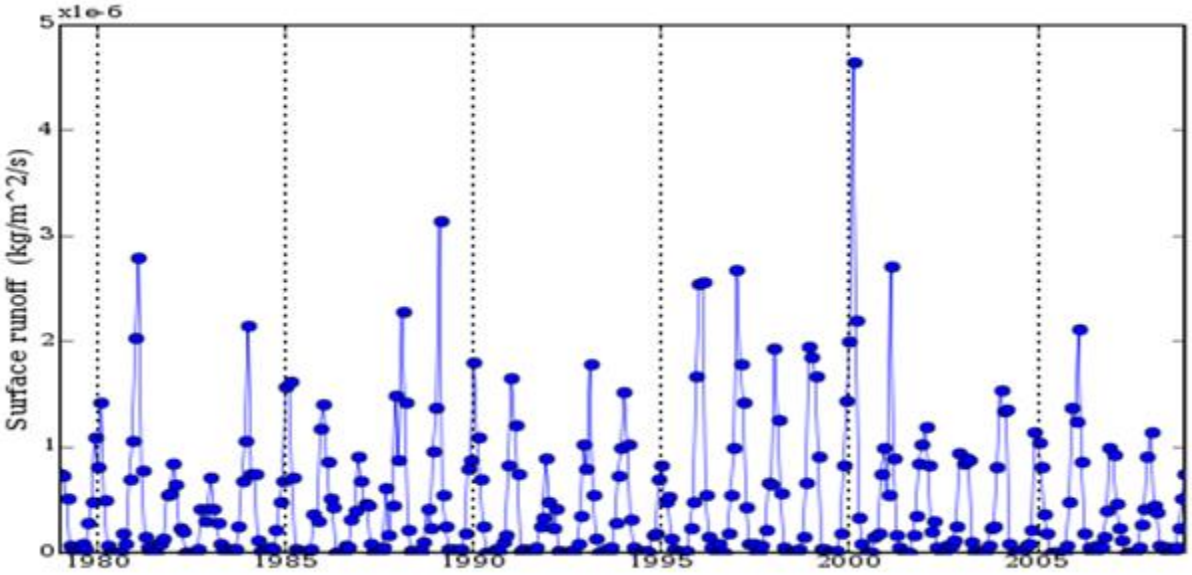

Figure 6:15 Interannual variability of NASA Giovanni surface runoff (kgm^{-2}s^{-1}) over southern Africa (averaged over 22-32E; 15-28S)

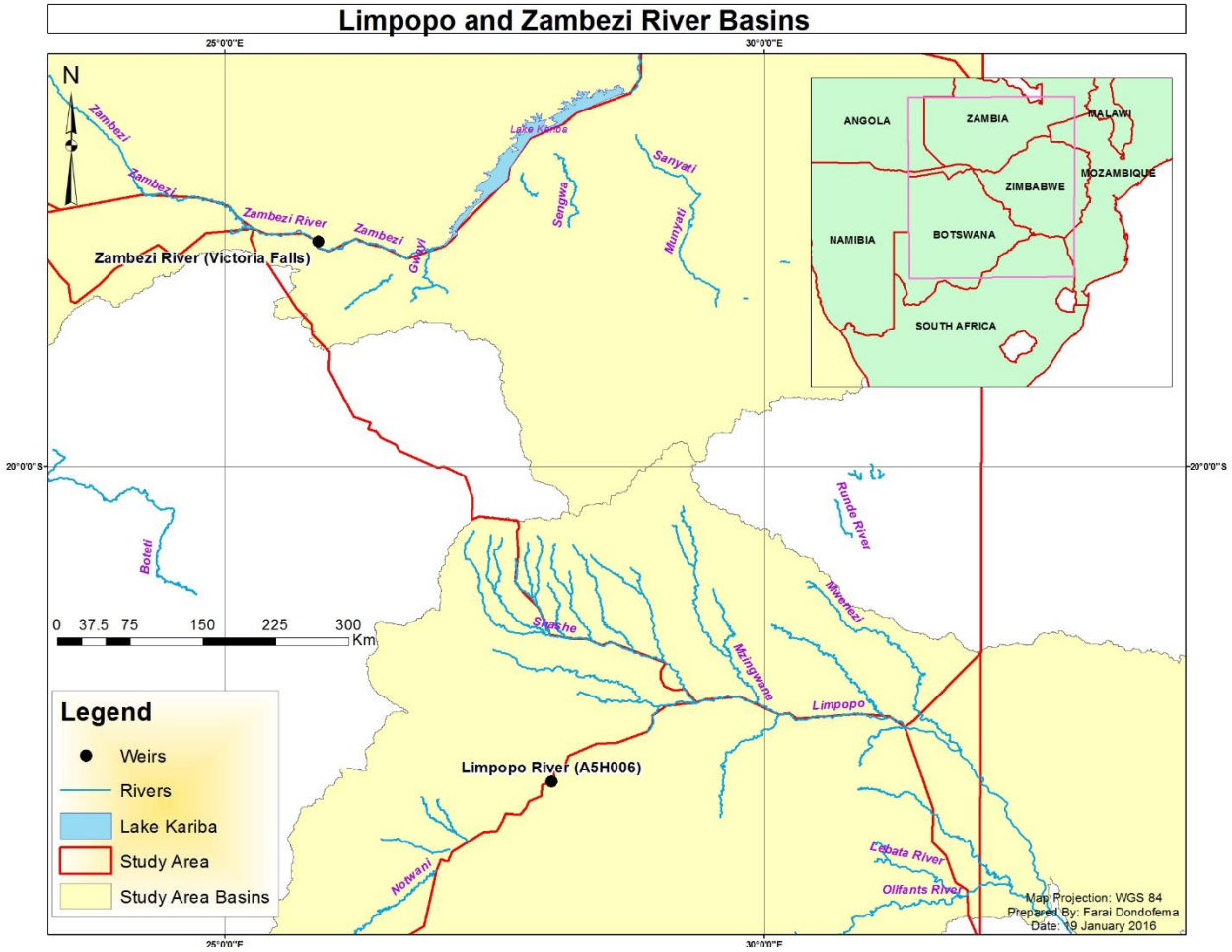

Figure 6:16 Drainage basins of the Zambezi and Limpopo Rivers with weirs shown upstream. Lake Kariba is also shown along the Zambezi between Zambia and Zimbabwe.

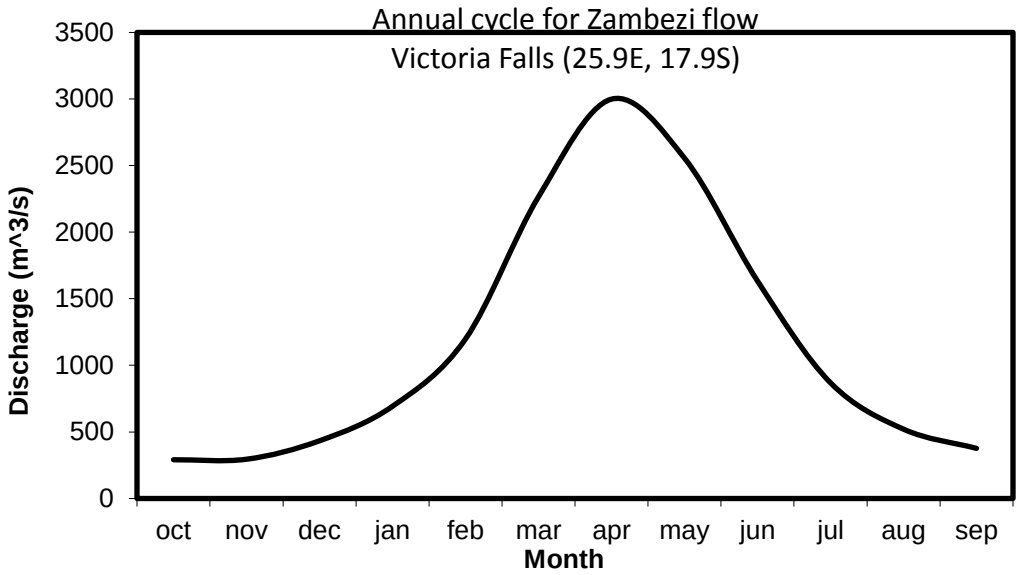

Figure 6:17 Mean annual cycle of Zambezi River flows (m^3s^{-1}) at Victoria Falls

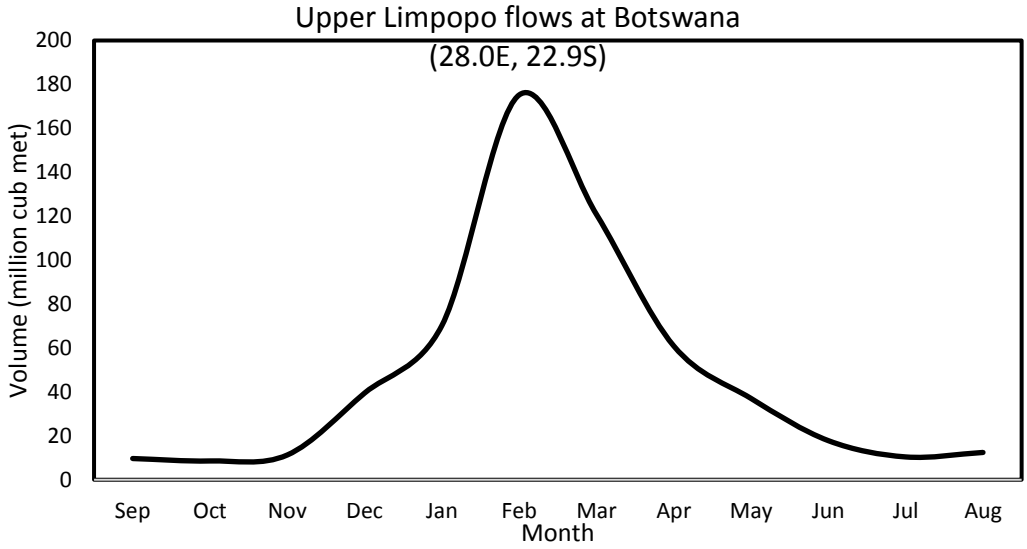

Figure 6:18 Mean annual cycle of flow volumes (mill cub met) of the upper Limpopo River at Botswana (A5H006)

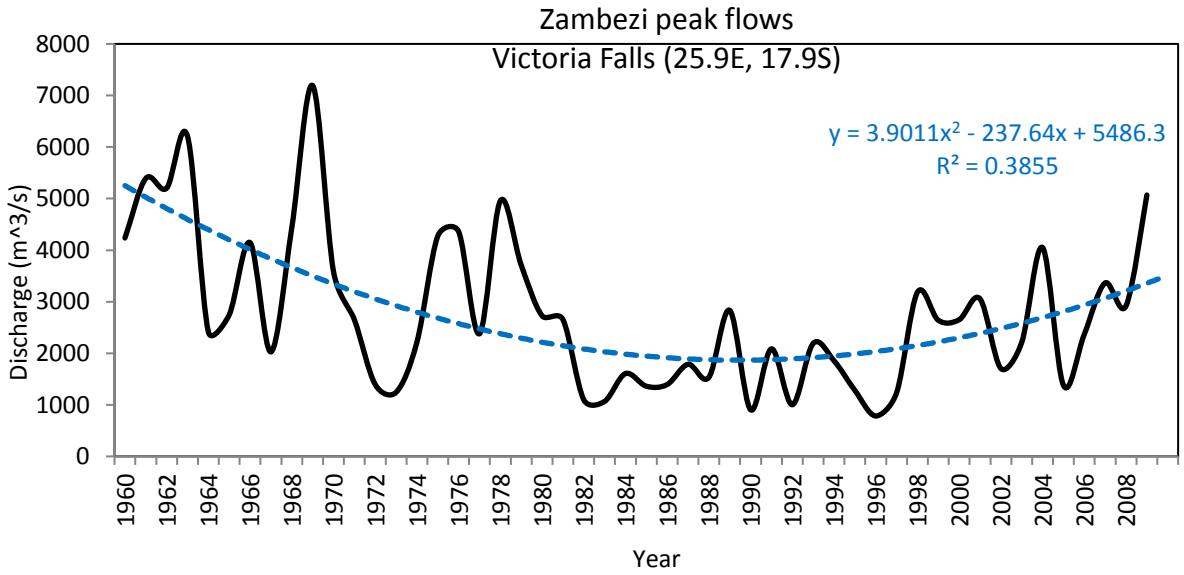

Figure 6:19 Interannual variability of ZRA Zambezi River peak flow (m^3s^{-1}) at Victoria Falls

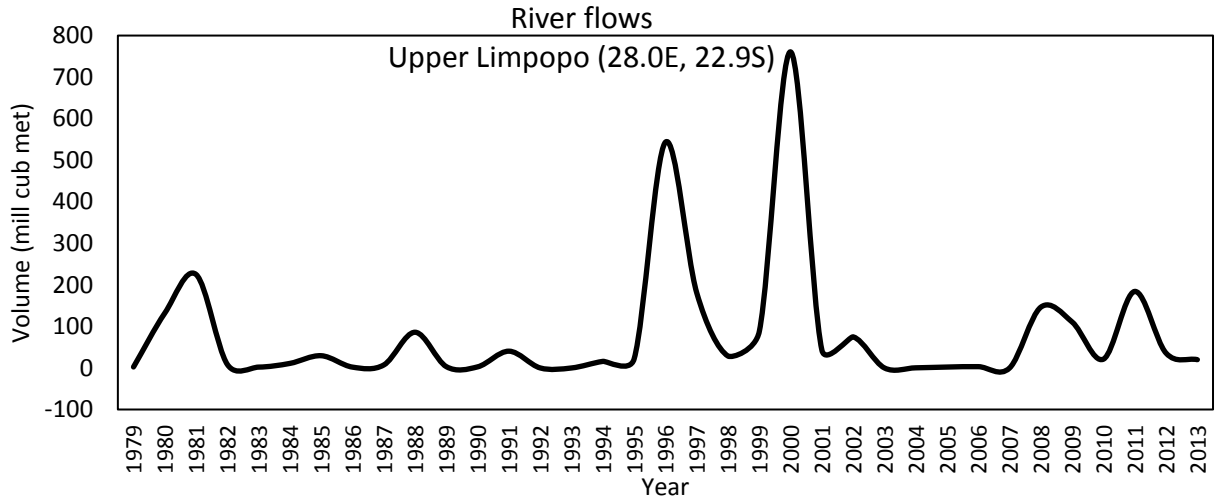

Figure 6:20 Interannual variability of late summer flows (mill cub met) of the upper Limpopo River at Botswana

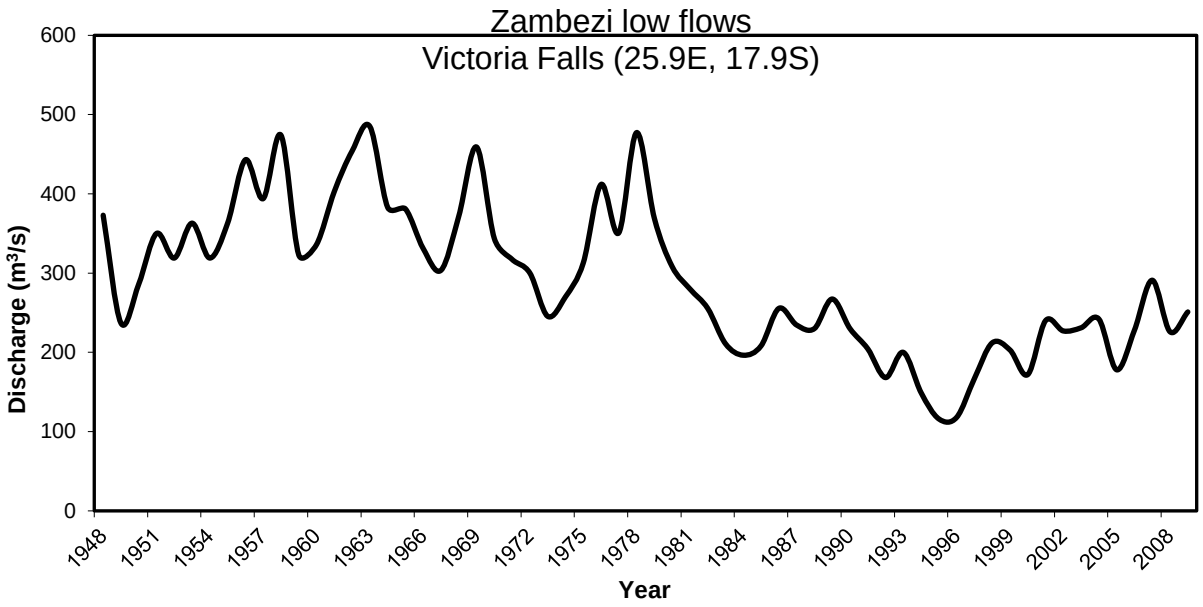

Figure 6:21 Annual minimum flows (m^3s^{-1}) of the Zambezi River at Victoria Falls (1948-2010)

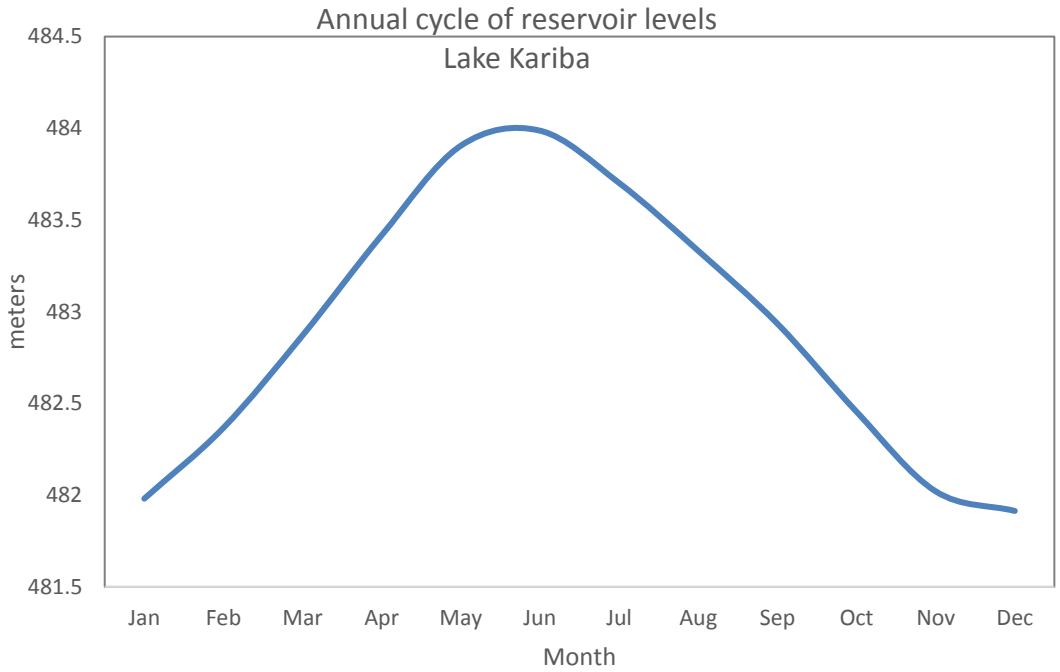

Figure 6:22 Mean annual cycle of reservoir levels (m) at Lake Kariba along the Zambezi River

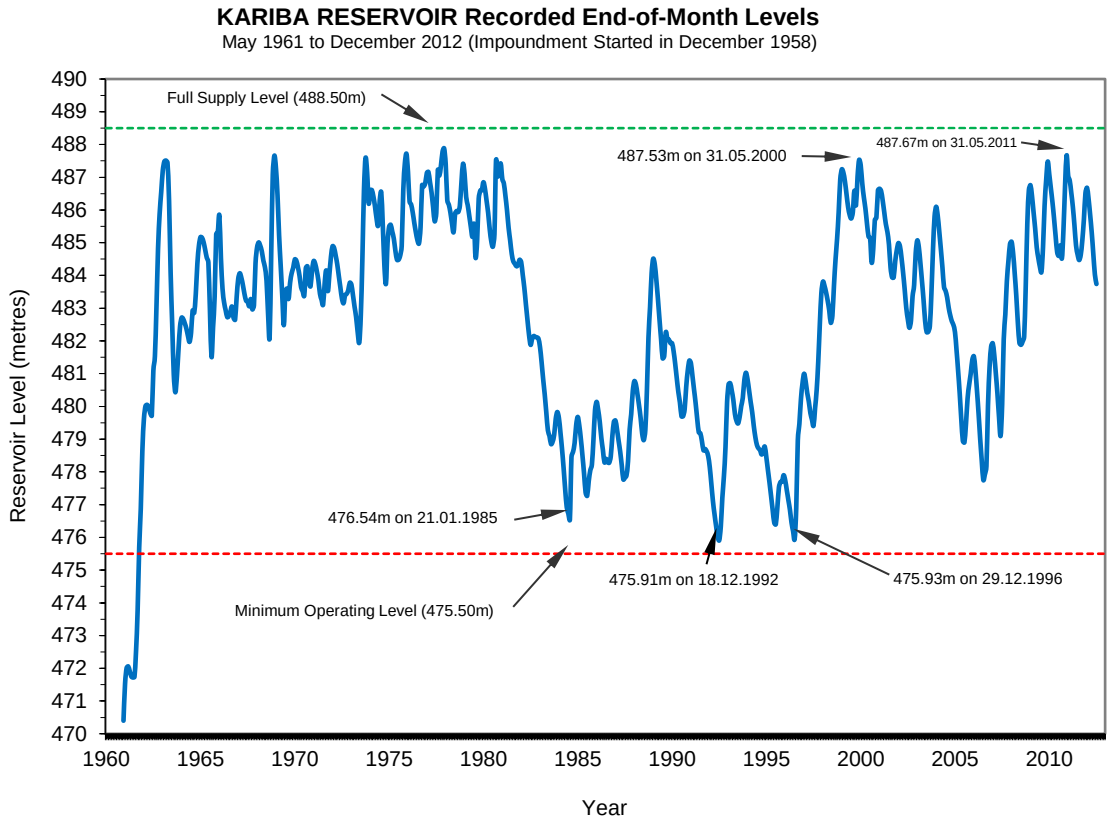

Figure 6:23 Variability of Lake levels (m) at Kariba: 1960-2012 (source: Zambezi River Authority)

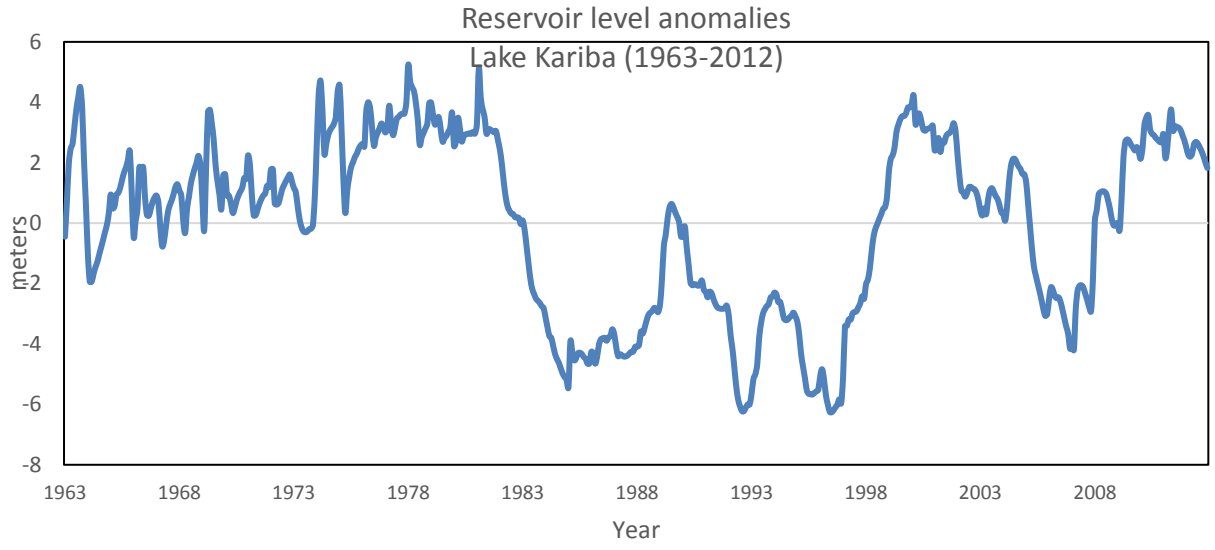

Figure 6:24 Anomalies of reservoir levels (m) for Lake Kariba: 1963-2012 (data source: Zambezi River Authority)

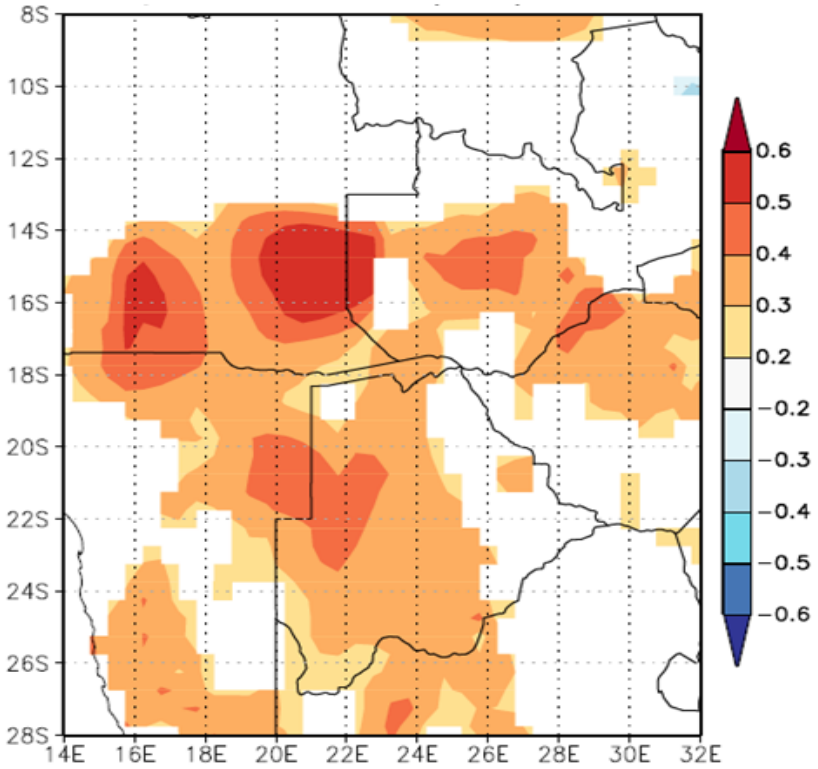

Figure 6:25 May-July averaged Kariba Reservoir Index correlated with DJF precipitation. The shaded grids are at 90% significance or more.

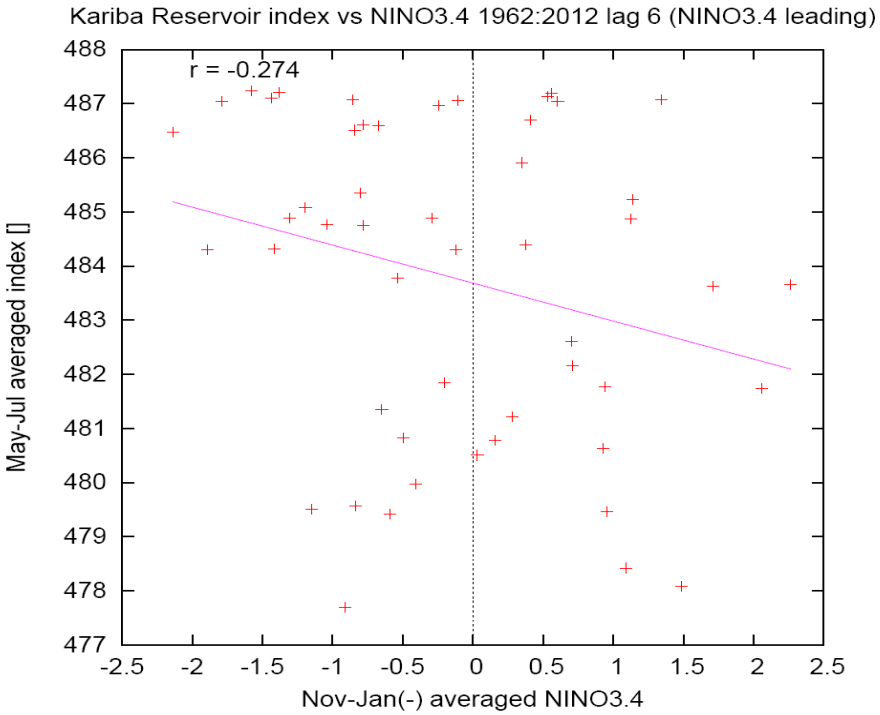

Figure 6:26 Nov-Jan averaged Nino 3.4 correlated with Kariba Reservoir Index lagged (90% significance)

Chapter 7

CONCLUSIONS AND FUTURE WORK

7.1 Introduction

The primary aim of this thesis was to map, quantify and analyze the nature and impacts of meteorological drought events over southern Africa using satellite observations and reanalysis models spanning the period from the summer of 1979-80 to that of 2011/12. The main focus was on an area on the central southern African plateau, bounded by 15-28°S and 22-32°E which includes Botswana, northern South Africa, southern Zambia and most of Zimbabwe. It was recognized from the onset that some climate drivers of drought and its impacts may lie outside the lateral boundaries of this focus area.

Whilst the drought problem has been studied extensively globally, this thesis has employed station observations and satellite-derived climate reanalyses at high resolution. Satellite estimates of evapotranspiration, potential evaporation and soil moisture were not readily available only ten years ago, especially for data-sparse regions such as southern Africa. Significantly, this is also the first time that a drought index based on an anomaly of the surface water balance is used in a study of drought in southern Africa. Drought is also analyzed here over a larger domain than most previous studies. In addition, this thesis provides a unique and new contribution to understanding the nature of an old problem which has evolved over time.

Statistical approaches and climate models have been employed to analyze various datasets and display fields of oceanic, terrestrial and atmospheric variables. It was shown in Chapter 3 that not all automatic stations in southern Africa report in real-time such that comparisons needed to be made between datasets for validation. Due to the continuous nature of datasets analyzed here, time series analysis dominated the methods, whilst anomalies from long-term means are important to show the drought signal. Composite analyses and some case studies have also been given to provide greater insights into the drought problem, its causes, characteristics and impacts.

This chapter provides a summary and synthesis of the key findings of this thesis mainly from Chapters 3-6, and how they contribute to the body of knowledge. A discussion of the links between drought and other emerging global issues is also offered. Research questions and insights that arise from this thesis are recommended for future studies. In conclusion, some solutions to drought management are offered with a focus on water supply problems in semi-rural communities and strategies for water efficiency.

7.2 Thesis findings and conclusions

7.2.1 Recent drought events: 1979-2012

As indicated in Chapter 2, the several definitions of drought that exist hold back the study of drought. The definition proposed in this thesis is based on an anomaly of the surface water balance and has been used to identify meteorological drought events over southern Africa during 1979-2012. Assuming that Runoff and Infiltration are a < 10% fraction of Precipitation, the main drivers of the surface water balance are then *P-E*. This index is an expression of the anomaly in supply (precipitation) minus demand (potential evapotranspiration). It has been shown in Chapter 3 that the *P-E* anomaly index is closely related to the self-calibrating Palmer Drought Severity Index (scPDSI) and is applicable to semi-arid southern Africa where potential evaporation and transpiration exceed precipitation.

The drought index identified seven distinct drought events over southern Africa during 1979-2012. Extreme drought occurred during 1992 and 1982, severe drought during 1983 and 1995, and moderate drought conditions during 1984, 1987 and 2003. Successive droughts occurred during 1982-84 and as such, the early part of the study period (1981-1995) was considerably drier and characterized by more severe droughts than the later. This may be part of a multi-decadal oscillation (~18-20 year) which has also been identified in previous studies. In this research, wavelet analysis has shown cycles of variability occurring at 2.5 and 4.5 years, which may be related to cycles of QBO and ENSO respectively.

7.2.2 Rainfall and evapotranspiration

It was found that PET exhibits a closer relation with SHF than with LHF and therefore SHF may be a useful indicator of losses in the surface water balance and drought conditions. In a study on global trends of PET, Matsoukos *et al.* (2011) also found that PET follows radiation fluxes more than vapour fluxes in most regions.

The datasets analyzed here do not support a recent drying trend over the summer rainfall region of southern Africa as trends are neutral. It appears there has been a recent recovery of rainfall from the severe droughts of the 1980s and 1990s. These patterns are also found in flows in the Zambezi River.

Whilst there is no significant variability of onset between drought and non-drought seasons, the cessation comes earlier than normal during drought resulting in a shorter duration of the rainy season. Thus the onset is not necessarily a useful indicator of the quality of a rainy season. This is consistent with the findings of Moeletsi *et al.* (2011) who found no significant link between onset during La Niña or onset during El Niño but that cessation was consistently earlier than normal during El Niño seasons.

For the period 1979-2012, this analysis has shown that the worst droughts in terms of intensity, duration and spatial extent have occurred over southern Africa during the 1980s and 1990s. The 1992 drought was the most severe. The impacts are also shown to be most significant during the same periods. The assumption of increasing drought is not necessarily supported here.

It is also noted that since the droughts of the 1990s, the occurrence of severe drought over southern Africa has declined during the study period. Long-term trends show a partial recovery of rainfall and hydrology since about 1995.

However, a regression trend of sensible heat flux using an ensemble of all CMIP5 models shows a positive value > 0.1 Wm^{-2} /yr in the period 1980-2050 over southern Africa. It is

one of the few places in the world that goes up, suggesting increasing evaporation losses in the near future. Thus, the changes in evaporation may be more significant and critical than those of precipitation in the surface water balance over southern Africa.

7.2.3 Radiation and temperature

Strong positive OLR anomalies are widespread over southern Africa, with maxima focused over Zimbabwe coinciding with the rainfall anomalies. This implies suppressed convection, reduced cloudiness and high surface temperatures over the region during drought. Whilst land surface temperature and maximum air temperatures also show strong positive anomalies during drought, the temperature anomalies are greatest over the western Limpopo and not over Zimbabwe. Adiabatic warming of subsiding air from the Botswana High may be the mechanism responsible for the warm anomalies over Botswana during this time.

A northwest-southeast band of negative OLR anomalies has been observed over the warm ocean east of Madagascar, supporting the relocation of TTTs and cloud bands there during drought. There is a strengthening of the north-south surface air temperature gradient (Tmax) associated with higher temperatures over the subcontinent. It has also been shown that summer air temperatures over the study area are negatively correlated with rainfall. The hottest temperatures are mostly associated with drought conditions as it is found that all seven droughts identified in this study were among the ten hottest summers in southern Africa during 1979-2012. However, the hottest temperatures are not all associated with drought conditions.

7.2.4 Meteorological propagation and diagnostics

Considerable progress has been made in understanding the synoptic scale circulation and weather systems that cause drought (Gustard *et al.* 2004). Weather systems cause drought by their unusual timing and persistence, or location (Stahl and Hisdal 2004). Anticyclonic anomalies dominate the surface and low level circulation over southern Africa during drought events.

Upper level vorticity over the Mozambique Channel is cyclonic guiding upper anomalous flow equatorward over southern Africa, which must sink according to conservation of absolute vorticity. Upper level convergence (hence sinking motion) is found over central South Africa and Botswana during drought periods. Some upper divergence observed along the west coast suggests uplift there and hence wet anomalies may affect the extreme west coast and the Namib when drought is widespread over the rest of the subcontinent. This may be due to the influence of Benguela Niños.

The vertical structure of the circulation has been used to illustrate how the Botswana High induces drought over the subcontinent. While it is accepted that subsidence is a prevailing characteristic of the subtropics (Tyson and Preston-Whyte 2000), it is enhanced during drought. Composite mean zonal and meridional circulation from the surface to 100 hPa show strengthening of upper westerlies such that subsidence is enhanced in the area between 18-38°E and between 10-30°S. The drought situation is associated with a strengthening and an equatorward displacement of the subtropical jet stream south of Africa.

The Botswana High is thus the immediate cause of meteorological droughts in southern Africa. The establishment, strengthening and persistence of the Botswana High results in the retreat of tropical rain belts equatorward whilst cloud bands are displaced to the Indian Ocean east of Madagascar. The Angola Low is also shallow and weakened causing a reduction of tropical inflows as the ITCZ retreats equatorward. The moisture flux onto the subcontinent is often weakened by a diffluent flow towards east of Madagascar. Instead, westerly wind anomalies at the surface from the Atlantic Ocean are dominant in some drought seasons.

Significant drying occurs throughout the depth of the troposphere from the surface to 200 hPa over southern Africa. This finding is consistent with the dominance of the Botswana High and the high pressure anomalies at the surface. It appears both St. Helena High and the Mascarene High have an important role in the subsidence occurring over the

subcontinent during drought periods. It has been found previously that the Mascarene High variability also affects (Morioka *et al.* 2013b).

It has also been shown that high tropical cyclone days in the Mozambique Channel (east of 40°E) may act to enhance the persistence of dry (drought) conditions even in the absence of remote influences. It was shown in Chapter 5 that cyclonic vorticity is enhanced over the Mozambique Channel during drought periods. Westerly surface wind anomalies are observed west of the Mozambique Channel with easterly anomalies in the east resulting in convergence and uplift around 40°E. Subsidence induced by the cyclone on its western flank sustains dry conditions (Chikoore *et al.* 2015). Conversely, land falling tropical cyclones may bring relief and unseasonal rainfall amounts during prolonged drought. Tropical cyclones Domoina and Imboa brought such drought relief to southern Mozambique, Swaziland and South Africa's eastern districts during the drought of 1984.

7.2.5 Remote influences

Sometimes anomalies in the circulation and weather systems are linked to oscillations of remote large scale ocean-atmosphere interactions (Stahl and Hisdal 2004). Nearly all the droughts identified in this study period occurred during an El Niño event suggesting a strong dominance of the El Niño Southern Oscillation (ENSO) signal. However, the 1981/82 drought occurred in a neutral season whilst the 1983/84 drought coincided with a weak La Niña event. Strong El Niño events occurred during 1982-3 and 1997-98. It has also been found that successive El Niños occurred during 1986-88 and 1992-95 whilst a prolonged La Niña episode continued through 1998-2001.

The consecutive droughts of 1982-84 occurred under different ENSO phases, from ENSO-neutral in 1982, strong El Niño in 1983 to weak La Niña in 1984.

The 1997/98 El Niño and more recently the 2009/10 have shown that El Niño does not always cause drought in southern Africa. Reason and Jagadheesha (2005) have shown the important role of the Angola Low, which was strengthened allowing for cloud bands and more rain than was expected during a strong El Niño. Even so, a weak El Niño may

produce a more severe drought compared to a stronger El Niño. The SW Indian Ocean plays an important role in determining the ENSO impact on seasonal rainfall over southern Africa. Warm Sea-Surface Temperature (SST) anomalies over the western Indian Ocean reinforce the occurrence and severity of drought in southern Africa.

Tropical cyclone (TC) days also appear to be influenced by cycles of ENSO. El Niño causes reduced moisture flux from the Indian Ocean resulting in prolonged dry spells and warmer weather. The mid-tropospheric Botswana High becomes established pushing cloud bands to the Indian Ocean.

Southern Africa is too remote from the Pacific Ocean to have pure ENSO influence - there are intermediaries such as upper westerlies from the Atlantic Ocean or a warmer tropical Indian Ocean via the IOD. Successive El Niños have shown that their impact may be different due to the state of the western Indian Ocean. Warmer western Indian Ocean (positive IOD) would act to enhance drying over southern Africa due to El Niño. A positive IOD coincided with El Niño during four droughts identified in this study (1983, 1987, 1992 and 1995) even though the coincidence did not produce droughts during 1988 and 1998.

Both the IOD and ENSO peak in the austral autumn but the IOD decays in winter earlier than ENSO the following spring. Manatsa *et al.* (2011) determined that the ENSO impact has gradually become more dominant as the IOD influence has diminished. A most significant finding is the link between the upper divergence field and the Indian Ocean Dipole during drought periods.

The South Atlantic Ocean has received less research attention with regards its influence on seasonal rainfall over southern Africa. A cooler/warmer ocean in the Atlantic Ocean adjacent to Africa (~5-15°S) results in anomalously higher/lower SLP over the ocean and adjacent interior. Higher pressure anomalies associated with a cooler Atlantic Ocean result in a weakening of the Angola Low whilst cloud band formation is inhibited. Warm Benguela Ni Niños result in anomalously wet weather along the Angola/Namibia coastal area (Hansingo and Reason 2009; Jury 2016).

7.2.6 Space-time variability

Whereas, hydrological extremes such as floods may occur over localized areas, droughts tend to persist while affecting large areas (Stahl and Hisdal 2004). Thus, the use of monthly data in the analysis of drought is justified. It has also been shown here that subsidence and dry weather covers an area extending from South Africa to the Congo and from the Kalahari to the Mozambique Channel (west of 40°E). Thus, drought tends to be widespread in southern Africa with regional variations in impact. Spatial heterogeneity in drought areas has also been found in other studies (e.g. Stahl and Hisdal 2004). Drought severity may require multiple indicators as crop and hydrological impacts exhibit different spatial variations from rainfall patterns.

It is important to show the area affected by drought, variability of drought intensity in the affected area and also recurring patterns from one drought to another (Stahl and Hisdal 2004). The deficits caused by drought in southern Africa appear to maximize over Zimbabwe as all seven droughts analyzed in this study have affected the country. The dominant drought mode (EOF1) and ENSO Niño 3.4 signal also maximize over Zimbabwe. However, while rainfall, OLR and soil moisture composite anomalies are greatest over Zimbabwe, potential evapotranspiration, surface air temperature and vegetation anomalies are greatest over the western Limpopo valley.

An analysis of rainfall anomalies during drought seasons shows that no drought is similar to another, suggesting that predictability of area covered by drought and its severity is still an enormous task for seasonal climate forecasters. However, it appears the more intense a drought is, the larger the area affected by anomalies. As drought ravages much of southern Africa, some wet anomalies seem to occur over the Angola/Namibia coastal margins due to the Benguela Niño phenomenon which results in warm SST anomalies and lower pressure and a stronger Angola Low.

The spatial extent of drought is related to the intensity of El Niño. In an earlier study on spatial extent of drought in southern Africa, Lyon (2004) found that a strong El Niño affects more than twice the land area affected during a weak El Niño.

Temporally, drought develops slowly and its impacts may be slow to emerge. Drought indices such as the PDSI and SPI exhibit positive trends during 1979-2012 suggesting a decrease in drought intensity during the study period. It is not clear whether these trends are temporary or how they are influenced by the prolonged droughts of the 1980s and 1990s.

7.2.7 Drought impact

It is long established that drought impacts are multidimensional and may be either short-term or may only appear in the long-term. It has been said in Chapter 2 that since drought impacts are non-structural, they are difficult to quantify (Heim 2002; Murthy *et al*. 2009).

Drought impact can be severe (Peters *et al.* 1991) and most significant in semi-arid regions, in countries whose economies are dominated by agriculture (Dube 2008). In industrialized countries, drought impact is greater due to economic losses than by famine (Stahl and Hisdal 2004). Even so, it has been found that drought may affect the agriculture sector directly or indirectly (e.g. Vogel 1994). Impacts of drought may also depend on the rainfall received during the preceding season. Successive droughts have occurred over southern Africa during 1982, 1983 and 1984 compounding the impacts and relief efforts over the region. The other four drought events (1987, 1992, 1995 and 2003) were followed by a relatively wetter season, allowing for a quicker recovery from the drought impact.

Soil moisture is an important variable that regulates energy and water cycles at the surface. It is found that rainfall deficits lead the soil moisture deficits which in turn lead the declines in surface runoff. Soil moisture exhibits strong seasonality over southern Africa with a peak during March and is at its lowest during September. This finding may provide useful information about land preparation by farmers before the onset of the rainy season as tilling the land in early October may act to expose the subsoil to further evaporative

losses. Plumes of dust may also affect air quality when winds blow across dry cultivated soils.

In addition to soil moisture, poor quality of soils may also affect yields of maize (Vogel 1994) and vegetation NDVI. Total maize yields for southern Africa have shown a slight upward trend since the 1995 drought. However, the productivity for Botswana and Zimbabwe has been declining steadily due to other non-climatic factors. NDVI anomalies are an indicator of biomass productivity including agricultural activity and may be used to determine the state of the veld and how that affects wildlife populations. The months of March and February are key periods with regards the drought impact on biomass productivity and agricultural output.

However, temporally, it appears most droughts reach the peak during the late summer which coincides with critical stages of crop growth. Farm management practices and political factors also influence the crop yields and agricultural productivity. Whilst perhaps the greatest impact of drought on maize yield and water resources may be social, it has been found in this study that economies are also significantly affected. Vogel (1994) found that drought impacts on agriculture need to be considered together with (mis) management and economic influences.

The value of agricultural productivity experiences huge losses during drought periods such as the drop to USD752 during 1992 from an average of about USD810 000 according to FAOSTAT data. Comparatively, river flows on the Zambezi account for hydro-electricity generation on Lake Kariba and in Cahorra Bassa downstream. Losses of up to USD102 million to Zambia, Zimbabwe and Mozambique have been observed due to declines in electricity generation capacity along the Zambezi (Muchuru *et al.* 2014).

River flows of a high volume river and a low flow river (Zambezi and Limpopo respectively) in southern Africa were studied and represented conditions of the basins upstream of the gauging stations. Reservoir levels for Lake Kariba have shown a strong response to drought during the 1980s and 1990s and to the Pacific Ocean ENSO.

The 1992 drought is by far distinct from other droughts in this study in terms of anomalies in the surface water balance, circulation, influences of the oceans and the devastating impacts.

7.3 Implications: Drought in a wider context

Drought occurs over southern Africa which is a region already stressed by other natural and man-made challenges. It results from complex interaction between the natural hazard and demand for water resources and food production from human systems (Wilhite *et al*. 2007). It is also difficult to determine whether drought characteristics are evolving over southern Africa due to climate change as each drought has a unique signature.

Climate change affects temperature, potential evaporation and precipitation patterns (e.g Stahl and Hisdal 2004) having influence on meteorological drought. Individually, changes in precipitation or evaporation may act as drivers of drought but may also intensify drought if they act in concert (Cook *et al.* 2014). Several climate change projections also suggest that drought will occur more frequently in regions such as southern Africa (e.g. Hoerling *et al.* 2006; Shongwe *et al.* 2011; Kay and Washington 2008). However, there is still some disagreement and uncertainty between the observations and models as to how drought will evolve in a future warmer climate.

Even if climate change does not affect the frequency or intensity of drought in future, the impacts of drought will likely become more harmful as a result of population growth and increased demand for water (AMS 1997). Human activities such as urbanization, population growth and a greater demand for water resources will exacerbate impacts of drought (AMS 2013). Additionally, land use changes affect streamflow and lower the water table (van Lanen *et al.* 2004) whilst excessive abstraction of groundwater for industry and domestic use may lead to hydrological drought (van Lanen *et al.* 2004).

The economies of southern Africa are largely agro-based and vulnerable to a highly variable climate. Poor economies have resulted in recent civic unrest in South Africa

following an influx of immigrants from neighboring countries. Funding from African governments for drought relief is therefore not always guaranteed. Whilst good management practices cannot prevent the occurrence of drought in future, it has potential to moderate the impact of the drought (Gustard *et al.* 2004).

As drought is a regular feature of the summer climate of southern Africa, the need to strengthen capacity for drought monitoring and forecasting is evident. In the past, impacts of drought have been compounded by a lack of preparedness (WMO 1997) and mismanagement. If the pattern of precipitation from the time of planting is unknown, farm management is likely to be aimed at minimizing risk, which often means settling for low inputs and low but stable yields (Phillips *et al.* 1998). Drought prediction may need to be integrated into an early warning system. Dissemination of scientific information to policy makers and the remote rural communities for decision support systems is imperative. What is important is to communicate the limitations of climate science and key uncertainties to users of weather and climate information. Operational staff in meteorology, hydrology and agronomy also need to remain up to date with advances in drought research.

Drought may have negative and far reaching consequences on society, including human health. As shown in Chapter 4, droughts are often accompanied by high land surface and air temperatures or heat waves which may cause an increase in mortality due to cardio-vascular related complications especially on the elderly and vulnerable. Poor water quality and food shortages may result in malnutrition and water borne diseases such as cholera. Pre-existing conditions such as HIV and AIDS may compound the drought impact. In contrast drought affects life cycles of the malaria vector (*anopheles* mosquito) and the *plasmodium* parasite such that periods of drought are periods of fewer malaria outbreaks and epidemics.

Advances in remote sensing of the environment have contributed to improved drought monitoring over southern Africa. Satellite observations of rainfall, soil moisture and vegetation are available for early warning. National Meteorological Services of the region

need to invest in deployment of real-time automatic weather observing systems to improve monitoring and predictability. The Indian Ocean is an important source of climate signal for southern Africa and also needs an improved observing network building on the successes of the Climate and Ocean – Variability, Predictability, and Change (CLIVAR). A regional effort to monitor and forecast drought through a specialized regional center may help provide a link between science and society.

7.4 Future work

This study has focused on historical drought in a summer rainfall region of southern Africa for the satellite era from 1979. The satellite record is still rather short to determine decadal-scale variability of drought and other climate variables and that may be considered a caveat of this study. The winter rainfall region has also been left out of this analysis and may require a separate investigation considering the projected drying in the winter rainfall area due to expansion of the subtropical highs and retreat of the cold fronts.

Whilst the role of the oceans in modulating drought in southern Africa has been analyzed and discussed in Chapter 5, it appears the Atlantic Ocean may be a significant contributor to rainfall variability in southern Africa than was previously thought. In addition, global phenomena such as the Southern Annular Mode (SAM), Quasi-Biennial Oscillation (QBO) and the Sunspot Cycle may have significant impact on drought in southern Africa and may require rigorous investigation.

The contribution of cross-equatorial waves in suppressing convection over southern Africa and displacing cloud bands to the Indian Ocean leading to periods of drought needs follow up after Ratnam *et al*. (2015).

A significant percentage of semi-arid rangelands in southern Africa are not suitable for cultivation and are used for grazing livestock herds and as wildlife sanctuaries. The wealth and livelihoods of rural communities in these regions are dependent on the size and health of livestock herds. It is necessary to investigate drought impacts on livestock herds (cattle and goats) and rural livelihoods.

There is some disagreement on the trends of drought and the influence of global warming on drought characteristics in future (e.g. Sheffield *et al.* 2012). Uncertainties in climate model physics and model projections depending on low mitigation or high mitigation scenarios affect decision making on adaptation. Thus, the climate change question is still elusive and requires further investigation. Most of the research globally on drought and drought monitoring using indices has focused on the conterminous United States. Such efforts could be targeted at the southern Africa region where rainfall is unreliable and where drought is regular and recurrent and where the impacts can be severe on communities and economies.

Although this study has employed lower resolution NCEP1 reanalyses, the high-resolution MERRA hourly reanalysis is now available for future research at IRI under NASA GSFC. It is quite similar to the new version of ECMWF (which is restricted access). The MERRA reanalysis has a resolution six times better than NCEP1, and model data assimilation technology that is 20 years newer.

The skill of climate models to simulate future evolution of droughts is also due to important sub-grid processes such as convection. Unorganized and deep convection are key features of the southern Africa summer climate.

The drought phenomenon is complex and has several dimensions. Some of the following research questions and insights arise from this study and may be considered for future studies:-

a) How will drought characteristics in southern Africa evolve under climate change?
b) How will climate change affect the El Niño phenomenon and its impacts?
c) What is the impact of drought on livestock herds and wildlife in southern Africa?
d) How skillful or effective are seasonal predictions of drought in southern Africa in agricultural and water management?
e) What coping strategies may be applicable to rural communities of southern Africa at risk of future drought?

7.5 Solutions in drought management

In response to the drought problem analyzed in this thesis and to some of the questions posed above, this section proffers some opportunities and strategies to 'live with drought' in southern Africa. The focus is on dual issues of local water resources in semi-urbanized places and farm management for water conservation in smallholdings.

During drought, some ephemeral rivers may run dry including wells and small dams making water supply one of the greatest challenges affecting local authorities. Rainwater harvesting is also a strategy to conserve water during drought periods. Collecting tanks from corrugated roofs into closed tanks may also supply water for domestic supply. One may argue that during severe drought, there may be few rainy days such that there may be little water to harvest. Thus, semi-rural communities of southern Africa could cope better with drought through the extension of municipal water management to farming areas. Contingencies may be made for bringing in water trucks to fill central community holding tanks. This may require funding from humanitarian organizations or through imposing a 'drought levy or tax'.

In deeper rural areas of southern Africa, groundwater may become a critical source of water supply. Water wells are often shallow and may dry up easily during drought periods. Community boreholes which can be up to 100 m deep may be a solution to water supply problems. In Zimbabwe, efforts are being made to abstract groundwater from an aquifer (Nyamandlovu) in the semi-arid southwest Matabeleland region. However, the future of groundwater has not been tested as groundwater is seldom included in drought studies.

In addition to climate constraints on rain-fed agriculture over southern Africa, there are also constraints related to soils and terrain. For example, the state and rate of land degradation will affect productivity of the land and therefore crop yields. Of all the world's uncultivated arable land, 60% is found in Africa (http://democracyinafrica.org/africa-feed-world-smallholders-will-key/). There is therefore opportunity to explore the increase in

land under cultivation to offset losses due to drought. Smallholder agriculture may become crucial in the expansion of land under cultivation.

In southern Africa, large scale commercial farmers are better resourced with large tracks of land for rotational grazing, water reservoirs and irrigation facilities. They also have better access to loans from banks and finance houses. Impacts of drought are therefore greatest on the smallholder farmer whose agriculture is rain-fed in a region of unreliable rainfall and whose livelihood depends on crop yields and domestic livestock.

It has been shown in this study that rain trends in southern Africa are neutral but sensible heat flux is significantly upward leading to increased evaporation from the land surface. That happens via the land surface warming faster than the air. Therefore, mulching may be a solution to water losses at a local scale, and perhaps preservation of ground cover at a larger scale. A mulch is composed of dead organic material which may be spread around crops. Mulches promote soil water retention by reducing evaporation and retard weeds and increase yields (Ramakrishna *et al.* 2006). Deng *et al.* (2006) also found that mulching increases water-use efficiency by between 10-20% in a study in North China.

During the 2003 drought in a community in northeast South Africa, Jury *et al.* (2008) demonstrated that mulching at the surface and compositing in the root layer significantly improve crop yields. Both caused more soil water retention, reducing surface soil temperatures by up to 10°C and potential evaporation by ~50%. That type of 'farm' management could only be applied at very small scales (usually referred to as 'intensive organic' farming), not industrial. Another indirect solution in drought management may be to intensify rural electrification programs so as to limit firewood collection and biomass burning.

Advances in seasonal climate prediction allow for early warnings of drought. Smallholder farmers may plan to plant drought resistant or short seasoned varieties of maize. Small grains such as sorghum and millet also provide alternative crops during drought periods as they can tolerate high temperatures and low rainfall. Staggering of planting dates also

spreads the risk of crop failure and may be a useful strategy to cope with drought. Diversification of livelihood options may also be considered to reduce drought risk.

The ultimate goal is for resource-poor and vulnerable rural communities of southern Africa to adapt and cope with the harsh realities of recurrent drought in a changing climate.

REFERENCES

Alley, W.M., 1984. The Palmer Drought Severity Index: Limitations and assumptions. *J. Climate Appl. Meteor.,* 23, 1100-1109

AMS, 1997. AMS policy statement on meteorological drought. Accessed online http://www.ametsoc.org/policy/drought2.html on 27 December 2013.

AMS, 2013. Drought: An information statement of the American Meteorological Society. *Adopted by AMS Council on 19 September 2013.* Accessed online http://www.ametsoc.org/POLICY/2013drought_amsstatement.html on 13/12/2013

Andrews, W.R.H. and L. Hutchings, 1980. Upwelling in the southern Benguela Current. *Prog. Oceanog.*, 9, 1-81

Anyamba, A. and C.J. Tucker, 2012. Historical perspectives on AVHRR NDVI and vegetation drought monitoring. In: *Remote sensing of drought, innovative monitoring approaches* [Wardlow, B.D., Anderson, M.C. and Verdin, J.P. (eds.)] CRC Press, Boca Raton, USA

Anyamba, A., Tucker, C.J. and J.R. Eastman, 2001. NDVI anomaly patterns over Africa during the 1997/98 ENSO warm event. *Int. J. Remote Sensing,* 22, 1847-1859

Anyamba, A., Tucker, C.J., and R. Mahoney, 2002. From El Niño to La Niña: vegetation response patterns over east and southern Africa during the 1997-2000 period. *J. Climate,* 15, 3096-3103

Ash, K.D. and C.J. Matyas, 2012. The influences of ENSO and the subtropical Indian Ocean Dipole, on tropical cyclone trajectories in the southwestern Indian Ocean. *Int. J. Climatol.*, 32, 41-56

Ashok, K., Behera, S.K., Rao, S.A., Weng, H. and T. Yamagata, 2007. El Niño Modoki and its possible teleconnection. *J. Geophys. Res.*, 112, C11007, doi:10.1029/2006JC003798

Barry, R.G. and R.J. Chorley, 2003. Atmosphere, weather and climate. 8th ed. *Routledge, London* 421 pp.

Behera, S. K., R. Krishnan, and T. Yamagata, 1999. Unusual ocean-atmosphere conditions in the tropical Indian Ocean during 1994. *Geophys. Res. Lett.*, 26, 3001–3004

Behera, S.K., Luo, J.J., Masson, S., Delecluse, P., Gualdi, S., Navarra, A., and T. Yamagata, 2005. Paramount impact of the Indian Ocean dipole on the East African short rains: a CGCM study. *J. Climate*, 18, 4514-4530.

Behera, S.K. and T. Yamagata, 2001. Subtropical SST dipole events in the southern Indian Ocean. *Geophys. Res. Lett.*, 28, 327-330

Behera, S.K. and T. Yamagata, 2003. Influence of the Indian Ocean dipole on the Southern Oscillation. *Journal of the Meteorological Society of Japan,* 81, 169-177

Beraki, A.F., DeWitt, D.G., Landman, W.A. and C. Olivier, 2014. Dynamical seasonal climate prediction using an ocean-atmosphere coupled climate model developed in partnership between South Africa and the IRI. *J. Climate,* 1719-1741

Bradford, R.B., 2000. Drought events in Europe. In: Drought and drought mitigation in Europe [Vogt, J. and F. Somma (eds)], *Advances in Natural and Technological Hazards Research, Vol 14. Kluwer Academic Publisher, Dordrecht, the Netherlands, pp 7-20*

Buckle C., 1996. Weather and Climate in Africa. *Longman: Harlow; 312 pp*.

Byun, H., 1996. On the atmospheric circulation associated with Korean drought. *J. Korean Meteor. Soc.,* 32**,** 455–469.

Byun, H. and D.A. Wilhite, 1999. Objective quantification of drought severity and duration. *J. Climate,* 12, 747-756

Cai, W., Cowan, T., Briggs, P. and M. Raupach, 2009. Rising temperature depletes soil moisture and exacerbates severe drought conditions across southeast Australia. *Geophys. Res. Lett.,* 36, L21709

Cai, W., Zhang, Y., Chen, Q. and Y. Yao, 2015. Spatial patterns and temporal variability of drought in Beijing-Tianjin-Hebei Metropolitan areas in China. *Advances in Meteorology*, doi.org/10.1155/2015/289471

Calow, R.C., MacDonald, A.M., Nicol, A.L. and N.S. Robins, 2010. Groundwater security and drought in Africa: Linking availability, access, and demand. *Groundwater,* 48, 246-256

Camberlin, P., Moron, V., Okoola, R., Philippon, N. and W. Gitau, 2009. Components of rainy seasons' variability in Equatorial East Africa: onset, cessation, rainfall frequency and intensity. *Theor. Appl. Climatol.,* doi 10.1007/s00704-009-0113-1

Challinor, A.J., Slingo, J.M., Wheeler, T.R., Craufurd, P.Q., and D.I.F. Grimes, 2003. Toward a combined seasonal weather and crop productivity forecasting system: Determination of the spatial correlation scale. *J. Appl. Meteorol.,* 42, 175-192

Challinor, A.J., Wheeler, T.R., Slingo, J.M., Craufurd, P.Q., and D.I.F. Grimes, 2005. Simulation of crop yields using ERA-40: Limits to skill and non-stationarity in weather-yield relationships. *J. Appl. Meteorol., 44, 516-531*

Chang, F.-C., Wallace, J.M., 1987. Meteorological conditions during heat waves and droughts in the United States Great Plains. *Mon. Wea. Rev.,* 1253-1269

Chikoore, H., 2005. Vegetation feedback on the boundary layer climate of southern Africa. *MSc. thesis, Univ. Zululand*

Chikoore, H. and M.R. Jury, 2010. Intraseasonal variability of satellite-derived rainfall and vegetation over southern Africa. *Earth Interactions,* 14, 1-26

Chikoore, H., Vermeulen, J.H. and M.R. Jury, 2015. Tropical cyclones in the Mozambique Channel: January to March 2012. *Nat. Hazards,* 77, 2081-2095

Christensen, J. and Co-authors, 2007. Climate change 2007: the physical science basis. Contribution of Working Group I to the Fourth Assessment Report of the Intergovernmental Panel on Climate Change, Cambridge: Cambridge University Press, chapter Regional climate projections. pp. 847-940.

Cook, B.I., Bonan, G.B. and S. Levis, 2006. Soil moisture feedbacks to precipitation in southern Africa. *J. Climate,* 19, 4198-4206

Cook, B.I., Smerdon, J.E., Seager, R. and S. Coats, 2014. Global warming and 21st century drying. *Clim. Dyn.*, 43, 2607-2627

Cook, C., Reason, C.J.C. and B.C. Hewitson, 2004. Wet and dry spells within particularly wet and dry summers in the South African summer rainfall region. *Clim. Res.,* 26, 17-31

Cook, E.R., Seager, R., Cane, M.A. and D.W. Stahle, 2007. North American drought: reconstructions, causes and consequences. *Earth-Science reviews,* 81, 93-134

Cook, K.C. 2000. The South Indian Convergence Zone and interannual rainfall variability over southern Africa. *J. Climate,* 13, 3789-3804

D'Abreton, P.C. and J.A. Lindesay, 1993. Water vapour transport over southern Africa during wet and dry early and late summer months. *Int. J. Climatol.,* 13, 151-170

Dai, A., 2011a. Characteristics and trends in various forms of the Palmer Drought Severity Index during 1900-2008. *J. Geophys. Res.,* 116, D12115, doi: 10.1029/2010JD015541

Dai, A., 2011b. Drought under global warming: A review. *Wiley Interdisciplinary Reviews: Clim. Change*, 2, 45-65

Dai, A., 2012. Increasing drought under global warming in observations and models. *Nature Climate Change,* 3, 52-58, doi: 10.1038/nclimate633

Deng, X., Shan, L., Zhang, H. and N.C. Turner, 2006. Improving agricultural water use efficiency in arid and semiarid areas of China. *Agricultural Water Management*, 80, 23-40

Didan, K., 2015. MOD13C1 MODIS/Terra Vegetation Indices 16-Day L3 Global 0.05Deg CMG V006. NASA EOSDIS Land Processes DAAC. http://doi.org/10.5067/ MODIS/MOD13C1.006

Dube, C., 2008. The impact of Zimbabwe's drought policy on Sontala rural community in Matabeleland South Province. *MSc. thesis, Stellenbosch Univ.*

Dube, L.T. and M.R. Jury, 2003. Structure and precursors of the 1992/93 drought in KwaZulu-Natal, South Africa from NCEP reanalysis data. *Water SA,* 29, 201-207

Eden, U., 2012. Drought assessment by evapotranspiration mapping in Twente, the Netherlands. *MSc. thesis, Univ. Twente*

Engelbrecht, C.J., Landman, W.A., Engelbrecht, F.A. and J. Malherbe, 2015. A synoptic decomposition of rainfall over the Cape south coast of South Africa. *Clim. Dyn.*, 44, 2589-2607

Fan, Y. and H. van den Dool, 2004. Climate Prediction Center global monthly soil moisture data set at 0.5 degree resolution for 1948 to present. *Geophysical Research*, 109, D10102, doi: 10.1029/2003JD004345

Farrar, T.J., Nicholson, S.E. and A.R. Lare, 1994. The influence of soil type on the relationships between NDVI, rainfall and soil moisture in semiarid Botswana. II. NDVI response to soil moisture. *Remote Sens. Environ.,* 50, 121-133

Fauchereau, N., Pohl, B., Reason, C.J.C., Rouault, M. and Y. Richard, 2009. Recurrent daily OLR patterns in the southern Africa/Southwest Indian Ocean region, implications for South African rainfall and Teleconnections. *Clim. Dyn.,* 32, 575-591

Fennel, W., 1999. Theory of the Benguela upwelling system. *J. Phys. Oceanogr.*, 29, 177-190

Florenchie, P., Lutjeharms, L.R.E. and C.J.C. Reason, 2003. The source of Benguela Niños in the South Atlantic Ocean. *Geophys. Res. Lett.,* 30, 1505, doi: 10.1029/2003GL017172

Feng, J., Dunxin, H.U. and Y.U. Lejiang, 2014. How does the Indian Ocean subtropical dipole trigger the tropical Indian Ocean dipole via the Mascarene high? *Acta Oceanol. Sin.*, 33, 64-76

Gandure, S., 2005. Coping with and adapting to drought in Zimbabwe. *PhD thesis, Univ. Witwatersrand*

Gibbs, W.J. and J.V. Maher, 1967. Rainfall deciles as drought indicators. *Bureau of Meteorology Bulletin,* 48, Commonwealth of Australia, Melbourne

Glad, P.A., 2010. Meteorological and hydrological conditions leading to severe regional drought in Malawi. *MSc. thesis, Univ. Oslo*

Goward, S.N., Xue, Y. and K.P. Czajkowski, 2002. Evaluating land surface moisture conditions from the remotely sensed temperature/vegetation index measurements: An exploration with the simplified simple biosphere model. *Rem. Sens. Environ.,* 79, 225-242

Grinsted, A., Moore, J.C. and S. Jevrejeva, 2004. Application of cross wavelet transform and wavelet coherence to geophysical time series. *Nonlinear Processes in Geophysics*, 11, 561-566

Gustard, A., van Lanen, H.A.J. and L.M. Tallaksen, 2004. Outlook. In: *Hydrological Drought, Processes and estimation methods for streamflow and groundwater. Developments in Water Science, 48* [Tallaksen, L.M. and H.A.J. van Lanen (eds)]. Elsevier, Amsterdam and Oxford, 579 pp.

Hansingo, K., 2008. An investigation into the impacts of the Benguela Niño on rainfall over southern Africa. *PhD thesis, Univ. Cape Town*

Hansingo, K. and C.J.C. Reason, 2009. Modelling the atmospheric response over southern Africa to SST forcing in the southeast tropical Atlantic and southwest tropical Indian Oceans. *Int. J. Climatol.*, 29, 1001-1012

Harris, I., Jones, P.D., Osborn, T.J. and D.H. Lister, 2013. Updated high-resolution grids of monthly climatic observations – the CRU TS3.10 dataset. *Int. J. Climatol.,* 34, 623-642

Harrison, M.S.J., 1984. A generalized classification of South African summer rain-bearing systems. *J. Climatology,* 4, 547-560

Harrison, M., Troccoli, A., Coughlan, M. and J.B. Williams, 2008. Seasonal Forecasts in Decision Making. In: *Seasonal Climate: Forecasting and managing risk [*Troccoli, A., Harrison, M., Anderson, D.L.T. and S.J. Mason (eds)*]*. Springer, Dordrecht, the Netherlands 467 pp.

Hart, N.C.G., Reason C.J.C. and N. Fauchereau, 2010. Tropical-extratropical interactions over southern Africa: three cases of heavy summer season rainfall. *Mon. Wea. Rev.,* 138, 2608–2623

Hart, N.C.G., Reason C.J.C. and N. Fauchereau, 2012. Building a tropical-extratropical cloud band metbot. *Mon. Wea. Rev.,* 140, 4005–4016

Hart, N.C.G., Reason C.J.C. and N. Fauchereau, 2013. Cloud bands over southern Africa: seasonality, contribution to rainfall variability and modulation by the MJO. *Clim. Dyn*., 41, 1199-1212

Hayes, M.J., 2011. What is drought? *Drought Indices. Available from: www.drought.unl.edu, Accessed on 15 June 2011.*

Hayes, M.J., Svoboda, M.D., Wilhite, D.A. and O.V. Vanyarkho, 1999. Monitoring the 1996 drought using the Standardized Precipitation Index. *Bull. Amer. Met. Soc.,* 80, 429-438

Hayes, M., Svoboda, M., LeCompte, D., Redmond, K. and P. Pasteris, 2005. Drought monitoring: new tools for the 21st Century. In: *Drought and Water Crises: Science, Technology and Management Issues* [Wilhite, D. (ed)], CRC Press, Boca Raton, pp. 53-69

Hayes, M.J., Svoboda, M.D., Wardlow, B.D., Anderson M.C. and F. Kogan, 2012. Drought monitoring: historical and current perspectives. In: *Remote sensing of drought, innovative monitoring approaches* [Wardlow, B.D., Anderson, M.C. and Verdin, J.P. (eds.)] CRC Press, Boca Raton, USA

Heim, R.R. Jr., 2000. Drought indices: A review. In: *Drought: A global assessment* [Wilhite, D.A. (ed)], Routledge, London, pp. 159-167

Heim, R.R. Jr., 2002. A review of Twentieth-Century drought indices used in the United States. *Bull. Amer. Met. Soc.,* 83, 1149–1165

Hirst, A.C. and S. Hastenrath, 1983. Atmosphere-ocean mechanisms of climate anomalies in the Angola-Tropical Atlantic sector. *J. Phys. Oceanogr.*, 13, 1146-1157

Hisdal, H., Tallaksen, L.M., Claussen, B., Peters, E., amd A. Gustard, 2004. Hydrological drought characteristics. In: *Hydrological Drought, Processes and estimation methods for streamflow and groundwater.* Developments in Water Science, 48 *[*Tallaksen, L.M. and H.A.J. van Lanen (eds)]. Elsevier, Amsterdam and Oxford, 579 pp.

Hoffman, M.T., Carrick, P.J., Gillson, L. and A.G. West, 2009. Drought, climate change and vegetation response in the succulent Karoo, South Africa. *S. Afr. J. Sci.,* 105, 54-60

Hoerling, M., Hurrel, J., Eischeid, J. and A. Phillips, 2006. Detection and attribution of twentieth-century northern and southern African rainfall change. *J. Climate*, 19, 3989-4008

Hollinger, S.E., Isard, S.A. and M.R. Welford, 1993. A new soil moisture drought index for predicting crop yields. Preprints, *Eight conf. on Applied Climatology,* 187 – 190, Amer. Met. Soc., Anaheim CA,

Holton, J.R., 2004. An introduction to dynamic meteorology. Fourth edition. *Elsevier Academic Press, London, 535 pp.*

Hsu, C.P.F. and J.M. Wallace, 1976. The global distribution of annual and semiannual cycles in precipitation. *Mon. Wea. Rev.,* 104, 1093-1101

Hughes, D.A., Hannart, P. and D. Watkins, 2003. Continuous baseflow separation from time series of daily and streamflow data. *Water SA,* 29, 43-48

Huete, A. and Co-authors, 2002. Overview of the radiometric and biophysical performance of the MODIS vegetation indices. *Remote Sens. Environ.* 83, 195-213

Huffman, G.J., Adler R.F., Bolvin, D.T. and G.J. Gu, 2009. Improving the global precipitation record: GPCP Version 2.1. *Geophys. Res. Lett.*, 36, art. no. L17808

IPCC, 2007. Summary for Policymakers. In: *Climate Change 2007: The Physical Science Basis. Contribution of Working Group I to the Fourth Assessment Report of the Intergovernmental Panel on Climate Change.* [Solomon, S., Qin, D., Manning, M., Chen, Z., Marquis, M., Averyt, K.B., Tignor, M., and H.L. Miller (eds)]. Cambridge, United Kingdom and New York, NY, USA

Izumo, T., Vialard, J., Lengaigne, M., de Boyer Montégut, C., Behera, S.K., Luo, J.J., Cravatte S., Masson S., and T. Yamagata, 2010. Influence of the state of the Indian Ocean Dipole on following year's El Niño. *Nature Geosci*., 3, 168-172.

Iizuka, S., Matsuura, T. and Yamagata, T., 2000. The Indian Ocean SST dipole simulated in a coupled general circulation model. *Geophys. Res. Lett., 27, doi: 10.1029/2000GL011484. issn: 0094-8276.*

Jury, M.R., 1992. A climatic dipole governing the interannual variability of convection of SW Indian Ocean and SE Africa region. *Theor. Appl. Climatol.,* 50, 103-115

Jury, M.R., 1999. Intra-seasonal convective variability over southern Africa: Principal components analysis of pentad outgoing longwave radiation departures 1976-1994. *Theor. Appl. Climatol.,* 62, 133-146

Jury, M.R., 2012. An inter-comparison of model-simulated east-west climate gradients over South Africa. *Water SA,* 38, 467-477

Jury, M.R., 2013. Climate trends in southern Africa. *S. Afr. J. Sci.,* 109, doi.org/10.1590 /sajs.2013/980

Jury, M.R., 2016. Climate influences on Vaal River flow. *Water SA*, 42, 232-242

Jury, M.R. and K.M. Levey, 1993. Climatology and characteristics of drought in the Eastern Cape of South Africa. *Int. J. Climatol.,* 13, 629-641

Jury, M.R., Valentine, H.R. and J.R.E. Lutjeharms, 1993a. Influence of the Agulhas current on summer rainfall along the southeast coast of South Africa. *J. Appl. Meteorol., 32, 1282-1287*

Jury, M.R., Pathack, B., Wang, B., Powell, M. and N. Raholijao, 1993b. A destructive tropical cyclone season in the SW Indian Ocean: January-February 1984. *S. Afr. Geog. J.*, 75, 53-59

Jury, M.R., McQueen, C., and K. Levey, 1994. SOI and QBO signals in the African region. *Theor. Appl. Climatol.,* 50, 103-115

Jury, M.R., Weeks, S. and M.P. Gondwe, 1997a. Satellite-derived vegetation as an indicator of climate variability over southern Africa. *S. Afr. J. Sci.,* 93, 34-38

Jury, M.R., Rouault, M., Weeks, S. and M. Schormann, 1997b. Atmospheric boundary-layer fluxes and structure across a land-sea transition zone in south-eastern Africa. *Boundary-Layer Meteorology 83:311-330.*

Jury, M.R. and N.D. Mwafulirwa, 2002. Climate variability in Malawi, Part I: Dry summers, statistical associations and predictability. *Int. J. Climatol.,* 22, 1289-1302

Jury, M.R., Nyathikazi, N. and E. Bulfoni, 2008. Sustainable agricultural for a community in a nature reserve on the Maputaland coast of South Africa. *Scientific Research and Essays*, 3, 376-382

Kabanda, T.A., 2005. Climatology of longterm drought in the northern region of the Limpopo province of South Africa. *PhD thesis, Univ. Venda*

Kalma, J.D., McVicar, T.R. and M.F. McCabe, 2008. Estimating land surface evaporation: A review of methods using remotely sensed surface temperature data. *Surv. Geophys.,* 29, 421-469

Kalnay, E., Kanamitsu, M., Kistler, R. and Co-authors 1996. The NCEP/NCAR 40 year reanalysis project. *Bull. Amer. Met. Soc.,* 77, 437-471

Kanamitsu, M., Ebisuzaki, W., Wollen, J., Yang, S-K., Hnilo, J.J., Fiorino, M. and G.L. Potter, 2002. NCEP-DOE AMIP-II Reanalysis (R-2). *Bull. Amer. Met. Soc*., 83, 1631-1643

Karnieli, A., Agam, N., Pinker, R.T. and Co-authors, 2009. Use of NDVI and land surface temperature for drought assessment: merits and limitations. *J. Climate,* 618-633

Kay, G. and R. Washington, 2008. Future southern African summer rainfall variability related to a southwest Indian Ocean dipole in HadCM3. *Geophys. Res. Lett.*, 35, L12701, doi: 10.1029/2008GL034180

Keyantash, J. and J.A. Dracup, 2002. The quantification of drought: An evaluation of drought indices. *Bull. Amer. Met. Soc.,* 83, 1167-1180

Kidd, C., 2001. Satellite rainfall climatology: A review. *Int. J. Climatol,* 21, 1041-1066

Kogan, F.N., 1997. Global drought watch from space. *Bull. Amer. Met. Soc.,* 78, 621-636

Kruger, A.C., 1999. The influence of the decadal-scale variability of summer rainfall on the impact of El Niño and La Niña events in South Africa. *Int. J. Climatol.,* 59-68

Kruger, A. C., and S. Shongwe, 2004. Temperature trends in South Africa: 1960-2003. South Africa. *Int. J. Climatol.*, 24, 1929-1945

Kusky, T.M., 2009. Climate change: shifting glaciers, deserts, and climate belts. The Hazardous Earth Set, New York: Facts on File, 156 pp. (ISBN-13: 978-0-8160-6466-3. ISBN-10: 978-0-8160-6466-0)

Landman, W. A., and S. J. Mason, 1999. Operational long-lead prediction of South African rainfall using canonical correlation analysis. *Int. J. Climatol.*, 19, 1073-1090.

Landman, W.A., DeWitt, D., Lee, D.E., Beraki, A. and D. Lotter, 2012. Seasonal rainfall skill over South Africa: one- versus two-tired forecasting systems. *Weather Forecast,* 27, 489-501

Lau, N-C, 1997. Interactions between global STT anomalies and the midlatitude atmospheric circulation. *Bull. Amer. Met. Soc.,* 78, 21-33

Lau, K.-M. and P.J. Sheu, 1988. Annual cycle, quasi-biennial oscillation and southern oscillation in global precipitation. *J. Geophys. Res. Atmos.*, 93, 10975-10988

Lau, K.-M. and H.-Y. Weng, 1995. Climate signal detection using wavelet transform: How to make a time series sing. *Bull. Amer. Met. Soc*., 12, 2391--2402

Lenters, J.D. and K.H. Cook, 1997. On the origin of the Bolivian High and related circulation features of the South American climate. *J. Atmos. Sci.*, 54, 656-677

Levey, K.M., 1993. Intra-seasonal oscillations of convection over southern Africa. *Unpublished MSc. thesis, Oceanography Dept., Univ. Cape Town*

Levey, K.M. and M.R. Jury, 1996. Composite intraseasonal oscillations of convection over southern Africa. *J. Climate*, 9, 1910-1920

Lewis, L.A. and L. Berry, 1988. African Environments and Resources. *Unwin Hyman, Boston*

Lindesay, J., 1998. Present Climates of Southern Africa. In: Climates of the Southern Continents. Past, present and future. [Hobbs, J.E., Lindesay, J.A. and H.A. Bridgman (eds)], *John Wiley & Sons, Chichester, 297 pp*

Lloyd-Hughes, B. and M.A. Saunders, 2002. A drought climatology for Europe. *Int. J. Climatology,* 22, 1571-1592

Lockwood, J.G., 1986. The causes of drought with particular reference to the Sahel. *Prog. Phys. Geog.,* 10, 111-119

Luo, J-J., Zhang, R., Behera, S.K., Masumoto, Y., Jin, F-F., Lukas, R. and T. Yamagata, 2010. Interaction between El Niño and extreme Indian Ocean dipole. *J. Climate*, 23: 726–742

Lutgens, F.K. and E.J. Tarbuck, 2010. The atmosphere: An introduction to meteorology *eleventh edition*. *Prentice Hall, New York, 508 pp.*

Lutjeharms, J.R.E., Biastoch, A., van der Werf, P.A., Ridderhinkhof, H. and W.P.M. de Ruijter, 2012. On the discontinuous nature of the Mozambique Current. *S. Afr. J. Sci*., 108, http://dx.doi.org/10.4102/sajs.v108i1/2.428

Lyon, B., 2004. The strength of El Niño and the spatial extent of tropical drought. *Geophys. Res. Lett.,* 31, doi: 10.1029/2004GL020901

Lyon, B., 2009. Southern Africa summer drought and heat waves: Observations and coupled model behaviour. *J. Climate,* 22, 6033-6046

Lyon, B. and S.J. Mason, 2007. The 1997-98 summer rainfall season in southern Africa. Part I: Observations. *J. Climate,* 20, 5134-5148

Lyon, B. and S.J. Mason, 2009. The 1997/98 summer rainfall season in southern Africa. Part II: Model simulations and coupled model forecasts. *J. Climate,* 22, 3802-3818

MacKellar, N., New, M. and C. Jack, 2014. Observed and modelled trends in rainfall and temperature for South Africa: 1960-2010. *S. Afr. J. Sci., 110, doi.org/10.1590/sajs.2014/20130353*

Macron, C., Pohl, B. and Y. Richard, 2014. How do tropical temperate troughs form and develop over southern Africa? *J. Climate*, 27, 1633-1647

Madden, R.A. and J. Williams, 1978. The correlation between temperature and precipitation in the United States and Europe. *Mon. Wea. Rev.,* 106, 142-147

Makarau, A., 1995. Intra-seasonal oscillatory modes of the southern Africa summer circulation. *PhD thesis, Univ. Cape Town*

Makarau, A. and M.R. Jury, 1997. Predictability of Zimbabwe summer rainfall. *Int. J. Climatol.,* 17, 1421-1432

Malawi Meteorological Services, 2011. Climate of Malawi. Accessed online from www.metmalawi.com on 22 June 2011

Malherbe, J., Engelbrecht, F.A., Landman, W.A. and C.J. Engelbrecht, 2012. Tropical systems from the southwest Indian Ocean making landfall over the Limpopo River Basin, southern Africa: a historical perspective. *Int J. Climatol*, 32, 1018-1032

Malherbe, J., Landman, W.A., Olivier, C., Sakuma and J-J. Luo, 2014. Seasonal forecasts of the SINTEX-F coupled model applied to maize yield and streamflow estimates over north-eastern South Africa. *Meteorol. Appl.*, 21, 733-742

Manatsa, D. and S.K. Behera, 2014. On the major shifts in the IOD during the last century, the role of the Mascarene High displacements. *Int. J. Climatol.,* 34, doi: 10.1002/joc.3820

Manatsa, D. and C.H. Matarira, 2009. Changing dependence of Zimbabwean rainfall variability on ENSO and the Indian Ocean dipole/zonal mode. *Theor. Appl. Climatol.,* doi: 10.1007/s00704-009-0114-0

Manatsa, D., Chingombe, W., Matsikwa, H. and C.H. Matarira, 2007. The superior influence of Darwin sea level pressure anomalies over ENSO as a drought predictor for Southern Africa. *Theor. Appl. Climatol.,* doi: 10.1007/s00704-007-0315-3

Manatsa, D., Chingombe, W. and C.H. Matarira, 2008. The impact of the positive Indian Ocean dipole on Zimbabwe droughts. *Int. J. Climatol.,* 28, 2011-2029

Manatsa, D., Matarira, C.H. and G. Mukwada, 2011. Relative impacts of ENSO and Indian Ocean dipole/zonal mode on east SADC rainfall. *Int. J. Climatol.,* 31, 558-577

Manatsa, D., Morioka, Y., Behera, S.K., Yamagata, T. and C.H. Matarira, 2013. Link between Antarctic ozone depletion and summer warming over southern Africa. *Nat. Geosci.,* doi: 10.1038/NGEO1968

Martyn, D., 1992. Climates of the world. *Developments in Atmospheric Science 18, Polish Scientific Publishers, Warsaw.*

Mason, S.J., 1995. Sea-surface temperature – South African rainfall associations, 1910 – 1989. *Int. J. Climatol.,* 15, 119-135

Mason, S.J. and M.R. Jury, 1997. Climatic variability and change over southern Africa: a reflection on underlying processes. *Prog. Phys. Geogr.,* 21, 23-50

Mason, S.J. and J.A. Lindesay, 1993. A note on the modulation of Southern Oscillation-South African rainfall associations with the Quasi-Biennial Oscillation. *J. Geophys. Res.,* 98, 8847-8850

Mason, S.J., Lindesay, J.A. and P.D. Tyson, 1994. Simulating drought in southern Africa using sea surface temperature variations. *Water SA, 20, 15-22*

Mason, S.J. and P.D. Tyson, 1992. The modulation of sea-surface temperature and rainfall associations over southern Africa with solar activity and the Quasi-Biennial Oscillation. *J. Geophys. Res.,* 97, 5847-5856

Matarira, C.H., 1990. Drought over Zimbabwe in a regional and global context. *Int. J. Climatol.*, 10, 609-625

Matarira, C.H. and M.R. Jury, 1992. Contrasting meteorological structure of intra-seasonal wet and dry spells in Zimbabwe. *Int. J. Climatol.,* 12, 165-176

Matsoukas, C., Benas, N., Hatzianastassiou, N. and Co-authors, 2011. Potential evaporation trends over land between 1983-2008: driven by radiative fluxes or vapour-pressure deficit? *Atmos. Chem. Phys.,* 11, 7601-7616

McKee, T.B., Doesken, N.J. and J. Kleist, 1993. The relationship of drought frequency and duration to time scales. *8th conference on Applied Climatology, 17-22 January 1993, Anaheim, California*

Meyer, S.J., Hubbard, K.G. and D.A. Wilhite, 1993. The development of a crop-specific drought index for corn. Part I: Model development and validation. *Agron. J.,* 85, 388-395

Mika, J., Horvath, Sz., Makra, L. and Z. Dunkel, 2004. The Palmer Drought Severity Index (PDSI) as an indicator of soil moisture. *Phys. Chem. Earth,* 30, 223-230

Moeletsi, M.E., 2010. Agroclimatological risk assessment in rainfed maize production for the Free State province of South Africa. *PhD thesis, Univ. Free State*

Moeletsi, E.M., Walker, S and W.A. Landman, 2011. ENSO and implications on rainfall characteristics with reference to the Free State Province of South Africa. *Phys. Chem. Earth,* 715-726

Mo, K.C., Paegle, J.N. and R.W. Higgins, 1997. Atmospheric processes associated with summer floods and drought in the central United States. *J. Climate,* 10, 3028-3046

Morioka, Y., Ratnam, V., Sasaki, W. and Y. Masumoto, 2013a. Generation mechanism of the South Pacific subtropical dipole. *J. Climate,* 26, 6033-6045

Morioka, Y., Tozuka, T. and T. Yamagata, 2013b. How is the Indian Ocean subtropical dipole excited? *Clim. Dyn.*, 41, 1955-1968

Morioka, Y., Masson, S., Terray, P., Prodhomme, C., Behera, S.K. and Y. Masumoto, 2014. Role of tropical SST variability on the formation of subtropical dipoles. *J. Climate*, 27, 4486-4507

Morioka, Y., Takaya, K., Behera, S.K., Masumoto, Y. and Y. Masumoto, 2015a. Local SST impacts on the summertime Mascarene High variability. *J. Climate*, 28, 678-694

Morioka, Y., Engelbreacht, F. and S.K. Behera, 2015b. Potential sources of decadal climate variability over southern Africa. *J. Climate,* 28, 8695-8709

Msangi, J.P., 2004. Drought hazard and desertification management in the drylands of southern Africa. *Environmental Monitoring and Assessment,* 99, 75-87

Muchuru, S., Landman, W.A., Dewitt, D. and D. Lötter, 2014. Seasonal rainfall predictability over the Lake Kariba catchment area. *Water SA,* 40, 461-470

Muchuru, S., Botai, J.O., Botai, C.M., Landman, W.A. and A.M. Adeola, 2015. Variability of rainfall over Lake Kariba catchment area in the Zambezi river basin, Zimbabwe. *Theor. Appl. Climatol.,* doi 10.1007/s00704-015-1422-1

Mudenda, O.S. and Z.L.S. Mumba, 2004. The unusual storm of January 1996. *Proceedings of the EUMETSAT meteorological satellite conference*, 31 May – 4 June 2004, Prague, Czech Republic

Mugara, R.K., 1997. Intraseasonal variation of convection over southern Africa. *PhD thesis, Univ. Reading*

Mulenga, H.M., 1998. Southern African Climatic Anomalies, Summer Rainfall and the Angola Low. *PhD thesis, Univ. Cape Town*

Mulenga, H.M., Rouault, M. and C.J.C. Reason, 2003. Dry summers over northeastern South Africa and associated circulation anomalies. *Clim. Res.,* 25, 29-41

Muller, A., Reason, C.J.C. and N. Fauchereau, 2008. Extreme rainfall in the Namib Desert during late summer 2006 and influences of regional ocean variability. *Int. J. Climatol.,* 28, 1061-1070

Murthy, C.S., Sesha Sai, M.V.R., Naresh Kumar, M. and P.S. Roy, 2009. Temporal divergence in cropping pattern and its implications on geospatial drought assessment. *Geocarto International,* 24, 377-395

Namias, J., 1983. Some causes of United States drought. *J. Climate and Applied Meteorology, 22, 30-39*

Nelson, G. and L. Hutchings, 1983. The Benguela upwelling area. *Prog. Oceanog.*, 12, 333-356

New, M., Washington, R., Jack, C. and B. Hewitson, 2003. Sensitivity of southern African climate to soil-moisture. *CLIVAR Exchanges*, No. 8, International CLIVAR Project Office, Southampton, United Kingdom, pp 45–47

New, M., Hewitson, B., Stephenson, D.B. and Co-authors, 2006. Evidence of trends in daily climate extremes over southern and west Africa. *J. Geophys. Res.,* 111, D14102, doi:10.1029/2005JD006289

Nicholson, S.E., Kim, J. and J. Hoopingarner, 1988. Atlas of African rainfall and its interannual variability. *Dept. of Meteorology, Florida State Univ., Tallahassee, 237 pp.*

Nicholson, S.E. and T.J. Farrar, 1994. The influence of soil type on the relationships between NDVI, rainfall and soil moisture in semi-arid Botswana: I. NDVI response to rainfall. *Rem. Sens. Environ.*, 50, 107-120

Nicholson, S.E., Leposo, D. and J. Grist, 2001. The relationship between El Niño and drought over Botswana. *J. Climate,* 14, 323-335

O'Farrell, P.J., Anderson, P.M.L., Milton, S.J. and W.R.J. Dean, 2009. Human response and adaptation to drought in the arid zone: lessons from southern Africa. *S. Afr. J. Sci.,* 105, 34-39

Oglesby, R.J. and D.J. Erikson III, 1989. Soil moisture and the persistence of North American drought. *J. Climate*, 2, 1362-1380

Olivier, C., Landman, W.A. and A.F. Beraki, 2013. River flow predictions for the South African mid-summer using a coupled general circulation model. *Paper presented at the annual conference of the South African Society for the Atmospheric Sciences, Durban, 26-27 September 2013*

Palmer, W.C., 1965. Meteorological Drought. *Research Paper No. 45, U.S. Weather Bureau* [NOAA Library and Information Services Division, Washington, D.C. 20852]

Palmer, W.C., 1968. Keeping track of soil moisture conditions, nationwide: The new crop moisture index. *Weatherwise,* 21, 156-161

Peters, A.J., Rundquist, D.C. and D.A. Wilhite, 1991. Satellite detection of the geographic core of the 1988 Nebraska drought. *Agr. Forest Meteorol.,* 57, 35-47

Phillips, J.G., Cane, M. and C. Rosenzweig, 1998. ENSO, seasonal rainfall patterns and simulated maize yield variability in Zimbabwe. *Agr Forest Meteorol*, 90, 39–50

Pinheiro, A.C., Tucker, C.J., Entekhabi, D. and J.A. Berry, 2001. Assessing the relationship between surface temperature and soil moisture in southern Africa. *Remote Sensing and Hydrology,* [Proceedings of a symposium held at Santa Fe, New Mexico, USA, April 2000], AHS Publ. no. 267, 2001

Pohl, N., Fauchereau, N., Richard, Y., Rouault, M. and C.J.C Reason, 2009. Interactions between synoptic, intraseasonal and inter-annual convective variability over southern Africa. *Clim. Dyn.,* 33, 1033-1050

Ramakrishna, A., Tam, H.M., Wani, S.P. and T.D. Long, 2006. Effect of mulch on soil temperature, moisture, weed infestation and yield of groundnut in northern Vietnam. *Field Crops Research,* 95, 115-125

Ratna, S.B., Behera, S., Ratnam, J.V., Takahashi, K. and T. Yamagata, 2013. An index for tropical temperate troughs over southern Africa. *Clim. Dyn.*, 41, 421-441

Ratnam, J.V., Behera, S.K., Masumoto, Y., Takahashi, K. and T. Yamagata, 2012a. A simple regional coupled model experiment for summer-time climate simulation over southern Africa. *Clim. Dyn.*, 39, 2207-2217

Ratnam, J.V., Behera, S.K., Masumoto, Y., Takahashi, K. and T. Yamagata, 2012b. Anomalous climatic conditions associated with the El Niño Modoki during the boreal winter of 2009. *Clim. Dyn.*, doi: 10.1007/s00382-011-1108-z

Ratnam, J.V., Behera, S.K., Masumoto, Y. and T. Yamagata, 2014. Remote effects of El Niño and Modoki events on the austral summer precipitation of southern Africa. *J. Climate,* 27, 3802-3815

Ratnam, J.V., Behera, S.K. and T. Yamagata, 2015. Role of cross-equatorial waves in maintaining long periods of low convective activity over southern Africa. *J. Atmos. Sci.*, 72, 682-692

Reason, C.J.C., 1999. Interannual warm and cool events in the subtropical/midlatitude south Indian Ocean region. *Geophys. Res. Lett.,* 26, 215-218

Reason, C.J.C., 2001a. Subtropical Indian Ocean SST dipole events and southern Africa rainfall. *Geophys. Res. Lett.,* 28, 2225-2227

Reason, C.J.C., 2001b. Evidence for the influence of the Agulhas Current on regional atmospheric circulation patterns. *J. Climate,* 14, 2769-2778

Reason, C.J.C., 2002. Sensitivity of the southern African circulation to dipole sea-surface temperature patterns in the Indian Ocean. *Int. J. Climatol.,* 22, 377-393

Reason, C.J.C., 2007. Tropical cyclone Dera, the unusual 2000/01 tropical cyclone season in the southwest Indian Ocean and associated rainfall anomalies over southern Africa. Meteorol Atmos Phys, 97, 181–188

Reason, C.J.C, 2016. The Bolivian, Botswana, and Bilybara Highs and Southern Hemisphere drought/floods. *Geophys. Res. Lett.,* 43, 1280-1286

Reason, C.J.C, Allan, R.J., Lindesay, J.A., and T.J. Ansell, 2000. ENSO and climatic sig nals in the Indian Ocean basin in the global context: Part 1, inter-annual composite patterns. *Int. J. Climatol.,* 20, 1285-1327

Reason, C.J.C. and A. Kiebel, 2004. Tropical cyclone Eline and its unusual penetration and impacts over the southern African mainland. *Weather Forecast.,* 19, 789-805

Reason, C.J.C., Hachigonta, S. and R.F. Phaladi, 2005. Interannual variability in rainy season characteristics over the Limpopo region of southern Africa. *Int. J. Climatol.,* 25, 1835-1853

Reason, C.J.C. and D. Jagadheesha, 2005. A model investigation of recent ENSO impacts over southern Africa. *Meteorol. Atm. Phys.*, 89, 181-205

Reason, C.J.C., Landman, W. and W. Tennant, 2006. Seasonal to decadal prediction of southern African climate and its links with variability of the Atlantic Ocean. *Bull. Amer. Met. Soc.*, doi:10.1175/BAMS-87-7-941

Reason, C.J.C. and H. Mulenga, 1999. Relationships between South African rainfall and SST anomalies in the Southwest Indian Ocean. *Int. J. Climatol.,* 19, 1651-1673

Reason, C.J.C. and M. Rouault, 2002. ENSO-like decadal variability and South African rainfall. *Geophys. Res. Lett.*, 29, 1638, doi 10.1029/2002GL014663

Rees, G., Marsh,T.J., Roald, L., Demuth, S., van Lanen, H.A.J. and L. Kasparek, 2004. Hydrological data. In: Hydrological drought: processes and estimation methods for streamflow and groundwater [Tallaksen, L.M. and H.A.J. van Lanen (eds.)], *Elsevier, Amsterdam 579 pp.*

Reynolds, R.W., Rayner, N.A., Smith, T.M., Stokes, D.C. and W. Wang, 2002. An improved in situ and satellite SST analysis for climate. *J. Climate*, 15, 1609-1625

Richard, Y., Fauchereau, N., Poccard, I., Rouault, M. and S. Trzaska, 2001. 20th century droughts in southern Africa: temporal variability, teleconnections with oceanic and atmospheric conditions. *Int. J. Climatol.*, 21, 873-885

Richard, Y. and I. Poccard, 1998. A statistical study of NDVI sensitivity to seasonal and interannual rainfall variations in southern Africa. *Int. J. Remote Sens.,* 19, 2907-2920

Richard, Y., Trzaska, S., Roucou, P. and M. Rouault, 2000. Modification of the southern African rainfall variability/ENSO relationship since the late 1960s. *Clim. Dyn.,* 16, 883-895

Rocha, A. and I. Simmonds, 1997. Interannual variability of southern Africa summer rainfall, 1: Relationships with air-sea interaction processes. *Int. J. Climatol.,* 17, 235-265

Ropelewski, C.F. and M.S. Halpert, 1987. Global- and regional-scale precipitation patterns associated with El Nino/Southern Oscillation. *Mon. Wea. Rev.,* 115, 1606-1626

Rouault, M., Florenchie, P., Fauchereau, N. and C.J.C. Reason, 2003. South east tropical Atlantic warm events and southern African rainfall. *Geophys. Res. Lett.*, 30, doi:10.1029/2002GL014840

Rouault, M. and Y. Richard, 2003. Intensity and spatial extension of drought in South Africa at different time scales. *Water SA,* 29, 489-500

Rouault, M. and Y. Richard, 2005. Intensity and spatial extent of droughts in southern Africa. *Geophy. Res. Lett.,* 32, L15702, 4PP. 2005 doi:10.1029/2005GL022436

Rutherford, M.C. 2004. Categorization of biomes. In: Vegetation of southern Africa [Cowling, R.M., Richardson, D.M. and S.M. Pierce (eds)], *Cambridge University Press, Cambridge, pp. 91-98*

Rutherford, M.C. and R.H. Westfall, 1986. The biomes of southern Africa – an objective categorization, 1st ed. *Memoirs of the Botanical Survey of South Africa,* 54, 1-98

Saha, S. and Co-authors, 2010. The NCEP Climate Forecast System Reanalysis. *Bull. Amer. Met. Soc.,* 91, 1015-1057

Saji, N.H., Goswami, B.N., Vinayachandran, P.N., and T. Yamagata, 1999. A dipole mode in the tropical Indian Ocean. *Nature*, 401, 360-363.

Schubert, S.D., Suarez, M.J., Pegion, P.J., Koster, R.D. and J.T. Bacmeister, 2004. Causes of long-term drought in the US Great Plains. *J. Climate,* 17, 485-503

Schulze, R.E., 1997. South African Atlas of Agrohydrology and – Climatology. *Water Research Commission, Pretoria, Report TT82/96*

Shafer, B.A. and L.E. Dezman, 1982. Development of a surface water supply index (SWSI) to assess the severity of drought conditions in snowpack and runoff areas. *Proc. Western Snow Conf.,* 164-175

Shaw, E.M., 1994. Hydrology in Practice, Third Edition. *Chapman & Hall, London, 569 pp.*

Sheffield, J. and E.F. Wood, 2008. Global trends and variability in soil moisture and drought characteristics, 1950-2000, from observation-driven simulations of the terrestrial hydrologic cycle. *J. Climate,* 21, 432-458

Sheffield, J., Andreadis, K.M., Wood, E.F. and D.P. Lettenmaier, 2008. Global and continental drought in the second half of the twentieth century: Severity-area-duration analysis and temporal variability of large scale events. *J. Climate,* 22, 1962-1981

Sheffield, J., Wood, E.F. and F. Munoz-Arriola, 2010. Long-term estimates of evapotranspiration for Mexico based on downscaled ISCCP data. *J. Hydrometerol.,* 11, 253-275

Sheffield, J., Wood, E.F. and M.L. Roderick, 2012. Little change in global drought over the past 60 years. *Nature,* 491, 435-438

Shillington, F.A., Reason, C.J.C., Duncombe Rae, C.M., Florenchie, P. and P. Penven, 2006. Large scale physical variability of the Benguela Current Large Marine Ecosystem (BCLME). *Large Marine Ecosystems,* 14, 49-69

Schneider, U., Becker, A., Finger, P. and Co-authors, 2014. GPCC's new land surface precipitation climatology based on quality-controlled in situ data and its role in quantifying the global water cycle. *Theor Appl Climatol.,* 115: 15. doi:10.1007/s00704-013-0860-x

Shongwe, M.E., van Oldenborgh, G.J., van Den Hurk, B. and M. van Aalst, 2011. Projected Changes in Mean and Extreme Precipitation in Africa under Global Warming. Part II: East Africa. *J. Climate*, 24, 3718-3733

Singleton, A.T. and C.J.C. Reason, 2007. Variability in the characteristics of cut-off low pressure systems over subtropical southern Africa. *Int. J. Climatol.*, *27*, 295-310

Smakhtin, V.Y., 2001. Low flow hydrology: a review. *J. Hydrol.,* 240, 147-186

Stahl, K. and H. Hisdal, 2004. Hydroclimatology. In: Hydrological drought: processes and estimation methods for streamflow and groundwater [Tallaksen, L.M. and H.A.J. van Lanen (eds.)], *Elsevier, Amsterdam 579 pp.*

Stringer, L.C., Dyer, J.C., Reed, M.S., Dougill, A.J., Twyman, C. and D. Mkwambisi, 2009. Adaptations to climate change, drought and desertification: local insights to enhancepolicy in southern Africa. *Environmental Science and Policy,* 12, 748-765

Sun, D. and M. Kafatos, 2007. Note on the NDVI-LST relationship and the use of temperature-related drought indices over North America. *Geophys. Res. Lett.,* 34, L24406, doi:10.1029/2007GL031485

Tadross, M.A., Hewitson, B.C. and M.T. Usman, 2005. The interannual variability of the onset of the maize growing season over South Africa and Zimbabwe. *J. Climate,* 18, 3356-3372

Tallaksen, L.M. and H.A.J. van Lanen, 2004. Introduction. In: Hydrological drought: processes and estimation methods for streamflow and groundwater [Tallaksen, L.M. and H.A.J. van Lanen (eds.)], *Elsevier, Amsterdam 579 pp.*

Tate, E.L., Meigh, J., Prudhomme, C and M. McCartney, 2000. Drought assessment in southern Africa using river flow data. *DFID Report 00/4, Institute of Hydrology, Willingford and Department for International Development (DFID), UK*

Tennant, W. and B.C. Hewitson, 2002. Intra-seasonal rainfall characteristics and their importance to the seasonal prediction problem. *Int. J. Climatol.,* 22, 1033-1048

Thornthwaite, C., 1948. An approach towards a rational classification of climate. *Geographical review, 38, 55-94*

Todd, M.C. and R. Washington, 1999. Circulation anomalies associated with tropical-temperate troughs over southern Africa. *Clim. Dyn.,* 15, 937-951

Todd, M.C., Washington, R. and P.I. Palmer, 2004. Water vapour transport associated with tropical-temperate trough systems over southern Africa and the southwest Indian Ocean. *Int. J. Climatol.,* 24, 555-568

Torrance, J.D., 1972. Malawi, Rhodesia and Zambia. In: *World Survey of Climatology*, *10,* Climates of Africa [J.F. Griffiths (ed.)], pp 409-418

Torrence, C. and G.P. Compo, 1998. A practical guide to wavelet analysis. *Bull. Amer. Met. Soc.,* 79, 61-78

Torrence, C., P.J. Webster, 1999. Interdecadal changes in the ENSO-monsoon system. *J. Climate,* 2679-2690

Trenberth, K.E. and G.W. Branstator, 1992. Issues in establishing causes of the 1998 drought in North America. *J. Climate,* 5, 159-172

Trenberth, K. E. and C.J. Guillemot, 1996. Physical processes involved in the 1988 drought and 1993 floods in North America. *J. Climate,* 9, 1288-1298

Trenberth, K.E. and D.J. Shea, 2005. Relationships between precipitation and surface temperature. *Geophys. Res. Lett.,* 32, L14703, doi: 10.1029/2005GL022760

Trenberth, K.E., Dai, A., van der Shrier, G. and Co-authors, 2014. Global warming and changes in drought. *Nature Climate Change*, 4, 17-22

Trzaska, S., 2010. Regional impacts from El Niño on Southern Africa. Accessed online at http://medias.obs-mip.fr/www/Reseau/Lettre/12/en/elnino/impacts_afr_aus.html on 5 August 2010.

Tsakiris, G. and H. Vangelis, 2005. Establishing a drought index incorporating evapotranspiration. *European water, 9/10, 3-11*

Tucker, C.J., 1979. Red and photographic infrared linear combinations for monitoring vegetation. *Remote Sen. Environ.,* 8, 127-150

Tucker, C.J., Pinzon, J.E., Brown, M.E., Slayback, D.A., Pak, E.W., Mahoney, R., Vermote, E.F. and N. El Saleous, 2005. An extended AVHRR - 8 km NDVI dataset comparable with MODIS and SPOT vegetation NDVI data. *Int. J. Remote Sens.,* 26, 4485-4498

Tyson, P.D., 1990. Modeling climatic change in Southern Africa: A review of available methods. *S. Afr. J. Sci.*, 86, 318-330

Tyson, P.D. and R.A. Preston-Whyte, 2000. The weather and climate of southern Africa. *Oxford University Press Southern Africa, Cape Town 396 pp.*

Tyson, P.D., Cooper, G.R.J. and T.S. McCarthy, 2002. Millenial to multi-decadal variability in the climate of southern Africa. *Int. J. Climatol., 22, 1105-1117*

UNEP, 2008. Vital water graphics: an overview of the state of the world's fresh and marine waters – 2nd edition. Accessed online at http://www.unep.org/dewa/vitalwater/article28.html on 30 December 2013.

Unganai, L.S. and T. Bandason, 2005. Monitoring agricultural drought in South Africa: Monitoring and predicting agricultural drought – a global study. *Oxford University Press, Oxford and London, UK pp 266-275*

Unganai, L.S. and F.N. Kogan, 1998. Southern Africa's recent droughts from space. *Adv. Space Res.,* 21, 507-511

Unganai, L.S. and S.J. Mason, 2001. Spatial characterization of Zimbabwe summer rainfall during the period 1920-1996. *S. Afr. J. Sci.,* 97, 425-432

Unganai, L.S. and S.J. Mason, 2002. Long-range predictability of Zimbabwe summer rainfall. *Int. J. Climatol.,* 22, 1091-1103

Usman, M.T. and C.J.C. Reason, 2004. Dry spell frequencies and their variability over southern Africa. *Clim. Res.,* 26, 199-211

Vancutsem, C., Ceccato, P. Dinku, T. and S.J. Connor, 2010. Evaluation of MODIS land surface temperature data to estimate air temperature in different ecosystems over Africa. *Rem. Sens. Environ.,* 114, 449-465

Van Lanen, H.A.J., Kasparek, L., Novicky, O. and Co-authors, 2004. Human influences. In: Hydrological drought: processes and estimation methods for streamflow and groundwater [Tallaksen, L.M. and H.A.J. van Lanen (eds.)], *Elsevier, Amsterdam 579 pp.*

Van Rooy, M.P. 1965. A rainfall anomaly index independent of time and space, *Notes*, 14, 43

Van Zyl, J., 1993. The last straw: drought and the economy. *Indicator SA,* 10, 47-51

Vicente-Serrano, S.M., Lopez-Moreno, J.I., Gimeno, L. and Co-authors, 2011. A multi-scalar global evaluation of the impact of ENSO on droughts. *J. Geophys. Res.,* 116, D20109, doi: 10.1029/2011JD0116039

Vigaud, N., Richard, Y., Rouault, M. and N. Fauchereau, 2009. Moisture transport between the south Atlantic Ocean and southern Africa: relationships with summer rainfall and associated dynamics. *Clim. Dyn.,* 32, 113-123

Vitart, F., Anderson, D. and T. Stockdale, 2003. Seasonal forecasting of tropical cyclone landfall over Mozambique. *J. Climate,* 16, 3932-3945

Vogel, C., 1994. The impact of extreme drought events. *Report submitted to the HSRC Human Needs, Resources and the Environment Programme supported by the Department of Environment Affairs*

Vogel, C., 2000. Climate and climatic change: causes and consequences. In: *The geography of South Africa in a changing world* [Fox, R. and K. Rowntree (eds.)], *Oxford University Press, Cape Town, 509 pp*

Von Storch, H., and F.W. Zwiers, 1998. Statistical Analysis in Climate Research. *Cambridge University Press, Cambridge, 485 pp.*

Walker, N.D., 1990. Links between South African summer rainfall and temperature variability of the Agulhas and Benguela Currents systems. *J. Geophys. Res.,* 95, 3297-3319

Wang, J., Rich, P.M. and K.P. Price, 2003. Temporal responses of NDVI to precipitation and temperature in the central Great Plains, USA. *Int. J. Remote Sens.,* 24, 2345-2364

Webster, P.J., Moore, A.M., Loschingg, J.P. and R.R. Leben, 1999. Coupled ocean-atmosphere dynamics in the Indian Ocean during 1997-98. *Nature*, 401, 356-360.

Wells, N., Goddard, S. and M.J. Hayes, 2004. A self-calibrating Palmer Drought Severity Index. *J. Climate*, 17, 2335-2351

Wessels, P. and A. Rooseboom, 2009. Flow-gauging structures in South African rivers. *Water Sci. Adv.,* 35, 1-19

Wilhite, D.A., 1992. Drought: its physical and social dimensions. In: Natural and technological disasters: causes, effects and preventive measures [Majumdar, S.K., Forbes, G.S., Miller, E.W. and Schmultz, R.F. (eds)] Pennsylvania Academy of SCience, Easton, Pennsylvania, pp 239-253

Wilhite, D.A. and M.H. Glantz, 1985. Understanding the drought phenomenon: the role of definitions. *Water International,* 10,111-120

Wilhite, D.A., Svoboda, M.D. and M.J. Hayes, 2007. Understanding the complex impacts of drought: A key to enhancing drought mitigation and preparedness. *Water Resour. Manage.,* 21, 763-774

WMO, 2012. Standardized Precipitation Index: User Guide. *WMO bulletin No. 1090,* Geneva, Switzerland

Xie, S.P., Annamalai, H., Schott, F.A. and J.P. McCreary, 2001. Structure and mechanism of south Indian Ocean climate variability. *J. Climate*, 15, 864-878

Yamagata, T., Behera, S.K., Rao, S.A., Guan, Z., Ashok, K. and H. N. Saji, 2002. The Indian Ocean Dipole: A physical entity. *CLIVAR Exch.*, 24, 15–18

Yamagata, T., Behera, S.K., Rao, S.A., Guan, Z., Ashok, K. and H. N. Saji, 2003. Comments on “Dipoles, Temperature Gradients, and Tropical Climate Anomalies”. *Bull. Amer. Met. Soc.*, 84, 1418-1422

Yeshanew A. and M.R. Jury, 2007. North African climate variability, part 1: tropical thermocline coupling. *Theor Appl. Climatol.*, doi10.1007/s00704-006-0242-8.

Yamagata, T., Morioka, Y. and S. Behera, 2016. Old and new faces of climate variations. In: Indo-Pacific climate variability and predictability [Behera, S.K. and T. Yamagata (eds)]. *World Scientific Series on Asia-Pacific Weather and Climate – Vol. 7, Singapore, pp. 1-23*

Yue, W., Xu, J., Tan, W. and L. Xu, 2007. The relationship between land surface temperature and NDVI with remote sensing: application to Shanghai Landsat ETM + data. *Int. J. Remote Sens.*, 28, 3205-3226